THE ORBIT OF THE MOON

by

Martin Alphonse Slade, III

S.B.(1964), S.M.(1967)
Massachusetts Institute of Technology

SUBMITTED IN PARTIAL FULFILLMENT
OF THE REQUIREMENTS FOR THE
DEGREE OF DOCTOR OF
PHILOSOPHY

at the

Massachusetts Institute of Technology

September 1971

Signature of Author: ______________________________
Department of Earth and Planetary
Sciences, September 1971

Certified by: ______________________________
Thesis Supervisor

Accepted by: ______________________________
Chairman, Departmental Graduate
Committee

To the memory of Dr. Wallace J. Eckert

1902-1971

TABLE OF CONTENTS

The Orbit of the Moon

THE ORBIT OF THE MOON

by

Martin A. Slade, III

Submitted to the Department of Earth and Planetary Sciences in September 1971, in partial fulfillment of the requirements for the degree of Doctor of Philosophy.

ABSTRACT

The position of the moon is calculated very precisely by numerically integrating the equations of motion. The initial conditions for the integration, along with various other parameters, are estimated from observations of the moon which include

a) meridian transits

b) Surveyor spacecraft tracking data

c) radar observations

The expression for the force on the moon in the equations of motion includes parameters characterizing the following small perturbations:

a) a general relativistic effect - the "geodesic precession"

b) tidal friction in the earth-moon system

c) a possible time variation of the gravitational coupling constant G

Estimation of these parameters from the lunar observations in combination with radar and optical observations of the inner planets leads to the following conclusions. The tidal interaction effect on the moon's mean motion $n_{☾}$ is not determined uniquely from this data set due to correlations with the variations in the earth's rotation rate and the possible variation in the gravitational constant. Upper limits can be placed on these variations, however, as follows:

$$\left|\frac{dn_{☾}}{dt}\right| < 33 \text{ seconds of arc/century}^2$$

$$\left|\frac{dG}{dt}\right| < 6\times10^{-11} \text{ G/year}$$

The geodesic precession is found to be (1.5 ± 0.6) seconds of arc/century, compared with the theoretical value from General Relativity of 1.92 seconds of arc/century.

Thesis Supervisor: Irwin I. Shapiro
Professor of
Geophysics and
Physics

CHAPTER I.

Introduction

Predictions of the position of the moon as a function of time have been attempted by man since the earliest known cultures. With the rise of modern science, observations of the lunar motion provided impetus for the development of Newton's theory of gravitation, as well as for several convincing tests of it. The theory of the motion of the moon was the rationale behind much mathematical work in the 18th and 19th centuries, notably by Euler, Laplace, and Poisson. The analytical theory for the lunar ephemeris incorporated in today's national almanacs (developed for navigational purposes) is due to G.W. Hill (1884). This theory was fully developed by E.W. Brown (1910), with recent revisions by W.J. Eckert (1966).

The space program has provided a new challenge to improve the accuracy of the lunar ephemeris for the traditional purpose of celestial navigation (in a more literal sense). The gravitational theories of Einstein and others have supplied sound scientific reasons for desiring more accurate tests of predictions for the positions of solar system bodies. At the same time very sensitive data types such as planetary radar ranging, spacecraft tracking data, and laser ranging have become available. The development of the modern electronic computer has been essential to the improvement of the calculations, both in quality and quantity, necessary for these purposes.

This thesis describes an effort to develop the theory of the lunar ephemeris to the point that the predicted effects of the following very small perturbations might be reliably distinguished in the complicated motion of the moon:

a) the general relativistic correction to the Newtonian gravitational interaction ("geodesic precession"),
b) the earth-moon interaction due to frictionally delayed tides,
c) a possible time variation in the gravitational coupling constant G.

A very accurate lunar ephemeris is also desired to satisfy the stringent prediction requirements necessary for successful laser ranging to the corner reflectors left by the Apollo missions. For all these purposes we generate the lunar ephemeris by numerical integration of the equations of motion in rectangular coordinates. We then rigorously calculate the values for the observables from the theory. The free parameters in the theory, such as initial conditions and the parameters characterizing the perturbations of scientific interest, are then estimated from the observations simultaneously.

Chapter II describes the model for the various forces that are included in the equations of motion. The lunar position and velocity as functions of time derived from the equations of motion can then be used to compute theoretical values for the observable quantities. The details of the calculation for the different types of observables are given in Chapter III. Chapter IV outlines the numerical techniques used, including the method of numerical integration applied to the equations of motion. Chapter V describes the "maximum likelihood" algorithm used to extract the parameter estimate from the (redundant) data set. Chapters VI and VII are devoted to a description and discussion of the various solutions obtained. Possible directions for future work are briefly indicated.

The extensive calculations necessary for this thesis were performed within the structure of a computer program called the Planetary Ephemeris Program (PEP), which has been developed over the past seven years at M.I.T.'s Lincoln Laboratory primarily by Michael E. Ash, Irwin I. Shapiro, and William B. Smith. PEP is a very general program able to treat many types of astronomical observations. In the following chapters only those features of the program relevant to the processing of lunar data will be discussed in detail.

One result of this work is a best-fitting ephemeris plus the (integrated) partial derivatives with respect to initial conditions and other parameters (See Section II.E) as functions of time. The latter quantities enable the ephemeris to be improved as more data types are added and/or more data collected. The usefulness of this ephemeris does not depend upon the validity of the purely scientific conclusions reached herein. In fact intermediate ephemerides produced during this work have been used successfully at Haystack Observatory for lunar radar mapping purposes, and have also been used for laser ranging prediction by groups at the Air Force Cambridge Research Laboratory, the Smithsonian Astrophysical Observatory, and the French Laser Group.

CHAPTER II

Theoretical Model for the Lunar Motion

A. Coordinate System

The basic theoretical framework underlying the calculation of the ephemeris used in the parameter estimation process to be described below (Chapter V) has been outlined previously by Ash, Shapiro, and Smith (1967). The right-handed coordinate system chosen has its origin at the Newtonian center of mass (barycenter) of the solar system with the axis directions defined by the mean equinox (x-axis) and equator (plane normal to the z-axis) of 1950.0. This system is assumed to be inertial; the axis directions are approximately those of the FK4 stellar system (Fricke and Kopff, 1963). The difference in orientation with respect to the FK4 catalogue at 1950.0 (as represented by the U.S. Naval Observatory lunar meridian circle observations reduced to the FK4) is explicitly estimated (see Section III.B below). Although the ephemeris is calculated in inertial space, the various kinds of observations are obtained in coordinate systems that, in general, are rotating with respect to inertial space (and not necessarily as rigid bodies). This problem is dealt with in Section II.C.

The physical units are chosen to agree as much as possible with conventional astronomical practice. The mass of the sun $M_\odot$ is set equal to unity. The unit of time chosen is the atomic time (A.1) second. The A.1 second is defined by setting the transition frequency ν_{43} of the $^2S_{1/2}$ state of cesium-133 between the hyperfine levels $(F=4,\ m_F=0) \leftrightarrow (F=3, m_F=0)$ at zero magnetic field to the precise value (Markowitz _et al._, 1958):

$$\nu_{43} = 9{,}192{,}631{,}770 \text{ cycles/A.1 second.}$$

The unit of length is the astronomical unit (A.U.), specified by defining

$$\frac{\sqrt{G(t_0)M_\odot}}{86{,}400} \equiv 0.01720209895\ (\text{A.U.})^{\frac{3}{2}}(\text{A.1 sec})^{-1}$$

where G is the gravitational constant. An epoch t_0 is associated with G because we may wish to solve for a time-variation which some cosmological theories have suggested as occurring in G. The appropriate epoch is the epoch of the determination of the initial conditions for the planets.

B.1 Time and Earth Rotation

The equations of motion for the solar system bodies are functions of an independent variable which we call coordinate time (C.T.). Atomic time, A.1, is related to C.T. in a theory-dependent manner. We choose to identify A.1 as a time with a uniform (but not identical) rate with respect to proper time for a terrestrial observer in the context of general relativity. The rate and origin of coordinate time are chosen to be

$$C.T. = A.1 + 32\overset{s}{.}15 + D(t) + Y(t) + M(t) + \ldots$$

The terms D(t), etc. are small periodic terms from the theory which average to zero; they are not observable for any of the work reported here. Unlike Ephemeris time* (E.T.), the coordinate time here does not depend upon the equinox to which the lunar ephemeris is referred.

The unit of time in the numerical integrations is the C.T. day. The C.T. second is $\frac{1}{86,400}$ of a C.T. day. The C.T. second can be considered equal to the A.1 second with negligible error for our applications.

Atomic time, and thus coordinate time, is related to universal time (U.T.1.) by measurements of the U.S. Naval Observatory. U.T.1 is the universal time appropriate for determining the orientation of the earth in inertial space, using Newcomb's relation between U.T.1 and sidereal time

---

* See the Explanatory Supplement, Section III.D

[see the Explanatory Supplement to the Ephemeris, Section III.B.3]. The differences between atomic time and U.T.1 are very irregular; a more uniform universal time, U.T.2, can be derived by removing the so-called "seasonal variations" (see below). Atomic time and U.T.2 differ by unpredictable variations in the rotation rate of the earth. The generic term commonly applied to these differences is ΔT, although this term strictly applies to the difference between Ephemeris Time (E.T.) and U.T.1. The variations were tentatively identified during the early twentieth century by a number of investigators, and demonstrated to be variations in the earth's rotation by Spencer Jones (1939). The currently accepted values for E.T. - U.T. come from the classic work of Brouwer (1952) for the years 1621 to 1948.5, and from the U.S. Naval Observatory for later times.

The geophysical explanation for ΔT is uncertain, but the variations seem to be related to the fluctuations in flow at the core-mantle boundary, as first suggested by Bullard et al. (1950). According to their model, changes in the length of day should cause opposite and proportional changes in the geomagnetic westward drift. A very high correlation ($\sim$0.93) between such changes has apparently been found by Ball et al. (1968) for a lag time between the change in rotation period and the change in drift of seven years. This time lag is consistent with the expected lag for propagation of the magnetic disturbance through a mantle thickness of conductivity $\sim 5 \times 10^{-9}$ e.m.u., a plausible average value (Vestine and Kahle, 1968). The explanation above for the physical origin of ΔT, however, still lacks general acceptance.

Published records of the differences between atomic time and universal time exist only from 1955 onward. Previous to 1955, the differences between coordinate time and U.T.2 must be derived from the data along with the other unknown quantities. The model for this variation was chosen after examination of accurate recent data for A.1. - U.T.2 [Markowitz, 1970], as well as of Brouwer's results. The adopted model assumes that ΔT changes at a uniform rate for several years at a time. The intervals over which the slope of ΔT vs. time remains constant can be chosen to be irregular in length, but we have chosen almost all to have nominal lengths of 4 years. This spacing appears more than sufficiently small since, for example, in the period 1925-1968, significant changes in slope of E.T. - U.T.1 occurred at intervals of 14, 12, 12, and 5 years (Klock and Scott, 1970).

The parameters in our model are the values of $\Delta T' \equiv$ C.T. - U.T.2 at the beginnings of successive 4-year intervals. (Since atomic time is only an intermediate quantity in the relation to C.T., it is unnecessary here.) As a boundary condition we have the defined difference A.1. + 32.15 - U.T.2 in 1955. The model is described graphically in Figure 1. The value of C.T. - U.T.2 at the time t_i at the beginning of the interval (t_i, t_{i+1}) is y_i. We see that the value of $\Delta T'$ as a function of time t is given by

$$\Delta T'(t) = \begin{cases} y_{i-1} + \frac{(y_i - y_{i-1})}{(t_i - t_{i-1})}(t - t_{i-1}) & \text{for } t_{i-1} \leq t \leq t_i \\ \\ y_i + \frac{(y_{i+1} - y_i)}{(t_{i+1} - t_i)}(t - t_i) & \text{for } t_i \leq t \leq t_{i+1} \end{cases}$$

The partial derivatives necessary to estimate the parameters y_i are given by

$$\frac{\partial \Delta T'}{\partial y_i} = \begin{cases} 0 & t < t_{i-1} \\ \\ \frac{t - t_{i-1}}{(t_i - t_{i-1})} & t_{i-1} \leq t \leq t_i \\ \\ 1 - \frac{(t - t_i)}{(t_{i+1} - t_i)} & t_i \leq t \leq t_{i+1} \\ \\ 0 & t > t_{i+1} \end{cases}$$

Thus the adopted model for C.T. - U.T.2 is composed of continuous piecewise linear expressions in time over pre-specified time intervals. The a priori values of y_i were taken from the smoothed values of Brouwer, and are given in Table 1. We accept the values from the U.S. Naval Observatory for A.1.+32.15 -U.T.2 from 1955 to the present, and then work backward in time to derive ΔT'. This approach takes advantage of the higher accuracy of recent observations -- a philosophy followed everywhere possible in our approach.

The seasonal variations ΔS.V. between U.T.1 and U.T.2 are necessary to complete the relation C.T. - U.T.1. These periodic variations have been accurately determined from the variations in latitude as measured by the Bureau International de l'Heure (B.I.H.), and are thought to have their origin in motions of oceanic and atmospheric masses (Munk and MacDonald, 1960). In our model, we have allowed for a possible linear change with time in the amplitudes of the variations, which change might be caused by long-term climatic changes with consequent changes in global weather patterns. The model has the analytic expression

$$\Delta S.V. = (a_1+b_1T)\cos S + (a_2+b_2T)\sin S$$

$$+(c_1+d_1T)\cos 2S + (c_2+d_2T)\sin 2S$$

n	ΔT' (seconds)	Julian Day Number	Interval	
			Days	Years
0.	31.3669	2435490	1295	3.546
1.	30.2900	2434195	1461	4.000
2.	28.1500	2432734	1461	4.000
3.	26.0800	2431273	1461	4.000
4.	24.3000	2429812	1461	4.000
5.	23.5800	2428351	1461	4.000
6.	23.5000	2426890	1461	4.000
7.	22.9200	2425429	1461	4.000
8.	22.2900	2423968	1461	4.000
9.	20.4800	2422507	1461	4.000
10.	17.3700	2421046	1461	4.000
11.	12.9500	2419585	1461	4.000
12.	7.5100	2418124	1461	4.000
13.	1.8000	2416663	1461	4.000
14.	-3.7900	2415202	1461	4.000
15.	-7.1900	2413741	1461	4.000
16.	-8.0400	2412280	1461	4.000
17.	-7.5800	2410819	1461	4.000
18.	-8.0700	2409358	1461	4.000
19.	-8.1400	2407897	1461	4.000
20.	-7.6700	2406436	1461	4.000
21.	-4.4800	2404975	1461	4.000
22.	0.2000	2403514	1461	4.000
23.	2.2600	2402053	1461	4.000
24.	3.3200	2400592	1461	4.000
25.	3.4600	2399131	1461	4.000
26.	2.9000	2397670	1461	4.000
27.	2.1200	2396209	1461	4.000
28.	1.1300	2394748	1461	4.000
29.	-0.0600	2393287	1461	4.000
30.	-0.0400	2391826	1461	4.000
31.	1.4900	2390365	1461	4.000
32.	2.3700	2388904	1461	4.000
33.	3.4900	2387443	1461	4.000
34.	5.3200	2385982	1461	4.000
35.	5.0400	2384521	1461	4.000
36.	4.7600	2383060	1461	4.000
37.	5.0000	2381599	1461	4.000
38.	5.4000	2380138	1461	4.000

Table 1. ΔT' = (C.T. - U.T.2) Values at Given Dates (Brouwer, 1952)

n	ΔT' (seconds)	Julian Day Number	Interval	
			Days	Years
39.	5.8000	2378677	1461	4.000
40.	6.4250	2377216	1461	4.000
41.	7.0500	2375755	1461	4.000
42.	7.6750	2374294	1461	4.000
43.	8.3000	2372833	1461	4.000
44.	7.3300	2371372	1461	4.000
45.	6.3600	2369911	1461	4.000
46.	5.3900	2368450	1461	4.000
47.	4.4200	2366989	1461	4.000
48.	3.4500	2365528	1461	4.000
49.	2.4800	2364067	1461	4.000
50.	1.5100	2362606	1461	4.000
51.	-0.0874	2360200	2406	6.587

Table 1. (Continued) ΔT' = (C.T. - U.T.2) Values at Given Dates (Brouwer, 1952).

where $S = 2\pi T$, and T is time in years of 365.2421988 days from Jan 1, 1962, 0 hrs U.T.2. The nominal values for the parameters (Guinot and Feissel, 1969) are

$$a_1 = +0.022 \text{ sec.}$$

$$a_2 = -0.012 \text{ sec.}$$

$$c_1 = -0.006 \text{ sec.}$$

$$c_2 = +0.007 \text{ sec.}$$

$$b_1 = b_2 = d_1 = d_2 = 0.$$

In computing theoretical values for observations of the moon, we must derive the positions of the earth-based observing sites in our inertial reference frame. A site position is composed of the vector sum of the position of the center of mass of the earth relative to the solar system barycenter and vector position of the site relative to the center of mass of the earth. In computing the latter position in our program, we assume that the motion of the earth about its center of mass is known except for the modifications discussed in Section II.C.2 below. The formulation of the rotation of the earth is taken from the expressions in the Explanatory Supplement to the American Ephemeris and Nautical Almanac; the implementation in the program is outlined in this section. Applying this information about the rotation of the earth to the vector position of the site as seen in a frame fixed to the earth's crust, together with the time relations of Section B, yields the position of the site at any time relative to the inertial frame.

The nominal values for the coordinates of the optical observatories in body-fixed coordinates have been taken from standard sources such as the American Ephemeris and Nautical Almanac. The positions of the Deep Space Network stations of the Jet Propulsion Laboratory (referred to the mean north pole and Greenwich meridian of 1900-05) were taken from Melbourne et al., 1968. These nominal values are listed in Table 2; since meridian observations are reported as if they were made from the center of mass of the earth, only the site longitude is necessary to calculate theoretical values for this observable. The effect of errors in the reduction to geocentric values will be examined in Chapter III, Section A. For the Surveyor doppler observations,

Table 2

Nominal Positions for Observing Sites

Site name		Radius (km)	Longitude (deg)	Geocentric Latitude (deg)
1.	HAYSTACK	6368.551653028	71.4886666667	42.4315183830
2.	MILLSTON	6368.563831130	71.4913888889	42.4256609690
3.	ARECIBO	6376.560245971	66.7530277778	18.2287613852
4.	85JPLVNS	6372.177000000	116.7940075000	35.0665981000
5.	11DSPION*	5206.350322378	116.8497745987	3673.7851760000
6.	12DSECHO*	5212.050800000	-243.1946300000	3665.6468000000
7.	14DSMARS*	5203.997400000	-243.1105900000	3677.0630000000
8.	41DSWOOM*	5450.197800000	-136.8875900000	-3302.3262000000
9.	42DSCANB*	5205.361028200	-148.9809579880	-3674.6129890000
10.	51DSJOHA*	5742.938000000	-27.6854600000	-2768.7193000000
11.	61DSMADR*	4862.604400000	-355.7510900000	4114.8518000000
12.	62DSCEBR*	4860.811400000	-355.6322900000	4116.9660000000
13.	AFLASER*	5391.827000000	110.7244167000	3400.6790000000
14.	6USNAVAL		77.0660375000	
15.	8USNAVAL		77.0655416667	
16.	9USNAVAL		77.0654625000	
17.	MUSNAVAL		77.0655416667	
18.	CAPETOWN		-18.4765833333	
19.	GRENWICH		0.0	
20.	CAMBRIDG		-0.0947916652	
21.	RADCLIFF		1.2516666667	
22.	OTTAWA		75.7164583200	
23.	PARIS		-2.3371249980	
24.	TOULOUSE		-1.4624999600	
25.	NICE		-7.3004166650	
26.	BESANCON		-5.9892499600	
27.	UCCLE		-4.3582083333	
28.	GTOKYO		-139.5407500000	
29.	STRASBRG		-7.7683333333	
30.	BERLIN		-13.1066666667	
31.	EDINBRG		3.1833333333	

*Cylindrical Coordinates [equatorial radius (km), longitude (deg), z(km)] the relevant body-fixed cooordinates were in the set of solved-for parameters. These results will be described in Chapter VII.

The transformation from earth body-fixed coordinates $\underset{\sim}{r}_B$ to inertial coordinates $\underset{\sim}{r}_{50.0}(t)$ is given by

$$\underset{\sim}{r}_{50.0}(t) = \underline{U}\, \underset{\sim}{r}_B$$

where

$$\underline{U} = (\underline{W}\ \underline{F}\ \underline{N}\ \underline{P})^T$$

$$= \underline{P}^T \underline{N}^T \underline{F}^T \underline{W}^T$$

$\underline{W}$, $\underline{F}$, $\underline{N}$, and $\underline{P}$ are matrices described below, and the superscript T denotes transpose. The time t is associated with $\underset{\sim}{r}_{50.0}$ because a constant vector in the (left-handed) body-fixed frame (pole and Greenwich meridian of 1900-05 conventionally is a function of time in the inertial coordinates. P is the precession matrix, transforming from coordinates referred to the earth's mean equator and equinox of 1950.0 to coordinates referred to the mean equator and equinox of date. This matrix will be discussed in more detail below. $\underline{N}$ is the nutation matrix, transforming from coordinates referred to mean equinox and equator of date to coordinates referred to the true equinox and true equator of date:

$$\underline{N} = \begin{bmatrix} 1 & -\Delta\psi \cos \varepsilon & -\Delta\psi \sin \varepsilon \\ \Delta\psi \cos \varepsilon & 1 & -\Delta\varepsilon \\ \Delta\psi \sin \varepsilon & \Delta\varepsilon & 1 \end{bmatrix}$$

where $\Delta\psi$ is the nutation in longitude, $\Delta\varepsilon$ is the nutation in obliquity, and ε is the obliquity of the ecliptic. $\Delta\psi$ and $\Delta\varepsilon$ were taken from series in the Explanatory Supplement. The matrix $\underline{F}$ rotates the coordinates referred to the true equinox and equator of date into the body-fixed frame of date:

$$\underline{F} = \begin{bmatrix} \cos \theta & \sin \theta & 0 \\ -\sin \theta & \cos \theta & 0 \\ 0 & 0 & 1 \end{bmatrix}$$

where θ is the apparent sidereal time.* The wobble matrix $\underline{W}$ transforms from the right-handed body-fixed frame of date to the left-handed frame of 1900-05 by accounting for polar

*Explanatory Supplement, 3B.2

motion:

$$\underline{W} = \begin{bmatrix} 1 & 0 & \lambda \\ 0 & -1 & \mu \\ -\lambda & \mu & 1 \end{bmatrix}$$

where λ and μ are the components of the angular position of the instantaneous pole at the time t in the 1900-05 frame, with λ measured along the meridian toward Greenwich and μ along the meridian 90° to the west of Greenwich.

The precession matrix mentioned above is given by

$$\underline{P} = \begin{bmatrix} \cos\xi_0\cos w\cos z - \sin\xi_0\sin z & -\sin\xi_0\cos w\cos z - \cos\xi_0\sin z & -\sin w\cos z \\ \cos\xi_0\cos w\sin z + \sin\xi_0\cos z & -\sin\xi_0\cos w\sin z + \cos\xi_0\cos z & -\sin w\sin z \\ \cos\xi_0\sin w & -\sin\xi_0\sin w & \cos w \end{bmatrix}$$

in which the angles are

$$\xi_0 = 2304''.948T_{50} + 0''.302T_{50}^2 + 0''.0179T_{50}^3$$

$$z = 2304''.948T_{50} + 1''.093T_{50}^2 + 0''.0192T_{50}^3$$

$$w = 2004''.255T_{50} - 0''.426T_{50}^2 - 0''.0416T_{50}^3$$

where T_{50} is the time t measured in tropical centuries of 36524.21988 days measured from 1950.0 (J.E.D. 2433282.423). These angles have the following significance. Suppose we wish to relate coordinates at some initial epoch t_0 to coordinates at a later epoch t. The angle $90°-\xi_0$ is the right ascension of the ascending node of the equator at t on the initial equator at t_0, measured from the equinox at t_0. The angle $90° + z$ is the right ascension of the node from the equinox at t. The angle w is the inclination of the equator at t with respect to the initial equator at t_0. To make the transformation from the initial system to the final system, we must perform rotations of: $-\xi_0$ about the original polar axis; +w about the new y axis; and -z about the new polar axis. These expressions are due to Simon Newcomb (1895).

B.2 Possible Errors in Observational Coordinate-System Motion

The accuracy of Newcomb's prescription for relating astronomical coordinate systems at different epochs must be very good since no corrections larger than relative motions of approximately one second of arc per century have been found in a variety of investigations [e.g., Fricke, 1967b (FK4 stars); Clemence, 1966 (inner planets)]. We will discuss the numerical values found by Fricke (1967a, 1967b) in Appendix 1. We assume that the observations can be regarded as reduced to a reference frame rotating uniformly with angular velocity $\vec{\omega}$ with respect to the inertial frame. The magnitude of $\vec{\omega}$ is expected to be small ($|\vec{\omega}| < 1''$ century^{-1}) so that the apparent acceleration due to this rotation is a small perturbation. For a planet at a position $\vec{r}_p$ with velocity $\vec{V}_p$, the apparent acceleration is

$$\Delta\vec{a} = 2(\vec{\omega}\times\vec{V}_p) - \vec{\omega}\times(\vec{\omega}\times\vec{r}_p)$$

The system of differential equations for the partial derivatives with respect to the components of $\vec{\omega}$ is needed to solve for these quantities and is quite simple:

$$\frac{d}{dt}\left(\frac{\partial\vec{r}}{\partial\omega_j}\right) = \frac{\partial\vec{V}_p}{\partial\omega_j}$$

$$\frac{d}{dt}\left(\frac{\partial \vec{V}_p}{\partial \omega_j}\right) = -(\hat{U}_j \times \vec{V}_p) - \hat{U}_j \times (\vec{\omega} \times \vec{r}_p) \; - \vec{\omega} \times (\hat{U}_j \times \vec{r}_p)$$

where $\hat{U}_j$ is a unit vector in the j^{th} coordinate axis direction.

The Coriolis term $-2\vec{\omega}\times\vec{V}_p$ will dominate for all bodies in the solar system since $\vec{V}_p >> (\vec{\omega}\times\vec{r}_p)$. We could include this force in the integration of the equations of motion.

A slightly different approach has been used with the computer program, since we wished to avoid integrating the variational equations above. We have approximated the effect of the rotation by multiplying the precession matrix $\underline{P}$ by another matrix $\underline{\Delta}$, where $\underline{\Delta}$ is given by

$$\underline{\Delta} = \begin{bmatrix} 1 & \omega_3 T_{50} & -\omega_2 T_{50} \\ -\omega_3 T_{50} & 1 & \omega_1 T_{50} \\ \omega_2 T_{50} & -\omega_1 T_{50} & 1 \end{bmatrix}$$

so that $\underline{\Delta}$ is orthogonal if we can neglect terms of order $(\omega_i \omega_j)$. To this order, the matrix procedure is equivalent to integrating the equations of motion with the additional acceleration as described above (see Appendix 2).

Some confusion exists in recent literature (Eckert, 1965; Baierlein, 1967) on a point related to the discussion above. The observability of the effect of geodesic precession on the motion of the moon has been questioned, since geodesic precession also affects the rotation of the earth. The algorithm for estimating $\vec{\omega}$ described above answers, in practice, any questions about the effects of observing the moon from a rotating (non-inertial) platform -- the earth. In principle, the geodesic precessional effects on earth rotation and on the motion of the moon can both be measured with respect to inertial space. (As a simple example, consider a synchronous satellite in orbit about the earth. The orbit of the satellite can be accurately determined by comparison with the star background, even through the motion of the satellite relative to the earth observer is very small.) A solution for geodesic precession and $\underline{\Delta}$ together with the associated formal errors will settle the question of observability. With sufficiently accurate data, the effects will both be determinable.

C. Rotation of the Moon

The rotation of the moon about its center of mass is also regarded as perfectly known for the processing of the data types treated in this thesis. The selenocentric coordinate system which we use has its origin at the center of mass of the moon, the z-axis along the axis of rotation of the moon, the x-axis in the mean direction of the earth, and the y-axis completing the right-hand system. We assume that these coordinate axes are also principal axes of inertia. Now let $\utilde{R}$ be the coordinates of the center of mass of the moon relative to the center of mass of the earth in the inertial coordinates in which we integrate the equations of motion. Let $\utilde{r}$ be the coordinates of the center of mass of the earth relative to the center of mass of the moon in the selenocentric system described above. Then the desired relationship for describing the rotation of the moon is given by

$$\utilde{r} = - \underline{B}\ \utilde{R}$$

where $\underline{B}$ is the orthogonal matrix formed from

$$\underline{B} = \underline{\Sigma}\ \underline{V}\ \underline{P}$$

in which $\underline{P}$ is the precession matrix, with $\underline{V}$ given by

$$\underline{V} \equiv \begin{bmatrix} 1 & 0 & 0 \\ 0 & \cos\,\varepsilon_0 & \sin\,\varepsilon_0 \\ 0 & -\sin\,\varepsilon_0 & \cos\,\varepsilon_0 \end{bmatrix}$$

where ε_0 is the obliquity at 1950.0, and with $\underline{\Sigma}$ having elements

$$\Sigma_{11} = \cos\psi\,\cos\phi - \sin\psi\,\sin\phi\,\cos\theta$$

$$\Sigma_{12} = \sin\psi\,\cos\phi + \cos\psi\,\sin\phi\,\cos\theta$$

$$\Sigma_{13} = -\sin\phi\,\sin\theta$$

$$\Sigma_{21} = -\cos\psi\,\sin\phi - \sin\psi\,\cos\phi\,\cos\theta$$

$$\Sigma_{22} = -\sin\psi\,\sin\phi + \cos\psi\,\cos\phi\,\cos\theta$$

$$\Sigma_{23} = -\cos\phi\,\sin\theta$$

$$\Sigma_{31} = -\sin\psi\,\sin\theta$$

$$\Sigma_{32} = \cos\psi\,\sin\theta$$

$$\Sigma_{33} = \cos\theta$$

(See M.E. Ash [1965a], Appendix B). This particular combination of matrices is only chosen for convenience. The precession matrix, for example, appears only because the angles in $\underline{\Sigma}$ are referred to the coordinates of date.

The angles used to express the elements of Σ can be defined as follows. Let ☾ be the mean longitude of the Moon, measured in the ecliptic from the mean equinox of date to the mean ascending node of the lunar orbit and then along the orbit. Let Ω be the longitude of the mean ascending node of the lunar orbit on the ecliptic measured from the mean equinox of date. Finally, let I be the inclination of the mean lunar equator to the ecliptic. Then the angles ψ, θ, ϕ are (Koziel, 1962)

$$\psi = \Omega + \sigma$$

$$\theta = I + \rho$$

$$\phi = 180^\circ + (☾ - \Omega) + (\tau - \sigma)$$

where σ, ρ and τ are the physical librations in node, inclination, and longitude, respectively.

We now determine the quantities on the right hand side of First, the inclination of the mean lunar equator on the ecliptic is (Koziel, 1962)

$$I = 1°32'20'' = 1\overset{\circ}{.}53889$$

$$= 0.0268587 \text{ radian}$$

Next, according to the Explanatory Supplement, p. 107, we have

$$\Omega = 259\overset{\circ}{.}183275 - 0\overset{\circ}{.}052953922d$$

$$+ 1\overset{\circ}{.}557 \times 10^{-12}d^2 + 5\overset{\circ}{.}0 \times 10^{-20}d^3$$

$$☾ - \Omega = 11\overset{\circ}{.}250889 + 13\overset{\circ}{.}2293504490d$$

$$-2\overset{\circ}{.}407 \times 10^{-12}d^2 - 1\overset{\circ}{.}1 \times 10^{-20}d^3$$

where d is the number of days that have elapsed from J.E.D. 2415020.0. Finally, the physical libration of the Moon is given by Koziel as

$$\tau = -12\overset{''}{.}9 \sin \ell - 0\overset{''}{.}3 \sin 2\ell + 65\overset{''}{.}2 \sin \ell'$$

$$+9\overset{''}{.}7 \sin (2F-2\ell) + 1\overset{''}{.}4 \sin (2F-2D) + 2\overset{''}{.}5 \sin (D-\ell)$$

$$-0\overset{''}{.}6 \sin (2D-2\ell+\ell') - 7\overset{''}{.}3 \sin (2D-2\ell)$$

$$-3\overset{''}{.}0 \sin (2D-\ell) - 0\overset{''}{.}4 \sin 2D + 7\overset{''}{.}6 \sin \Omega;$$

$$\rho = -106'' \cos \ell + 35''\cos(2F-\ell) - 11''\cos 2F$$

$$-3''\cos(2F-2D) - 2''\cos(2D-\ell) \;;$$

$$I(\tau-\sigma) = 108''\sin \ell - 35''\sin(2F-\ell) + 11''\sin 2F$$

$$+3''\sin(2F-2D) + 2''\sin(2D-\ell)$$

where I is measured in radians, and where the arguments ℓ, ℓ', F and D are given in the Explanatory Supplement as functions of time. The relations between the arguments ℓ, ℓ', F and D, and the arguments g, g', ω and ω' of Koziel are given by

$$\ell = g \qquad\qquad g = \ell$$

$$\ell' = g' \qquad\qquad g' = \ell'$$

$$D = g' - g' + \omega - \omega' \qquad\qquad \omega = F - \ell$$

$$F = g + \omega \qquad\qquad \omega' = F - D - \ell'$$

The subsequent revision by Koziel (1967) of his results, and further work on the physical libration by D. Eckhardt (1970) have been examined in the context of our types of observations.

These newer results are found to have negligible effect on τ, ρ, and σ for the data in this thesis. The lunar laser ranging data, of course, necessitate the incorporation of an improved libration model.

D. Equations of Motion

D.1 Newtonian terms

D.1.a. Definitions and Notation

The basic equations for the motion of the moon about the earth in inertial coordinates are dominated by the Newtonian centers of mass interactions with the earth and sun. Smaller perturbing forces are due to the Newtonian centers of mass interactions with the other 8 planets. Still other perturbing forces are designated as $\vec{F}_E$ and $\vec{F}_M$ acting on the earth and moon, respectively.

Let the subscript E denote the earth, M the moon, and j(j=1,2,...8) the j^{th} perturbing planet. The vector positions of the earth relative to the sun are given by $\vec{X}_E$. The coordinates of the moon relative to the sun are $\vec{X}_M$, and the coordinates of the j^{th} planet relative to the sun are $\vec{X}_j$. Further we define

$$\vec{X}_{ME} \equiv \vec{X}_M - \vec{X}_E \qquad \vec{X}_{jM} \equiv \vec{X}_j - \vec{X}_M$$

$$\vec{X}_{jE} \equiv \vec{X}_j - \vec{X}_E$$

$$r_E \equiv |\vec{X}_E|$$

$$r_{ME} \equiv |\vec{X}_{ME}|$$

$$r_{jE} \equiv |\vec{X}_{jE}| \qquad , \text{ etc.}$$

The mass of the earth is M_E, the moon's mass is M_M, and M_j the mass of the j^{th} perturbing planet. Newton's laws of motion and gravity then give

$$\frac{d^2\vec{X}_E}{dt^2} = -GM_\odot \frac{\vec{X}_E}{r_E^3} + GM_M \frac{\vec{X}_{ME}}{r_{ME}^3} + G\sum_{j=1}^{8} (M_j \frac{\vec{X}_{jE}}{r_{jE}^3}) + \frac{1}{M_E}\vec{F}_E$$

$$\frac{d^2\vec{X}_M}{dt^2} = -GM_\odot \frac{\vec{X}_M}{r_M^3} - GM_E \frac{\vec{X}_{ME}}{r_{ME}^3} + G\sum_{n=1}^{8} (M_j \frac{\vec{X}_{jM}}{r_{jM}^3}) + \frac{1}{M_M}\vec{F}_M$$

The equations of motion for $\vec{X}_{ME}$ are obtained by subtraction:

$$\frac{d^2\vec{X}_{ME}}{dt^2} = -GM_\odot \frac{(M_E+M_M)}{M_\odot} \frac{\vec{X}_{ME}}{r_{ME}^3} + \vec{D} + \vec{P} + (\frac{1}{M_M}\vec{F}_M - \frac{1}{M_E}\vec{F}_E)$$

where

- $$\vec{D} = GM_\odot (\frac{\vec{X}_E}{r_E^3} - \frac{\vec{X}_M}{r_M^3})$$

$$\vec{P} = GM_{\odot}\left[\sum_{\substack{j=1\\ j\neq 3}}^{9} \frac{M_j}{M_{\odot}} \left(\frac{\vec{X}_{jM}}{r_{jM}^3} - \frac{\vec{X}_{jE}}{r_{jE}^3}\right)\right]$$

Table 3 lists the masses used in this expression for the numerical integrations. The positions of the planets were obtained from ephemerides supplied on magnetic tape by M.E. Ash (private communication).

The additional effects represented by inclusion of the term $(\frac{1}{M_M}\vec{F}_M - \frac{1}{M_E}\vec{F}_E)$ are:

$\vec{Q}$ - the acceleration due to the harmonics higher than the central force term in the expansion of the earth's gravitational potential

$\vec{H}$ - the acceleration due to higher harmonics in the moon's gravitational potential

$\vec{R}$ - the acceleration due to general relativistic effects

$\vec{T}$ - acceleration due to tidal friction in the earth-moon system

$\vec{V}$ - acceleration due to a time variation in the gravitational constant G.

Table 3

Reciprocal Planetary Masses as Used in

Moon Numerical Integrations

(Not all digits are significant)

PLANET	$\left(\frac{M_\odot}{M_{planet}}\right)$
Mercury	6,031,916.0
Venus	408,522.0
Earth + Moon	328,900.1
Mars	3,098,700.0
Jupiter	1,047.4
Saturn	3,499.0
Uranus	22,900.0
Neptune	19,400.0
Pluto	4,000,000.0
$\frac{\text{Mass of Earth+Moon}}{\text{Mass of Moon}}$	82.301

The well known accelerations $\vec{Q}$ and $\vec{H}$ will be discussed first.

D.1.b Harmonics of the Earth's Gravitational Potential

The gravitational potential U of the earth can be expanded in spherical harmonics as

$$U(r,\phi,\lambda) = -\frac{GM_E}{r}\left[1 - \sum_{n=2}^{\infty} J_n \left(\frac{a_E}{r}\right)^n P_n(\sin\phi)\right.$$

$$\left. + \sum_{\ell=2}^{\infty} \sum_{m=1}^{\ell} \left(\frac{a_E}{r}\right)^n P_{\ell m}(\sin\phi)\{c_{\ell m}\cos m\lambda + s_{\ell m}\sin m\lambda\}\right]$$

where r is the distance from the center of mass of the earth; ϕ,λ are the geocentric latitude and longitude, a_E is the equatorial radius of the earth, and the Legendre functions are those given by, e.g., Hildebrand (1948) as

$$P_n(z) = \frac{1}{2^n n!}\frac{d^n}{dz^n}(z^2-1)^n \; ; \qquad n = 0,1,2,\ldots$$

$$P_{n\ell}(z) = (1-z^2)^{\ell/2}\frac{d^\ell P_n(z)}{dz^\ell} \; ; \quad \ell = 0,1,2,\ldots n$$

The earth rotates on its axis in ~24 hours. Compared with the $\sim 27\frac{1}{3}$ day period of the moon, the temporal variation of the earth's field is very rapid (as viewed from inertial space). Therefore let us average the potential over the longitude λ, as follows

$$\hat{U}(r,\phi) \equiv \frac{1}{2\pi}\int_0^{2\pi} U(r,\phi,\lambda)\,d\lambda$$

We see immediately that the double summation term vanishes, and we are left with

$$\hat{U}(r,\phi) = -\frac{GM_E}{r} + \frac{GM_E}{r}\sum_{n=2}^{\infty} J_n\left(\frac{a_E}{r}\right)^n P_n(\sin\phi)$$

The first term is the center of mass potential, which we must exclude to find the perturbation.

We can relate the geocentric coordinates r,ϕ to the inertial coordinates using the matrices from Section II.C.1. Let us first construct rectangular geocentric coordinates. The z'-axis by definition is normal to the true equator of date; since we have averaged over λ, we are free to choose the x'-axis along the true equinox of date:

$$x' = r\cos\phi\cos\lambda'$$

$$y' = r\cos\phi\sin\lambda'$$

$$z' = r\sin\phi$$

where $\underset{\sim}{\lambda}'$ is "longitude" from the equinox of date. Let $\underset{\sim}{G}$ be a position vector in a geocentric coordinate system with axis directions parallel to the axis directions of the inertial coordinate system. Then $\underset{\sim}{E} = (x',y',z')$ and $\underset{\sim}{G}$ describe the same point if they are related by

$$\underset{\sim}{E} = \underline{N}\ \underline{P}\ \underset{\sim}{G} \equiv \underline{A}\ \underset{\sim}{G}$$

where the nutation matrix $\underline{N}$ and the precession matrix $\underline{P}$ were described above.

Suppose the moon were located at $\underset{\sim}{G} = \underset{\sim}{X}_{ME}$ in inertial coordinates ($r = r_{ME} = |\underset{\sim}{G}|$). Then

$$\frac{z'}{r} = \sin\phi_M = \frac{1}{r_{ME}} \sum_{\ell=1}^{3} A_{3\ell} (\underset{\sim}{X}_{ME})_\ell$$

We are now in a position to calculate $\vec{Q}$. The force on the moon due to the earth's potential is

$$\vec{F}_M = -M_M \vec{\nabla}_G \hat{U}$$

The force exerted on the earth by the moon is the negative of the force exerted by the earth on the moon. We can compute (from these forces) the perturbing acceleration

$$\vec{Q} = \frac{1}{M_M} \vec{F}_M - \frac{1}{M_E} \vec{F}_E$$

The explicit expression for $\vec{Q}$ is given below after a brief discussion of an approximation made as follows.

In the programming of $\vec{Q}$, the summation in the potential has been terminated at n = 3. To estimate the effects of neglecting J_4, the secular rates of change of the osculating orbital elements can be calculated from Lagrange's planetary equations. Using Groves' (1960) results for the effects of zonal gravitational harmonics, and a value for $J_4 = -1.6 \times 10^{-6}$, we find that the only secular changes are in the ascending node Ω, the perigee ω, and the mean anomaly ℓ_0 at the epoch t_0

Ω: 5×10^{-4} "/century

ω: -4.6×10^{-4} "/century

ℓ_0: -2×10^{-7} "/century

The rate of change of the semi-major axis truly vanishes. The variation in eccentricity is proportional to sin 2ω, with amplitude of $\overline{\dot{e}/e}$ smaller than $(\frac{\dot{\Omega}}{e})$ by $\sin^2 i$. The inclination variation is also proportional to sin 2ω, and is smaller by $e^2 \sin i$. These changes appear to be completely unobservable. The expression for $\vec{Q}$ that is programmed is therefore

$$\vec{Q} = \frac{GM_{\odot}}{r_{ME}^2} \frac{(M_E+M_M)}{M_{\odot}} \{(\frac{a_E}{r_{ME}})^2 J_2[\frac{\vec{X}_{ME}}{r_{ME}} (\frac{15}{2} \sin^2\phi_M - \frac{3}{2}) - 3\vec{A}_3 \sin\phi_M]$$

$$+(\frac{a_E}{r_{ME}})^3 J_3[\frac{\vec{X}_{ME}}{r_{ME}} (\frac{35}{2} \sin^3\phi_M - \frac{15}{2} \sin\phi_M)$$

$$-\vec{\underset{\sim}{A}}_3(\frac{15}{2} \sin^2\phi_M - \frac{3}{2})]\}$$

where

$$\underset{\sim}{A}_3 = [(\underline{A})_{31}, (\underline{A})_{32}, (\underline{A})_{33}]$$

The values used for J_2 and J_3 were obtained from earth satellite observations. They are (Kozai, 1969)

$$J_2 = 1.082639 \times 10^{-3}$$

$$J_3 = -2.565 \times 10^{-6}$$

with

$$a_E = 6378.166 \text{ meters}$$

and

$$GM_E = 3.986011765 \times 10^5 \text{ km}^3/\text{sec.}$$

D.1.c Interaction of the Moon's Nonspherical Gravitational Potential with the Earth

Let $\vec{L}$ be the force on the center of mass of the earth due to the moon's gravitational potential. The center of mass of the earth, in selenocentric coordinates, is located at

$$\underset{\sim}{X} = -\underline{B}\, \underset{\sim}{X}_{ME}$$

where $\underset{\sim}{X}_{ME}$ is the position of the center of mass of the moon relative to the center of mass of the earth in our inertial coordinate system used in the numerical integration, and $\underline{B}$ is the orthogonal matrix defined, along with our selenocentric coordinates, in Chapter II, Section C. Let U be the gravitational potential of the moon, found by integration of the potential due to the mass elements $d\mu(\vec{x}')$ located at selenocentric positions $\vec{x}'$. Then we have

$$U(x,y,z) = \iiint_{\text{vol. of moon}} \frac{d\mu(x')}{[(x-x')^2+(y-y')^2+(z-z')^2]^{1/2}}$$

The force on the center of mass of the earth is

$$\vec{L} = -M_E \vec{\nabla} U$$

where M_E is the mass of the earth.

The potential U can be expanded in spherical harmonics as follows

$$U(r,\theta,L) = -\frac{GM_M}{r_{ME}}\left[1-\sum_{n=2}^{\infty}\sum_{m=0}^{n}\left\{\left(\frac{R_m}{r_{ME}}\right)^n P_{nm}(\cos\theta) f_{nm}(L)\right\}\right]$$

where

$$f_{nm}(L) = c_{nm}\cos(mL) + s_{nm}\sin(mL)$$

where M_M is the mass of the moon, R_m is the mean radius of the moon, r_{ME} is the radial separation between the centers of mass, and (θ,L) describe the angular location of the center of mass of the earth in selenocentric coordinates:

$$\sin\theta\cos L = -\sum_{\ell=1}^{3} \underset{\sim}{B}_{1\ell}\frac{(\underset{\sim}{X}_{ME})_\ell}{r_{ME}}$$

$$\sin\theta\sin L = -\sum_{\ell=1}^{3} \underset{\sim}{B}_{2\ell}\frac{(\underset{\sim}{X}_{ME})_\ell}{r_{ME}}$$

$$\cos\theta = -\sum_{\ell=1}^{3} \underset{\sim}{B}_{3\ell}\frac{(\underset{\sim}{X}_{ME})_\ell}{r_{ME}}$$

In our numerical integrations, we have included only terms through n=2 in the potential. The effects of the third order terms are approximately one-third of the direct effect due to the fourth harmonic in the earth's gravitational field, which was shown to be ignorable in the preceeding section. The resulting potential can be simplified further by using the assumption that the axes of our selenocentric system coincide with the principal axes of inertia, that is

$$c_{21} = \frac{I_{xz}}{M_M R_m^2} = 0$$

$$s_{21} = \frac{I_{yz}}{M_M R_m^2} = 0$$

$$s_{22} = \frac{I_{xy}}{M_M R_m^2} = 0$$

We make use of the relationships:

$$c_{20} = -\frac{1}{M_M R_m^2} [I_{zz} - \frac{(I_{xx}+I_{yy})}{2}]$$

$$c_{22} = \frac{1}{4M_M R_m^2} [I_{yy}-I_{xx}]$$

to express our results in terms of the moments of inertia. The force on the moon is minus the force on the earth, so dividing by the masses and subtracting the accelerations gives the acceleration of the moon relative to the earth:

$$\vec{H} = GM_{\odot} \frac{(M_E+M_M)}{r_{ME}^2 M_{\odot}} \left(\frac{R_m}{r_{ME}}\right)^2 \left\{\frac{(I_{yy}-I_{xx})}{M_m R_m^2} \left[\frac{\vec{X}_{ME}}{r_{ME}} \left(\frac{15}{2} D_2^2-\frac{3}{2}\right)-3D_2\vec{B}_2\right]\right.$$

$$\left. + \frac{(I_{zz}-I_{xx})}{M_m R_m^2} \left[\frac{\vec{X}_{ME}}{r_{ME}} \left(\frac{15}{2} D_3^2 - \frac{3}{2}\right)-3D_3\vec{B}_3\right]\right\}$$

where

$$D_j = \sum_{\ell=1}^{3} (\underline{B})_{j\ell} (\underset{\sim}{X}_{ME})_{\ell}$$

$$\underset{\sim}{B}_i = \{\underline{B}_{i1}, \underline{B}_{i2}, \underline{B}_{i3}\}$$

(See M.E. Ash (1965a) for a more complete derivation.)

An important restriction on the parameters GM_M and R_m should be recognized in connection with the values of c_{20} and c_{22}. The value of R_m is conventional; that is, a value is assumed and must always be used in formulae such as above in connection with the related values of c_{20} and c_{22}. The value of GM_M was solved for from the Lunar Orbiter data; the value appropriate to the values for c_{20} and c_{22} below is 4902.87 km^3/sec (with the value for c fixed at 299792.5 km/sec). The appropriate value of R_m is 1738 km. One must not treat GM_M + R_M as variables for any partial derivatives that might be taken. GM_M, of course, can still be estimated from the center of mass effects.

The values for c_{20} and c_{22} used in the numerical integration were average values from analyses of Lunar Orbiter data (Michael _et al._, 1969; Lorell, 1970; Laing and Liu, 1971). They were

$$c_{20} = -2.022 \times 10^{-4}$$

$$c_{22} = 2.286 \times 10^{-5}$$

The uncertainties in these numbers and their effect on our results will be discussed below. The values for the other second-degree coefficients give information about the relationship between the principal axes of inertia and the body axes of the moon. Forming and diagonalizing the inertia matrix constructed from the second-degree coefficients and using an assumed value of $(I_{zz}-I_{xx})/I_{zz} = 6.29 \times 10^{-4}$, Michael _et al._ (1969) find that the principal axes are displaced by less than two degrees from the body axes. This result gives credibility to the assumption that the two sets of axes coincide.

How do uncertainties in these values of the 2nd harmonics affect the secular motions of the node ($d\Omega_{☾}$) and perigee ($d\pi_{☾}$)? From the equations given by Eckert (1965), we can calculate the following sensitivities to $\Delta(d\Omega_{☾})$ and $\Delta(d\pi_{☾})$ about our nominal values:

$$\Delta(d\Omega_{☾}) = (6.95\times10^{4}\ \Delta c_{20}$$

$$-1.39\times10^{5}\ \Delta c_{22})\ \frac{\text{sec of arc}}{\text{century}}$$

with

$$d\Omega_{☾} = -17''.3\ \text{century}^{-1}$$

for the values of c_{20} and c_{22} given above, and

$$\Delta(d\pi_{☾}) = (-0.39\times10^{4}\ \Delta c_{20}$$

$$+0.41\times10^{5}\ \Delta c_{22})\ \frac{\text{sec of arc}}{\text{century}}$$

with

$$d\pi_{☾} = 1''.7 \text{ century}^{-1}$$

From the formal errors of the various solutions, reasonable uncertainties appear to be

$$\Delta c_{20} \approx \Delta c_{22} \approx 3 \times 10^{-6}$$

These values yield (worst case) uncertainties of 0''.5 century^{-1} in $d\Omega_{☾}$ and 0''.1 century^{-1} in $d\pi_{☾}$, compared with the relativistic effect of 2"/century. In retrospect, the partial derivatives for these quantites probably should have been integrated. These partials could be produced, and the differential adjustments due to refinements of values for c_{20} and c_{22} could then be made to the position and velocities. Another possibility would be to reintegrate with improved values for c_{20} and c_{22}, then to recompute the theoretical values and solve for a new consistent set of initial conditions from the new normal equations. Of course, a better, but currently impractical, method would be to process Lunar Orbiter data simultaneously with our data set in order to solve for the moon's gravitational potential. The effect of the uncertainty in these harmonic coefficients on our results could be at the level of 10 - 20% of the geodesic precession. We will return to the uncertainties in c_{20} and c_{22} at an appropriate place in discussing the final conclusions.

D.2 General Relativistic Corrections

The additional perturbing force on the moon $\vec{R}$ due to effects of general relativity is computed via the post-Newtonian approximation. All formulae in this discussion follow the development and notation of Weinberg (1972), Chapter 9. In harmonic coordinates the appropriate line element is

$$ds^2 = g_{00}dt^2 - 2g_{i0}dx^i dt - g_{ij}dx^i dx^j$$

where the components of the metric tensor are

$$g_{00} = -1-2(\phi+\psi)-2\phi^2-2\psi$$

$$g_{ij} = \delta_{ij}-2\phi\delta_{ij}$$

$$g_{i0} = \xi_i$$

In the above equations, ϕ, ψ, and $\vec{\xi}$ are potentials derived from the energy-momentum tensor $T^{\mu\nu}$:

$$\phi(\vec{x},t) = -G\iiint d^3\vec{x}' \frac{\overset{0}{T}{}^{00}(\vec{x}',t)}{|\vec{x}-\vec{x}'|}$$

$$\psi(\vec{x},t) = -G\iiint \frac{d^3x'}{|\vec{x}-\vec{x}'|} \Big[\overset{2}{T}{}^{00}(\vec{x}',t)+\overset{2}{T}{}^{ii}(\vec{x}',t)$$

$$+ \frac{1}{4\pi G} \frac{\partial^2\phi(\vec{x}',t)}{\partial t^2}\Big]$$

$$\vec{\xi} = -4G\iiint \frac{d^3\vec{x}'}{|\vec{x}-\vec{x}'|} \overset{1}{T}{}^{i0}(\vec{x}',t)$$

For a collection of mass points m_n, with coordinate position $\vec{x}_n$ and velocities $\vec{V}_n(t)$, the elements of the energy momentum tensor are

$$\overset{0}{T}{}^{00} = \sum_n m_n \delta^3(\vec{x}-\vec{x}_n)$$

$$\overset{2}{T}{}^{00} = \sum_n m_n[\phi(\vec{x}_n) + \frac{1}{2}\vec{v}_n^{\,2}]\delta^3(\vec{x}-\vec{x}_n)$$

$$\overset{1}{T}{}^{i0} = \sum_n m_n v_n^i \delta^3(\vec{x}-\vec{x}_n)$$

$$\overset{2}{T}{}^{ii} = \sum_n m_n v_n^i v_n^i \delta^3(\vec{x}-\vec{x}_n)$$

where the notation $\overset{n}{T}$ is explained in Appendix 3.

The equation of motion for a particle in this gravitational field is

$$\frac{d\vec{v}}{dt} = -\vec{\nabla}(\phi+2\phi^2+\psi) - \frac{\partial\vec{\xi}}{\partial t} + 3\vec{v}\ \frac{\partial\phi}{\partial t} + \vec{v}\times(\vec{\nabla}\times\vec{\xi}) + 4\vec{v}\ (\vec{v}\cdot\vec{\nabla})\,\phi - \vec{v}^{\,2}\vec{\nabla}\phi$$

Coordinate time t and proper time τ are related by

$$\frac{d\tau}{dt} = 1 + \phi - \frac{1}{2}\vec{v}^{\,2} - \frac{1}{8}(2\phi-\vec{v}^{\,2})^2 + \phi^2 + \psi - \vec{\xi}\cdot\vec{v} + \phi\vec{v}^{\,2}$$

We will express the equation of motion in terms of the quantities defined in Section II.D and the definitions

$$\vec{V}_M \equiv \frac{d\vec{X}_M}{dt} \qquad \vec{V}_E \equiv \frac{d\vec{X}_E}{dt} \qquad \vec{V}_{ME} \equiv \frac{d\vec{X}_{ME}}{dt}$$

$\vec{x}_n$ takes on values $\vec{X}_M$ and $\vec{X}_E$; $\vec{v}_n$ equals $\vec{V}_M$ or $\vec{V}_E$.

By excluding the term $-\nabla\phi$ since we are interested only in the relativistic perturbation, we compute the accelerations

$d^2\vec{X}_M/dt^2$ and $d^2\vec{X}_E/dt^2$. Subtracting, we find

$$\vec{R} = \left.\frac{d^2\vec{X}_{ME}}{dt^2}\right|_{rel} = GM_\odot [\frac{\vec{X}_M}{r_M^3} f_1 - \frac{\vec{X}_E}{r_E^3} f_2 - \frac{\vec{X}_{ME}}{r_{ME}^3} f_3$$

$$+ \frac{\vec{V}_M}{c} \frac{1}{r_M^2} f_4 - \frac{\vec{V}_E}{c} \frac{1}{r_E^2} f_5]$$

where

$$f_1 = \frac{4GM_\odot + GM_M}{r_M c^2} + \frac{4GM_E + \frac{7}{2} GM_M}{r_{ME} c^2} + \frac{GM_E}{r_E c^2} - \frac{\vec{V}_M^2}{c^2}$$

$$f_2 = \frac{4GM_\odot + GM_E}{r_E c^2} + \frac{4GM_M + \frac{7}{2} GM_E}{r_{ME} c^2} + \frac{GM_M}{r_M c^2} - \frac{\vec{V}_E^2}{c^2}$$

$$f_3 = 2(2\frac{M_E}{M_\odot} + \frac{M_M}{M_\odot})(\frac{2GM_M + GM_E}{r_{ME} c^2}) + \frac{4GM_E + GM_M}{r_M c^2} + \frac{4GM_M + GM_E}{r_E c^2}$$

$$- (2\frac{M_E}{M_\odot} + \frac{M_M}{M_\odot}) \frac{\vec{V}_E^2}{c^2} - (2\frac{M_M}{M_\odot} + \frac{M_E}{M_\odot}) \frac{\vec{V}_M^2}{c^2} + 4(\frac{M_E}{M_\odot} + \frac{M_M}{M_\odot}) \frac{\vec{V}_E \cdot \vec{V}_M}{c^2}$$

$$+\ \frac{3}{2}\ \left(\frac{M_E}{M_\odot}\right)\ \frac{(\vec{V}_E\cdot\vec{X}_{ME})^2}{c^2 r_{ME}^2}\ +\ \frac{3}{2}\ \frac{M_M}{M_\odot}\ \frac{(\vec{V}_M\cdot\vec{X}_{ME})^2}{c^2 r_{ME}^2}$$

$$-\ \frac{1}{2}\ GM_E\ \frac{(\vec{X}_{ME}\cdot\vec{X}_E)}{r_E^3\ c^2}\ +\ \frac{1}{2}\ \frac{GM_M(\vec{X}_{ME}\cdot\vec{X}_M)}{r_M^3\ c^2}$$

$$f_4\ =\ \frac{4\vec{X}_M\cdot\vec{V}_M}{r_M c}\ +\left(\frac{r_M}{r_{ME}}\right)^2\left(4\ \frac{M_E}{M_\odot}\ +\ 3\frac{M_M}{M_\odot}\right)\left(\frac{\vec{V}_M}{c}\cdot\ \frac{\vec{X}_{ME}}{r_{ME}}\ \right)$$

$$-\ \left(3\ \frac{M_E}{M_\odot}\ +\ \frac{4M_M}{M_\odot}\right)\left(\frac{r_M}{r_{ME}}\right)^2\left(\frac{\vec{V}_E}{c}\right)\cdot\left(\frac{\vec{X}_{ME}}{r_{ME}}\ \right)$$

$$f_5\ =\ 4\left(\frac{\vec{X}_E}{r_E}\cdot\ \frac{\vec{V}_E}{c}\right)\ +\ \left(4\frac{M_E}{M_\odot}\ +\ 3\frac{M_M}{M_\odot}\right)\left(\frac{r_E}{r_{ME}}\right)^2\left(\frac{\vec{X}_{ME}}{r_{ME}}\right)\cdot\ \frac{\vec{V}_M}{c}$$

$$-\ \left(3\frac{M_E}{M_\odot}\ +\ 4\frac{M_M}{M_\odot}\right)\left(\frac{r_E}{r_{ME}}\right)^2\left(\frac{\vec{X}_{ME}}{r_{ME}}\right)\cdot\ \frac{\vec{V}_E}{c}$$

Note that all factors of G and c are explicitly present above, and that the f_i are dimensionless. [See Tausner (1966) for a derivation of the equations of motion from a Lagrangian point of view.]

This acceleration has been implemented in the program with an adjustable constant λ multiplying it. Thus, $\lambda = 0$ corresponds to pure Newtonian interaction and $\lambda = 1$ implies general relativity is correct.* The partial $\partial\vec{R}/\partial\lambda$ is simply the equation for $\vec{R}$ above.

The addition of this force to the central force will produce an evolution in time of the osculating orbital

---

*Determining the parameter λ is equivalent [Weinberg, 1972] to determining the combination $\frac{2+2\gamma-\beta}{3}$ where γ and β are parameters in the Eddington-Robertson harmonic coordinate metric

$$ds^2 = [1 - \frac{2MG}{R}\alpha + (\gamma - 1 + 2\beta)\frac{M^2G^2}{R^2} + \dots]\,dt^2$$

$$- [1 + (3\gamma - \alpha)\frac{MG}{R} + \dots]\,d\underset{\sim}{x}^2$$

$$- [(\alpha - \gamma)\frac{MG}{R} + \dots](\underset{\sim}{x}\cdot d\underset{\sim}{x})^2/R^2$$

where $\alpha = 1$ by definition of mass.

elements. In order to verify the proper coding of these equations in PEP, the following procedure was adopted. An integration of the moon's orbit was carried out with no forces acting between the earth and moon except for the central force and general relativity. For comparison, an integration with only the central forces was done. The positions and velocities were converted to osculating elliptic elements. The differences from the values of the elements at epoch were then found by subtraction. These differences for the central force only are plotted in Figure 2. The oscillations and secular trends in this figure are due solely to the build-up of error terms in the numerical integration which was done with a step size of 1/4 day (as opposed to the actual ephemeris calculations which were with a step size of 1/8 day).

The behavior of the differences of the orbital elements from those at epoch for general relativity is shown in Figure 3. For our data set, the observable effect caused by this force is a rotation of the moon's orbit with respect to inertial space. The orbital angular momentum is shown in Appendix 3 to precess with angular velocity

$$\vec{\Xi} = -\frac{1}{2}\vec{\nabla}\times\vec{\xi} - \frac{3}{2}\vec{V}\times\vec{\nabla}\phi$$

The major possible contributions are from

$$\phi_{\odot} = -\frac{GM_{\odot}}{r_M}$$

$$\phi_{\oplus} = -\frac{GM_E}{r_{ME}}$$

$$\vec{\xi}_{\oplus} = \frac{2G}{r_{ME}^3}(\vec{X}_{ME} \times J_{\oplus})$$

$$\vec{\xi}_{\odot} = \frac{2G}{r_M^3}(\vec{X}_M \times J_{\odot})$$

where

$$(J_K)_{\odot,\oplus} = \int d^3\vec{x}'\, \varepsilon_{ijk} x^i_{\odot,\oplus}\, T^{j0}_{\odot,\oplus}$$

[See Appendix 3]. The precession angular velocity is therefore given with sufficient accuracy by

$$\vec{\Xi} = 3GM_{\odot}\frac{(\vec{x}_M \times \vec{V}_M)}{2r_M^3} + 3GM_E\frac{(\vec{x}_{ME} \times \vec{V}_{ME})}{2r_{ME}^3} + 3G\frac{\vec{x}_{ME}(\vec{x}_{ME} \cdot J_{\oplus})}{r_{ME}^3} - \frac{G\vec{J}_{\oplus}}{r_{ME}^3}$$

$$+ 3G\vec{x}_M\frac{(\vec{x}_M \cdot \vec{J}_{\odot})}{r_M^5} - \frac{G\vec{J}_{\odot}}{r_M^3}$$

For the moon's orbit, only the first term is greater than a few hundredths of a second of arc per century. This term, the <u>geodesic</u> precession, is approximately 2 seconds of arc per century.* The geodesic term was first discussed by De Sitter (1916).

Let us compute more exactly the magnitude of this term. The moon moves about the sun in the orbit of the earth-moon barycenter if we average over times of about a month. The earth-moon barycenter orbit is approximately elliptical and can be described by the standard formula

$$r_B = \frac{L}{1+e\cos(\theta-\theta_0)}$$

where L is the semi-latus-rectum and e the eccentricity. The value of $\vec{X}_M \times \vec{V}_M$ is of magnitude $\sqrt{LM_\odot G}$. The result for $\vec{\Xi}$ is found to satisfy

$$|\bar{\vec{\Xi}}| \simeq \frac{3GM_\odot \sqrt{M_\odot G}\,\sqrt{a}\,\sqrt{1-e^2}\,[1-e\cos(\theta-\theta_0)]^3}{2a^3(1-e^2)^3}$$

$$\simeq 1''94\ [1-3e\cos(\theta-\theta_0)] \text{ per century}$$

where $\bar{\Xi}$ signifies an average over a time scale shorter than about a month.

*The analogue of the advance of a planet's perihelion (~43"/century for Mercury) -- one of the classical tests of general relativity -- is quite negligible for the moon moving about the earth: 0''06 per century.

Examining the graph in Figure 3 for the evolution of the right ascension of the ascending node of the lunar orbit on the ecliptic we see small monthly oscillations, an annual oscillation of amplitude $\sim 0''.1$/century, and a secular trend of $1''.94$/century as expected. Reliably verifying this secular contribution in the observations of the moon would constitute a verification of the predictions of equation 5 in Appendix 3, and is one of the goals of this thesis.

We now come to the formulation of the more controversial forces in the earth-moon system: tidal friction and the effect of a time-varying gravitational constant.

D.3.a. Effects of Tidal Friction on the Moon

A quadratic term in time in the mean longitude of the moon -- unaccounted for in any purely gravitational theory -- was found first by Halley soon after Newton developed his lunar theory. The value for the amplitude of this term that is incorporated into the national ephemerides was derived by Spencer Jones (1932). Although the formal error found by Spencer Jones is small, recent treatment by Van Flandern (1970) of stellar occultations by the moon have increased the suspicion of many workers that a large correction may be necessary to the amplitude of this effect.

The qualitative explanation for the origin of the quadratic term in the mean longitude is tidal friction. A simple heuristic model for the torques in the earth-moon system due to the (frictionally delayed) lunar tides on the earth was developed by MacDonald (1964), as follows. He assumes that the lunar disturbing potential produces a second harmonic distortion of the earth, with a magnitude proportional to the Love number K_2. This tide, however, does not exhibit maximum values directly under the moon. The tide is carried to an angle δ ahead of the moon by the relative angular velocity of the earth and moon because of frictional delay.

The potential external to the earth at a time t is then

$$U = - \frac{GM_M R_\oplus^5}{r_{ME}^3(t)\, r_{ME}^3(t-\frac{\delta}{n})} K_2 P_2(\xi)_{\xi=\delta}$$

where ξ is the zenith angle of the moon, r_{ME} is the distance of the moon from the earth, n is the mean lunar motion, $R_\oplus$ is the mean earth radius, and G the gravitational constant.

This potential produces an acceleration on the moon acting in the direction of motion of the tidal bulge of magnitude

$$\left| - \frac{1}{r_{ME}} \frac{\partial U}{\partial \xi} \right|_{\xi=\delta} = \frac{3GM_M R_\oplus^5}{2r_{ME}^4(t) r_{ME}^3(t-\frac{\delta}{n})} K_2 \sin(2\delta)$$

The extra lunar potential due to the tidal deformation of the moon by the earth is

$$U_{☾} = - \frac{GM_E^2 R_m^5 K_{☾2}}{M_M r_{ME}^6(t)}$$

where we have assumed that the tidal lag angle for the moon is zero. This treatment of the lunar potential is correct over the short time (∿200 yrs) of our observations since the only perceptible effect is the main effect, i.e., tidal friction in the earth. The radial component of the acceleration on the moon is then

$$R = -\frac{\partial}{\partial r_{ME}} (U + U_{☾})$$

$$R = -\frac{3}{2} \frac{GM_M R_\oplus^5}{r_{ME}^4(t) r_{ME}^3(t-\frac{\delta}{n})} K_2 \{3 \cos^2\delta - 1 + \frac{2K_{☾2}}{K_2}(\frac{M_E}{M_M})^2 (\frac{R_m}{R_\oplus})^5\}$$

$$\equiv - \frac{A}{r_{ME}^4 r_{ME}^3(t-\frac{\delta}{n})} \{3 \cos^2\delta - 1 + D\}$$

To express the other accelerations explicitly, let us set up the following coordinate system: take the z'' axis along the moon's orbital angular velocity vector $\vec{n}$, and the x'' axis along the line of intersection of the earth's equatorial plane and the orbital plane of the moon, the line of nodes. (See Figure 4.) The earth's axis of rotation is then in the y''-z'' plane. The angular velocity of the earth, $\vec{\Omega}$, and a unit vector to the moon, $\hat{u}$, have components

$$\vec{\Omega} = (0,\ \Omega \sin \varepsilon,\ \Omega \cos \varepsilon)$$

$$\hat{u} = (\cos\phi',\ \sin\phi',\ 0\ )$$

in this coordinate system (where the angles are defined in Figure 4). Note also that $n = |\vec{n}|$. As seen in inertial space, this coordinate system will undergo small oscillations of 18.6 year period about the mean position of the coordinate axes. This effect is due to the regression of the line of nodes on the ecliptic. In addition, the coordinate system also partakes of the general precession. Both of these effects are small enough so that the forces calculated in this frame differ from those calculated in an inertial frame by a negligible amount for the purpose of calculating tidal-friction effects.

A unit vector along the direction of motion of the earth's tidal bulge in the coordinate system of Figure 4 is

$$\hat{b} = \frac{(\vec{\Omega} - \vec{n}) \times \hat{u}}{|(\vec{\Omega} - \vec{n}) \times \hat{u}|}$$

The unit vector $\hat{b}$ has components

$$\hat{b} = [- \frac{(\Omega \cos \varepsilon - n)}{\Omega_0} \sin \phi', \frac{(\Omega \cos \varepsilon - n)}{\Omega_0} \cos \phi',$$

$$- \frac{\Omega \sin \varepsilon}{\Omega_0} \cos \phi']$$

where $\Omega_0 \equiv |(\vec{\Omega} - \vec{n}) \times \hat{u}|$. The average acceleration normal to the orbit plane is

$$W = - (\frac{1}{r_{ME}} \frac{\partial U}{\partial \xi}\bigg|_{\xi=\delta}) \hat{b} \cdot \hat{k}$$

and the average acceleration in the orbit plane is given by

$$S = - (\frac{1}{r_{ME}} \frac{\partial U}{\partial \xi}\bigg|_{\xi=\delta}) \hat{b} \cdot (-\hat{i} \sin \phi' + \hat{j} \cos \phi')$$

Since these accelerations are only approximate, we will ignore the very small difference between $r_{ME}(t)$ and $r_{ME}(t-\frac{\delta}{n})$. We define a new constant $A' = (A/a)^7$ where a is the semi-major axis of the moon's orbit, and also define $C(r_{ME}) = (a/r_{ME})^7$. Then

$$R = -A'C(r_{ME})\{3 \cos^2\delta - 1 + D\}$$

$$S = A'C(r_{ME})\sin(2\delta)\{(\Omega \cos \varepsilon - n)/\Omega_0\}$$

$$W = -A'C(r_{ME})\sin(2\delta)\,\frac{\Omega \sin \varepsilon \cos \phi'}{\Omega_0}$$

and ε is defined by

$$\cos \varepsilon = \frac{\vec{\Omega}\cdot\vec{n}}{\Omega n}$$

Assuming $K_{2☾} = K_2$ for the earth in the absence of any other information, MacDonald finds that D = 1.33.

If these results are to be considered reasonable, it should be possible to account for the astronomically observed acceleration of the moon with a small value for the parameter 2δ. The torque on the moon is given by

$$\vec{T}_{☾} = \vec{X}_{ME}\times\vec{F}$$

where

$$\vec{F} = M_m\{(R \cos \phi' - S \sin \phi')\hat{i} + (R \sin \phi' + S \cos \phi')\hat{j} + W\,\hat{k}\}$$

or

$$\vec{T}_{☾} = M_m(r_{ME}W \sin \phi'\hat{i} - r_{ME}W \cos \phi'\hat{j} + r_{ME}S\ \hat{k})$$

The torque averaged over a lunar orbit is then

$$\vec{T}_{☾\text{-}av} = M_m\ (-\overline{r_{ME}W \cos \phi'}\ \hat{j} + \overline{r_{ME}S}\ \hat{k})$$

The astronomical determinations of earth-moon tidal friction from solar eclipses have recently been reviewed by Newton (1969). He finds that the rate of change of the mean motion of the moon as given by studies of past solar eclipses is best represented by

$$\dot{n} = -(22.0 \pm 1.1) + (3.3 \pm 1.2)T + (0.114 \pm 0.059)T^2$$

$$(\text{arc-seconds})/(\text{century})^2$$

where T is time in centuries from 1900.0. The present value is -20.0"/(century)^2, not very different from the estimate of Spencer Jones (1939) of 22."44/(century)^2. We can relate the torque to the rate of change of the mean motion as follows:

$$\vec{T}_{☾\text{-}av} \cdot \frac{\vec{n}}{n} = M_m\overline{r_{ME}S} = \frac{d}{dt}(M_m a^2 n) = 2M_m an\ \frac{da}{dt} + M_m a^2\dot{n}$$

But from Kepler's law,

$$n^2 a^3 \simeq G(M_E+M_m)$$

or

$$\frac{d}{dt}(n^2a^3) = 0$$

Therefore,

$$\frac{da}{dt} + \frac{2}{3}\frac{a}{n}\dot{n} = 0$$

or

$$\vec{T}_{☾-av} \cdot \frac{\vec{n}}{n} = -\frac{1}{3} M_m a^2 \dot{n}$$

Using equation (60) of MacDonald (1964),

$$M_m \overline{r_{ME} S} = \frac{2M_m Aq'F(q)\sin 2\delta}{\pi a^6(1-e^2)^{9/2}} \{1+(\tfrac{3}{2}+\tfrac{3}{2}\cos\delta)e^2+\tfrac{3}{8}\cos\delta\ e^4\}$$

where

$$q' = \sqrt{1-q^2}$$

$$q^2 = \sin^2\varepsilon/[(\cos\varepsilon - \tfrac{n}{\Omega})^2+\sin^2\varepsilon]$$

and F(q) is the complete elliptic integral of the first kind, Newton's result can be expressed in terms of a value for the lag angle:

$$\sin 2\delta = 0.0687 - 0.01T - 0.0004T^2$$

where T is centuries from 1900.0. The parameters s_i chosen to be adjusted are $\sin 2\delta \equiv s_1 + s_2 T + s_3 T$ The numerical value of A' is about 1.88×10^{-17} km/sec^{2}m or,

$$A' = 9.37 \times 10^{-16} \text{ A.U.}/(\text{day})^2$$

Assuming that the result for sin 2δ is physically meaningful, we may interpret it in terms of a quality factor Q for the earth by the relationship given by Kaula (1969, p. 673):

$$\tan 2\delta \simeq \frac{1}{Q}$$

The value for Q from above is then ∿13. The detailed mechanisms for the dissipation of the energy in the tides are unknown. Seismological studies of the mantle (Anderson and Kovach, 1964; Press, 1966) and laboratory studies of granite (Knopoff and MacDonald, 1958) suggest a lower bound on Q of a few hundred. At the diurnal frequency of $\sim 10^{-5}$ Hz, the values of Q for the mantle range from Q = 100 for the upper

400 km, to Q = 2000 for the lower mantle. The value of Q for the oceans, on the other hand, has been estimated (Munk and MacDonald, 1960) as approximately 3 at $\sim 10^{-5}$ Hz. Another source of information on the Q of the earth is the variation of latitude or "Chandler wobble". If we accept the interpretation of the broadening of the spectral peak centered at the Chandler frequency as due to damping, then the relaxation time τ_R of the wobble is related (Munk and MacDonald, 1960) to Q by

$$Q \simeq \frac{\pi}{T_c} \tau_R$$

Rudnick (1956) found τ_R = 11 years which corresponds to a Q of 30; Jeffreys (1968) believes that the evidence favors $\tau_R > 30$ years, or $Q > 80$. The period T_c of the motion ($T_c \sim 434$ days) may make this Q irrelevant for the question of tidal friction however. Thus determination of a credible value of sin 2δ would be an important constraint on the theories of energy dissipation in the earth.

D.3.b. Other Effects of Tidal Friction

The torque due to tidal friction on the earth's spin angular momentum should cause the spin of the earth to be decreasing. However, the study by Newton (1969) has indicated that no clear evidence of such an effect can be found. If true, an acceleration of the earth's spin, due to non-tidal forces, must then be contributing

$$\dot{\Omega} \simeq +23 \times 10^{-9}\ \Omega/\text{century}$$

at present. The model for the relationship between universal time and coordinate time described in Section II.B should reflect a constant $\dot{\Omega}$ by a secular trend in the solution for $\Delta T'$.

Another variety of tidal interaction is the one between the earth's orbital motion and the solar tides. The solar tides raised on the earth can be shown to cause a negligible effect on the orbital motion of the earth, as follows. From Kepler's law, we showed above that

$$\dot{n} \simeq \frac{3T_{☾}}{M_M a_{☾}^2}$$

and the similar expression for the change in the mean orbital motion of the earth is

$$\dot{n}_{\oplus} \simeq - \frac{3T_{\odot}}{M_E a_{\odot}^2}$$

Therefore

$$\frac{\dot{n}_{\oplus}}{\dot{n}_{☾}} = \frac{M_M}{M_E} \; \frac{a_{☾}^2}{a_{\odot}^2} \; \frac{T_{\odot}}{T_{☾}}$$

Since the periods of the solar and lunar tides are not very different, we can assume that the value for sin $2\delta_{\odot}$ will be roughly that of the moon. Then we have

$$\frac{T_{☾}}{T_{\odot}} = \left(\frac{M_M^2}{a_{☾}^6} \right) / \left(\frac{M_{\odot}^2}{a_{\odot}^6} \right) = 5.1$$

We obtain then

$$\frac{\dot{n}_{\oplus}}{\dot{n}_{☾}} \simeq 10^{-8}$$

The solar tides raised on the earth will have no secular effect on the orbital motion of the moon, since their period is not commensurate with the lunar tides on the earth, causing the net torque to average to zero.

Goldreich (1964) investigated the long-term effects in the earth-moon system, using two models for the tidal effects. The first model was just that of part 3.a above; the second was a more elaborate model from Kaula (1964) taking solar tides and lunar-solar precession into account. The results of these two calculations were almost identical. The formulae presented in Section D.2 above appear to represent the only effect in the earth-moon system due to tidal friction that we need model in our equations.

These formulae were inserted into the program, and a numerical integration was carried out with only the earth-moon central force and the force due to tidal friction affecting the motion. The resulting evolution in time of the osculating orbital elements is shown in Figure 5 as the differences in the elements from their initial values. The rates of time variation of the elements are compared in Table 4 with the corresponding values as calculated by MacDonald (1967) and Kaula (1964). The good agreement lends confidence to the belief that the model is programmed correctly. Further details on programming of the tidal friction model, together with the partial derivatives with respect to sin 2δ, are given in Appendix 4.

D.4. Time Varying Gravitational Constant

Many theories of gravitational interaction other than that of Einstein have been proposed on various philosophical grounds [e.g.; Dirac, 1937; Brans and Dicke, 1961; Isham, Salam, and Strathdee, 1971]. A common feature of many theories is a predicted time variation in the coupling constant G. What is the predicted magnitude of this variation? In Dirac's cosmology, a specific prediction is made (see Weinberg, 1972):

Table 4

Time Variation of Orbital Elements under the Influence of Tidal Friction

Element	MacDonald	Kaula	This work
semi-major axis	+3.2 cm/yr	+3.4 cm/yr	+3.3 cm/yr
eccentricity	$+0.72\times10^{-11}$ yr^{-1}	$+1.2\times10^{-11}$ yr^{-1}	$+1.09\times10^{-11}$ yr^{-1}
inclination	-6.2×10^{-10} °/yr	-5.2×10^{-10} °/yr	-8.21×10^{-10} °/yr
node	0	0	$+5.84\times10^{-9}$ °/yr (0.002"/century)
perigee	$+2.8\times10^{-7}$ °/yr	not calculated	$+3.2\times10^{-7}$ °/yr (∿0.1"/century)

$$\left(\frac{\frac{dG}{dt}}{G}\right)_{present} = -3H_0$$

where H_0 is the Hubble constant, currently thought to have a value $\sim 10^{-10}$years. The Brans-Dicke theory gives a rate of decrease of between $4\times10^{-13}yr^{-1}$ (q_0 = 0.01, ω = 6) and $2\times10^{-11}yr^{-1}$(q_0 = 1, ω = 6) for "reasonable" values of the deceleration parameter q_0 and the scalar coupling constant ω (Weinberg, 1972).

The best experimental upper limit on the current value of $\dot{G}$ comes from an analysis of radar observations of the inner planets (Shapiro *et al.*, 1971):

$$\left(\frac{|\dot{G}|}{G}\right)_{present} \leq 4 \times 10^{-10} yr^{-1}$$

The existence of the atomic time scale during these measurements makes the determination of Shapiro *et al.* independent of the variations in the earth's rotation rate.

The model for the perturbing force due to $\dot{G}$ in our program consists of an *ad hoc* parameterization: the quantity $GM_{\odot}$ in the equations of motion is replaced by

$$(GM_\odot)_{t=t_0} + \left[\frac{d}{dt}\,(GM_\odot)\right]_{t=t_0}(t-t_1)$$

where the coordinate time t_0 is an arbitrary epoch at which the quantities are evaluated. The interpretation of d(GM d(GM_0)/dt as a variation in G is quite unambiguous to the level of $\sim 10^{-14}$G, since one can easily estimate that $dM_\odot/dt \simeq -10^{-14} M_\odot\ yr^{-1}$ (e.g., Brandt, 1970, p. 188; also see Dessler, 1967).

The implementation of this effect in the program was checked in a manner similar to that used for relativity and tidal friction. The central force plus a time variation in $GM_\odot$ was allowed (the mass ratios $M_j/M_\odot$ are assumed to be absolute constants in time). The evolution in time of the osculating orbital elements was computed; the differences from the values at spoch are plotted in Figure 6. The theoretical values corresponding to the case plotted can be estimated as follows:

Let:

$$(GM_\odot)\ \frac{(M_E+M_M)}{M_\odot} \equiv \mu \equiv \mu_0 + \dot{\mu}\ (t-t_1)$$

where t is measured from the epoch of integration, μ_0 is the value at the epoch t = 0. t_1 is the epoch for $\dot{\mu}$ also measured from the integration epoch. t_1 is not equal to zero due to a programming oversight in this calculation. In the case plotted, t_1 = 520 days. The disturbing function is radial and is equal to

$$R = -\frac{\dot{\mu}(t-t_1)}{r_{ME}^2}$$

where r_{ME} is the earth-moon distance. The equations for the behavior of the osculating elliptic elements as functions of time (Danby, 1962) are for this special case:

$$\frac{da}{dt} = \frac{2a^2}{(\mu p)^{1/2}} e (\sin f)R$$

$$\frac{de}{dt} = (\frac{p}{\mu})^{1/2} (\sin f)R$$

$$\frac{d\omega}{dt} = -\frac{1}{e} (\frac{p}{\mu})^{1/2} (\cos f)R$$

$$\frac{d\Omega}{dt} = \frac{di}{dt} = 0$$

$$\frac{d\sigma}{dt} = \frac{3n}{2a} t \frac{da}{dt} + (\frac{p}{\mu})^{1/2} \frac{(1-e^2)^{1/2}}{e(1-e \cos f)}$$

$$[\cos f-e(1+\sin^2 f)]R$$

with the definition

$$p \equiv a(1-e^2)$$

$$n^2 \equiv \frac{\mu}{a^3}$$

The variations from the initial values of the elements will be small, so the initial values, designated by subscript 0, can be used on the right hand side of these equations. Let us also approximate the equations by ignoring e^2 and higher powers of eccentricity.

Consider the equation for da/dt first

$$\frac{da}{dt} = -2n_0a_0 \frac{\dot{\mu}}{\mu_0} e_0(\sin f)(t-t_1)$$

$$\simeq -2n_0a_0 \frac{\dot{\mu}}{\mu_0} e_0(t-t_1)[\sin M + 2e \sin M \cos M + O(e^2)]$$

$$\simeq -2n_0a_0 \frac{\dot{\mu}}{\mu_0} (t-t_1)e_0 \sin M + O(e^2)$$

$$\simeq -2n_0a_0 \frac{\dot{\mu}}{\mu_o} (t-t_1)e_0 \sin (nt- {}_0)$$

where

$$g_0 = n\, t_{perigee}$$

Integrating from 0 to t, we have

$$a = a_0 - \frac{2a_0}{n_0} \frac{\dot{\mu}}{\mu_0} e_0\{[\cos g_0 - (\sin g_0)(n_0 t - n_0 t_1)]\sin n_0 t$$

$$+[\cos g_0 (n_0 t_1 - n_0 t) - \sin g_0]\cos n_0 t\}$$

At the epoch, the term $n_0 t_1$ is very large, so that inserting the values $\dot{\mu}/\mu_0 = 3\times10^{-11}$years^{-1}, e_0=0.05, $a_0 = 2.6\times10^{-3}$A.U., we find

$$|a-a_0|_{t=0} \simeq 2e_0 \frac{\dot{\mu}}{\mu_0} a_0 t_1 \cos g_0 = 1.3 \times 10^{-14}\text{A.U.}$$

Now we note that $de/dt=((1-e^2)/2ae)da/dt$, so that the amplitude of the e oscillation at t = 0 should be $\sim4\times10^{-11}$. Also we have

$$\left|\frac{d\omega}{dt}\right| \simeq \frac{1}{e} \left|\frac{de}{dt}\right|$$

The ω oscillation will therefore be 90° out of phase with the variation in <u>a</u>, and will have amplitude

$$|\omega-\omega_0|_{t=0} \simeq 4\times10^{-8} \text{ degree.}$$

These predictions are confirmed by inspection of Figure 6.

E. Variational Equations

In order to estimate the parameters in our theory from the data, we must have theoretical expressions for the partial derivatives of the observable quantities with respect to the parameters. Many partial derivatives of the observables are constructed, via the chain rule for partial derivatives, from the partial derivatives of position and/or velocity with respect to the parameters (together, of course, with the explicit dependences of the observables on position, velocity, and time). A system of differential equations for the partials of position and velocity, called the variational equations, can be constructed.

The set of equations for the earth-moon relative position $\vec{X}_{ME}$ and velocity $\vec{V}_{ME}$, from section D, are

$$\frac{d\vec{X}_{ME}}{dt} = \vec{V}_{ME}$$

$$\frac{d\vec{V}_{ME}}{dt} = (\vec{F}_M)_{tot} \equiv -GM_{\odot} \frac{(M_E+M_M)}{M_{\odot}} \frac{\vec{X}_{ME}}{r_{ME}^3} + \vec{D}+\vec{P}+\vec{Q}+\vec{H}+\vec{R}+\vec{T}+\vec{V}$$

with initial conditions

$$\vec{X}_{ME}(t_0) = \vec{X}_0 \qquad \vec{V}_{ME}(t_0) = \vec{V}_0$$

For a parameter β, we have the set of equations

$$\frac{d}{dt} \left(\frac{\partial \vec{X}_{ME}}{\partial \beta}\right) = \frac{\partial \vec{V}_{ME}}{\partial \beta}$$

$$\frac{d}{dt} \left(\frac{\partial \vec{V}_{ME}}{\partial \beta}\right) = \frac{\partial}{\partial \beta} \left(\frac{(\vec{F}_M)_{tot}}{M_M}\right)$$

The explicit functional form for the variational equations have been set down in detail in M.E. Ash (1965), Chapter 5, Section B. The partial derivatives not given there have been given along with the perturbing accelerations described above.

These equations, along with the equations of motion, must be integrated over the relevant period of time, as described in Chapter 4. The partial derivatives that were integrated for this thesis were with respect to the following parameters: six initial conditions, the relativity parameter, $(\dot{G}/G)_{present}$, sin 2δ, inverse mass of the earth+moon, and the ratio of the mass of the moon to the earth+moon mass.

CHAPTER III

Theoretical Values of Observations

A. Optical Observations

Observations of the moon have been made regularly by many observatories for several centuries. The basic observing program consists of recording the times of transit of the moon and the zenith distance at those times, together with similar observations for standard stars. (An object transits or culminates when it is on the observer's celestial meridian.) For an extended object like the moon, the transit refers to one or more of the limbs (north, south, east, west) or a point like the crater Mösting A.

The operational procedures in the observation program are complicated, but as a crude conceptual picture, the differences in sidereal time between the lunar and stellar transits give differences in geocentric right ascension. The east or the west limb is usually observed -- preferably both to facilitate the reduction to the center of figure of the moon. The catalogue right ascensions of the standard stars (referred to the true equinox and equator of date by applying precession, nutation, and proper motion) are used to convert the differences in right ascension to an absolute geocentric right ascension in the system of the catalogue used.

Usually during the course of a transit observation, the zenith distance at culmination is measured. For the moon the measurement refers to the north and/or south limb (or Mösting A). The differences in zenith distance between the moon and the standard stars can be used to calculate the difference in geocentric declination through a relation which depends on the parallax of the observing site relative to the center of mass of the earth (see below). Atmospheric refraction also must be taken into account due to the differing zenith distances of the various objects.

Corrections are often applied to both types of observables to produce the coordinates at transit of the center of figure of the moon. Usually these corrections are made through adopted values for vertical and horizontal semi-diameters of the moon. These values are sometimes derived from the observations in the course of the reductions by the observatory. A further sophistication is the use of Watt's (1963) corrections for the irregularities of the limb. Several series of observations used in our analysis consisted of limb observations referred to the transit time of either the center or the limb itself. The theoretical calculations were modified at the appropriate point in those instances in a manner described below.

A.1 Theoretical Calculations of Observables

The program calculates the geocentric right ascension and declination at transit for the <u>center of mass</u> of an object through an iterative process which starts with a first guess at the U.T.1 time of meridian crossing (which must be within twelve hours of the true time). From ΔT' and the seasonal variations, we can calculate the coordinate time corresponding to the value of U.T.1. A provisional first position for the center of mass of the moon at this coordinate time in the inertial reference frame, $\underset{\sim}{r}_{ME}^{(1)}$, can then be found from the ephemeris. The position referred to the true equator and equinox of the date of observation is obtained by applying the precession and nutation matrices:

$$(\underset{\sim}{r})_{date}^{(1)} = \underline{N}\ \underline{P}\ \underset{\sim}{r}_{ME}^{(1)}$$

The right ascension α and declination δ have their first values found from

$$\alpha^{(1)} = \tan^{-1}\left(\frac{y_{date}}{x_{date}}\right)$$

$$\delta^{(1)} = \sin^{-1}\left(\frac{z_{date}}{|\underset{\sim}{r}_{date}|}\right)$$

with proper account taken for quadrant in α. At meridian crossing, the right ascension equals the local sidereal time. The true sidereal time θ_t is calculated via Newcomb's formula which relates θ_t to U.T.1, together with the nutation in longitude $\Delta\psi \cos \varepsilon$. The correction $\underline{\Delta t}$ to the first guess for U.T.1 is given by

$$\Delta t = \theta_t - \lambda - \alpha^{(1)}$$

where λ is the west longitude of the observatory. Using this corrected time, we calculate $\underset{\sim}{r}_{ME}^{(2)}$, and then $\alpha^{(2)}$ and $\delta^{(2)}$. The iteration continues until Δt is less than some input accuracy constant.

Since the program calculates the position in the coordinate system in which we perform the integration, we must allow for the differences between that system and the system of the stellar catalogue to which the observations refer. For this purpose, we use a simple three-parameter model for each observation series that permits small corrections to the reference equator, equinox, and declination system. The corrected theoretical right ascension and declination are given by

$$\alpha^c = \alpha + \Delta E - \Delta I \cos \alpha \tan \delta$$

$$\delta^c = \delta + \Delta\phi + \Delta I \cos \alpha$$

where ΔE is the angular separation between the corrected and reference equinoxes; ΔI is the inclination of the corrected equator to the reference equator; and $\Delta\phi$ is the bias in the declination system. $\Delta\phi$ is considered to be, in part, a correction due to errors in the geocentric latitude. The series of observations are restricted in the time covered so that the time variation of ΔE, ΔI, and $\Delta\phi$ can be neglected.

A procedure preferable to this three-parameter model would involve the computation of differential corrections between the different star catalogues used for our data and the FK4 system. The labor involved was beyond our resources, however, and possibly would yield no better results since other systematic errors (telescope flexure, etc.) may be equally important.

The observations of an extended body like the moon are found to be strongly biased by the different lighting effects at different phases. In order to empirically determine these corrections for each series of observations, we parametize the vector $\Delta\vec{\rho}$, the projection perpendicular to the line of sight of the vector from the center of mass to the center of illumination, as follows:

$$\Delta\vec{\rho} = D \sum_n a_n \cos n\theta \, \frac{(\vec{r}_M \times \vec{r}_E) \times (\vec{r}_E - \vec{r}_M)}{(|\vec{r}_M \times \vec{r}_E| \, |\vec{r}_E - \vec{r}_M|)}$$

where the a_n are the parameters to be estimated. The angle θ is given by

$$\theta = \cos^{-1}\left[\frac{\vec{r}_M \cdot (\vec{r}_M - \vec{r}_E)}{|\vec{r}_M|\,|\vec{r}_M - \vec{r}_E|}\right] ; \qquad 0 \leq \theta \leq \pi$$

and $\vec{r}_E$, $\vec{r}_M$, and D are, respectively the vector from the sun to the earth, the vector from the sun to the moon, and the diameter of the moon. The algorithms for the phase corrections and the equator-equinox-declination corrections were developed by I.I. Shapiro. For further details, see a more complete description in M.E. Ash (1972).

The observations in each series may not be referred to the center of mass of the moon because, for example, the center of mass does not project onto the center of the Watts' datum. However a solution for further corrections, which would be highly correlated with those above, seemed to be unlikely to be worth the great effort that would be entailed.

A.2 Limb Observations

For those observations which were not corrected to the center of the moon at all, further corrections to the calculations needed to be formulated. These observations included all of those at Greenwich prior to 1830. These corrections are developed below. The geocentric right ascension of the center of the moon at the universal time t_L of transit of the east (first) or west (second) limb, $\alpha_c(t_L)$, is the "observed" quantity for several series. The quantity that is computed directly in PEP is the geocentric right ascension of the center at the instant of the transit of the center, $\alpha_c(t_c)$. When the limb is on the meridian, the local hour angle of the moon's center is $\pm S/(15 \cos \delta)$, where S is the apparent geocentric semidiameter in degrees, δ is the declination of the center at center passage, and + or - denotes first or second limb, respectively. The sidereal time T_c corresponding to t_c is known; the sidereal time of the limb transit, T_L, is given by

$$T_L = T_c \pm \frac{S}{15(1-\lambda)\cos \delta}$$

where λ is the rate of change of right ascension with respect to sidereal time in seconds of r.a. per second of sidereal time. Therefore

$$\alpha_c(t_L) = \text{sid. time at } t_L - \text{local hour angle of center at } t_L$$

$$\alpha_c(t_L) = T_c \pm \frac{S}{15(1-\lambda)\cos \delta} \mp \frac{S}{15 \cos \delta}$$

$$= \alpha_c(t_c) \pm \frac{\lambda S}{15(1-\lambda)\cos \delta}$$

Similarly, the declination of the center at the passage of the center $\delta_c(t_c)$ is clearly related to the center's declination at meridian passage of a limb (east or west),

$\delta_c(t_L)$, by

$$\delta_c(t_L) = \delta_c(t_c) \pm \lambda' \frac{S}{15(1-\lambda)\cos\ \delta}$$

where λ' is the rate of change of declination in seconds of arc per second of sidereal time.

The quantity λ is calculated from the rectangular coordinates of the center of the moon, referred to the mean equator and equinox of date -- x_1 x_2, x_3-- and their derivatives (with respect to coordinate time, τ) -- $\dot{x}_1$, $\dot{x}_2$. $\dot{x}_3$ -- as follows:

$$\alpha_c(\tau) = \tan^{-1} (\frac{x_2}{x_1})$$

$$\frac{d\alpha_c}{d\tau} = \frac{1}{x_1^2 + x_2^2} [x_1\dot{x}_2 - x_2\dot{x}_1]$$

Let t be universal time, and s be mean sidereal time

$$\tau = t + \Delta T'$$

$$s = s_0 + rt$$

Then we have

$$\frac{d\alpha_c}{ds} = \frac{d\alpha_c}{d\tau} \frac{d\tau}{dt} \frac{dt}{ds}$$

For purposes of limb corrections, $d\Delta T'/d\tau$ can be ignored, as can the difference between true and mean sidereal time. Then

$$\lambda = \frac{d\alpha_c}{ds} = \frac{1}{r} \frac{d\alpha}{d\tau}$$

The value of λ' can be calculated using the relationship

$$\delta_c = \sin^{-1}\left(\frac{x_3}{\sqrt{x_1^2 + x_2^2}}\right)$$

$$\frac{d\delta_c}{d\tau} = \frac{[x_1^2\dot{x}_3 + x_2^2\dot{x}_3 - x_1x_3\dot{x}_1 - x_2x_3\dot{x}_2]}{[x_1^2 + x_2^2]\sqrt{x_1^2 + x_2^2 - x_3^2}}$$

$$\lambda' = \frac{d\delta_c}{ds} = \frac{1}{r}\frac{d\delta_c}{d\tau}$$

The derivatives with respect to τ above ignore the derivatives of the precession-nutation matrix. The principal terms, however, should be on the order of $50''/365\times8.64\times10^4$ seconds and $9''/18.6\times365\times8.64\times10^4$ seconds. For making limb corrections, these are clearly negligible.

Some series (e.g., old Radcliffe observations) give α_L the right ascension of the limb at its transit over the meridian as the "observed" quantity. Then α_c and α_L are related, from above, by

$$\alpha_c = \alpha_L \pm \frac{S}{15(1-\lambda)\cos\delta}$$

Observations also exist of the declination of a point on the limb at the time that the limb (north or south) is on the meridian. In this case, the formula for correcting the declination is more complex. The correct relation is derived in Chauvenet (1891), p. 306:

$$\sin(\delta-\delta_1) = \sin P \pm \sin S - 2\cos\delta\sin\delta_1\sin^2(\tfrac{H}{2})$$

where

$$\sin P \equiv \rho\sin\pi\sin(\phi'-\delta_1)$$

and

δ_1 = observed declination of limb (corrected for refraction)

δ = the geocentric declination of the center of the moon

S = as before

ϕ' = the geocentric latitude of the observation

ρ = the radius to the place of observation

λ = as above

π = the moon's equatorial horizontal parallax

In the expression above, H is the true hour angle of the center at meridian passage of the limb. The upper or lower sign is used according to whether the north or south limb was observed. H is an "observed" quantity, since it can be calculated from the sidereal time of observation S_1, and the sidereal time of the center's transit S_2, from

$$H = (1-\lambda)(S_2-S_1)$$

This number is frequently on the observation records (but was not transferred to the punched cards). The value of δ above is referred to the time of the limb on the meridian. The reduction to δ_0, the value for the center on the meridian, is given by

$$\delta_0 = \delta + (S_2 - S_1)\lambda'$$

The terms involving S_2-S_1 are on the order of a second of arc and often less. According to an example in Chauvenet, Vol. II, p. 308, these terms are usually included in the reduction of the micrometer correction, and I have assumed, unless the explanations explicitly said otherwise, that the corrections involving H have been made by the observer.

From the formulae above, it is clear that the reduction of limb observations depends critically on the values for several astronomical constants adopted by the observers:

a) If the value of the semidiameter in right ascension S_α is in error by ΔS_α, the derived r.a. is in error by

$$\begin{matrix} +(1^{st}) \\ -(2^{nd}) \end{matrix} \frac{\Delta S_\alpha}{15(\cos\delta)}$$

b) the declination depends on errors in the semi-diameter in declination S_δ and other quantities in the reduction from topocentric to geocentric values as follows:

$$\Delta\delta = \begin{matrix} -(N) \\ +(S) \end{matrix} \Delta S_\delta + \rho\sin(\phi' - \delta_1)\Delta\pi'' + \pi''\sin(\phi' - \delta_1)\Delta\rho$$

$$+\rho\pi''\cos(\phi' - \delta_1)\Delta\phi''$$

where ΔS_δ is the error in semi-diameter in degrees ($\neq \Delta S_\alpha$ in general)

$\Delta\pi''$ is the error in parallax in seconds of arc

$\Delta\rho$ is the error in radius vector in units of earth radii

$\Delta\phi'$ is the error in geocentric latitude in radians.

A latitude correction which can be solved for is programmed in PEP. Unless a good "modern" value for the geocentric latitude of the old observatory location can be found, and unless the modern value is very different, the last term will be ignored and the correction will be solved for. The observers' explanations were examined for assumed values for the radius to the site and the constant of parallax, and corrections to the best modern values were made for some observations, as will be further documented in Chapter VII.

B. Radar Observations

The radar observables are the two-way time delay τ and the Doppler shift of the reflected signal f_d, both evaluated at the universal time of reception t_r. The calculation of time delay begins with the evaluation from the ephemeris (and our theoretical superstructure) of the vector position of the receiving site $\vec{S}_r(t_r)$. The vector position of the reflection point $\vec{R}(t_b)$ at the bounce time t_b can be found from the implicit equation:

$$t_b = t_r - \frac{|\vec{R}(t_b) - \vec{S}_r(t_r)|}{c}$$

where c is the speed of light. This equation can be solved by iteration. The vector position of the transmitter site $\vec{S}_T(t_t)$ at the time of transmission t_t is derived from the implicit relation

$$t_t = t_b - \frac{|\vec{R}(t_b) - \vec{S}_t(t_t)|}{c}$$

The time delay in coordinate time is then given by

$$\tau = t_r - t_t$$

The Doppler shift is given by (see Shapiro *et al.*, 1966):

$$f_d(t_r) = -f_0 \frac{d\tau}{dt_r}(t_r)$$

where f_0 is the transmitted frequency. The observations usually are of the subradar point, which is defined as the point where the line-of-sight from the radar to the center of mass of the moon intersects the surface of the moon.

The explicit formulation for these radar observables in terms of the quantities in the theory can be found in a report by M.E. Ash (1972).

C. Surveyor Doppler Observations

The Surveyor landed spacecraft carried transponders which received a "monochromatic" radio signal from an earth-based station, and retransmitted the signal to the ground after frequency multiplication by a constant factor c_1. The observations used in this thesis were all of "coherent counted" Doppler, that is, the transmitter reference oscillator frequency was available at the receiver. The receiver takes the reference frequency, multiplies it by c_1, and beats this frequency f_M against the incoming signal. The number M_0 of positive zero crossings of the differenced signal are counted for the duration of an observation, called the counting interval D_c. The observable is given as M_0/D_c.

The epoch of the observation is given at the midpoint of the counting interval. The details of the observational procedure, together with values for the various constants, are given by Holzman (1965).

The theoretical calculation of this observable is done by computing the difference between the phase delay at the end and that at the beginning of the counting interval. If the epoch of the observation is t_e, then the endpoints occurred at

$t_e \pm D_c/2$. The phase delay can be calculated, using the algorithm described for radar time delay above, at each end of the counting interval. The difference of these delays, divided by D_c and multiplied by f_M, is the theoretical value of the observable, except for corrections for atmospheric effects. The fact that the observations are of <u>phase</u> delay affects only the calculation of dispersive effects such as the ionospheric corrections.

Further correction of the "vacuum" theoretical value is necessary to account for the variation in phase delay due to the changing path length through the troposphere (lower neutral portion of the atmosphere) during the course of an observation. The correction $\Delta\rho_T(t_E \pm D_c/2)$ to the range at either end of the counting interval, to first order, is $(\ell_z/\sin E_{receive})$ + $(\ell_z/\sin E_{send})$ where ℓ_z is the extra contribution to the zenith range from the troposphere and E is the elevation angle. At low elevation angles, significant deviations occur due to the curvature of the earth's surface and ray bending effects. A semi-empirical correction has been found (C.C. Chao, 1970) by fitting to range corrections $\Delta\rho$ generated by a ray tracing program for a spherical earth.

The formula found by Chao, as used in our Surveyor reduction, is, in meters,

$$\Delta\rho_T(E) = \frac{K_{ij}\ell_z}{\sin E + \dfrac{A \cos E}{\sin E + B \cos E}}$$

where K_{ij} is a multiplicative factor to be adjusted for each observing site (i) and spacecraft (j). The quantities ℓ_z, A, and B are constants with values:

ℓ_z = 2 meters (light time equivalence)

A = 0.00143

B = 0.0445

The ionosphere causes an effect very similar to the neutral atmosphere, except that the equivalent additional path length is a function of the local electron density.

Due to the fact that the troposphere and ionospheric corrections are highly correlated, a solution for both is not contemplated. The neutral atmosphere model is adjusted; a fixed model for the ionosphere using measured electron content is programmed. The model used is based on that of Melbourne et al. (1968), and has the form

$$(\Delta\rho)_I = C_L \frac{N_e(t_I)}{N_0} \left(\frac{2.3\times10^9}{f_0}\right)^2 \Delta_0(E)$$

where $\Delta_0(E)$ is a function tabulated by Melbourne et al.; f_0 is the transmitter frequency in Hertz; $N_e(t_I)$ is the integrated electron content along the path to the spacecraft in electrons/meter^2 at the time of the observations t_I; N_0 = $8.069\times10^7\times$electrons/meter^2, and

$$C_L = \frac{\pi - 2|\phi_M|}{\pi - 2|\phi_M(\text{Stanford})|}$$

where ϕ_M is the geomagnetic latitude.

This empirical expression was developed by JPL to produce a good fit to a numerical calculation for the nominal values $f_0 = 2.3\times10^9$ Hz and $N_e = N_0$. The extrapolation for other parameter values comes from a theoretical basis. The factor C_L attempts to account for the latitudinal variation of the electron content. The integrated electron contents at half-hour intervals were supplied by M.J. Davies of the Stanford Electronic Laboratories (personal communication, 1971).

D. Stellar Occultations

Observations of occultations of stars by the moon consist of recording the time of disappearance and/or the time of reappearance of the star. The observation is thus independent of the star catalogue currently being used by the observatory (except for the small effect that the regulation of the observatory clock, i.e. the universal time, depends on the star catalogue). If the star were correctly identified as to catalogue number, name, etc., then the observation can be reduced at any later time using the best modern star positions. Thus this data type is clearly quite sensitive to the value of $\Delta T'$ at the time of observation.

The theoretical evaluation of the occultation observations has been implemented in the program. The partial derivatives of the observable with respect to the various parameters have not yet been checked out. The corrections for the topography of the limb from the charts of Watts (1963) have not yet been completely coded in the program. For these reasons, the observations of occultations have not been included in the data set for this thesis. The theoretical expressions for this observable will be given in a seperate report.

CHAPTER IV

Numerical Methods

A. Numerical Integration

The method of numerical integration is a second-order form of a classical predictor-corrector scheme. "Classical" in this connection means that the resulting values of the function being integrated are obtained at equally spaced intervals. Suppose we desire the solution of the three-dimensional system of 2^{nd} order ordinary differential equations of the form

$$Y^{(2)}(t) = F(t, Y(t), Y^{(1)}(t))$$

with initial conditions

$$Y(a) = Y_0 \ ; \ Y^{(1)}(a) = Y_0^{(1)}$$

in which Y is the vector [x,y,z], and the superscript (n) indicates the order of the derivative with respect to time.

The classical predictor-corrector scheme generates a sequence of vectors Y_p, approximating $Y(t_p)$, from the equation:

$$\sum_{i=-1}^{s} [a_i Y_{p-i} + hb_1 Y_{p-i}^{(1)} + h^2 c_i Y_{p-1}^{(2)}] + E = 0$$

at s+2 equally spaced points t_{p-i}, $i = -1,\ldots s$. Here h is the spacing $(t_i - t_{i-1})$, E is an error term, and a_i, b_i, c_i are coefficients which depend on s (and i). The equation is used to extrapolate Y_p forward in t when $b_{-1} = c_{-1} = 0$. Iterative application of the equation when some of the b_{-1}, c_{-1} are non-zero, make up the corrector, or interpolation, mode of this method. [See Hildebrand (1956), and W.B. Smith (1968) for more complete treatments.] In particular, we assume that we can form a polynomial approximation of degree p to $F(t,Y,Y^{(1)})$. Then

$$\nabla^2 Y_k \simeq h^2 \sum_{i=0}^{p} W_i \nabla^i Y_k^{(2)}$$

where

$$W_i = \left(\sum_{j=0}^{i} d_j\right) d_i$$

and the d_j are defined recursively from:

$$d_0 = 1$$

$$d_1 = -\frac{1}{2}$$

$$\vdots$$

$$d_m = -\sum_{\ell=1}^{m} \left(\frac{d_{\ell-1}}{m-\ell+2}\right)$$

The ∇^i are the standard backward differencing operators:

$$\nabla^\circ \equiv 1$$

$$\nabla^1 Z_k \equiv Z_k - Z_{k-1}$$

$$\nabla^n Z_k \equiv \underbrace{\nabla^1(\nabla^1(\nabla^1 \ldots (\nabla^1 Z_k)))}_{\text{n applications}}$$

In order to predict, we operate on both sides with the advancing operator $(1/(1-\nabla^1))$

$$\frac{1}{(1-\nabla^1)} \nabla^2 Y_k = \nabla^2 Y_{k+1} = \frac{1}{1-\nabla^1} h^2 \sum_{i=0}^{p} W_i \nabla^i Y_k^{(2)}$$

$$= [1+\nabla^1+\nabla^2+\nabla^3+\ldots]h^2 \sum_{i=0}^{p} W_i \nabla^i Y_k^{(2)}$$

$$= h^2 \sum_{i=0}^{p} e_i \nabla^i Y_k^{(2)}$$

where

$$e_i = \sum_{j=0}^{i} W_j$$

Now writing out $\nabla^2 Y_k$, and transposing terms we have

1. for prediction

$$Y_{k+1} \simeq -Y_{k-1}+2Y_k + h^2 \sum_{i=0}^{p} e_i \nabla^i Y_k^{(2)}$$

which requires the current Y_k, the Y_k just past, and the accelerations

$$Y_k^{(2)}, \quad k=0,\ldots -(p+1)$$

2. for correcting the current value:

$$Y_k \simeq -Y_{k-2} + 2Y_{k-1} + h^2 \sum_{i=0}^{p} W_i \nabla^i Y_k^{(2)}$$

The velocities are obtained by numerical differentiation from the corrected values:

$$Y_m^{(1)} = \sum_{k=0}^{q} r_k Y_{m-k}$$

where

$$r_k = \sum_{i=k}^{q} (-1)^k \binom{i}{k} f_i$$

$$f_i = \begin{cases} 0 & i=0 \\ \frac{1}{h}\left(\frac{1}{i}\right) & i\neq 0 \end{cases}$$

Note that this method is not self-contained, since the iterative procedure must have some initial values to fit with the polynomial. The starting procedure is the numerical integration method due to A. Nordsieck (1962). This method will not be described here; the important features are

1. The method is self-starting
2. the accuracy and stability of the "software" package are thought to be completely verified.

The fractional accuracy to be achieved per unit time interval is specified for the starting procedure, and the step size in the integration is automatically chosen to match this requirement. The accuracy specified for starting the moon integration was 1×10^{-16} (as high as double precision arithmetic allows).

Once the starting procedure has generated a sufficient number of values for the order of the polynomial fitting to be done, the predictor-corrector scheme may begin.

In the moon integrations, the predictor-corrector step size chosen was $\frac{1}{8}$ day. A 12-term expression in the accelerations (i.e., p = 11) was used. The output points were at tabular intervals of one half-day. The choice of these numbers is not unique and can be defended only on experimental grounds: e.g., $\frac{1}{4}$ day steps were tried and found to be unstable after $\sim$10 years. Whether $p = 11$ and $h = \frac{1}{8}$ are "sufficiently" accurate in any particular application must be settled by investigation. For our purposes, comparison with other integration methods and "closed-loop" integrations have led to the conclusion that the error of the integration at the end point (1750) is at most 5×10^{-10} A.U. ($\approx$ 75 meters). If observations of one second of arc ($\simeq$ 2 Km) standard error and strictly zero bias were made in 1750, then approximately 50 thousand observations of this quality would be necessary to require more accuracy from the ephemeris.

The integration packages used were developed and tested by William B. Smith of Lincoln Laboratory. Interfacing the moon acceleration software [the so-called right-hand side routine; since $\ddot{\vec{r}} = F(\vec{r}, \dot{\vec{r}}, t)$] to the integration routines was done with his assistance. The speed of this predictor-corrector method of integration was an important factor in insuring that computer time necessary for this task* was not exorbitant.

B. Everett Interpolation

The observations of the moon are generally made at times other than the times for which tabulated values of position and velocity are available. Therefore in processing observations in PEP, an interpolation method is applied to the tabulated values. The method chosen is Everett eighth-difference interpolation. The output tabular interval of the numerical integration (not to be confused with the step size h) must be short enough so that the error in interpolation is no larger than the error in the integration. This criterion governed the choice of half-day output for the moon.

Appendix 5 details the algorithm developed by Michael Ash for the Everett scheme.

---

* For example, twelve sets of equations were integrated with about 1 year's output requiring one minute of IBM 360/91 CPU time. For the Nordsieck method, nearly 10 times as much computer time would have been required.

C. Numerical Checks of Partial Derivative Coding

The formulae for partial derivatives of an observable quantity O with respect to a parameter q were checked for correct coding and self-consistency by computing the value of the function $\partial O/\partial q$ for two values of the parameter, say q_0 and q_1. The values of O for those parameter values with the other parameters fixed also were available. Forming a Taylor series for $O(q_1)$, we have

$$O(q_1) \simeq O(q_0) + \left.\frac{\partial O}{\partial q}\right|_{q_0} (q_1 - q_0) + \frac{1}{2} \left.\frac{\partial^2 O}{\partial q^2}\right|_{q_0} (q_1 - q_0)^2$$

if q_1 is close enough to q_0. Now if we compute

$$\frac{\Delta O}{\Delta q} \equiv \frac{O(q_1) - O(q_0)}{q_1 - q_0}$$

then

$$\frac{\Delta O}{\Delta q} \simeq \left.\frac{\partial O}{\partial q}\right|_{q_0} + \frac{1}{2} \left.\frac{\partial^2 O}{\partial q^2}\right|_{q_0} (q_1 - q_0)$$

We also have that

$$\left.\frac{\partial O}{\partial q}\right|_{q_1} = \left.\frac{\partial O}{\partial q}\right|_{q_0} + \left.\frac{\partial^2 O}{\partial q^2}\right|_{q_0} (q_1 - q_0)$$

If we average the values of $\partial O/\partial q$ at q_1 and q_0, we have

$$\frac{1}{2}\left(\left.\frac{\partial O}{\partial q}\right|_{q_1} + \left.\frac{\partial O}{\partial q}\right|_{q_0}\right) = \left.\frac{\partial O}{\partial q}\right|_{q_0} + \frac{1}{2}\left.\frac{\partial^2 O}{\partial q^2}\right|_{q_0}(q_1 - q_0)$$

Therefore the quantities to compare are the averaged partials and $\Delta O/\Delta q$. Care must be taken not to choose the increment $q_1 - q_0$ too large, since this would invalidate the Taylor series approximation. However, the increment cannot be too small or the check will reveal nothing for lack of precision. Tables 5 and 6 list the results of these comparisons for the variational equations and the partials of the observables, respectively, for the parameters listed in the left-hand columns. In the tables presented, the increments in checking the variational equations were sometimes not well chosen. This situation explains the somewhat variable level of agreement for the same parameter in different types of observables. These results confirm that the coding for the forces and the partials are self consistent, since coding errors (of which several were found) show up in the first -- rarely in the second--decimal place. The general fractional agreement is $\sim 10^{-4}$.

Table 5

Typical Fractional Disagreement in Variational Equations Check

(maximum of three components)

	Position	Velocity
Moon initial conditions	8×10^{-5}	2×10^{-4}
Mass (3')*	1×10^{-5}	5×10^{-4}
Mass (10)**	2×10^{-5}	5×10^{-5}
Relfct***	7×10^{-5}	4×10^{-4}
Tidal friction	5×10^{-5}	8×10^{-5}
$\dot{G}$	9×10^{-5}	2×10^{-4}

* inverse of earth+moon mass

** ratio of moon to earth+moon mass

*** relativity multiplicative factor

Table 6

Typical Fractional Disagreement in Check of Observation Partials

	Surveyor Doppler	Radar Delay	Radar Doppler	R.A.	Dec.
Moon i.c.	4×10^{-5}	1×10^{-4}	5×10^{-5}	3×10^{-4}	2×10^{-4}
Mass(3)*	1×10^{-4}	2×10^{-7}	8×10^{-5}	6×10^{-5}	4×10^{-5}
Mass(10)**	5×10^{-5}	2×10^{-5}	7×10^{-5}	3×10^{-4}	2×10^{-4}
Relfct ***	2×10^{-5}	3×10^{-5}	9×10^{-5}	6×10^{-5}	4×10^{-5}
Tidal Friction	2×10^{-5}	7×10^{-6}	4×10^{-5}	3×10^{-5}	2×10^{-5}
$\dot{G}$	3×10^{-5}	1×10^{-5}	5×10^{-5}	4×10^{-5}	7×10^{-6}

* inverse of earth+moon mass

** ratio of moon to earth+moon mass

*** relativity multiplicative factor

Table 6 Cont.

		Surveyor Doppler
Selenocentric Location of Surveyor Spacecraft	Radius	2×10^{-7}
	Longitude	3×10^{-5}
	Latitude	9×10^{-6}
Geocentric Location of Observatory	Equatorial radius	3×10^{-5}
	longitude	8×10^{-6}
	Distance along spin axis (Z)	4×10^{-5}

CHAPTER V

Maximum Likelihood Parameter Estimation

The parameters of our physical model are determined from a linearized, iterative, weighted least-squares solution. The mathematical formulation of this process will be given without proof below. (See Shapiro 1957 for a rigorous discussion.) Let an observable quantity 0 depend on a set of I parameters, q_i, and time, t:

$$0 = F(q_1, q_2, \ldots q_I, t)$$

where F is the theoretical expression for the observable 0. We wish to estimate the parameters q_i from the observations starting from a nominal set of values q_{i0}. We suppose that actual observations 0', of total number J, are made at times t_j. Let us form the following column vectors

$$\{\underset{\sim}{y}\}_j = \{0'_j - 0\,(q_1, q_2, \ldots q_I, t_j)\}; j=1,\ldots J$$

$$\{\underset{\sim}{x}\}_i \equiv \{q_i - q_{i0}\}\ ; \qquad i=1,2\ldots I$$

We also assume that there exists a (column) noise vector $\underset{\sim}{\varepsilon}$ of dimension J which represents the noise in each measurement. Assume that the noise can be characterized as random samples from a multivariate gaussian probability density distribution with zero means. We can expand $\underset{\sim}{y}$ in a power series about the q_{i0}'s as follows:

$$\underset{\sim}{y} = \underset{\sim}{y}_0 - A\,\underset{\sim}{x} + \text{terms of order } (q_i - q_{i0})^2$$

where

$$\underset{\sim}{y}_0 = \underset{\sim}{y}(\underset{\sim}{x}=0)$$

and the matrix $\underline{A}$ has elements

$$\{\underline{A}\}_{ij} = \left\{ \frac{\partial F(q_1,q_2,,,q_F,t_j)}{\partial q_i} \right|_{q_i=q_{i0},\ i=1\to I}$$

The equation that should hold true to sufficient accuracy to insure convergence on the "correct" minimum among the extrema of the weighted sums of the squares of the residuals is

$$\underset{\sim}{y}_0 = \underline{A}\,\underset{\sim}{x} + \underset{\sim}{\varepsilon}$$

The linearization error is presumed to be smaller than $\underset{\sim}{\varepsilon}$.

The maximum likelihood linearized approximation solution $\hat{\underset{\sim}{x}}$ can be shown to be the solution to the so-called "normal equations" obtained by weighting both sides by the matrix $\underline{\Lambda}_\varepsilon^{-1}$ (defined below) and then multiplying by $\underline{A}^T$:

$$\underline{A}^T \underline{\Lambda}_\varepsilon^{-1} \underset{\sim}{y}_0 = \underline{A}^T \underline{\Lambda}_\varepsilon^{-1} \underline{A}\, \hat{\underset{\sim}{x}}$$

or

$$\hat{\underset{\sim}{x}} = (\underline{A}^T \underline{\Lambda}_\varepsilon^{-1} \underline{A})^{-1} \underline{A}^T \underline{\Lambda}_\varepsilon^{-1} \underset{\sim}{y}_0$$

where $\underline{\Lambda}_\varepsilon$ is the noise covariance matrix $(\overline{\underset{\sim}{\varepsilon}\, \underset{\sim}{\varepsilon}^T})$ and the overbar denotes ensemble average or expectation. Terms of the order of $(\underset{\sim}{x})^T \underset{\sim}{x}$, $\underset{\sim}{x}^T \underset{\sim}{y}_0$, and $\underset{\sim}{y}_0^T \underset{\sim}{x}$ times second derivatives $\partial^2 F/\partial q_i\, \partial q_j$ have been neglected. This solution is in fact also the linearized minimum variance solution (see Solloway, 1965). The covariance matrix for this solution is

$$\underline{\Lambda}_x = (\underline{A}^T \underline{\Lambda}^{-1} \underline{A})^{-1}$$

The matrix inversion in PEP uses the Gauss-Jordan direct method with a routine supplied by N. Brenner. The documentation for this inversion is found in a report by M.E. Ash (1972) and references cited therein.

The linear estimate of the noise after the "best" set of parameters q_i are used in the theoretical expressions can be obtained from

$$\hat{\underline{\varepsilon}} = [\underline{I} - \underline{A}(\underline{A}^T \underline{\Lambda}_\varepsilon^{-1} \underline{A})^{-1} \underline{A}^T \underline{\Lambda}_\varepsilon^{-1}] \underset{\sim}{y}_0$$

where $\underline{I}$ is the identity matrix ($\{\underline{I}\}_{ij} = \delta_{ij}$).

In processing real observations, we generally make the restrictive assumption of independent (uncorrelated) measurement errors (i.e., $\underline{\Lambda}_\varepsilon$ is diagonal). To express $\underline{\Lambda}_x$, let us form the column vector

$$\underset{\sim}{\alpha}_m(t_j) = \begin{bmatrix} \frac{\partial O_m}{\partial q_1}(t_j) \\ \\ \frac{\partial O_m}{\partial q_2}(t_j) \\ \vdots \\ \frac{\partial O_m}{\partial q_I}(t_j) \end{bmatrix}$$

where O_m is the m^{th} type of observable. We assume that the errors in O'_m are gaussianly distributed with standard deviations σ_m. Then we have

$$(\underline{A}^T \underline{\Lambda}_\varepsilon^{-1} \underline{A})_m = \frac{1}{\sigma_m^2} \sum_{j=1}^{J} [\underset{\sim}{\alpha}_m^T(t_j)\underset{\sim}{\alpha}_m(t_j)]$$

whence

$$\underline{\Lambda}_x^{-1} = \sum_{m=1}^{M} (\underline{A}^T \underline{\Lambda}_\varepsilon^{-1} \underline{A})_m$$

where M is the total number of observable types.

The formal standard deviations of the parameter estimates are then

$$\sigma_i = \sqrt{\{(\underline{\Lambda}_x)\}_{ii}} \quad ; \quad i = 1,2,\ldots.I$$

and the normalized correlations between the estimates of parameters i and j are

$$c_{ij} = \frac{\{\underline{\Lambda}_x\}_{ij}}{\sigma_i \sigma_j} \; ; \quad i,j = 1,2,\ldots I$$

The linearization above demands that we must iterate until, by some criterion, convergence of the solution to the maximum likelihood estimate has been achieved. The criterion chosen is that the parameter adjustments are small fractions of their standard deviations.

PEP has several convenient related features for aiding in a judgment concerning the validity of a solution. For example the post-fit residuals can be linearly predicted, printed out, and/or plotted. The normal equations can be saved on magnetic tape so that additional solutions with parameter and/or data subsets can be explored.

CHAPTER VI.

Preliminary Solution for Observations from 1925-1969

The generation of a preliminary ephemeris was begun by obtaining initial conditions -- position and velocity in 1950.0 rectangular coordinates at the desired epoch (J.E.D. 2440000.5)*-- from values tabulated in the "Improved Lunar Ephemeris" (Eckert *et al.*, 1954) as supplied on magnetic tape by the Jet Propulsion Laboratory (designated as LE4).
A numerical integration of the motion and the derivatives with respect to initial conditions was carried out using these initial conditions. This integration covered a period of twelve years, 1956 to 1968, backward in time.

This ephemeris was then used to calculate theoretical values for observations made over this period of time in order to obtain improved initial conditions. The observational material used consisted of

1) meridian-circle observations from the U.S. Naval Observatory from 1956 to 1968.
2) time delay and Doppler observations of the sub-radar point of the moon made in 1966-1967.

These data are subsets of larger data sets which will be

*May 24, 1968

described in detail below. After two iterations, a converged solution was obtained. The converged solution did not differ significantly from the solution for the first iteration. With the initial conditions for this solution, an integration from 1968 backward in time to 1925 was carried out.

The date of 1925 for the intermediate ephemeris was chosen because a very homogeneous set of meridian-circle observations extending from 1968 back to 1925 became available when this step was being planned. This homogeneous data set is a careful reduction of meridian-circle observations made with the USNO 6 inch transit instrument. All positions are referenced to the system of FK4 (Adams *et al*., 1969). The extensive corrections made to these data are described in Adams *et al*. In brief, the data have been corrected for (1) limb irregularities using the limb corrections of Watts (1963), (2) refinements of the corrections for refraction, instrumental errors, diurnal aberration, and (3) parallax and orbital motion including the new IAU dimensions of the earth. Other data used in this solution were as follows: Greenwich observations from 1925 to 1954 were taken from the reference in Appendix 6, § 6 g-h. Observations at Capetown, South Africa, covering the period 1936-1959 were made available prior to publication by the observatory (personal communication, 1967). The radar data are taken from *Radar Studies of the Moon*, *Final Report*, *Vol. 2*; and unpublished

Table 7

Summary of Observations Fitted in Solution for Period 1925-1969

Observatory	Dates of Observations	Series Name	Number of Observations (r.a.+dec.)	r.m.s of post fit residuals r.a.	r.m.s of post fit residuals dec.	mean of post fit residuals r.a. (seconds of arc)	mean of post fit residuals dec. (seconds of arc)
U.S. Naval	1925-1969	6925	6394	∿0.″75	0.″8	-5.6×10^{-4}	-1.7×10^{-3}
Greenwich	1931-1954	5431	2923	1.″6	1.″3	2×10^{-3}	~ 0.0
	1931-1954	M531	1306*	1.″1	1.″1	4.7×10^{-4}	~ 0.0
	1925-1930	M300	692*	1.″0	1.″1	2×10^{-4}	~ 0.0
Capetown	1949-1959	5949	536	2.″0	2.″4	8×10^{-4}	~ 0.0
	1944-1949	4944	322	1.″6	2.″4	-7.7×10^{-5}	~ 0.0
	1936-1944	4436	500	1.″4	2.″3	3.7×10^{-4}	~ 0.0
Haystack	1966-1967	6766	128†	∿3 sec ∿0.15 Hz.			

*Observations of crater Mösting A reduced to center by observer instead of limb reduced to center.

†Time delay and Doppler observations.

observations made in 1968. The data are summarized in Table 7, which gives the number in each series of observations, the corresponding series "name" (as documentation for outside users of the lunar data compiled here) and some statistics for each series.

Sample plots of the residuals versus time for the converged solution for this data set are given in Figures 7 through 10. For the entire data set back to 1925, the most serious systematic trend in the residuals occurs in the Capetown observations. The observations for the period 1959-1949 in particular show annual oscillations, especially in the declination residuals, which are not found in other observation series. The amplitude of this oscillation is approximately two to three seconds of arc, and is the cause of the large root-mean-square (r.m.s) of the residuals for that series in Table 7. The results have been communicated to the South Africa observers for their comments.

In order to test the fundamental hypothesis that the observational errors are Gaussianly distributed with zero mean, we have fitted Gaussian distributions to the residuals in right ascension and declination. The parameters in the fit were the amplitude of the Gaussian distribution, the standard deviation, and the mean. The results for all right ascension observations combined are shown in Figure 11, and for declination in Figure 12. The overpopulation of the tails of the distributions relative to the fit is partly caused by the equal a priori standard error assigned for every series being one second of arc. The fit should have been made to the residuals divided by the r.m.s. error for the particular series. The solution for the parameter estimates should have been repeated with each series weighted appropriately. In fact, in the final solution that included observations from 1970 back to 1950 [per Chapter VII], this procedure has been followed. For the set of intermediate parameter estimates in the solution to 1925, this additional step was not taken. For this solution, the mean of the right ascension residual was 0".039 arc, with a standard deviation of 1".01. The corresponding declination values were 0".009 and 1".16 respectively.

The solution from data back to 1925 includes estimation of the values for ΔT' for 1956 to 1925. These results are presented in Figure 13 and illustrate a difficulty with solutions for ΔT' from lunar data alone: a secular trend in ΔT' is highly correlated through the mean motion with the estimate of the semimajor axis of the lunar orbit. A secular trend in ΔT' is also correlated with the estimated values for the multiplicative relativity parameter λ (see Chapter III) and the time variation for the gravitational constant. As we shall see in the next chapter, solutions with the moon and inner planets combined can be used to make a meaningful determination of $\Delta T'$ (provided we are willing to accept $\dot{G}$ or tidal friction from a priori information).

The initial conditions from this converged solution over the 43-year time interval (1925-1968) were used to integrate backward in time from 1968 to 1750. The latter date was chosen as the "break-even point" in the trade-off between decreasing observational accuracy and the increasing sensitivity to long-term trends in the motion.

CHAPTER VII

Solution for Observations from 1750 to 1970; Conclusions

The next step in improving the ephemeris of the moon was the fitting of a much larger data set than that discussed in the previous chapter. The general description of that data set, which includes observations extending back in time to 1750, is given by Tables 8 and 9. Table 8 describes the Surveyor Doppler observations which made up a part of this enlarged data set. The dates on which observations were obtained are within periods in which the Surveyor was in sunlight since the transmitter depended on solar power. Table 9 contains descriptive material on those optical observations which were not described in Chapter VI. The time ordering of the observation series in Table 9 reflect an order dictated by efficiency in computer processing of the observation cards. The bibliographic information for these observations can be found in Appendix 6.

Normal equations for these data were formed using the ephemeris described in Chapter VI. These normal equations were stored on magnetic tape. This system of equations was then augmented by various inner planet normal equation sets, for reasons to be described below, and the total system could

Table 8

SUMMARY OF SURVEYOR COUNTED DOPPLER OBSERVATIONS

Spacecraft	Observing Site	Dates Data Obtained	Total Number of Observations
Surveyor I	DS11	6/3/66 6/5/66-6/16/66 7/7/66-7/8/66 7/13/66	646
	DS42	6/3/66-6/15/66 7/6/66-7/9/66 7/12/66-7/13/66	928
Surveyor III	DS11	4/23/67 5/2/67-5/3/67	9
	DS12	4/25/67	63
	DS42	4/20/67 4/22/67-4/27/67 5/1/67-5/3/67	471
	DS51	4/26/67-4/27/67 4/29/67-4/30/67	122
	DS61	4/20/67 4/22/67-4/28/67 5/1/67-5/3/67	408

Table 8 (Cont.)

Spacecraft	Observing Site	Dates Data Obtained	Total Number of Observations
Surveyor V	DS11	9/11/67-9/13/67 9/16/67-9/24/67	748*
	DS42	9/11/67 9/13/67 9/16/67-9/24/67	1528*
	DS61	9/11/67-9/14/67 9/16/67-9/24/67	3170*
Surveyor VI	DS11	11/10/67-11/25/67	350
	DS42	11/10/67-11/12/67 11/14/67-11/16/67 11/18/67 11/20/67-11/23/67 11/25/67	457
	DS61	11/10/67-11/17/67 11/22/67-11/24/67	489
Surveyor VII	DS11	1/9/68-1/22/68	1604*
	DS42	1/10/68-1/15/68 1/17/68-1/23/68	1759*
	DS61	1/10/68-1/23/68	4651*

*Counting interval is 60 seconds. All others are 300 seconds.

Table 9

Summary of Series for Optical Observations

Observatory	Dates of Observations	Series Name	r.m.s error postfit residuals (sec of arc) r.a.	Decl.
6"U.S.Naval	1900-1903	M300	1.2	1.3
Greenwich	1900-1930	M000	1.8	1.4
Besançon	1908-1922	M790	2.2	4.1
Tokyo	1961-1962	M261	2.5	2.8
	1949-1960	M049*	2.8	2.3
Uccle	1928-1944	M428	2.2	2.3
9"U.S.Naval	1913-1925	M513	1.0	0.9
	1900-1901	M300	1.7	1.3
Greenwich	1931-1954	M531	1.1	1.1
	1905-1930	M300	1.2	0.9
Paris	1903-1904	B491	2.5	1.6
	1902-1902	P250	2.8	1.8
	1900-1906	A691*	2.0	1.6
	1900-1906	C688*	2.6	1.7
	1924-1935	3619	3.2	1.5
	1919-1923	L619*	1.6	4.1

* observations not of the center of the moon at transit of center

Table 9 (Cont.)

Summary of Series for Optical Observations

Observatory	Dates of Observations	Series Name	r.m.s error postfit residuals (sec of arc) r.a.	Decl.
9"U.S.Naval	1894-1899	M994	1.8	1.9
8"U.S.Naval	1866-1891	M166	2.0	2.1
U.S.Naval	1861-1865	M561*	3.0	3.0
Edinburgh	1838-1847	M538	2.3	2.4
Greenwich	1875-1899	M975	1.8	1.6
	1852-1874	M450	2.0	1.8
Strassburg	1888-1893	M388	1.7	1.9
	1882-1888	M882*	1.9	1.9
Greenwich	1836-1851	M131	2.3	2.2
	1831-1835	M131*	3.3	3.0
Besançon	1890-1895	M590	2.0	2.3
Cambridge	1838-1852	M238	2.5	2.2
	1833-1837	M728	3.6	3.2
	1832-1833	M728	3.6	X
Radcliffe	1841-1890	M040	3.0	2.1
Paris	1891-1893	C491*	2.1	1.0
	1850-1887	P250*	2.7	2.8

* observations not of the center of the moon at transit of center
X observable type missing

Table 9 (Cont.)

Summary of Series for Optical Observations

Observatory	Dates of Observations	Series Name	r.m.s error postfit residuals (sec of arc) r.a.	Decl.
Paris	1891-1899	A691*	2.7	2.3
	1887-1890	L087*	2.1	X
	1879-1885	J579*	2.7	2.0
	1888-1899	C688*	3.0	1.5
	1867-1887	G767*	3.0	3.9
	1863-1863	R363*	2.0	X
	1863-1863	S363*	2.0	2.3
	1837-1849	4930*	2.5	3.5
Greenwich	1812-1813	1312*	5.5	6.3
	1825-1830	3025*	3.6	2.7
	1824-1825	2524*	2.7	3.3
	1813-1824	2413*	3.2	4.0
	1800-1812	1000*	3.3	4.4
	1765-1799	0065*	3.4	4.2
	1753-1765	6553*	3.8	4.8
	1750-1753	5350*	4.3	4.9
	1810-1812	1210*	X	3.8
	1831-1831	M131*	3.0	2.0

* observations not of the center of the moon at transit of center

X observable type missing

then be solved using Gauss-Jordan direct elimination. Many solutions were then made for various choices of parameters. One rationale for these different solutions is that the variations in the solutions for the remaining parameters, as we add or subtract other subsets of parameters, give some indications of the systematic errors which are surely present that the formal standard error cannot evaluate. Our parameter solutions were also limited by computer storage to the inversion of a matrix of maximum dimension 375. For similar reasons, the data series which were included were also varied in order to explore the sensitivity of the results in other ways. For example, all observations during the nineteenth century at Paris could be eliminated to see how various parameter solutions depend on the time spanned and the observing program at a particular observatory.

For the purposes of a thesis, this vast collection of information is not well suited for presentation. The process of digesting all the information contained in these solutions is a continuing task which will occupy several years. The principal results, however, can be indicated by studying one particular well-chosen parameter solution which we shall call the nominal solution. The results of the other parameter solution sets will be mentioned at such points as I believe, with my current limited grasp of their full information, that a particular parameter solution or its formal error needs qualification.

This nominal solution is based upon the lunar data described in Tables 7, 8, and 9, plus meridian circle and radar observations of Mercury and Venus, and meridian circle observations of the Sun. These planetary data have been described by Ash et al. (1971) The nominal solution includes the estimation of the parameters for the geodesic precession, the first term in sin 2δ, and the time variation of the gravitational constant. In addition six initial conditions for the moon, for the earth-moon barycenter, for Mercury, and for Venus were estimated. The inclusion of the Surveyor observations made necessary the addition of parameters for the apparent Doppler shift introduced by the neutral atmosphere,* for the locations of the observing stations, and for the selenocentric coordinates of the Surveyor spacecraft . The parameters for $\Delta T'$ ($\equiv$ C.T.-U.T.2) and the optical catalogue orientation parameters were also included in this solution. The phase corrections were separately solved for due to the restrictions on matrix dimension. Other solutions show that the phase

* No model for the ionospheric effects included in nominal solution.

corrections are negligibly correlated with the other parameters of interest.

The values found for these parameters will be discussed below in the somewhat arbitrary order of, firstly, the parameters associated with the Surveyor observations, then the parameters associated with the optical observations, and finally the parameters of general scientific interest. On the basis of this nominal solution, the residuals that would result can be linearly predicted. These resulting residuals have been plotted as a function of time. The graphs of the predicted residuals will be discussed along with the relevant parameter solutions because these residuals are an important measure of the credibility of the solutions. The absence of systematic trends and a Gaussian distribution of the residuals about a zero mean are the required characteristics. As a partial summary of the information in these graphs, the second moments of the residuals on a series-by-series basis are included in Table 9 for the optical observations, and separately in Table 10 for the Surveyor observations.

Let us begin a closer look at the parameter solutions, starting with the Surveyor observations as indicated above. The behavior of the Surveyor residuals is illustrated in Figures 14 through 18. At the frequency of these observations

Table 10

Statistical Analysis of

Predicted Residuals for Surveyor Observations

		Mean (millihertz)	r.m.s. (millihertz)
SUR 1	DSS 11	- 0.22	2.4
	DSS 42	- 0.18	2.5
SUR 3	DSS 12	0.013	0.9
	DSS 42	0.093	6.3
	DSS 61	0.03	9.0
	DSS 51	0.0038	1.5
	DSS 11	2.2	5.0
SUR 5	DSS 11	- 1.8	5.5
	DSS 42	- 0.6	3.5
	DSS 61	- 0.1	42.
SUR 6	DSS 11	- 3.1	7.8
	DSS 61	0.96	3.3
	DSS 42	0.88	2.5
SUR 7	DSS 11	- 2.5	4.5
	DSS 42	- 1.5	3.0
	DSS 61	- 2.2	23.

(2.3×10^9Hz), 1 millimeter per second is equivalent to 15.4 milliHertz. The diurnal signatures remaining in some of the residuals could be due in part to ionospheric effects (maximum of $\sim 8 \times 10^{-3}$Hz) which were not included in this solution. If daytime observations were made (especially near local sunrise) for a particular tracking station, the ionospheric contributions might amount to the signatures present (but a detailed study has not been carried out). A more serious difficulty is the presence of non-zero daily means for several tracking stations, particularly on the later Surveyors. Typically the daily mean was 10 - 20 milliHertz. The contribution of these days is seen, for example, in the r.m.s. for Surveyors 5 and 7 (at DSS 61) in Table 10. The analysis of the Surveryor observations at the Jet Propulsion Laboratory (F. B. Winn, 1968) designates these daily passes of data collectively as "biased data". The origin of the bias is unknown, but is suspected to be instrumental.

Table 11 compares the solution obtained for the lunar locations of the Surveyor transponders with the solutions contained in <u>The Surveyor Project Final Report</u>, Vol. II (F. B. Winn, 1968). The most serious discrepancy is between the selenocentric radii found for Surveyor III - a difference of ~3km. The solution by Winn was constrained to the radius

Table 11

Surveyor Location Solutions Expressed as

Adjustments from JPL Solutions*

		Nominal Solution (± Formal	Standard Error)	JPL Standard Error
SUR 1	Δr, Km	- 0. 47	(± 0.07)	± 1.4
	Δλ, deg	0.038	(± 0.002)	± 0.09
	ΔØ, deg	0.046	(± 0.001)	± 0.06
SUR 3	ΔR, Km	- 3.1	(± 0.3)	± 0.3
	Δλ, deg	- 0.021	(± 0.005)	± 0.005
	ΔØ, deg	- 0.003	(± 0.001)	± 0.011
SUR 5	Δr, Km	0.45	(± 0.37)	± 0.3
	Δλ, deg	0.021	(± 0.005)	± 0.006
	ΔØ, deg	0.056	(± 0.003)	± 0.025
SUR 6	Δr, Km	0.16	(± 0.10)	± 0.84
	Δλ, deg	- 0.012	(± 0.001)	± 0.006
	ΔØ, deg	- 0.023	(± 0.001)	± 0.018
SUR 7	Δr, Km	- 0.28	(± 0.15)	± 0.31
	Δλ, deg	0.006	(± 0.02)	± 0.01
	ΔØ, deg	- 0.0008	(± 0.004)	± 0.008

r = distance from moon center of mass, $\Delta r = r_{MIT} - r_{JPL}$

λ = selenocentric longitude, $\Delta\lambda = \lambda_{MIT} - \lambda_{JPL}$

Ø = selenocentric latitude, $\Delta\phi = \phi_{MIT} - \phi_{JPL}$

* <u>Surveyor Project Final Report, Part II</u>

from the Lunar Aeronautical Charts (LAC) as compiled by the Aeronautical Chart and Information Center (ACIC). We might expect discrepancies of this order because systematic differences of this size exist between radar measurements of lunar topography (Shapiro _et al_., 1972) and the LAC charts. Also a comparison of the other JPL Surveyor solutions with the ACIC control points led to the conclusion that the ACIC datum center is 2.8 ± 0.7 km farther from the Earth than the center of mass (Haines, 1969). The differences between formal standard errors found here and those of Winn partly reflect different weighting given to observation sets. These differences are being currently examined in conjunction with JPL for possible problem areas.

Table 12 compares the solution for the location of the DSN tracking stations with recent JPL solutions (Mottinger, 1970). The agreement in radius and differential longitude is very good; the absolute longitudes show a large systematic discrepancy of magnitude 4.65×10^{-4} degrees. ($\sim$ 46 meters on the earth's surface). The JPL longitudes place the locations to the east of the M.I.T. determined locations. Recent comparisons between JPL and Smithsonian Astrophysical Observatory (SAO) solutions for the tracking station locations (Gaposchkin and Lambeck, 1970) yielded a systematic longitude difference of 2.3×10^{-4} degrees, with JPL location to the

Table 12

Comparison of DSN Station Location Solutions

Station		Nominal Solution (± formal standard error)	JPL LS24* (no Ionospheric Corrections)	JPL LS25* (With Ionosphere)
DSS 11 Pioneer	R_s, Km	5206.3388 (1.5×10^{-4})	5206.3381	5206.3419
	$\Delta\lambda$, deg	- 0.04395981 (5.1×10^{-6})	- 0.043930	- 0.043931
	Z, Km	3673.853 (1.6×10^{-2})	3673.759+	3673.763+
DSS 12 Echo	R_s, Km	5212.0511 (9.0×10^{-4})	5212.0497	5212.0535
	$\Delta\lambda$, deg	—	—	—
DSS 42 Weemala	R_s, Km	5205.3496 (1.2×10^{-4})	5205.3497	5205.3504
	$\Delta\lambda$, deg	- 94.213245 (2.6×10^{-6})	- 94.21326	- 94.213258
	Z, Km	- 3674.485 (5.3×10^{-3})	- 3674.628+	- 3674.646+
DSS 51 Johannesburg	R_s, Km	5742.9452 (7.3×10^{-4})	5742.9412	5742.9417
	$\Delta\lambda$, deg	-215.509158 (4.2×10^{-6})	-215.50915	- 215.509127
DSS 61 Robledo	R_s, Km	4862.6056 (1.9×10^{-4})	4862.6044	4862.6078
	$\Delta\lambda$, deg	112.556477 (2.8×10^{-6})	112.55646	112.556448

* Mottinger, 1970. Assigned formal standard errors are two meters in R_s and five meters in λ.

+ geodetic values, not in solution

east of the SAO locations. One possible explanation would be different origins of the right ascension system (the vernal equinox) in the various reductions of the data. The systematic longitude difference cannot be ascribed to the different U.T. 1 time systems used, as the comparison given in Table 13 shows. (A ten milli-second difference leads to $\sim 4.6 \times 10^{-5}$ degree change in longitude.)

Solutions for the Z components of station location (distance along spin axis) were made only for DSS 11 and 42 since all Surveyors had observations at these stations. Systematic differences compared with geodetic values exist in the solutions for position along the spin axis. These differences may be due to further rotational orientation differences between the star catalogues used, to different implicit definitions for the location of the center of mass of the earth, or to data biases, etc. Differences of similar magnitude exist between the North American Datum and the 1969 Smithsonian Standard Earth (Lambeck, 1971). Lambeck solves for the relationship between the NAD and the SSE by seven parameters: three translations, three rotations, and a scale change. The translational differences are the largest:

Table 13

Comparisons of Time Systems of Different Organizations

	MIT C.T. - U.T.C.	JPL E.T. - U.T.C.	BIH A.1.+32.15-U.T.C.
July 21, 1967	37.9684 sec	37.965 sec	37.9289 sec
Sept. 16, 1967	38.1149 sec	38.111 sec	38.078 sec
	MIT U.T.1 - U.T.C.	JPL U.T.1. - U.T.C.	BIH U.T.1 - U.T.C.
July 21, 1967	57. 8 milliseconds	66. milliseconds	52.2 milliseconds
Sept. 16, 1967	97.4 milliseconds	94. milliseconds	95.5 milliseconds

$$\Delta X = - \quad 31.8 \text{ meters}$$

$$\Delta Y = \quad 178.0 \text{ meters}$$

$$\Delta Z = \quad 177.6 \text{ meters}$$

The solutions for the Z-component of the station locations made in this thesis from the Surveyor data are not sufficiently numerous for any conclusions to be drawn as yet. The star catalogues' orientation parameters (see below) could easily account for the longitude bias; the Z-component differences are too large by a factor of three to be attributed to uncertanties in these parameters. The problem of these systematic biases needs further investigation.

The atmospheric corrections for the principal solution described here consisted only of tropospheric parameters for the zenith range. The values for the zenith range in meters from the solution are given in Table 14. These results have been compared with the average ranges computed from radiosonde balloon data (Ondrasik and Thuleen, 1970). The results from the Surveyor reductions were within twenty per cent for about half of the determinations. These results are given graphically in Figure 19. The anomalous results for Surveyor III at DSS 61 may be partly a compensation for a large ionospheric contribution (since the ionospheric effect on phase delay has the opposite sign from the tropospheric correction). The generally

Table 14

Zenith Tropospheric Thickness

ℓ_Z from Surveyor Solutions

Spacecraft	Tracking Station	ℓ_Z (meters) (formal standard error)	
Surveyor I	DSS 11	2.00	(.008)
	DSS 42	2.31	(.03)
Surveyor III	DSS 11	2.09	(.03)
	DSS 42	2.70	(.03)
	DSS 51	2.10	(.2)
	DSS 12	2.09	(.07)
	DSS 61	1.39	(.02)
Surveyor V	DSS 11	1.99	(.08)
	DSS 42	2.26	(.1)
	DSS 61	1.93	(.05)
Surveyor VI	DSS 11	1.99	(1.2)
	DSS 42	1.88	(.02)
	DSS 61	2.39	(.04)
Surveyor VII	DSS 11	1.94	(1.2)
	DSS 42	1.95	(.009)
	DSS 61	2.09	(.02)

smaller than measured ranges may be a manifestation of the same effect.

Now let us turn to an examination of the meridian circle observations and of the other related parameters. The predicted residuals for the optical observations are given in Figures 20 to 24. Note that, in Figure 24, the scale is approximately fifty percent larger than on the other figures for optical observations. The statistics for the optical observations were detailed in Table 9. The revised observatory positions used to obtain the corrections for parallax and time of meridian passage of the center (made via the formulae given in Chapter III) are shown in Table 15. The orientation parameters of the star catalogues for the observation series for which the adjustments were large multiples of their formal errors (hence statistically significant) are presented in Table 16. Note that the values for ΔE, ΔI, and $\Delta \emptyset'$ for the U.S. Naval series from 1925 to 1969 gives the differential orientation of the FK4 axes with respect to our inertial system which is defined by the totality of the observations. (This identification is true in so far as the reduction of the U.S.N.O. observations to the FK4 was complete and accurate.) Interpreted as distance on the surface of the earth, these adjustments amount to 25 meters in the equinox,

Table 15

Observatory Coordinates Used for

Non-Standard Observation Series

	ρ	θ	ϕ'
Radcliffe	6365.095	1.2516667 deg	51°.572505
Tokyo	6370.997	- 139.54075	35°.49038
U.S. Naval Observatory Series Name M561	6369.874	77.06554167	38°.73332
Greenwich	6365.371	0.0	50°.682965

ρ = geocentric radius in kilometers (a_e = 6378.166 Km)

θ = longitude in degrees

ϕ' = geocentric latitude in degrees

Table 16

Sample Solutions for Star Calalogue

Orientations for Moon Series

The numbers in parentheses are the magnitude of the adjustment in units of their formal standard errors.

	ΔE (sec of time)		ΔI (sec of arc)		Δ∅ (sec of arc)	
6 USN M925	5.8×10^{-2}	(34)	2.4×10^{-1}	(13)	-3.2×10^{-1}	(26)
Gren M431	6.2×10^{-2}	(24)	-3.9×10^{-1}	(10)	-6.1×10^{-1}	(23)
Gren 0065	3.8×10^{-2}	(11)	-1.7×10^{-2}	(0.7)	-2.32×10^{-1}	(14)
6 USN M300	4.34×10^{-2}	(11)	4.6×10^{-1}	(7)	-1.	(22)
Gren M000	4.99×10^{-2}	(22)	2.1×10^{-1}	(8)	-0.9	(50.2)
9 USN M513	9.2×10^{-3}	(3)	4.5×10^{-1}	(11)	-0.8	(28)

$\sim$ 7 meters in the equatorial adjustment and $\sim$10 meters in the latitude bias.

Observations of the inner planets were included in the nominal solution because a meaningful solution for a possibly changing gravitational constant and $\Delta T'$ cannot be determined from the moon alone, as we shall see below. The credibility of the solution is tested by the magnitudes of the adjustments to the inner planet parameters since the inner planet nominal values are based upon quite well converged solutions for these parameters from the solution involving the planet data alone (Ash et al., 1971). Table 17 gives the adjustments found for the initial conditions for the planets. Comparison with other solutions made by adjusting different parameters and/or omitting various data sets leads to the conclusion that the adjustments to the inner planet orbital elements are controlled almost completely by the radar data when included. The optical data alone for the inner planets, with or without the moon data included, do not produce adjustments to inner planet orbital elements similar to the radar values no matter what parameters are adjusted for all cases tried.* These results warn of the presence of systematic errors in the optical data. Table 18 gives the osculating orbital

* The differences in these adjustments are large compared to the formal errors of the solution.

Table 17

Inner Planet Solution Parameters Expressed as Adjustments from Input Values

(Numbers in parentheses are the magnitudes of adjustments in units of their formal standard errors.)

Body	Δa (A.U*)	Δe	Δi(deg)	$\Delta\Omega$(deg)	$\Delta\omega$(deg)	ΔM_0(deg)
☿ †	-7.4×10^{-10} (7.4)	-8.2×10^{-9} (3.9)	6.3×10^{-5} (2.9)	-3.3×10^{-5} (2.0)	9.0×10^{-5} (8.4)	-2.5×10^{-7} (0.4)
♀	-3.2×10^{-9} (15.)	3.2×10^{-9} (3.7)	6.1×10^{-5} (2.8)	-5.8×10^{-5} (3.8)	2.2×10^{-4} (17.)	-1.1×10^{-4} (14.)
Earth-Moon Bary-center	-7.1×10^{-9} (24.)	-9.6×10^{-10} (-1.1)	6.4×10^{-5} (3.0)	-4.6×10^{-5} (3.0)	1.3×10^{-4} (18.)	-3.0×10^{-5} (10.)

† Mass ☿ solution: 6,032,779 ± 2000 inverse solar masses

* Astronomical Unit in light-seconds solution: 499.0047940 ± .0000005

Table 18

Moon Initial Conditions from Nominal Solution at

Epoch J.E.D. 2440000.5

a	0.0025715142099	A.U.	$(\pm\ 5.\mathrm{x}10^{-12})$*
e	0.055615887		$(\pm\ 4.\mathrm{x}10^{-8})$*
i	28.3968891	deg.	$(\pm\ 8.\mathrm{x}10^{-7})$*
Ω	3.3128778	deg.	$(\pm\ 9.\mathrm{x}10^{-6})$*
ω	226.270822	deg.	$(\pm\ 1.\mathrm{x}10^{-5})$*
M_0	154.885985	deg.	$(\pm\ 1.\mathrm{x}10^{-5})$*

* formal standard error

elements at epoch for the moon which are associated with the nominal solution. The next lunar ephemeris used in continuing this work should be generated with these starting conditions.

Now let us turn to the estimation of the parameters of particular interest in this work: those for geodesic precession, a time varying gravitational constant, and tidal friction. The estimation of $\Delta T'$ will also be crucial here. To understand all these results, a digression on previous methods of estimating these quantities will be necessary.

For any body b in the solar system, comparison of the mean longitude of the body from the ephemeris (as a function of coordinate time) to the observed mean longitude (as a function of universal time) gives a difference which is found empirically to grow quadratically with time:

$$\Delta L_b = A_b + B_b\tau + C_b\tau^2$$

where τ is coordinate time. This (non-zero) value found for ΔL_b has the following possible theoretical interpretation:

$$2C_b = \dot{n}_b - n_b\left(\frac{\dot{\Omega}}{\Omega}\right)$$

where $\dot{n}_b$ is an (assumed constant) rate of change of the mean motion n_b, and $\dot{\Omega}$ is an (assumed constant) variation in the earth's rotation rate Ω. We may compare two different bodies as follows:

$$(\Delta\ddot{L})_1 - \frac{n_1}{n_2}(\Delta\ddot{L})_2 = \dot{n}_1 - n_1\frac{\dot{\Omega}}{\Omega} - \frac{n_1}{n_2}\dot{n}_2 + n_1\frac{\dot{\Omega}}{\Omega}$$

$$= \dot{n}_1 - \frac{n_1}{n_2}\dot{n}_2 \equiv \Delta_{12}$$

By comparing the moon to the inner planets and the sun, the quantities, $\Delta_{☾p}$ were found to be quite independent of the planet p involved. Since the ratios $n_{☾}/n_p$ are very large, the values of $\dot{n}_p$ must be negligible (it was argued). On this assumption, the $\Delta_{☾p}$ give $\dot{n}_{☾}$. This rate of change of the mean motion can be expressed in terms of the tidal friction parameter sin 2δ. The measured quantities

$$\frac{1}{n_p}\Delta\ddot{L}_p = \frac{\dot{n}_p}{n_p} - \frac{\dot{\Omega}}{\Omega}$$

should give $\dot{\Omega}/\Omega$ since $\dot{n}_p$ is assumed to be zero. Then ΔT is found from

$$\Delta T(t) = \int_{\tau = t_0}^{\tau = t} d\tau \int_0^{\tau} \dot{\Omega}(t')dt'$$

If the concept of a changing gravitational constant is introduced, the picture becomes more complex. For any planet, a rate of change of the mean motion caused by the variation in G is given by:

$$\frac{\dot{n}_p}{n_p} = 2\,\frac{\dot{G}}{G}$$

as follows from Kepler's law and conservation of orbital angular momentum. For the moon (ignoring other torques), a rate of change $\dot{G}/G = -3 \times 10^{-11}\ \text{yr}^{-1}$ causes a change of

$$\dot{n}_{☾} = -10''\ \text{century}^{-1}$$

or about half of the currently believed value due to tidal friction. Thus we see that the fact that $\Delta_{☾p}$ is independent of p does not give a unique value for $\dot{n}_{☾}$. The problem of determining $\dot{G}/G$, $\dot{\Omega}/\Omega$, and $\dot{n}_{☾}$ becomes one of determining three unknowns from the two equations of $\Delta_{☾p}$ and $\Delta\ddot{L}_p$. (Mercury and Venus do not separately provide independent equations because the data are not numerous enough for the accuracy required.)

With these remarks as background, let us discuss the results for the parameters given in Table 19. The results in this table for $\dot{\Omega}/\Omega$ are derived from the result for $\Delta T'$ as follows. The table of ΔT given by Brouwer depends on the expression for Ephemeris Time which has a value for $\dot{n}$ incorporated. In order to relate $\Delta T'$ to ΔT, allowance must be made for the difference in $\dot{n}_{☾}$ in the two results via

$$\delta(\Delta T) = 20.44 \left(\frac{\sin 2\delta}{0.0755} - 1\right)T^2$$

where T is in centuries. This correction is due to the T^2 term assumed by Brouwer in the moon's mean motion. After allowing for this difference, any residual T^2 coefficient is assumed due to $\dot{\Omega}/\Omega$. As expected from our discussion above, no unique determination of sin 2δ, $\dot{G}/G$, and $\Delta T'$ is possible. Different solutions are obtained for the parameters depending upon the parameter set adjusted. The result for the geodesic precession, however, is quite independent of the solution for these quantities. A qualitative understanding of this uncoupling can be reached by considering the observable quantities from which these parameters are determined. The mean longitude of the moon, as explained above, contains the primary information concerning $\dot{G}$, tidal friction, and $\Delta T'$. The geodesic precession, on the other hand, is principally determined through the motion of the node and perigee of the lunar orbit. Therefore we can expect the solution for the geodesic precession to be meaningful in spite of possible problems with quantities associated with the mean longitude.

The nominal solution for $\Delta T'$ is plotted in Figure 25. Except for the expected difference which grows quadratically

Table 19
Results

	Classical solution (in national ephemerides)	Solution with moon data, inner planet optical and radar data	Solution with moon data, inner planet optical data	Solution with moon data, inner planet optical and radar data
$\frac{\dot{G}}{G}$	0	Not in solution	Not in solution	-3.3×10^{-11} $\pm0.3\times10^{-11}$ per year
sin 2δ	0.0755	0.046 ±0.004	0.054 ±0.004	0.105 ±0.005
$(\frac{\dot{\Omega}}{\Omega})_{resid}$	0	-0.3×10^{-10} $\pm.05\times10^{-10}$ per year	-1.0×10^{-10} $\pm0.2\times10^{-10}$ per year	-0.1×10^{-10} $\pm.03\times10^{-10}$ per year
Centennial geodesic precession	1".92*	1".4 ± 0".25	1".55 ± 0".25	1".4 ± 0".25

*General relativistic value, 1".83 in current version of Brans-Dicke theory for $\omega = 6$.

with time, the general oscillations of $\Delta T'$ and the ΔT of Brouwer agree remarkably well.*

The errors quoted in Table 19 are the formal standard errors from the solution. The uncertainty in the result for the geodesic precession should also reflect the uncertainty in the gravitational harmonics of the moon. The contribution from this source can only be estimated, but a reasonable value is $0''.25$ century^{-1}. Combining the formal error with this and doubling the result yields a conservative estimate of the actual error of $0''.6$ century^{-1}.

Comparison of the solutions for various parameter sets allows us to place the following limits on the parameters involved:

$$0.03 < \sin 2\delta < 0.11$$

$$\left|\frac{\dot{G}}{G}\right| < 6 \times 10^{-11} \text{ yr}^{-1}$$

$$\left(\frac{\dot{\Omega}}{\Omega}\right) > -2 \times 10^{-10} \text{ yr}^{-1}$$

The geodesic precession is found to be

$$1''.5 \pm 0''.6 \text{ century}^{-1}$$

The solutions in Table 19 assume that general relativity is correct for the inner planets. Relaxing this constraint, we estimated the multiplicative factor for general relativity

*The seasonal variations ΔS.V. were not well determined from our data. The nominal solution holds these parameters at the values described in Ch. II.

λ_r for both the moon and the inner planets combined. The solutions for λ_r ranged from (0.995 ± 0.006) to (1.003 ± 0.006), where 1.000 would indicate that general relativity is correct. (J_2 for the sun was fixed at zero in these solutions so this result can shed no light on Dicke vs. Einstein, except in a model-dependent way.)

Any conclusions based on the solutions discussed in this thesis must be regarded as tentative, due to the following modeling and procedural problem areas. Firstly and probably most importantly, the solutions are not fully converged on the true maximum likelihood estimate since no iterations have been performed. Therefore the first step in any future work with these lunar data must be reintegrating the motion of the moon, recomputing the residuals, and forming new normal equations. The second problem area concerns the modeling of the motion of the observational coordinate system with respect to inertial space. As discussed in Chapter I, this motion has been parameterized as three rotations about orthogonal axes. The solutions discussed above do not include any attempts to solve for these parameters. Inclusion of these parameters in the next iteration may cause significant changes in the solutions.

As has been discussed above, the solutions obtained here contain indications of systematic errors of various types. Until the origins of these errors are better understood, we must be very cautious in the interpretation of the results here. Some of the questions concerning systematic errors can be approached by comparison of results obtained using different data types. Two data types come to mind immediately: laser ranging observations and stellar occultations by the moon.

The stellar occultation data were originally intended to form a part of this work and the calculation of the observable from the theory is checked out. The normal equations cannot be used, however, because the partial derivatives of the observable with respect to many parameter types have not yet been checked numerically for consistency with the observable itself. Work in this area is continuing.

The laser ranging data could have been processed by PEP for this thesis. At the time of this work, however, the availability of the data was restricted to members of the LURE team. These data should clearly be incorporated as quickly as possible into the solutions. The accuracy of the laser observations will require the eventual improvement of the model for the rotation of the moon about its center of mass. Within the context of PEP the logical direction for this improvement would be the numerical integration of these equations of motion. The knowledge of rotation of the earth about its center of mass is another area which will soon be inadequate for treatment of the laser data. Estimation of the Chandler wobble, solid earth tides, continental drift etc. will be necessary. All these effects to be modelled will degrade the sensitivity of the laser data to the parameters of fundamental physical interest such as the time variation of G unless other methods of estimating the same effects can be brought to bear. Parallel monitoring of these motions by a technique of comparable accuracy - Very Long Baseline Interferometry - would be highly desirable.

Index of Symbols

The following general principles have been adhered to in designating the various physical quantities. Vectors -- a magnitude and direction independent of coordinate system -- have been denoted by an arrow above the symbol (e.g. $\vec{X}$). A 3x1 matrix of components of a vector in some particular coordinate system are designated by a tilde under the symbol (e.g. $\utilde{x}$). Other matrices have their symbol underlined (e.g. $\underline{P}$). A dot above a letter denoted differentiation with respect to time. Subscripts 0 frequently indicate initial values.

The following index is not intended to be complete. Those symbols which are important or which may be ambiguous have been included. For those symbols which have multiple definition, it is hoped that the context will be sufficiently clear that no confusion will result.

A	coefficient of forces in tidal friction model
a	semi-major axis of ellipses
a_i, c_i	time-independent amplitudes of trigonometric seasonal variations in earth rotation
b_i, d_i	time-dependent amplitudes of seasonal variations in earth rotation
$\underline{B}$	moon rotation matrix
c	speed of light in vacuum
c_{ij}	correlation coefficients
$c_{\ell m}, s_{\ell m}$	coefficients in expansion of gravitational field in spherical harmonics.

D	term in lunar tidal friction model
$D(t)$	term in C.T.-A.1
D_c	counting interval
ds^2	line element in general relativity
e	eccentricity of elliptic orbit
$\underline{F}$	rotation matrix for the Earth about its center of mass
f_0	transmitter frequency
G	gravitational constant
g_{ij}	components of metric tensor
$\vec{H}$	acceleration on the moon due to the harmonics in lunar gravitational potential
I	inclination of mean lunar equator to the ecliptic
I_{ij}	components of inertia tensor
J_n	coefficient of zonal harmonics
K_2	Love number
L	semi-latus rectum of ellipse
ℓ_0	mean anomaly at epoch
ℓ_Z	atmospheric delay in zenith direction (converted to distance)
$M(t)$	term in C.T.-A.1.
M_E	mass of earth
M_j	mass of j^{th} planet
M_M	mass of the moon
$M_\odot$	mass of the sun
$\underline{N}$	nutation matrix

N_0, N_e	integrated electron content of ionosphere
$\vec{n}$	lunar orbital angular velocity vector
n	mean motion of the moon
O	observable quantity
$\vec{P}$	force on moon due to planets other than the earth
$\underline{P}$	precession matrix
$P_n, P_{\ell m}$	Legendre functions
$\vec{Q}$	acceleration of moon due to earth gravitational harmonics
Q	quality factor for the earth
$\vec{R}$	acceleration of moon due to general relativistic effects
R	radial acceleration of the moon due to tidal friction
S	acceleration of the moon due to tidal friction in the plane of the mean lunar orbit
s	sidereal time
T	as superscript, matrix transpose
$\vec{T}$	acceleration on moon due to tidal friction in earth-moon system
$T^{\mu\upsilon}$	energy-momentum tensor
t	universal time
t	coordinate time
t_i	point in AT' model at which a slope change occurs
t_0	some initial epoch

$\underline{U}$	the matrix $\underline{P}^T\underline{N}^T\underline{F}^T\underline{W}^T$
U	gravitational potential
$\vec{V}$	acceleration of moon due to time varying gravitational constant
$\underline{W}$	wobble (polar motion) matrix
W	acceleration of the moon due to tidal friction normal to the mean lunar orbit
w	angle in precession matrix
Y	vector in numerical integration
Y(t)	term in C.T.-A.1.
y_i	value of $\Delta T'$ at t_i
z	angle in precession matrix

α	right ascension
α	parameter in Robertson metric
β	parameter in Robertson metric
γ	parameter in Robertson metric
$\Delta\epsilon$	nutation is obliquity
$\Delta\Psi$	nutation in longitude
$\Delta T'$	coordinate time minus universal time U.T.2
δ	lag angle in tidal friction model
ϵ	obliquity of the ecliptic
Θ	apparent sidereal time
λ	geocentric longitude
λ	element of wobble matrix
μ	the combination GM
μ	element of wobble matrix
ν_{43}	transition in cesium - 133 defining A-1 second
Ξ	angular velocity of orbital angular momentum precession
$\vec{\xi}$	vector potential derived from $T^{\mu\nu}$
ξ_o	angle in precession matrix
π	lunar parallax
ρ	physical libration in inclination of moon
Σ	moon rotation matrix
σ	physical libration in the moon's node
τ	coordinate time
τ	proper time in general relations
τ	time delay
ϕ	scalar potential derived from $T^{\mu\nu}$
Ψ	$\Omega + \sigma$

Ω	longitude of mean ascending node of lunar orbit measured on the ecliptic from mean equinox of date
$\vec{\Omega}$	earth angular velocity
Ω	magnitude of $\vec{\Omega}$
ω	relative angular velocity vector between two coordinate systems
ω	argument of perigee of lunar orbit

Special Symbols

☉	sun
☿	Mercury
♀	Venus
⊕	Earth
♂	Mars
☾	The mean longitude of the moon; as a subscript, denotes a quantity associated with the moon.

Figure Captions

Figure 1. Schematic Illustration of Model for C.T.-U.T.2

Figure 2. Osculating Orbital Elements for the Moon as a Function of Time, with Newtonian Gravitational Interaction Only between Centers of Mass (Expressed as differences from elements at epoch).

Figure 3. Osculating Orbital Elements as a Function of Time with General Relativistic Gravitational Perturbations of the Sun Affecting the Moon-No Direct Solar Perturbations.

Figure 4. Coordinate System and Vector Used in Tidal Friction Calculation

Figure 5. Osculating Lunar Orbital Elements with Tidal Friction and Newtonian Interactions Affect the Lunar Motions

Figure 6. Osculating Orbital Elements for the Lunar Motion Affected by Newtonian Interaction and a Changing Gravitational Constant.

Figure 7. Right Ascension Residuals for the U.S. Naval Observatory with the Ephemeris of Chapter VI.

Figure 8. Declination Residuals for the U.S. Naval Observatory with the Ephemeris of Chapter VI.

Figure 9. Right Ascension Residuals for the Royal Greenwich Observatory with the Ephemeris of Chapter VI.

Figure 10. Declination Residuals for the Royal Greenwich Observatory with the Ephemeris of Chapter VI.

Figure 11. Gaussian Distribution Fitted to Right Ascension Residuals from Fit for 1925-to 1968.

Figure 12. Gaussian Distribution Fitted to Declination

Figure 13. Solution for $\Delta T'$ from Data for Period 1925-1968.

Figure 14. Predicted Residuals for Surveyor I from Nominal Solution from 1970 to 1750.

Figure 15. Predicted Residuals for Surveyor III from Nominal Solution from 1970 to 1750.

Figure 16. Predicted Residuals for Surveyor V from Nominal Solution from 1970 to 1750.

Figure 17. Predicted Residuals for Surveyor VI from Nominal Solution from 1970 to 1750..

Figure 18. Predicted Residuals for Surveyor VII from Nominal Solution from 1970 to 1750.

Figure 19. Zenith Range through Troposphere for Surveyor Solutions (Nominal for Period 1970 to 1750).

Figure 20. Predicted Meridian Circle Residuals for the Period 1970 to 1900, Part A.
For ease of reading Figures, here is table of Julian Day Numbers

1750	2360234	1950	2433282
1800	2378496	1955	2435108
1850	2396758	1960	2436934
1900	2415020	1965	2438761
1925	2424151	1970	2440587

Figure 21. Predicted Meridian Circle Residuals for Period 1970-1900; Part B (Nominal Solution)

Figure 22. Predicted Meridian Circle Residuals for Period 1900-1830; Part A (Nominal Solution)

Figure 23. Predicted Meridian Circle Residuals for Period 1900-1830; Part B

Figure 24 Predicted Meridian Circle Residuals for Period 1830-1750.

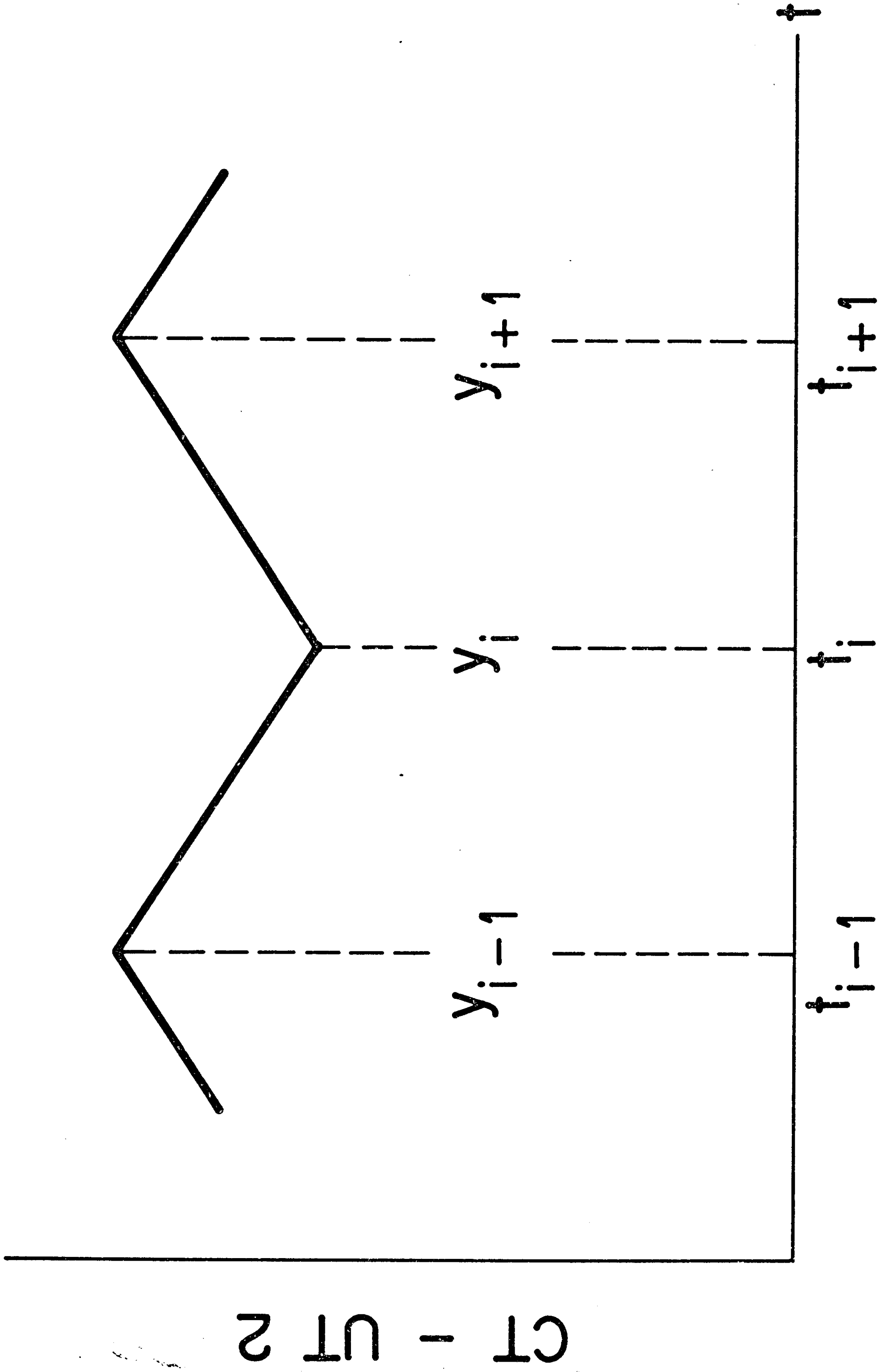

Figure 1.

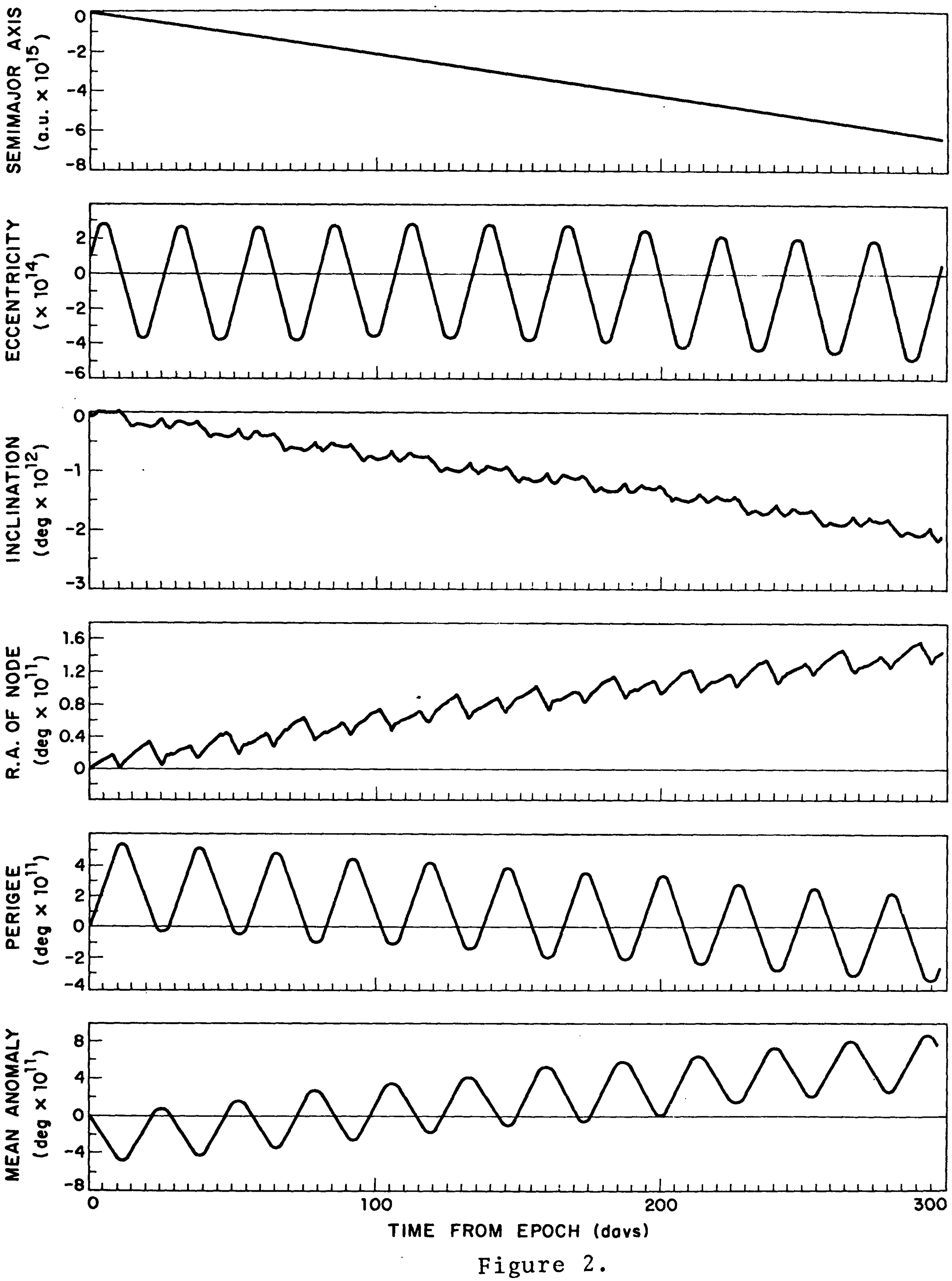
SEMIMAJOR AXIS (a.u. × 10^15)
0
-2
-4
-6
-8
ECCENTRICITY (× 10^14)
2
0
-2
-4
-6
INCLINATION (deg × 10^12)
0
-1
-2
-3
R.A. OF NODE (deg × 10^11)
1.6
1.2
0.8
0.4
0
PERIGEE (deg × 10^11)
4
2
0
-2
-4
MEAN ANOMALY (deg × 10^11)
8
4
0
-4
-8
0
100
200
300
TIME FROM EPOCH (days)

Figure 2.

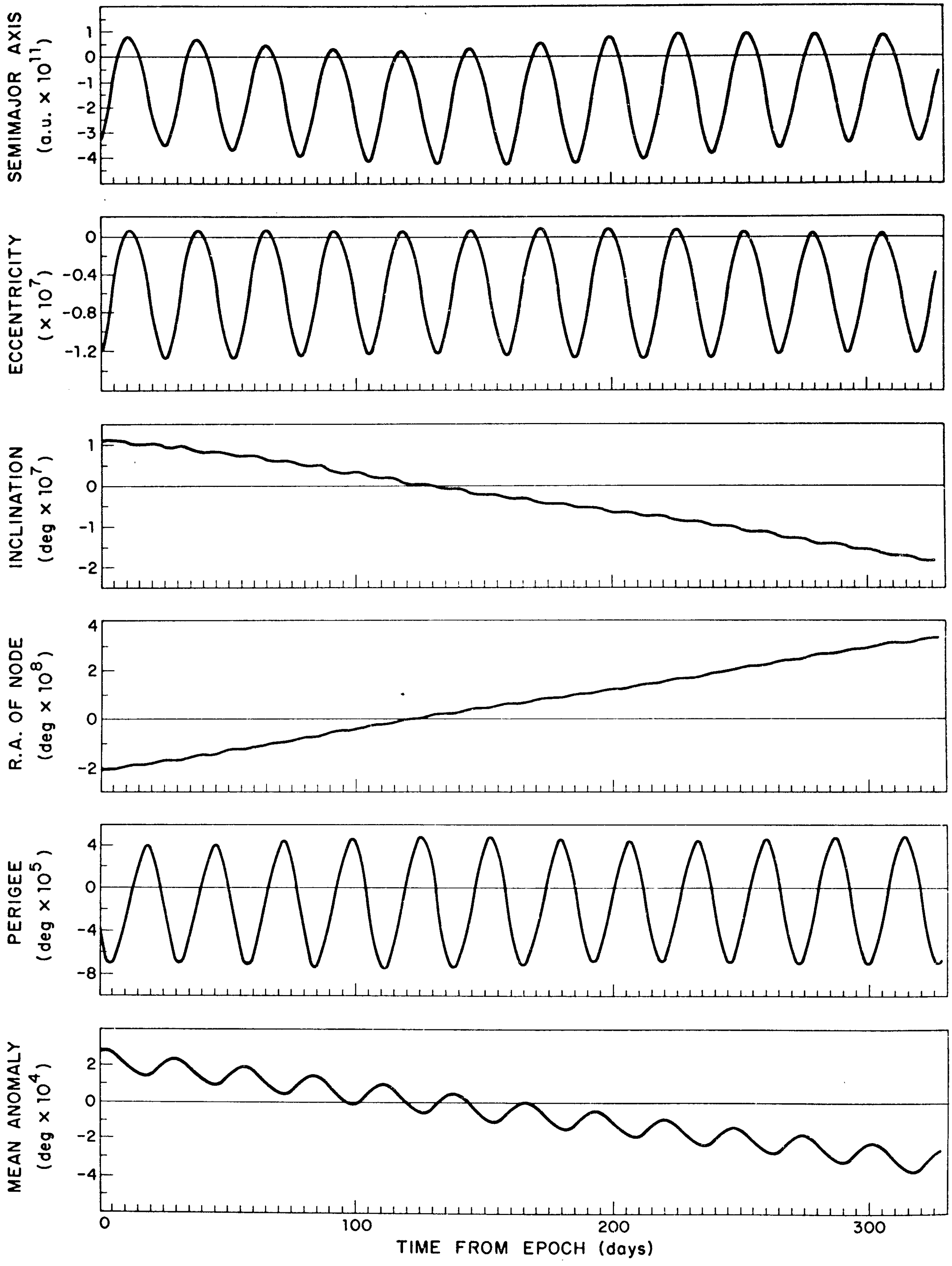
SEMIMAJOR AXIS (a.u. × 10^11)
1
0
-1
-2
-3
-4
ECCENTRICITY (× 10^7)
0
-0.4
-0.8
-1.2
INCLINATION (deg × 10^7)
1
0
-1
-2
R.A. OF NODE (deg × 10^8)
4
2
0
-2
PERIGEE (deg × 10^5)
4
0
-4
-8
MEAN ANOMALY (deg × 10^4)
2
0
-2
-4
0
100
200
300
TIME FROM EPOCH (days)

Figure 3.

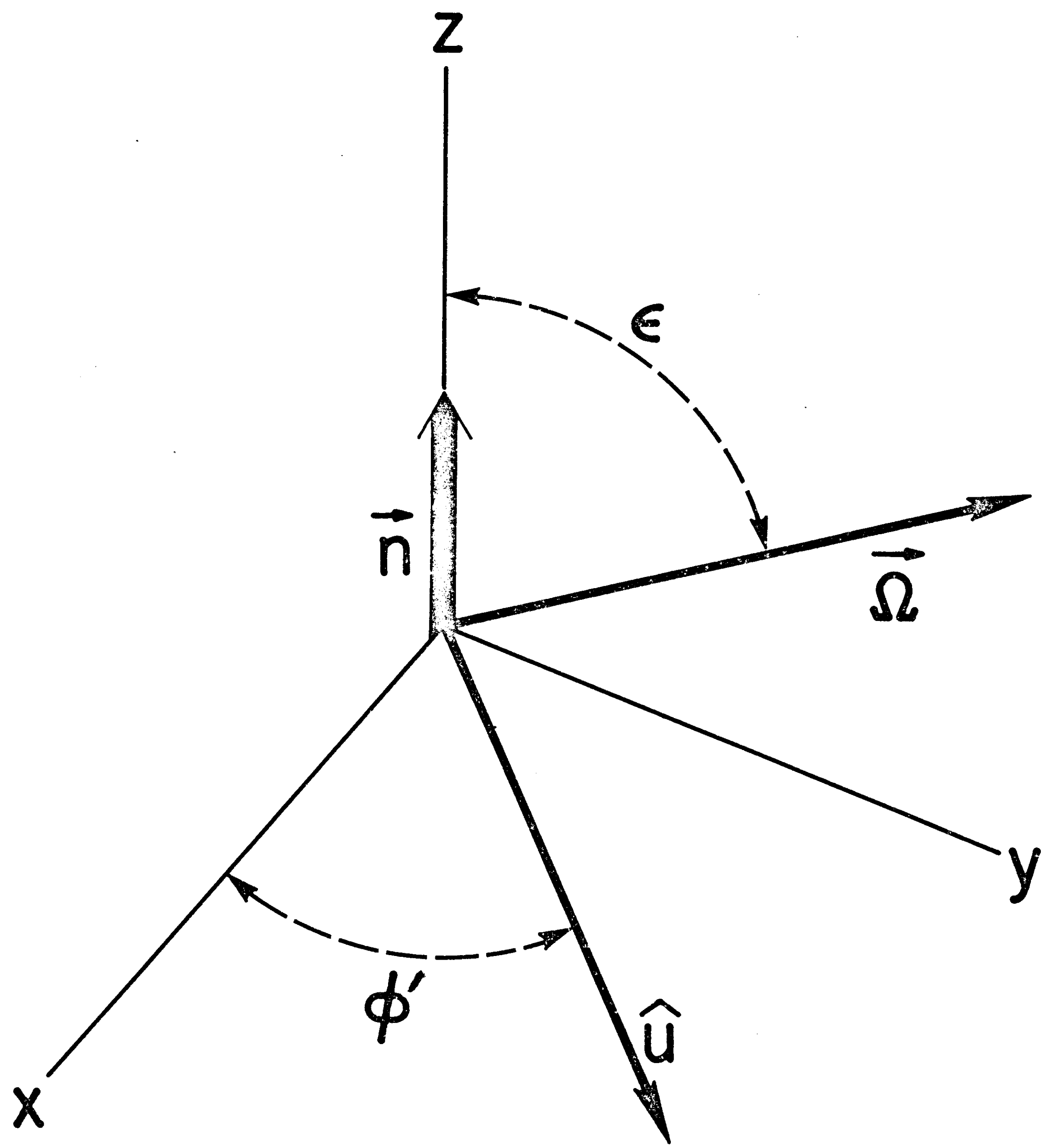

Figure 4.

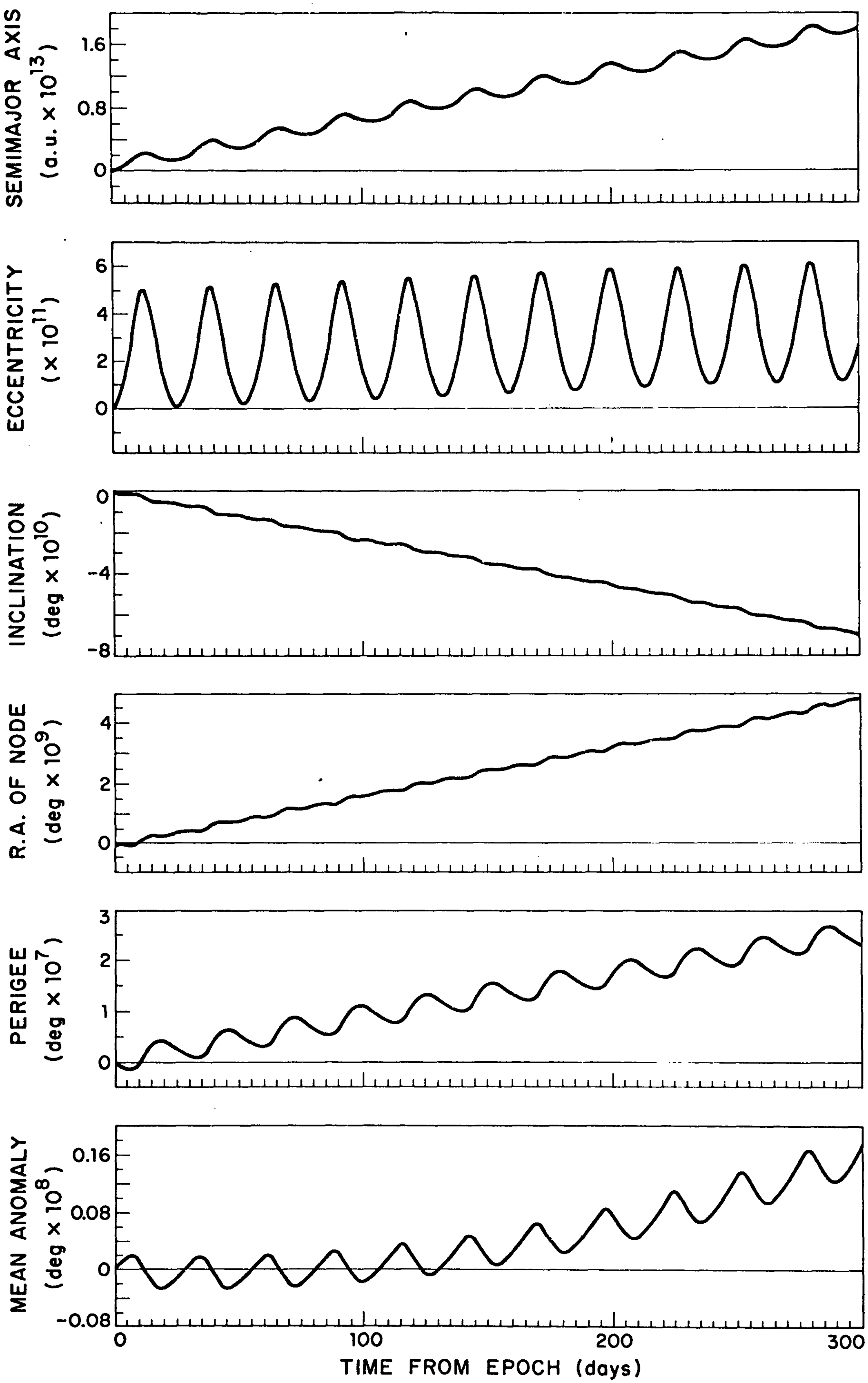
SEMIMAJOR AXIS
(a.u. × 10^13)
1.6
0.8
0
ECCENTRICITY
(× 10^11)
6
4
2
0
INCLINATION
(deg × 10^10)
0
-4
-8
R.A. OF NODE
(deg × 10^9)
4
2
0
PERIGEE
(deg × 10^7)
3
2
1
0
MEAN ANOMALY
(deg × 10^8)
0.16
0.08
0
-0.08
0
100
200
300
TIME FROM EPOCH (days)

Figure 5.

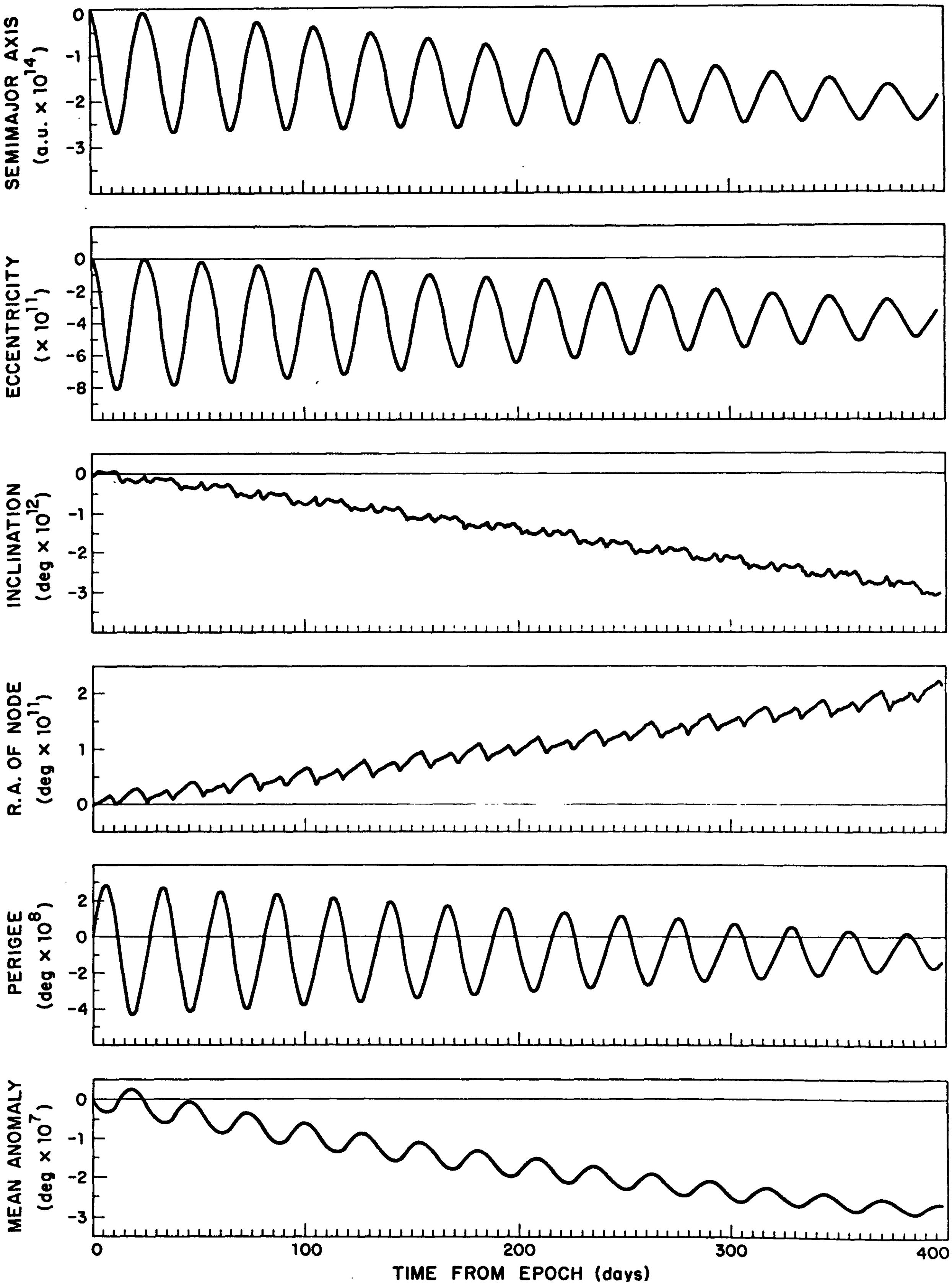
SEMIMAJOR AXIS (a.u. × 10^14)
0
-1
-2
-3
ECCENTRICITY (× 10^11)
0
-2
-4
-6
-8
INCLINATION (deg × 10^12)
0
-1
-2
-3
R.A. OF NODE (deg × 10^11)
2
1
0
PERIGEE (deg × 10^8)
2
0
-2
-4
MEAN ANOMALY (deg × 10^7)
0
-1
-2
-3
0
100
200
300
400
TIME FROM EPOCH (days)

Figure 6.

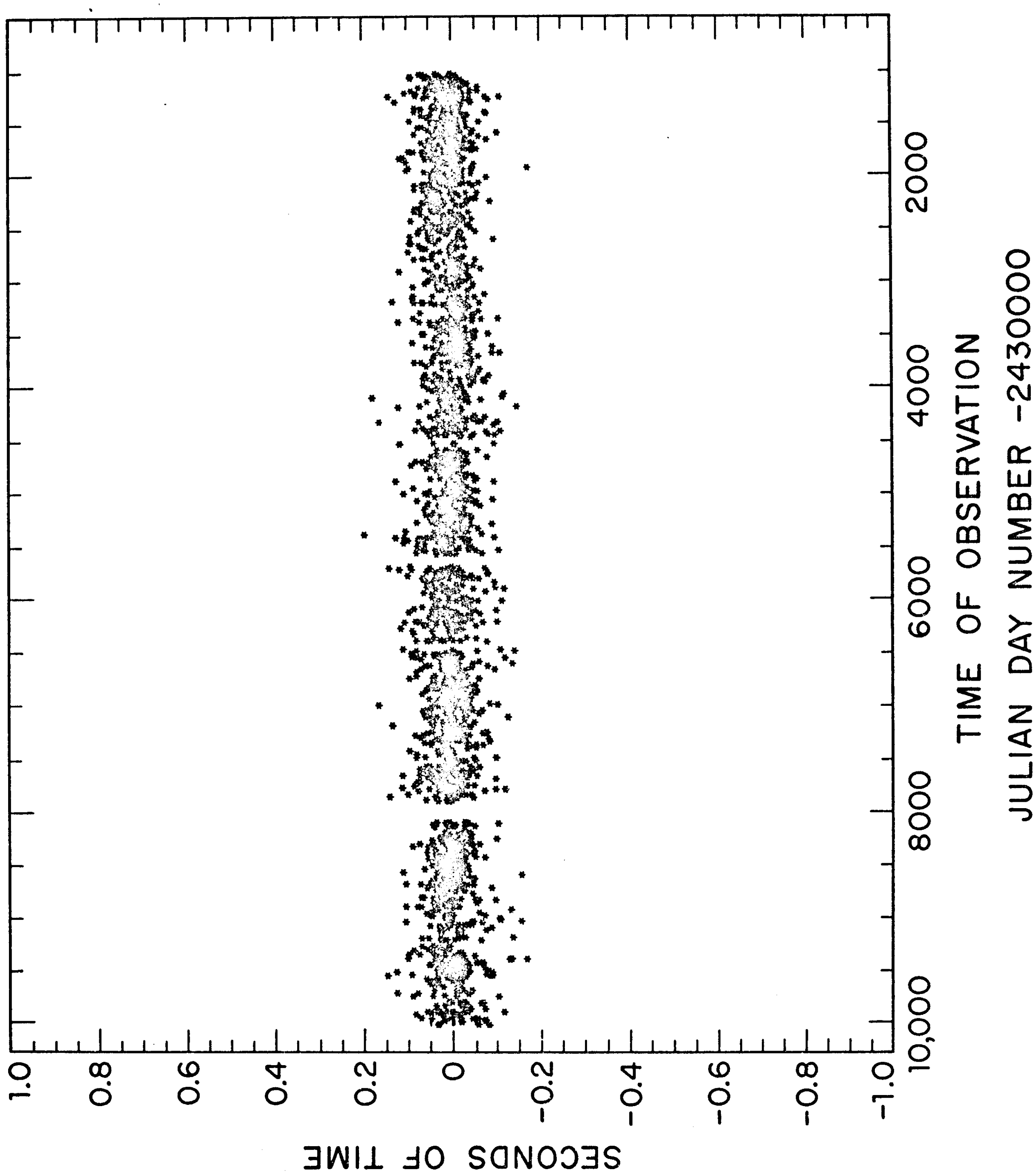
SECONDS OF TIME
1.0
0.8
0.6
0.4
0.2
0
-0.2
-0.4
-0.6
-0.8
-1.0
TIME OF OBSERVATION
JULIAN DAY NUMBER -2430000
2000
4000
6000
8000
10,000

Figure 7.

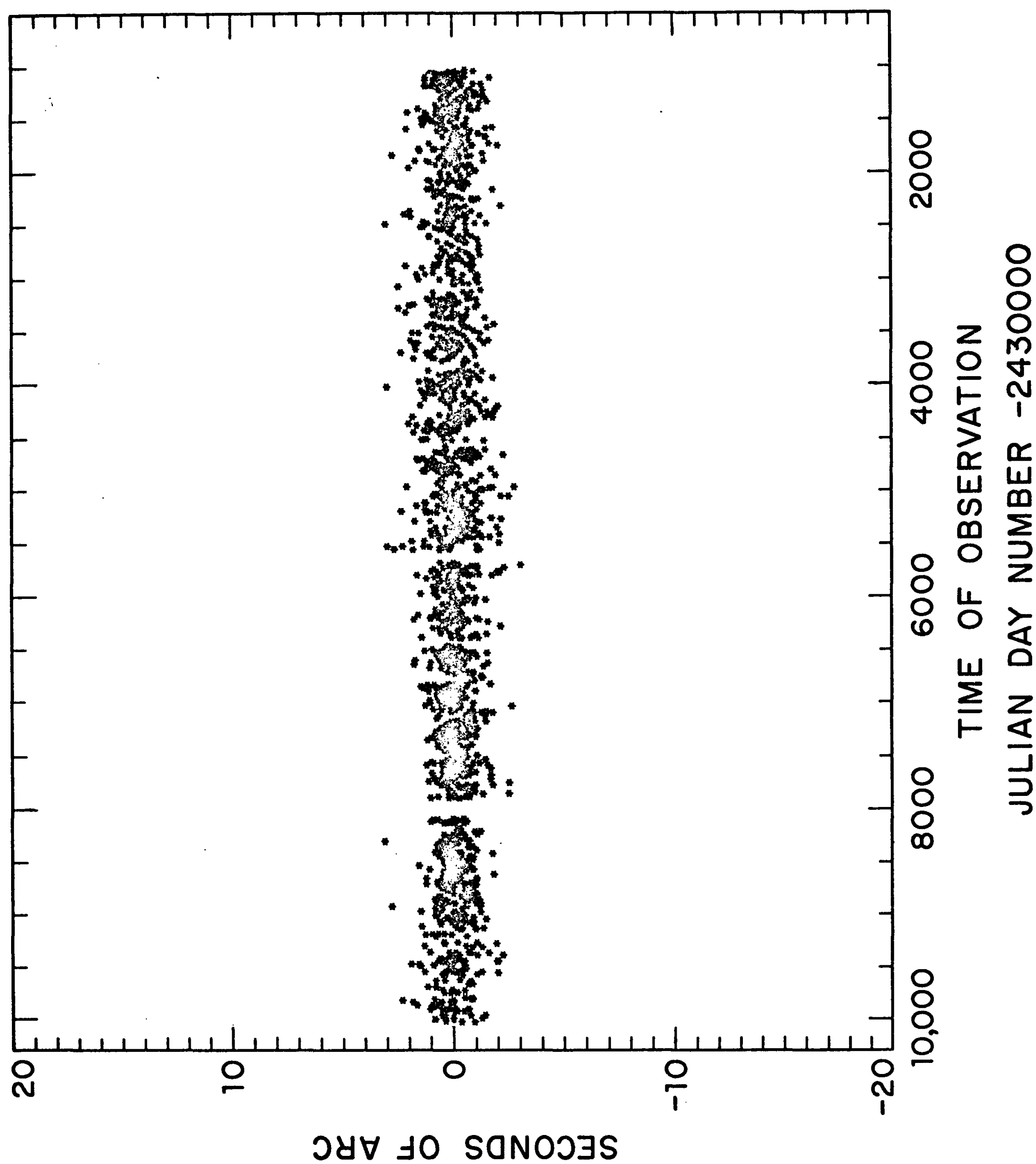
20
10
0
-10
-20
SECONDS OF ARC
10,000
8000
6000
4000
2000
TIME OF OBSERVATION
JULIAN DAY NUMBER -2430000

Figure 8.

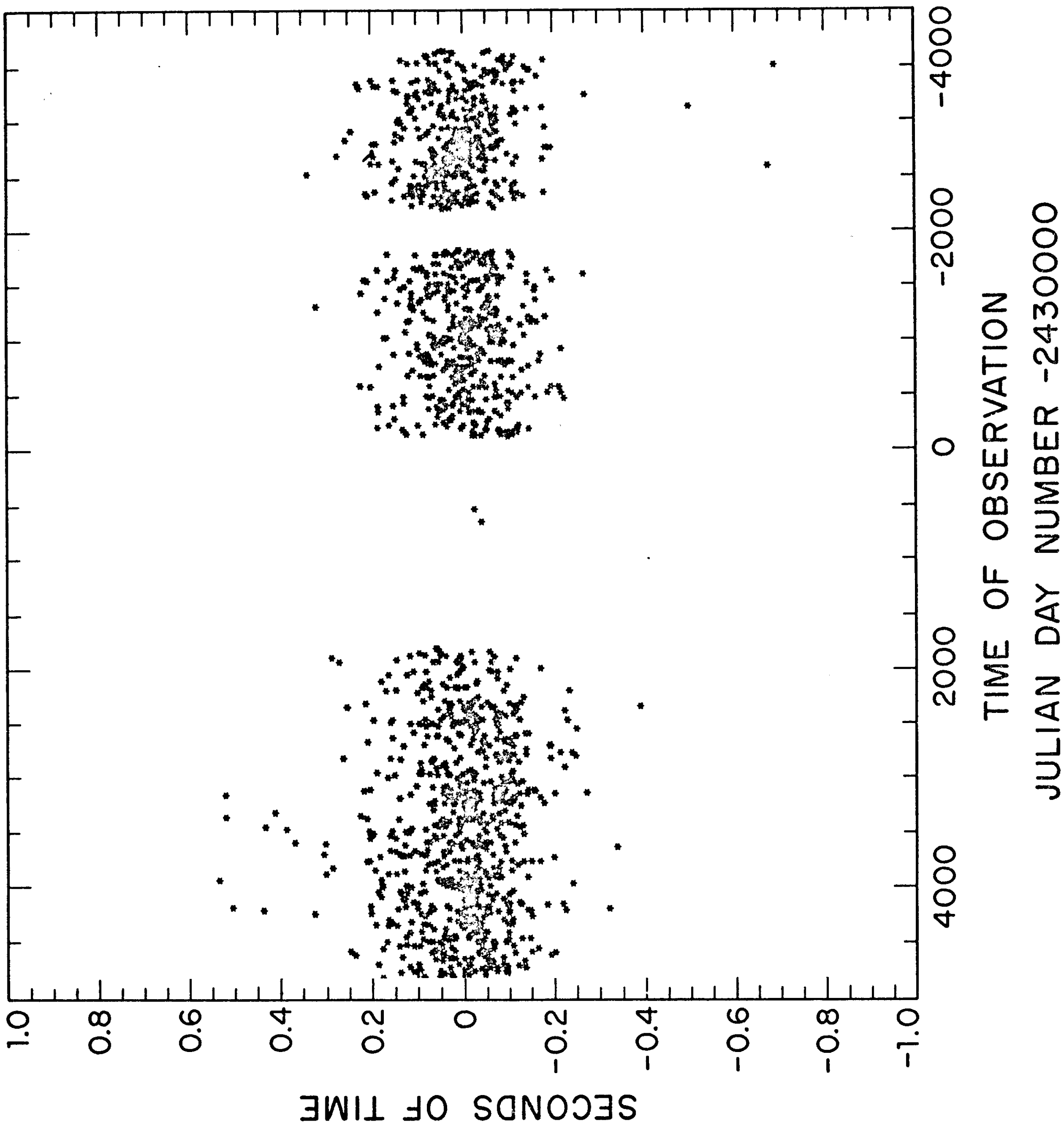
TIME OF OBSERVATION
JULIAN DAY NUMBER -2430000
SECONDS OF TIME
-4000
-2000
0
2000
4000
1.0
0.8
0.6
0.4
0.2
0
-0.2
-0.4
-0.6
-0.8
-1.0

Figure 9.

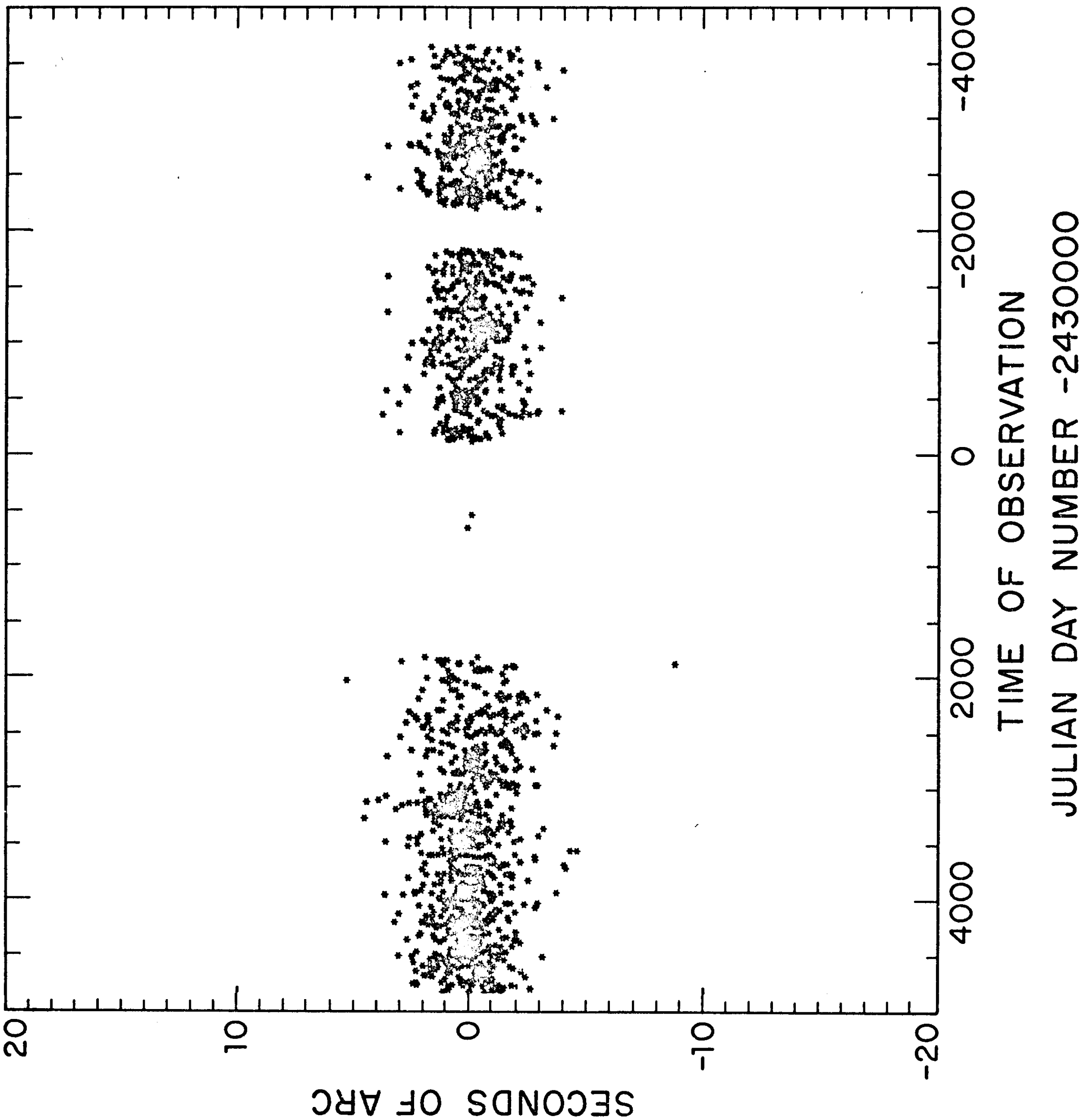
TIME OF OBSERVATION
JULIAN DAY NUMBER -2430000
-4000
-2000
0
2000
4000
SECONDS OF ARC
20
10
0
-10
-20

Figure 10.

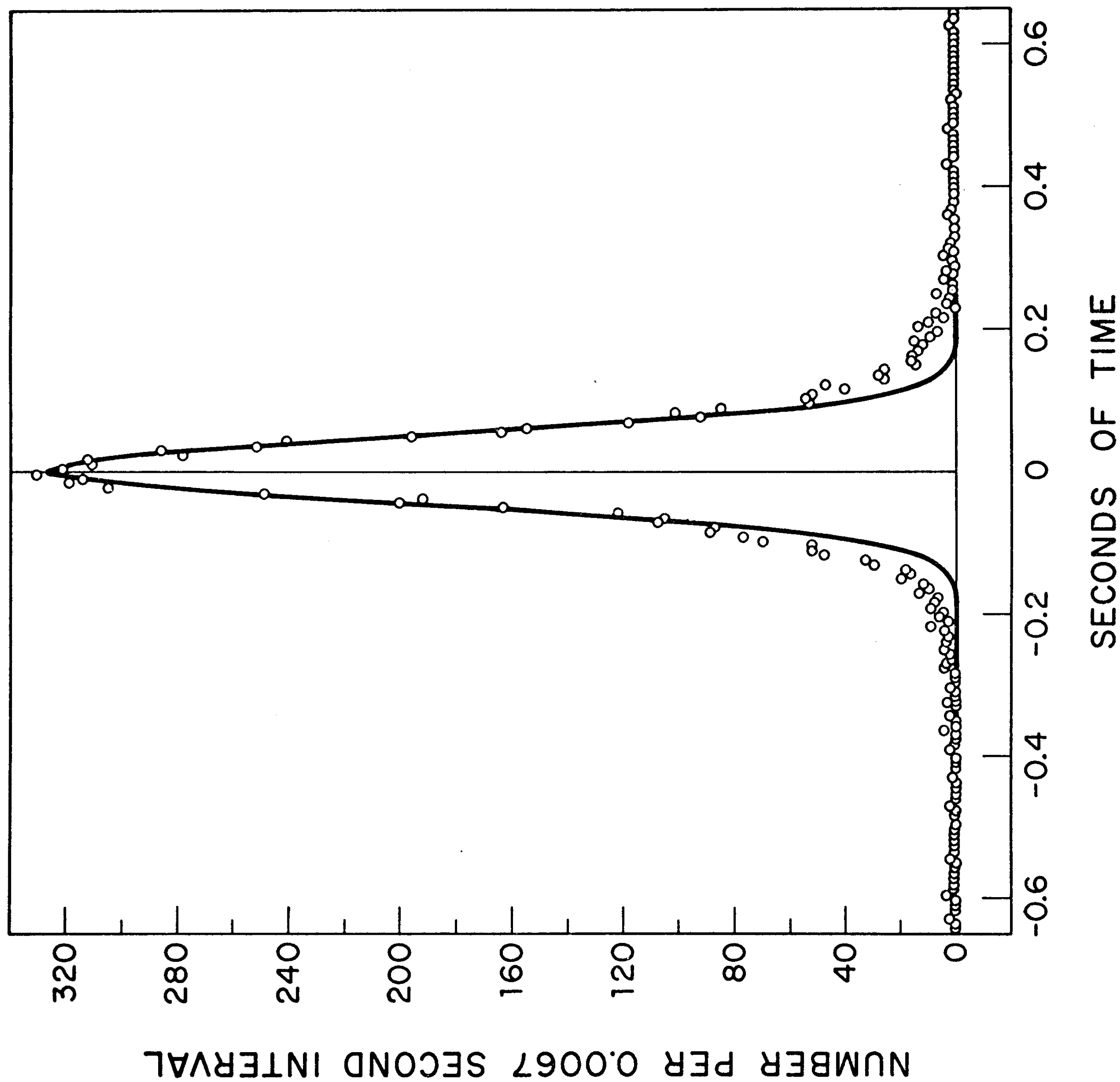
NUMBER PER 0.0067 SECOND INTERVAL
0
40
80
120
160
200
240
280
320
SECONDS OF TIME
-0.6
-0.4
-0.2
0
0.2
0.4
0.6

Figure 11.

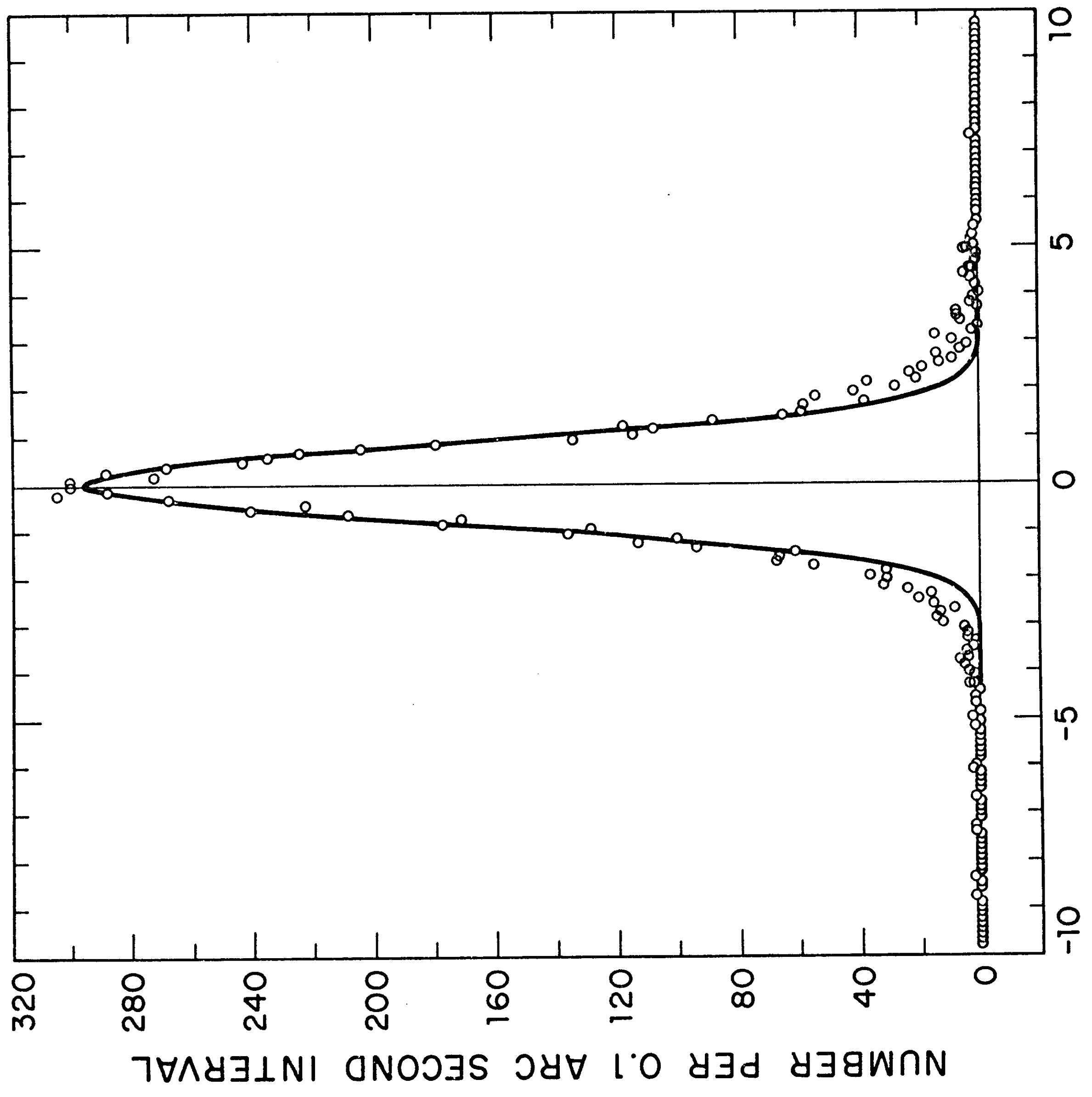
NUMBER PER 0.1 ARC SECOND INTERVAL
320
280
240
200
160
120
80
40
0
SECONDS OF ARC
-10
-5
0
5
10

Figure 12.

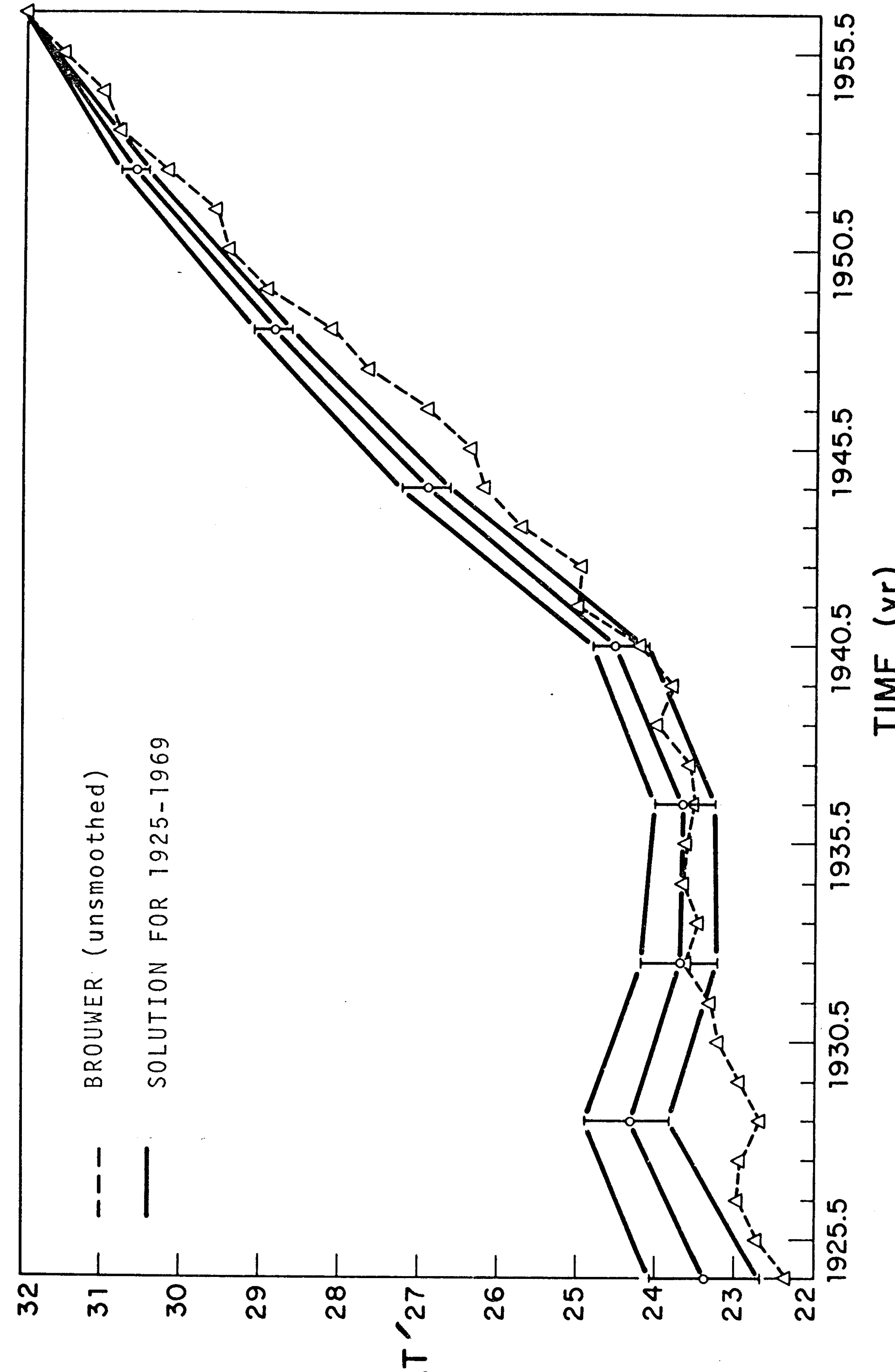

BROUWER (unsmoothed)
SOLUTION FOR 1925-1969
TIME (yr)
1925.5
1930.5
1935.5
1940.5
1945.5
1950.5
1955.5
ΔT′
32
31
30
29
28
27
26
25
24
23
22

Figure 13.

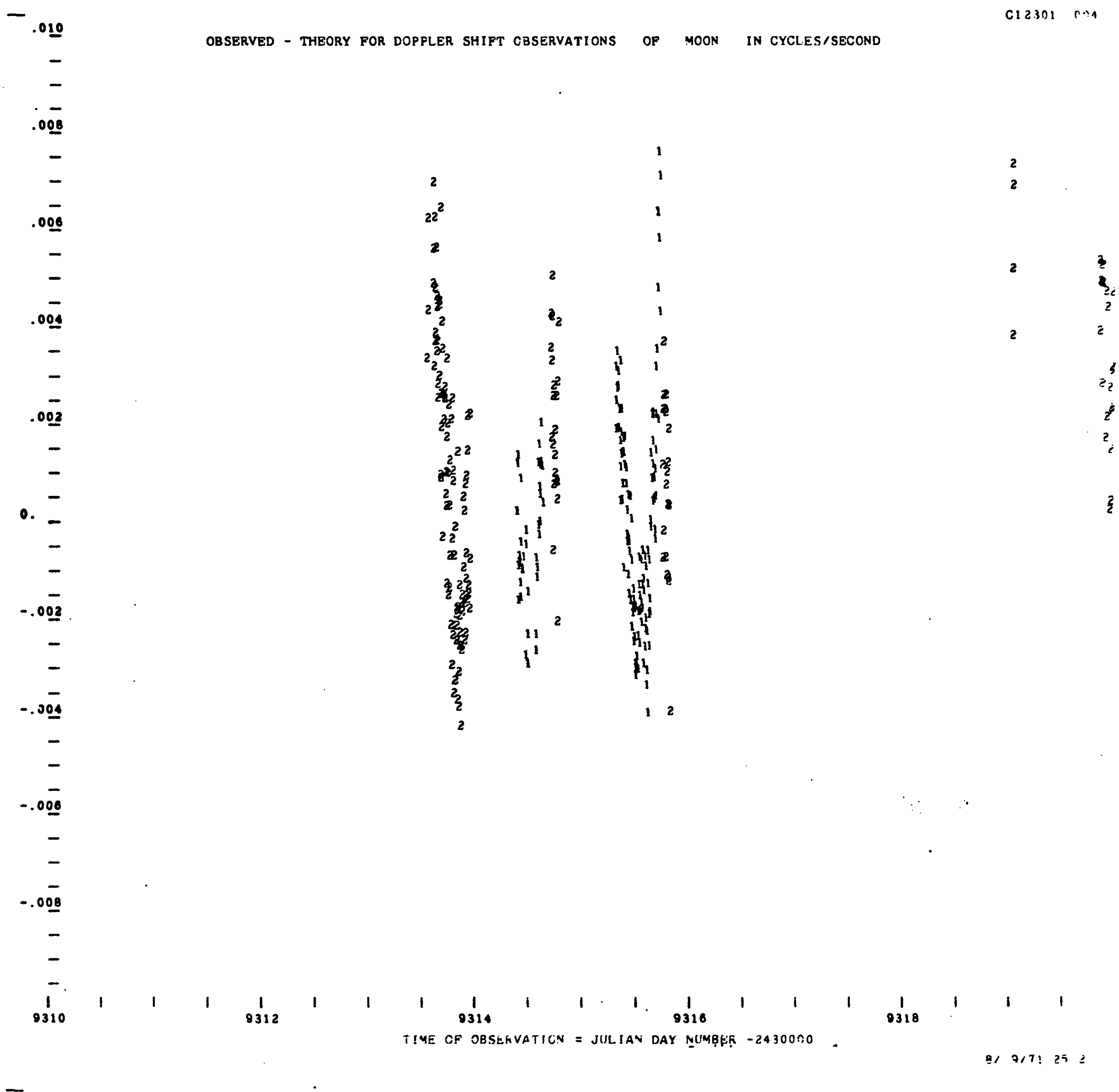
C12301 004
OBSERVED - THEORY FOR DOPPLER SHIFT OBSERVATIONS OF MOON IN CYCLES/SECOND
.010
.008
.006
.004
.002
0.
-.002
-.004
-.006
-.008
9310
9312
9314
9316
9318
TIME OF OBSERVATION = JULIAN DAY NUMBER -2430000

Figure 14.

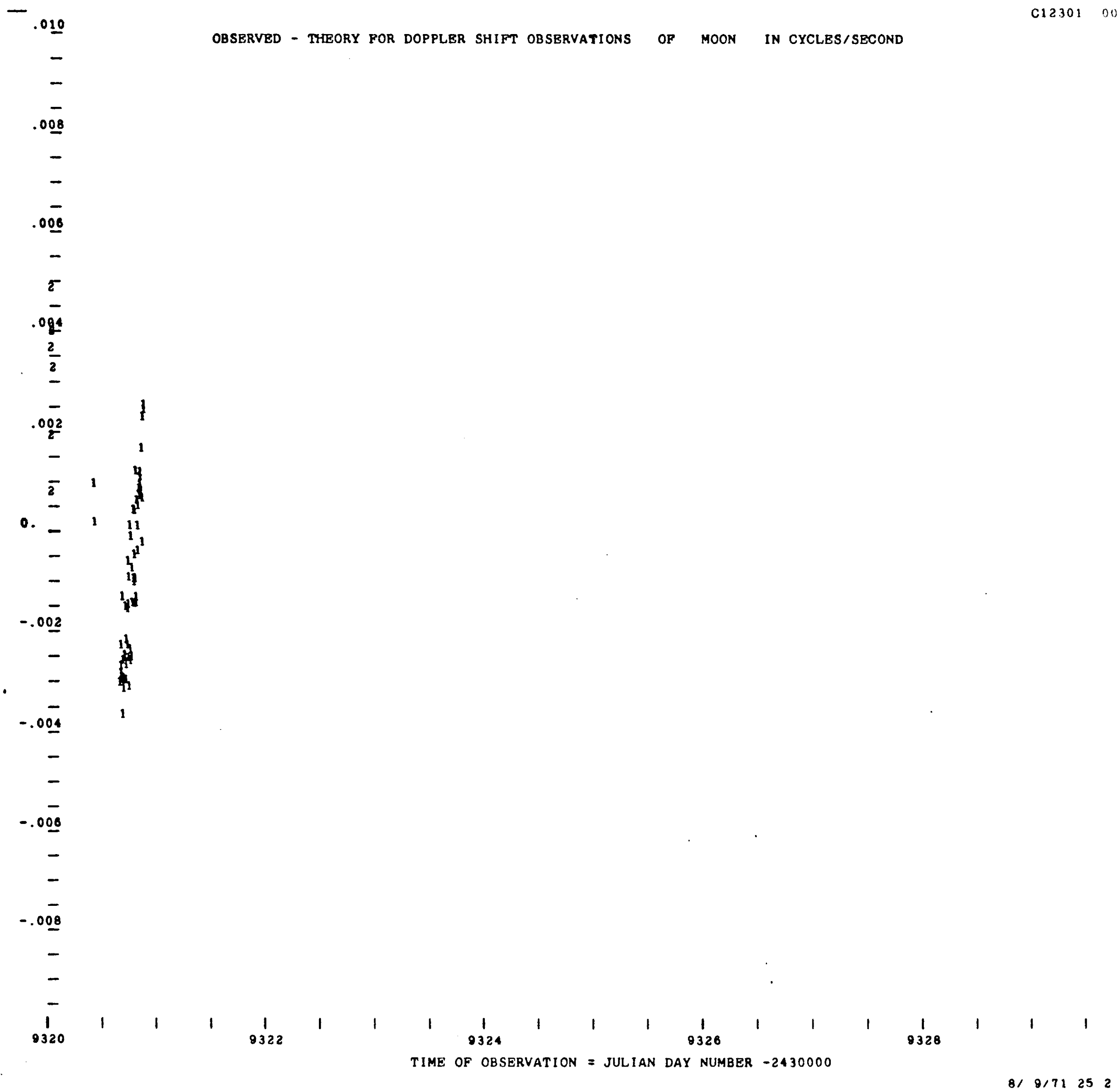
C12301 005
OBSERVED - THEORY FOR DOPPLER SHIFT OBSERVATIONS OF MOON IN CYCLES/SECOND
.010
.008
.006
.004
.002
0.
-.002
-.004
-.006
-.008
9320
9322
9324
9326
9328
TIME OF OBSERVATION = JULIAN DAY NUMBER -2430000
8/ 9/71 25 2

Fig. 14 (Cont.)

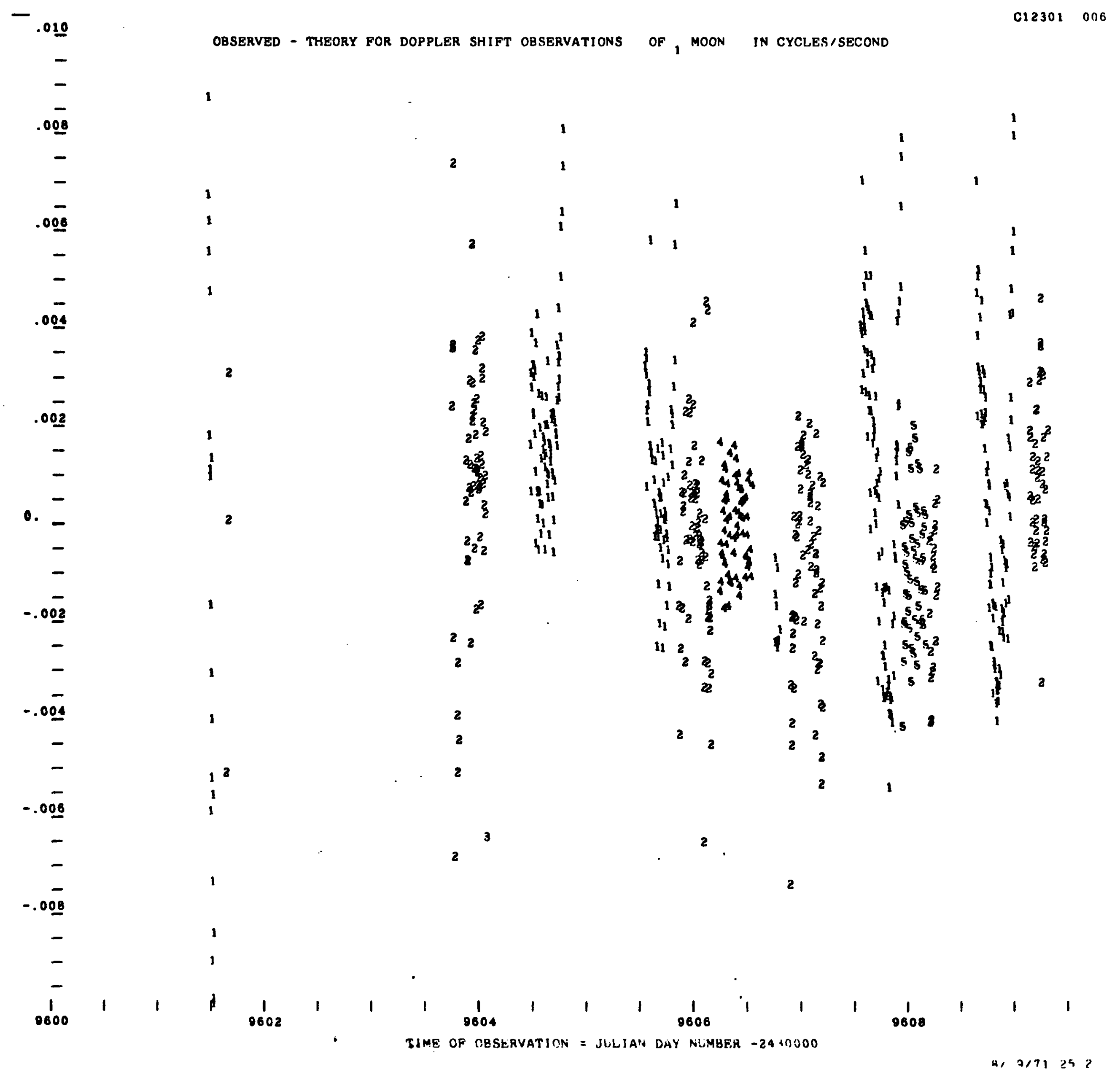
C12301 006
OBSERVED - THEORY FOR DOPPLER SHIFT OBSERVATIONS OF 1 MOON IN CYCLES/SECOND
.010
.008
.006
.004
.002
0.
-.002
-.004
-.006
-.008
9600
9602
9604
9606
9608
TIME OF OBSERVATION = JULIAN DAY NUMBER -2430000

Figure 15.

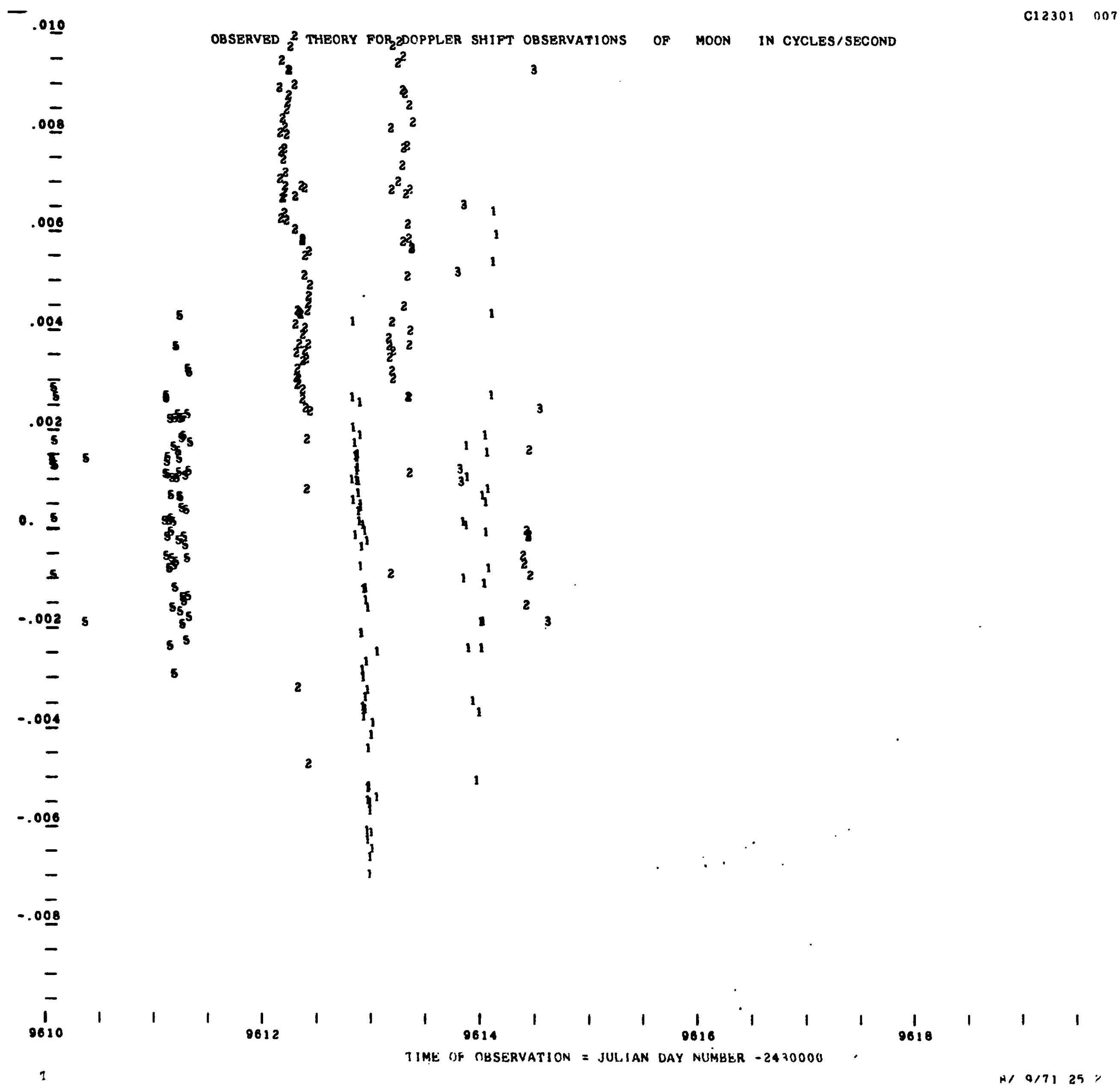
C12301 007
OBSERVED - THEORY FOR DOPPLER SHIFT OBSERVATIONS OF MOON IN CYCLES/SECOND
.010
.008
.006
.004
.002
0.
-.002
-.004
-.006
-.008
9610
9612
9614
9616
9618
TIME OF OBSERVATION = JULIAN DAY NUMBER -2430000

Fig. 15. (cont.)

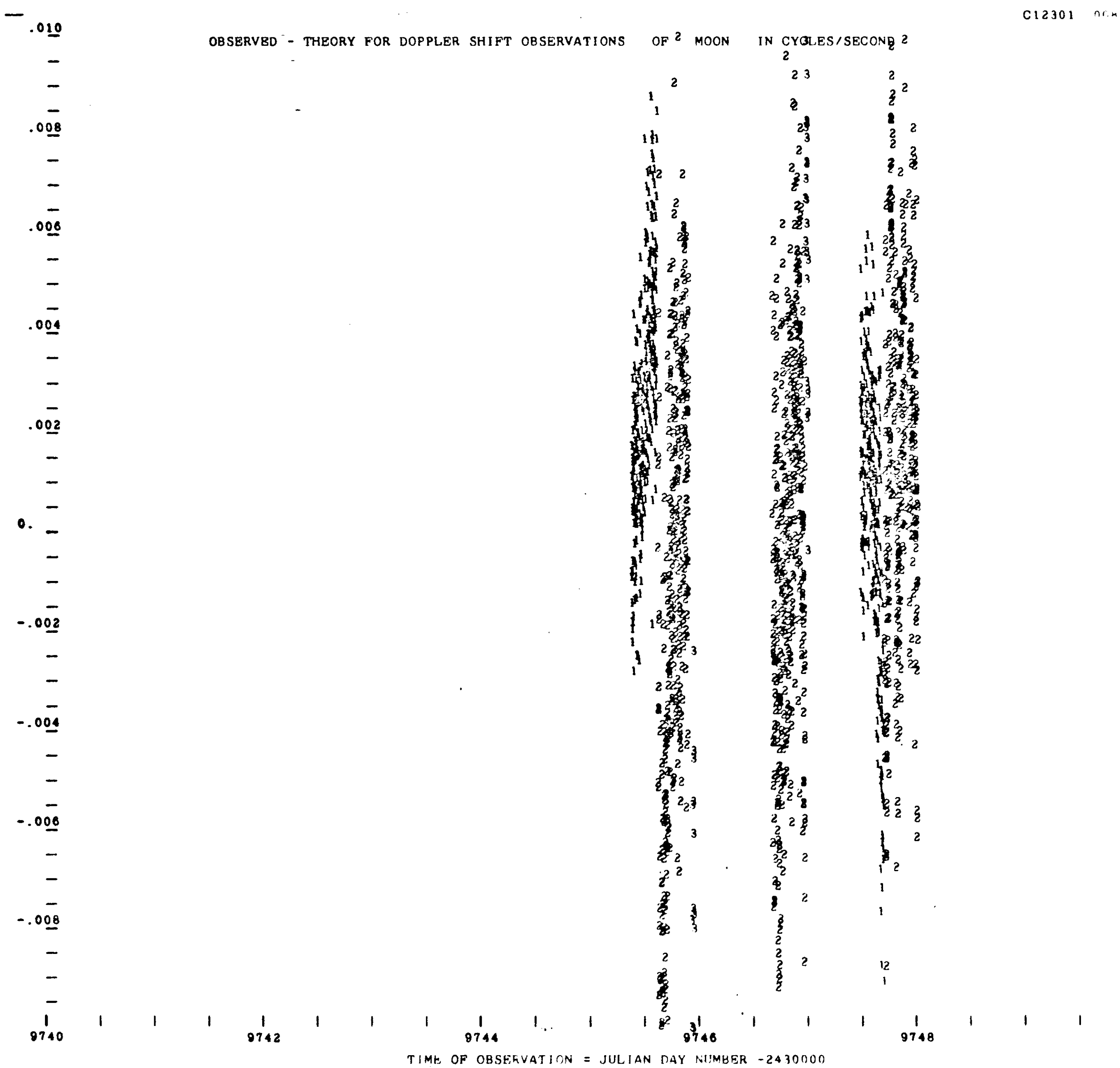

C12301
OBSERVED - THEORY FOR DOPPLER SHIFT OBSERVATIONS OF MOON IN CYCLES/SECOND
.010
.008
.006
.004
.002
0.
-.002
-.004
-.006
-.008
9740
9742
9744
9746
9748
TIME OF OBSERVATION = JULIAN DAY NUMBER -2430000

Fig. 16

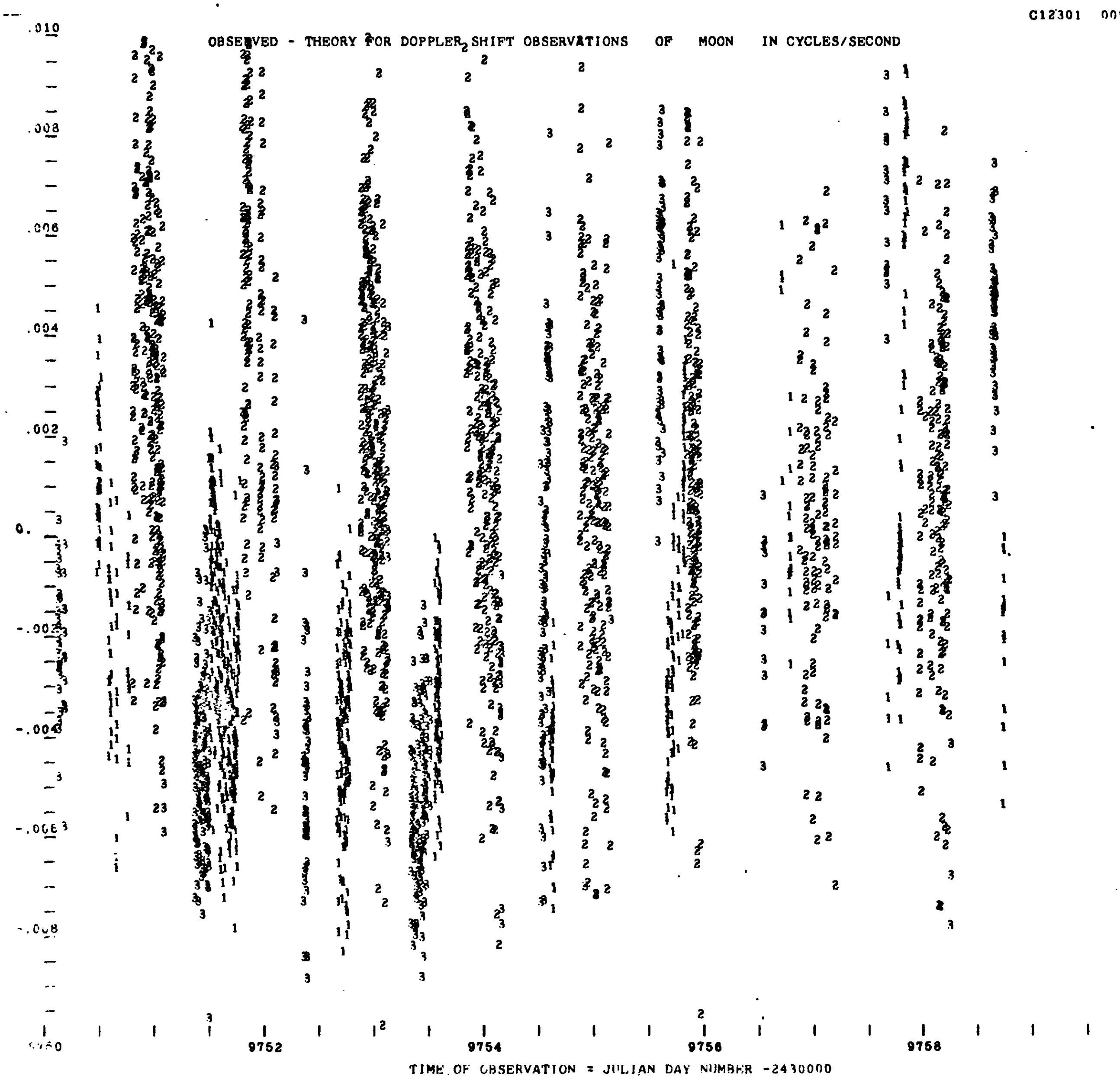
C12301 009
OBSERVED - THEORY FOR DOPPLER SHIFT OBSERVATIONS OF MOON IN CYCLES/SECOND
.010
.008
.006
.004
.002
0.
-.002
-.004
-.006
-.008
9752
9754
9756
9758
TIME OF OBSERVATION = JULIAN DAY NUMBER -2430000
8/11/71 25 2

Fig. 16 (Cont.)

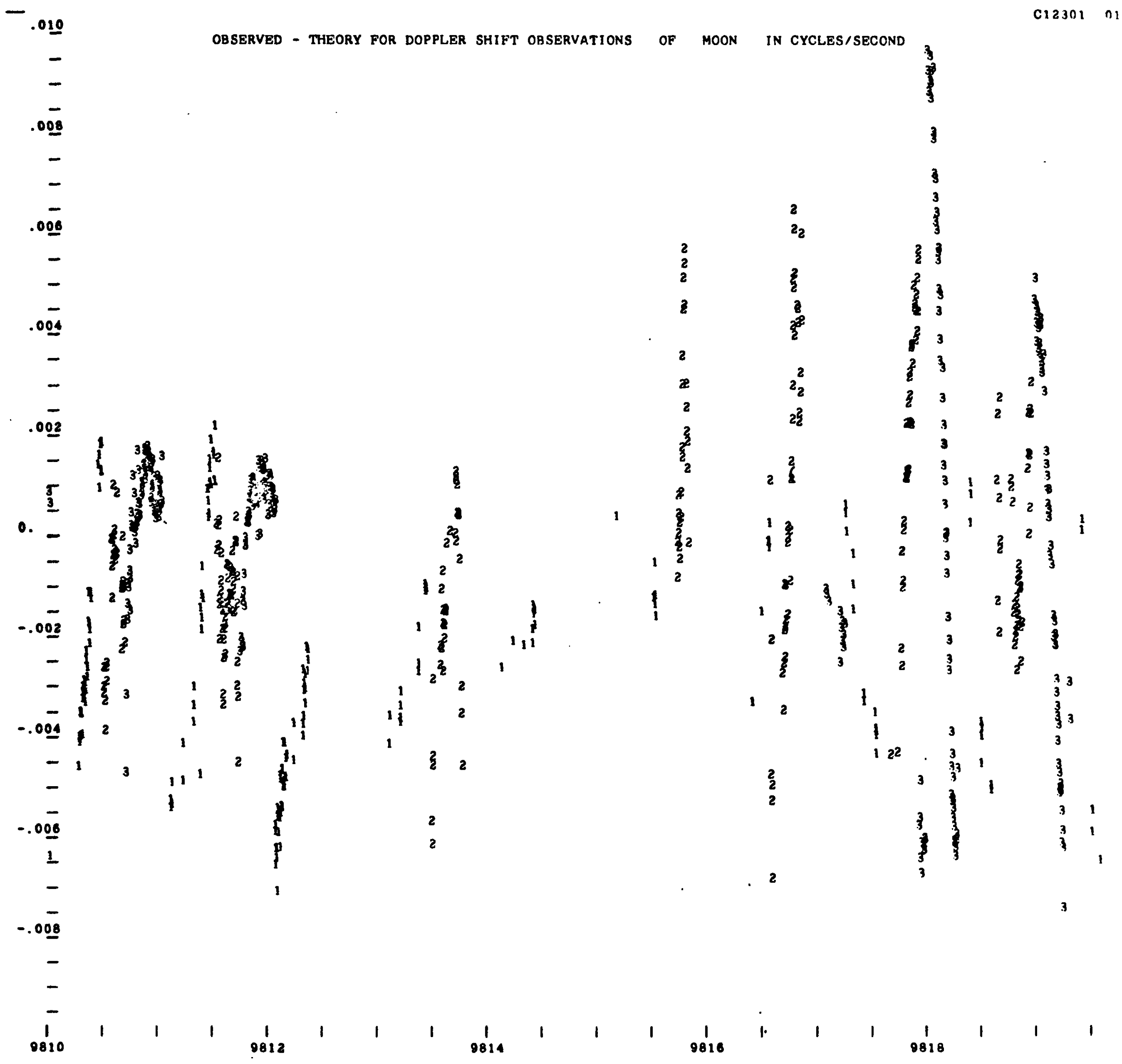
C12301 01?
OBSERVED - THEORY FOR DOPPLER SHIFT OBSERVATIONS OF MOON IN CYCLES/SECOND
.010
.008
.006
.004
.002
0.
-.002
-.004
-.006
-.008
9810
9812
9814
9816
9818
TIME OF OBSERVATION = JUL

Fig. 17.

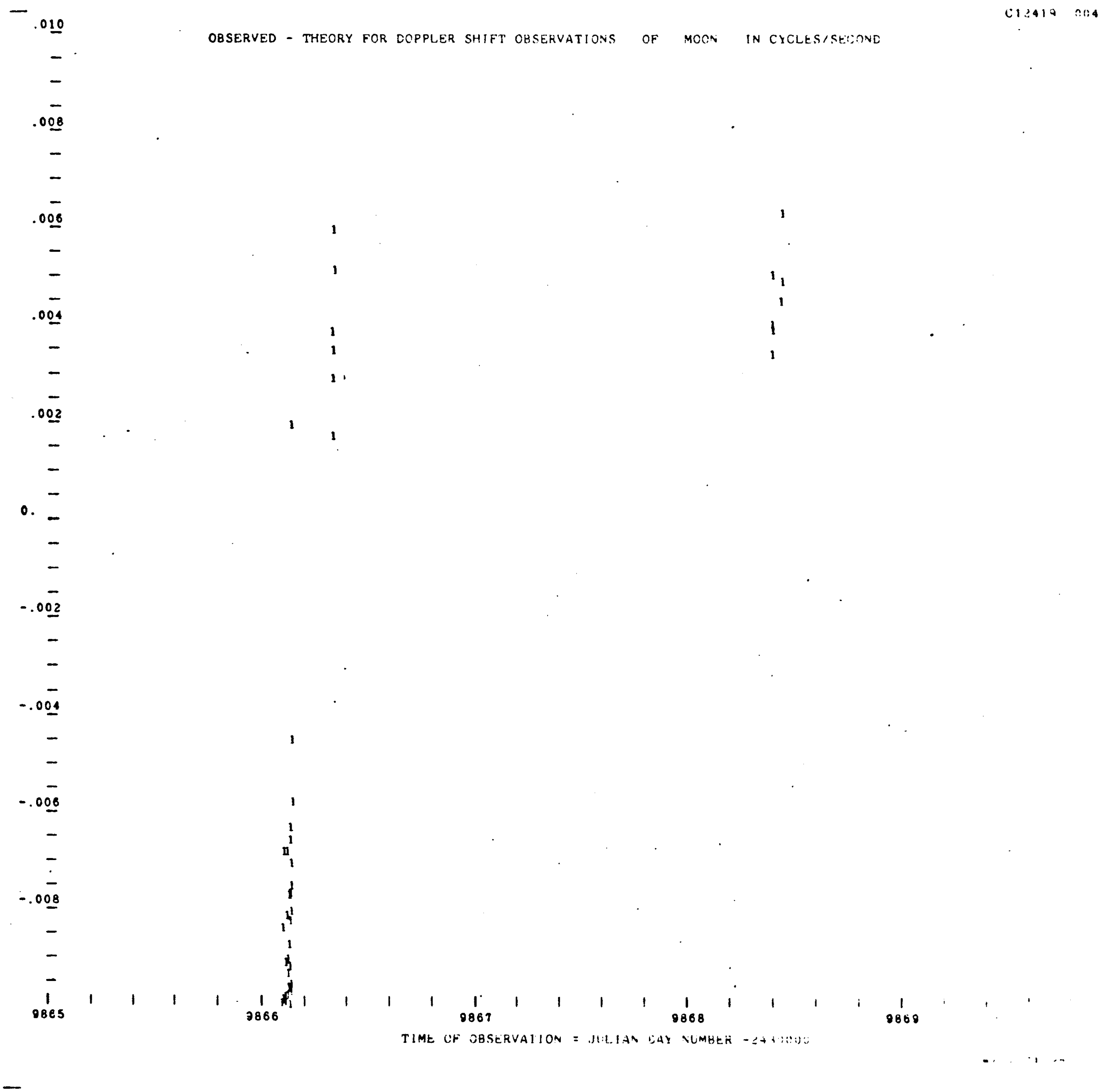

C12419 004
OBSERVED - THEORY FOR DOPPLER SHIFT OBSERVATIONS OF MOON IN CYCLES/SECOND
.010
.008
.006
.004
.002
0.
-.002
-.004
-.006
-.008
9865
9866
9867
9868
9869
TIME OF OBSERVATION = JULIAN DAY NUMBER

Figure 18.

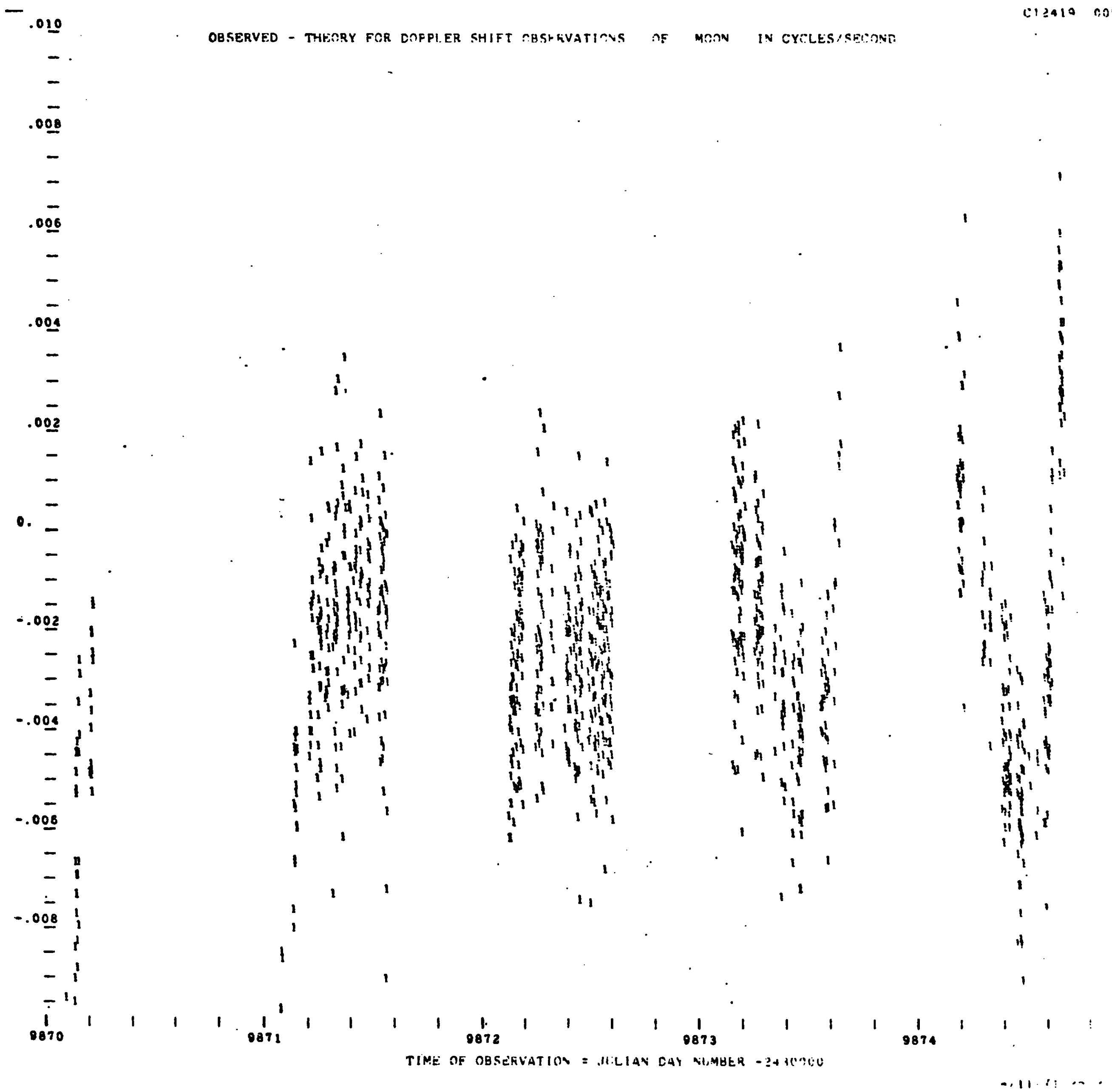

C12419 005
OBSERVED - THEORY FOR DOPPLER SHIFT OBSERVATIONS OF MOON IN CYCLES/SECOND
.010
.008
.006
.004
.002
0.
-.002
-.004
-.006
-.008
9870
9871
9872
9873
9874
TIME OF OBSERVATION = JULIAN DAY NUMBER -2430000

Fig. 18 (cont.)

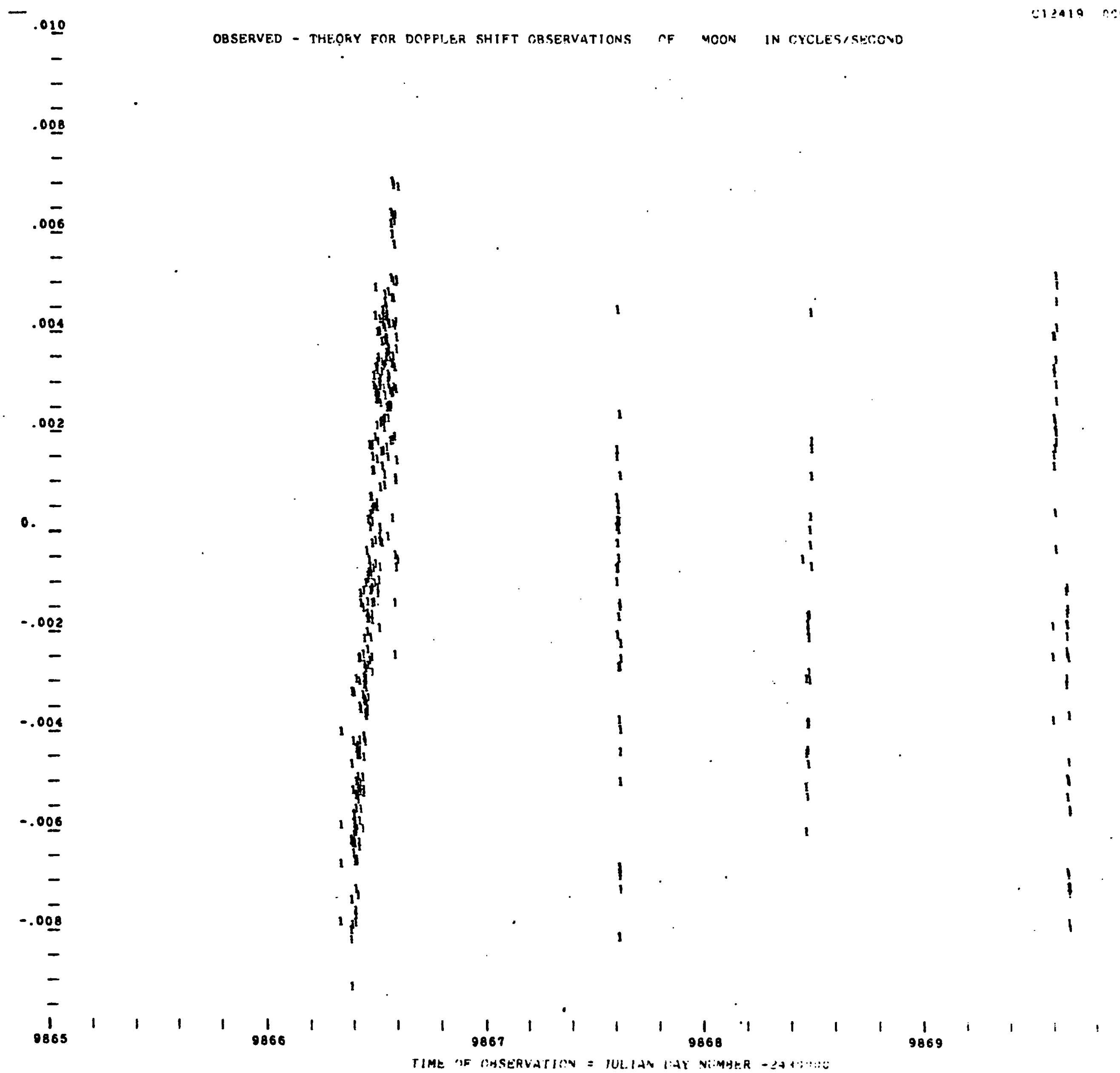
OBSERVED - THEORY FOR DOPPLER SHIFT OBSERVATIONS OF MOON IN CYCLES/SECOND
.010
.008
.006
.004
.002
0.
-.002
-.004
-.006
-.008
9865
9866
9867
9868
9869
TIME OF OBSERVATION = JULIAN DAY NUMBER

Fig. 18 (Cont.)

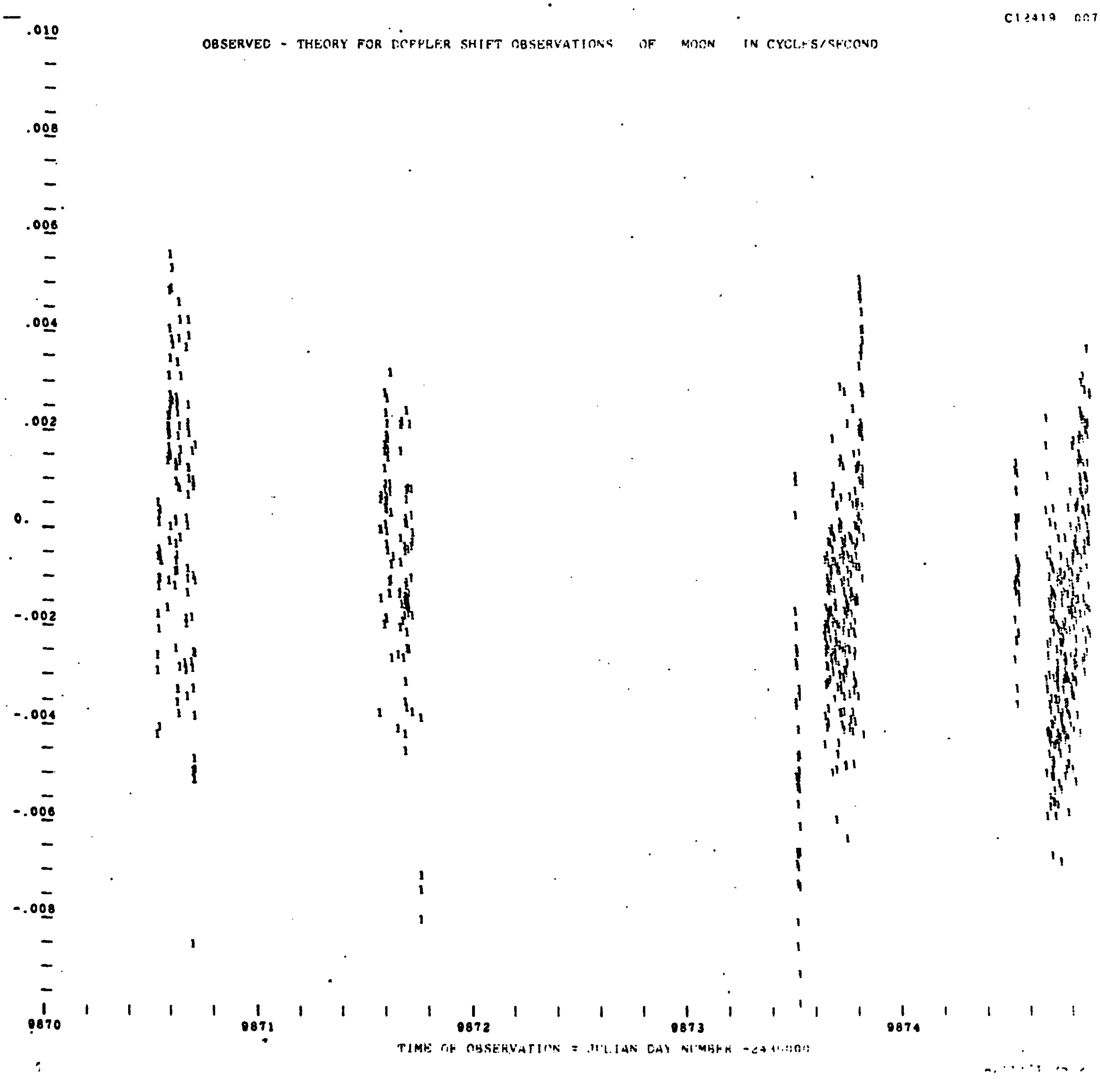
C12419 007
OBSERVED - THEORY FOR DOPPLER SHIFT OBSERVATIONS OF MOON IN CYCLES/SECOND
.010
.008
.006
.004
.002
0.
-.002
-.004
-.006
-.008
9870
9871
9872
9873
9874
TIME OF OBSERVATION = JULIAN DAY NUMBER

Fig. 18 (Cont.)

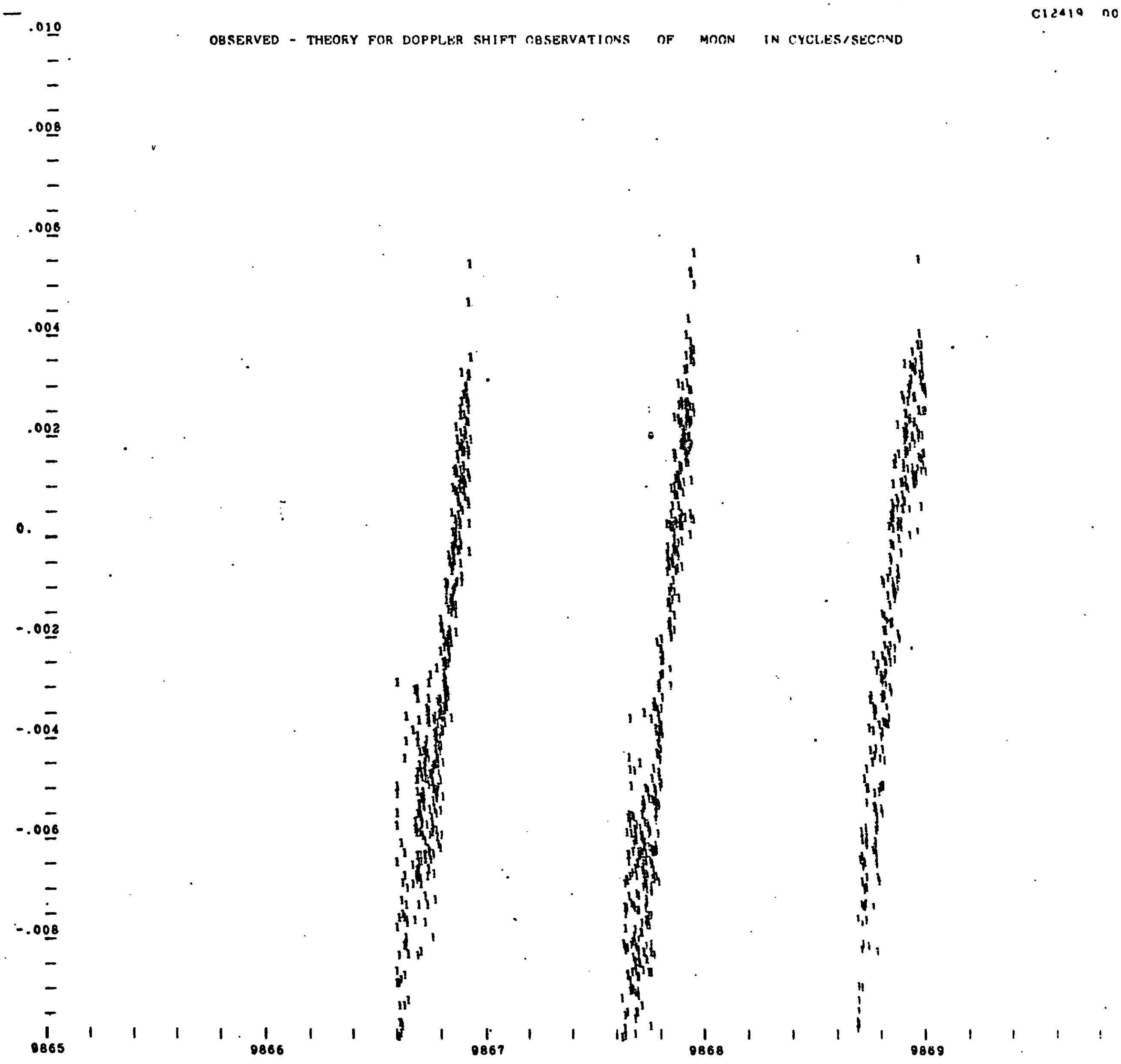

C12419 006
OBSERVED - THEORY FOR DOPPLER SHIFT OBSERVATIONS OF MOON IN CYCLES/SECOND
.010
.008
.006
.004
.002
0.
-.002
-.004
-.006
-.008
9865
9866
9867
9868
9869

Fig. 18 (Cont.)

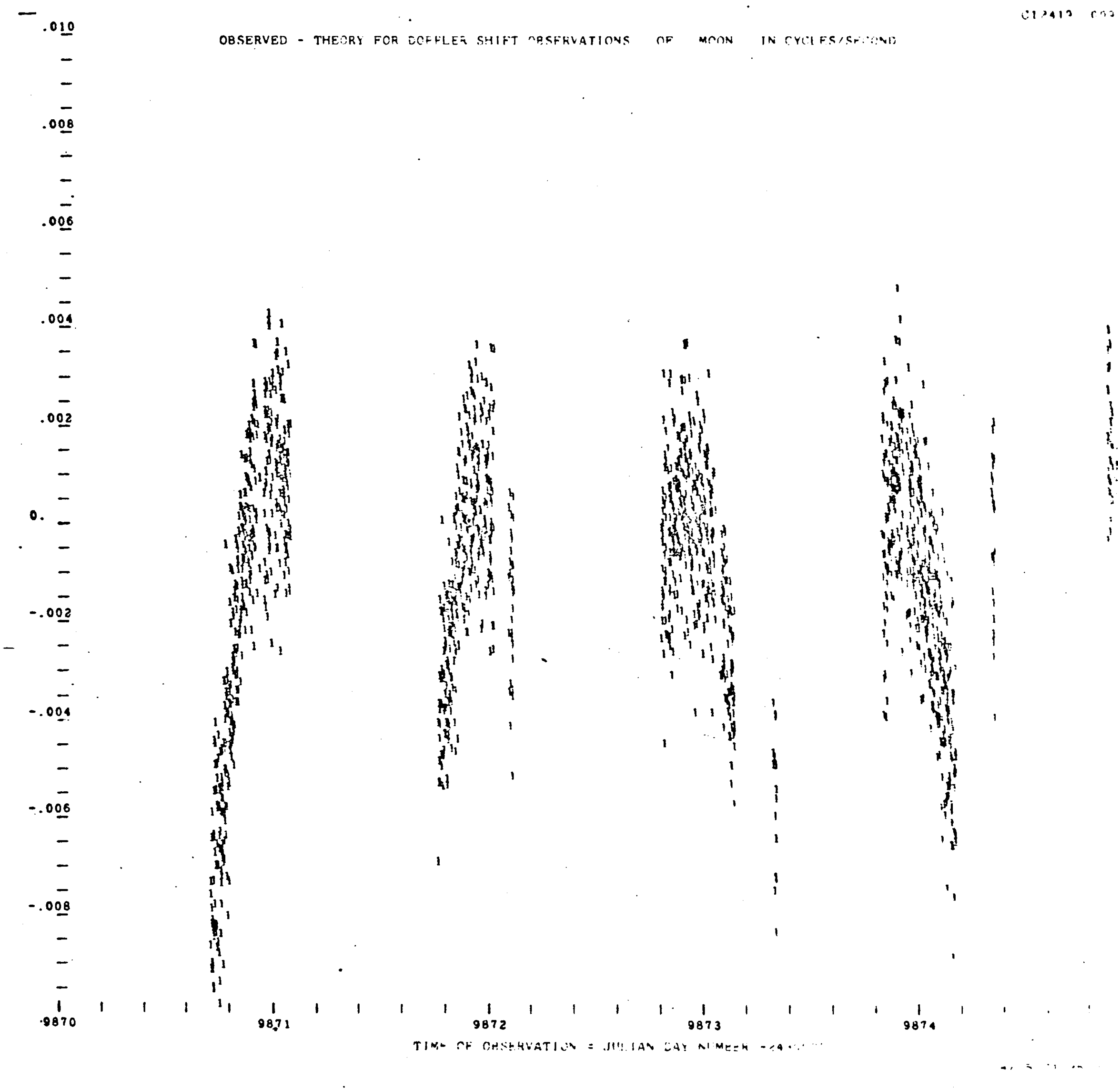
OBSERVED - THEORY FOR DOPPLER SHIFT OBSERVATIONS OF MOON IN CYCLES/SECOND
.010
.008
.006
.004
.002
0.
-.002
-.004
-.006
-.008
9870
9871
9872
9873
9874
TIME OF OBSERVATION = JULIAN DAY NUMBER

Fig. 18 (cont.)

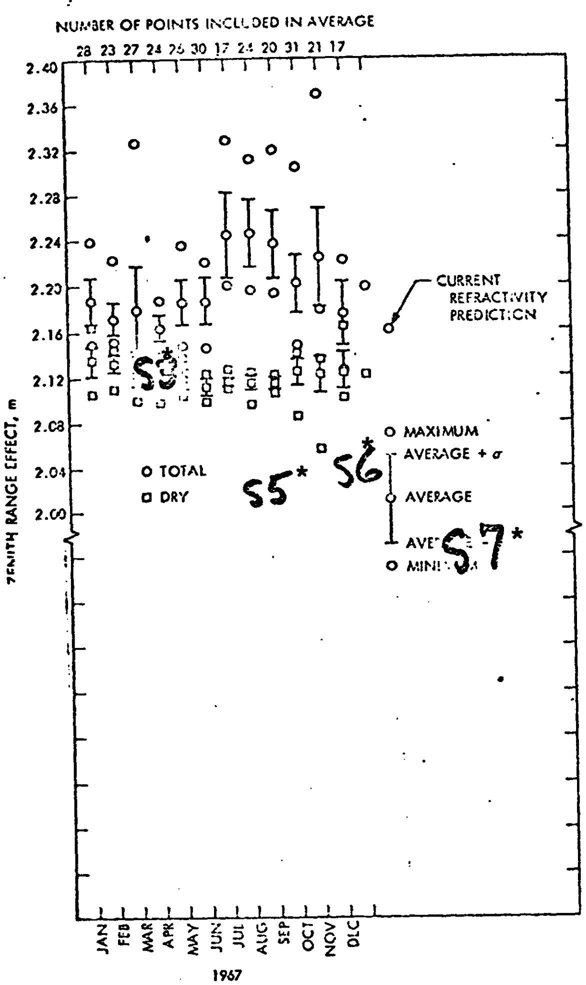

Monthly averages and standard deviations of total, and dry zenith range effects over California

Figure 19.

(Figure adapted from Ondrasik and Thuleen, 1970.)

$^{*}S_n$ denotes value for Surveyor n; n = 1, 3, 5, 6, and 7.

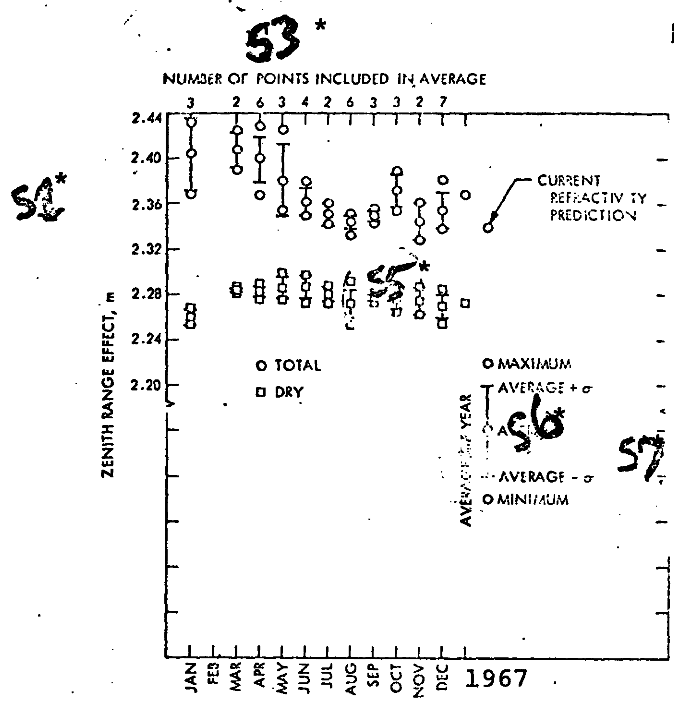

Monthly averages and standard deviations of total, and dry zenith range effects over Australia

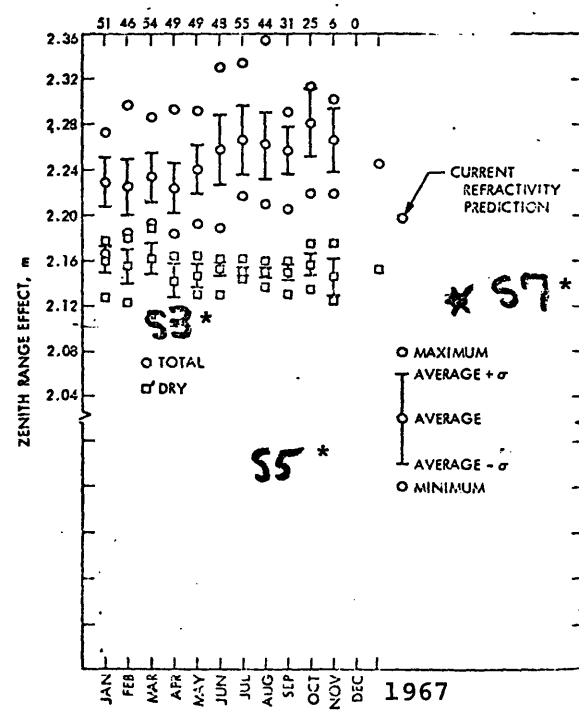

Monthly averages and standard deviations of total, and dry zenith range effects over Spain

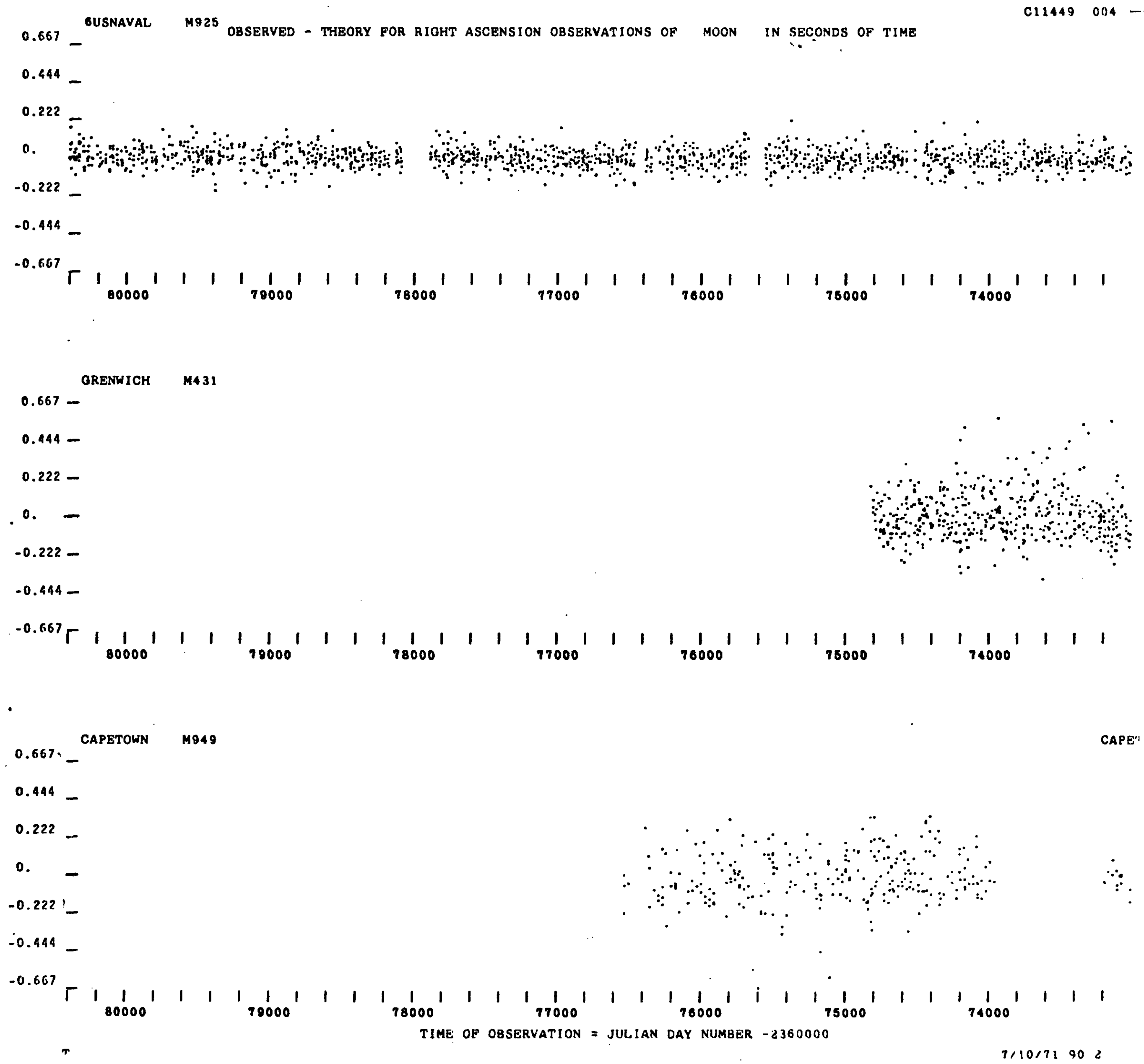

C11449 004
6USNAVAL M925 OBSERVED - THEORY FOR RIGHT ASCENSION OBSERVATIONS OF MOON IN SECONDS OF TIME
0.667
0.444
0.222
0.
-0.222
-0.444
-0.667
80000
79000
78000
77000
76000
75000
74000
GRENWICH M431
CAPETOWN M949
TIME OF OBSERVATION = JULIAN DAY NUMBER -2360000
7/10/71 90 2

Fig. 20

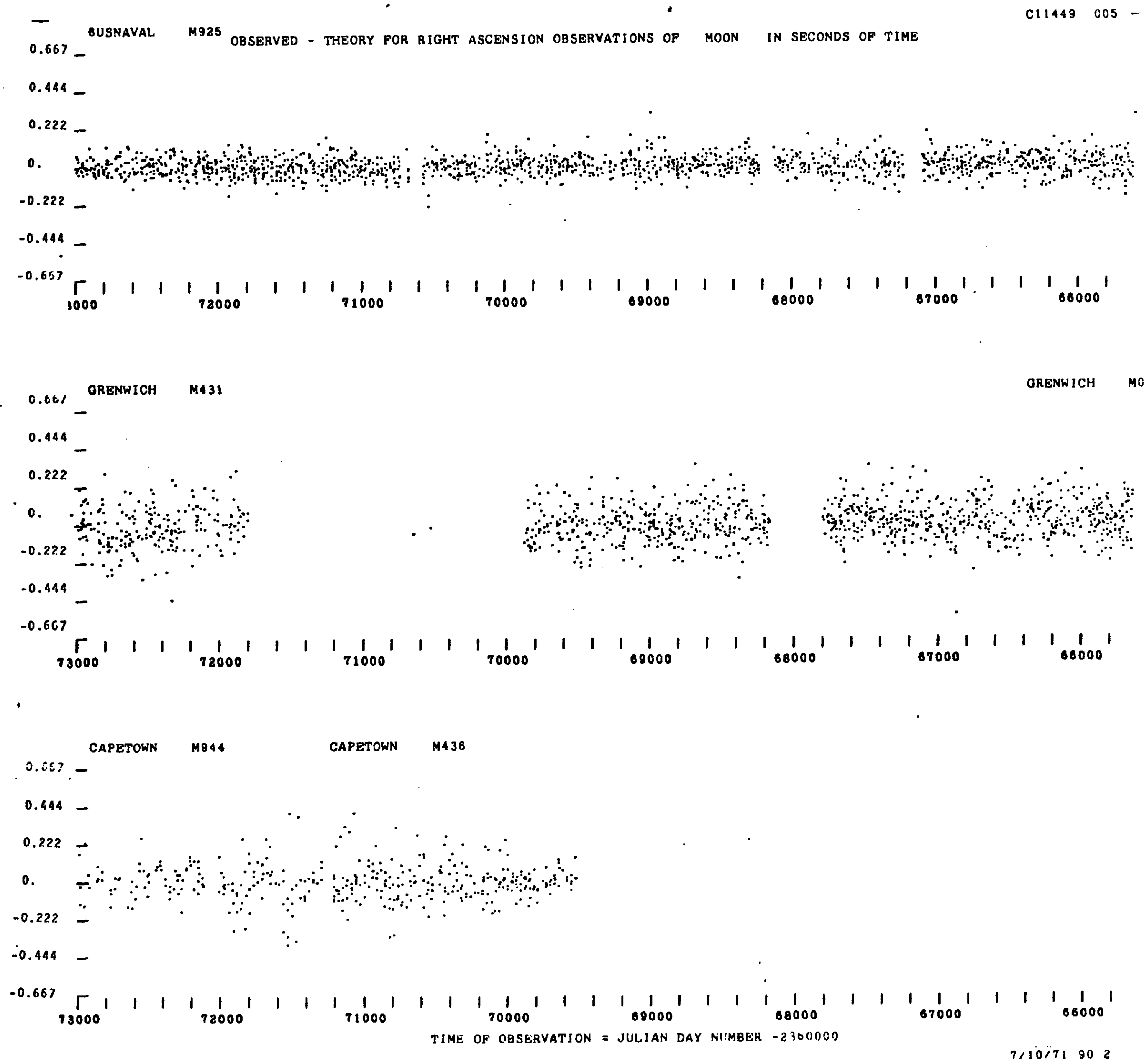
C11449 005
6USNAVAL M925 OBSERVED - THEORY FOR RIGHT ASCENSION OBSERVATIONS OF MOON IN SECONDS OF TIME
0.667
0.444
0.222
0.
-0.222
-0.444
-0.667
72000
71000
70000
69000
68000
67000
66000
GRENWICH M431
GRENWICH
73000
CAPETOWN M944
CAPETOWN M436
TIME OF OBSERVATION = JULIAN DAY NUMBER -2360000
7/10/71 90 2

Fig. 20 (Cont.)

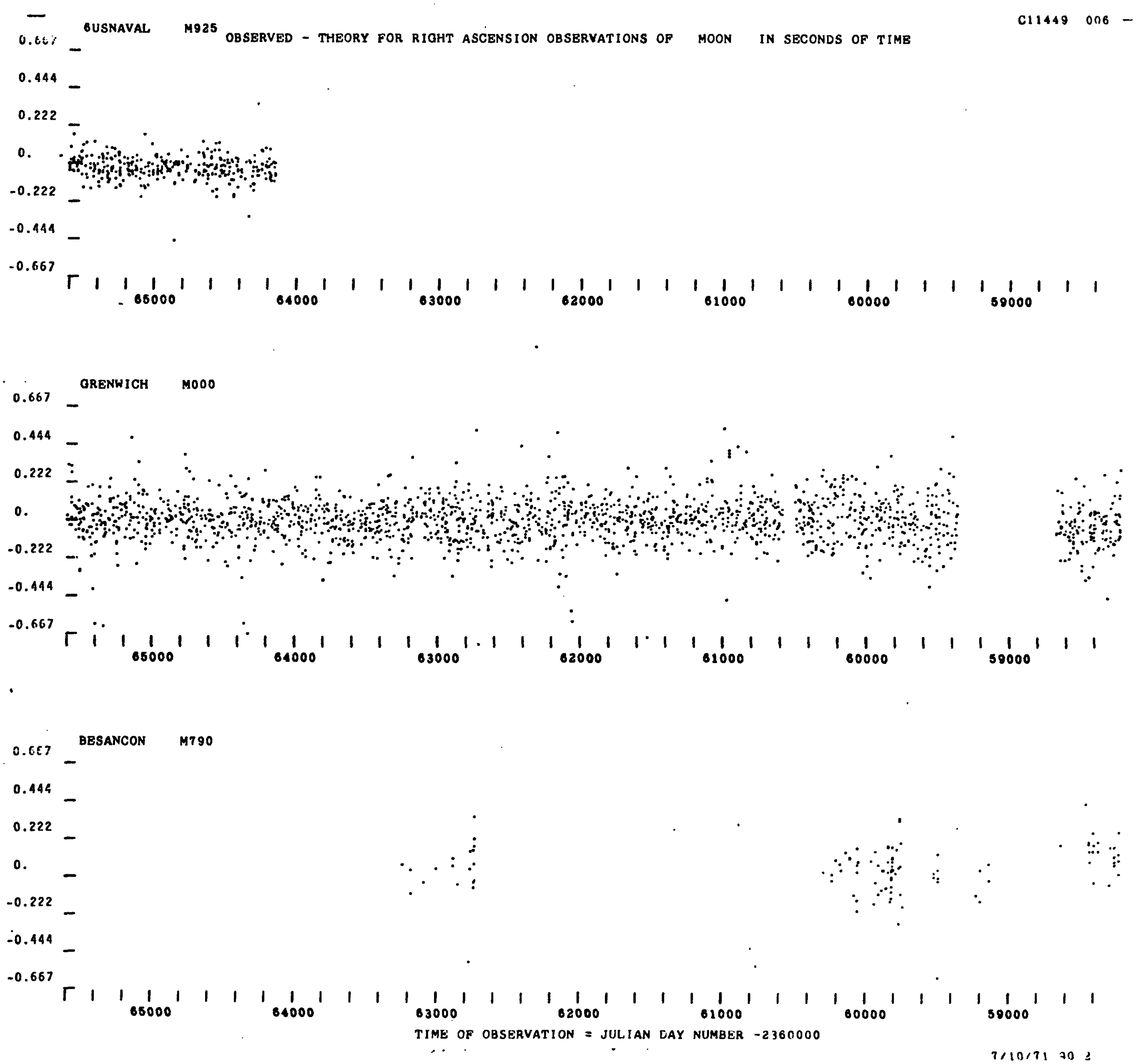
C11449 006
6USNAVAL M925
OBSERVED - THEORY FOR RIGHT ASCENSION OBSERVATIONS OF MOON IN SECONDS OF TIME
0.667
0.444
0.222
0.
-0.222
-0.444
-0.667
65000
64000
63000
62000
61000
60000
59000
GRENWICH M000
BESANCON M790
TIME OF OBSERVATION = JULIAN DAY NUMBER -2360000

Fig. 20. (Cont.)

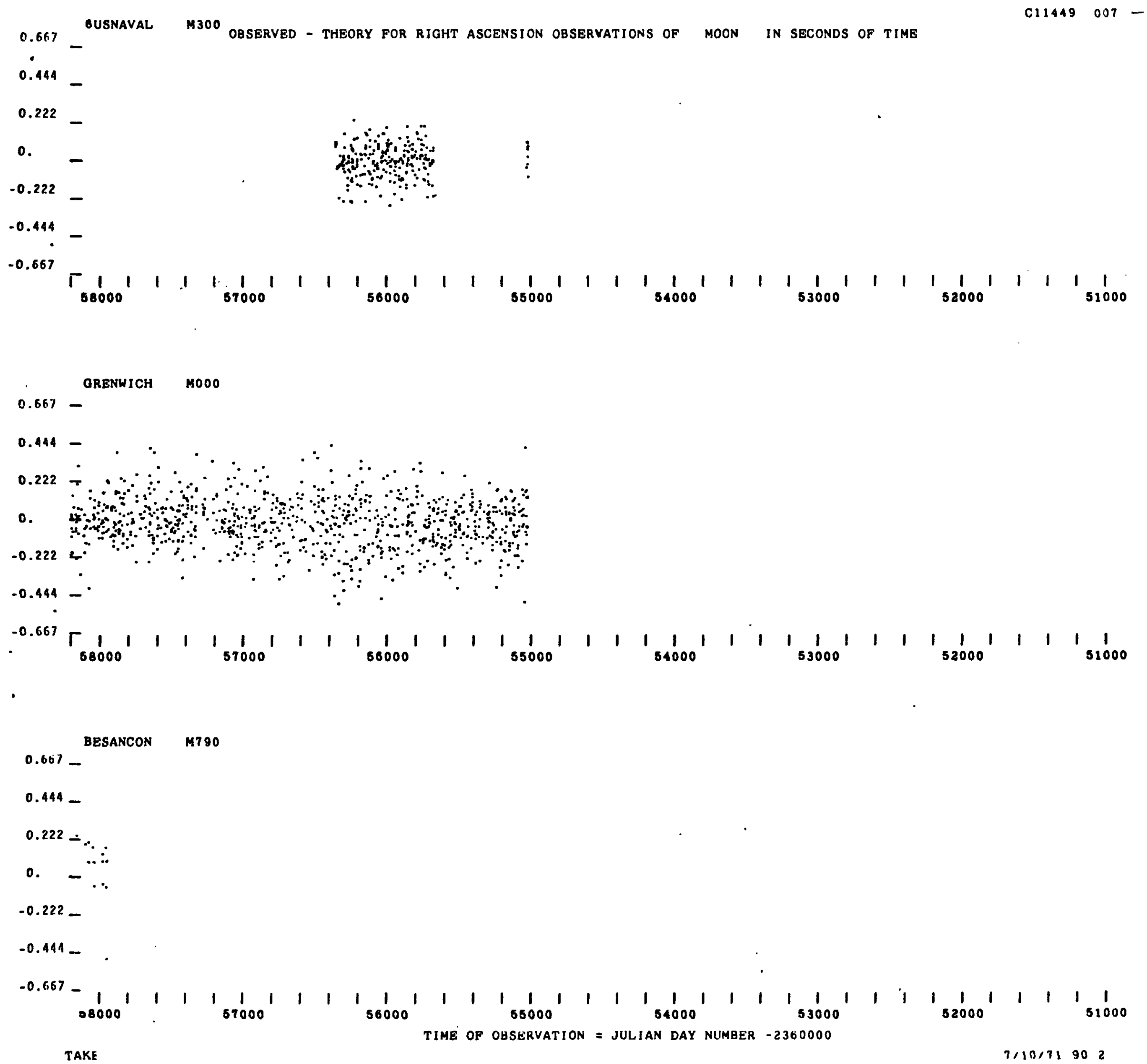
C11449 007
6USNAVAL M300
OBSERVED - THEORY FOR RIGHT ASCENSION OBSERVATIONS OF MOON IN SECONDS OF TIME
0.667
0.444
0.222
0.
-0.222
-0.444
-0.667
58000 57000 56000 55000 54000 53000 52000 51000
GRENWICH M000
0.667
0.444
0.222
0.
-0.222
-0.444
-0.667
58000 57000 56000 55000 54000 53000 52000 51000
BESANCON M790
0.667
0.444
0.222
0.
-0.222
-0.444
-0.667
58000 57000 56000 55000 54000 53000 52000 51000
TIME OF OBSERVATION = JULIAN DAY NUMBER -2360000
TAKE
7/10/71 90 2

Fig. 20 (Cont.)

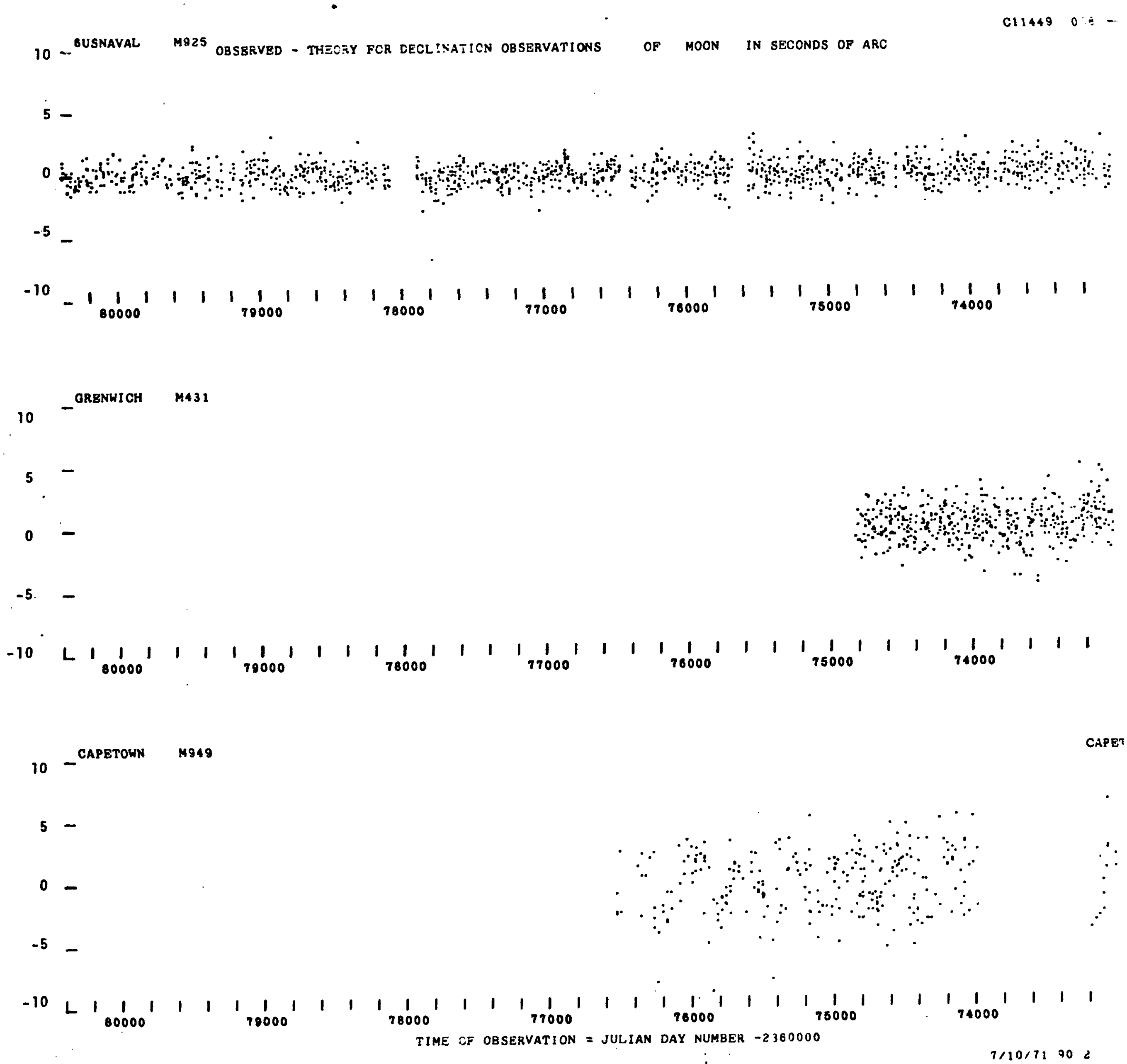
C11449
USNAVAL M925 OBSERVED - THEORY FOR DECLINATION OBSERVATIONS OF MOON IN SECONDS OF ARC
10
5
0
-5
-10
80000
79000
78000
77000
76000
75000
74000
GRENWICH M431
CAPETOWN M949
TIME OF OBSERVATION = JULIAN DAY NUMBER -2360000
7/10/71

Fig. 20 (Cont.)

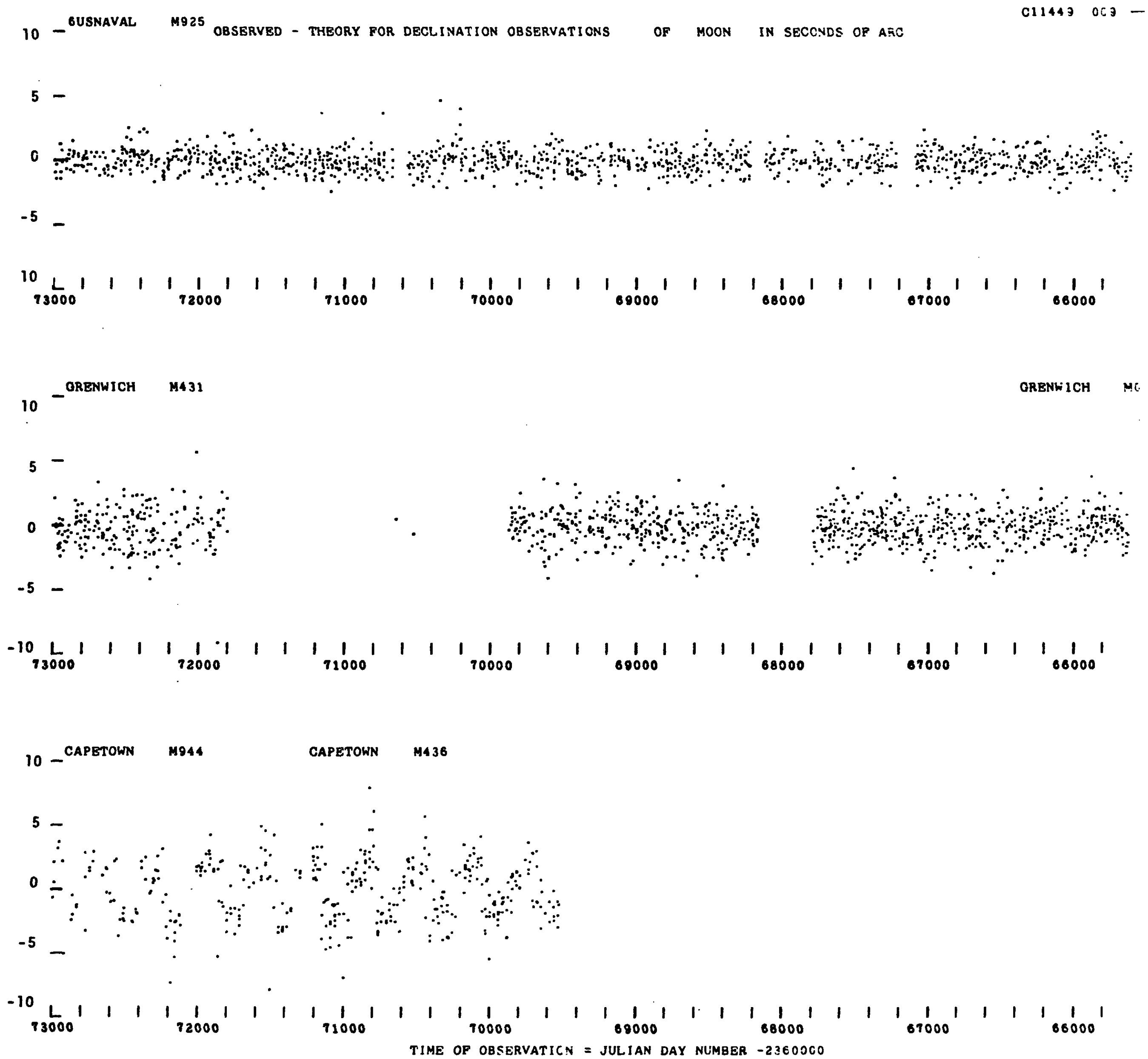
C11449 009
6USNAVAL M925 OBSERVED - THEORY FOR DECLINATION OBSERVATIONS OF MOON IN SECONDS OF ARC
GRENWICH M431
GRENWICH
CAPETOWN M944
CAPETOWN M436
TIME OF OBSERVATION = JULIAN DAY NUMBER -2360000
7/10/71 90 2

Fig. 20 (Cont.)

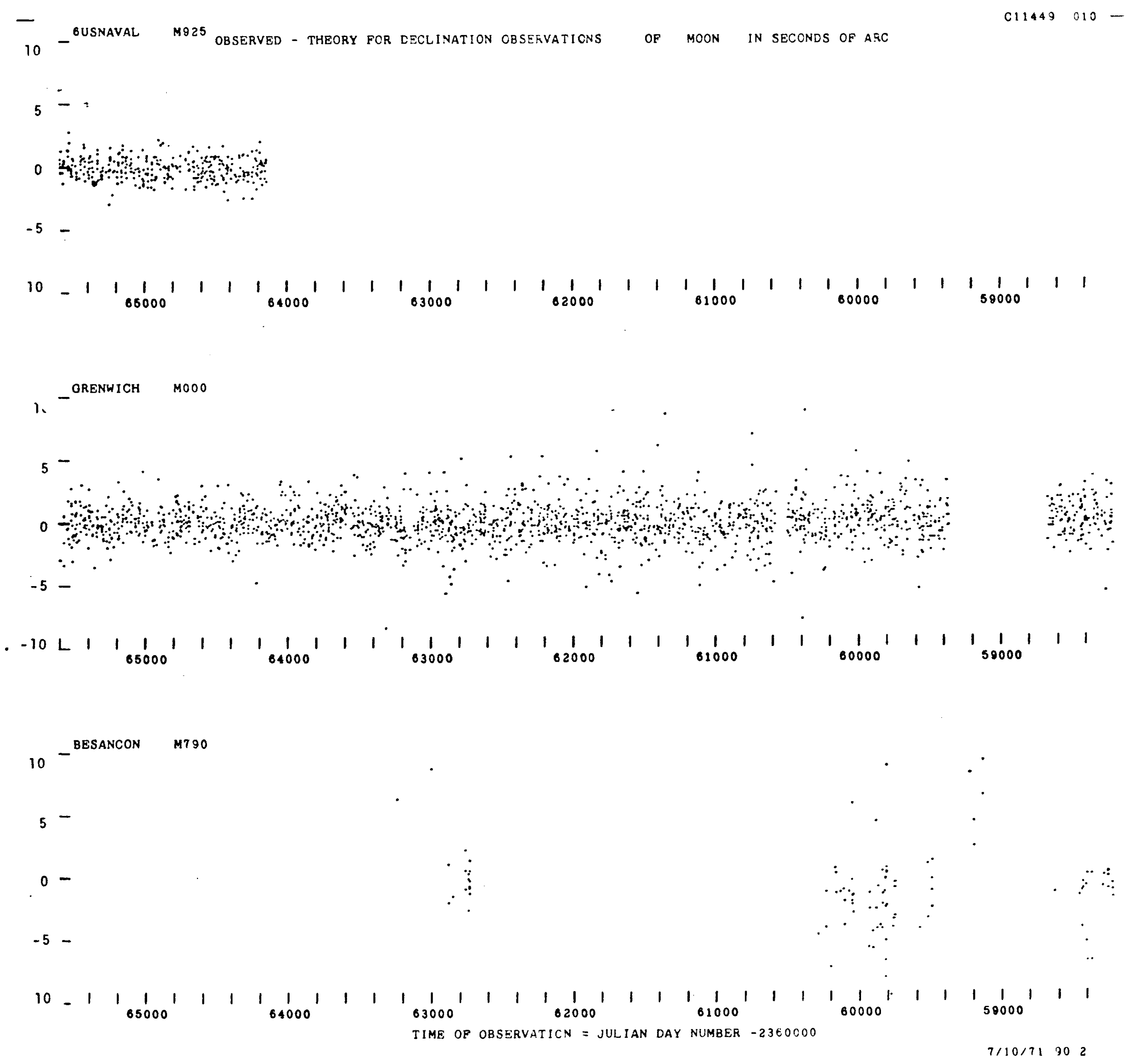
C11449 010
6USNAVAL M925 OBSERVED - THEORY FOR DECLINATION OBSERVATIONS OF MOON IN SECONDS OF ARC
10
5
0
-5
10
65000
64000
63000
62000
61000
60000
59000
GRENWICH M000
5
0
-5
-10
65000
64000
63000
62000
61000
60000
59000
BESANCON M790
10
5
0
-5
10
65000
64000
63000
62000
61000
60000
59000
TIME OF OBSERVATICN = JULIAN DAY NUMBER -2360000
7/10/71 90 2

Fig. 20(Cont.)

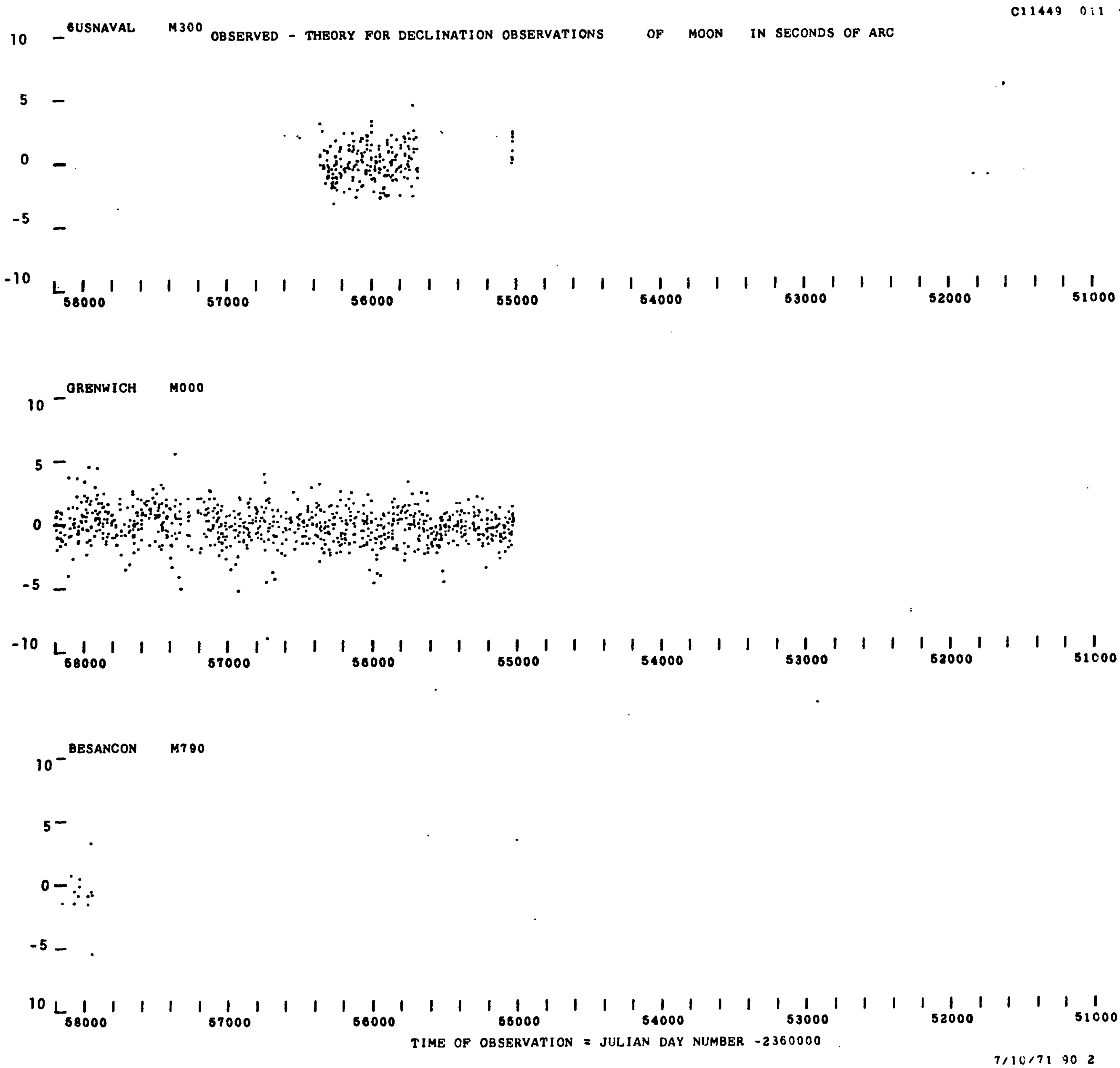
C11449 011 -
6USNAVAL M300 OBSERVED - THEORY FOR DECLINATION OBSERVATIONS OF MOON IN SECONDS OF ARC
10
5
0
-5
-10
58000
57000
56000
55000
54000
53000
52000
51000
GRENWICH M000
BESANCON M790
TIME OF OBSERVATION = JULIAN DAY NUMBER -2360000
7/10/71 90 2

Fig. 20 (Cont.)

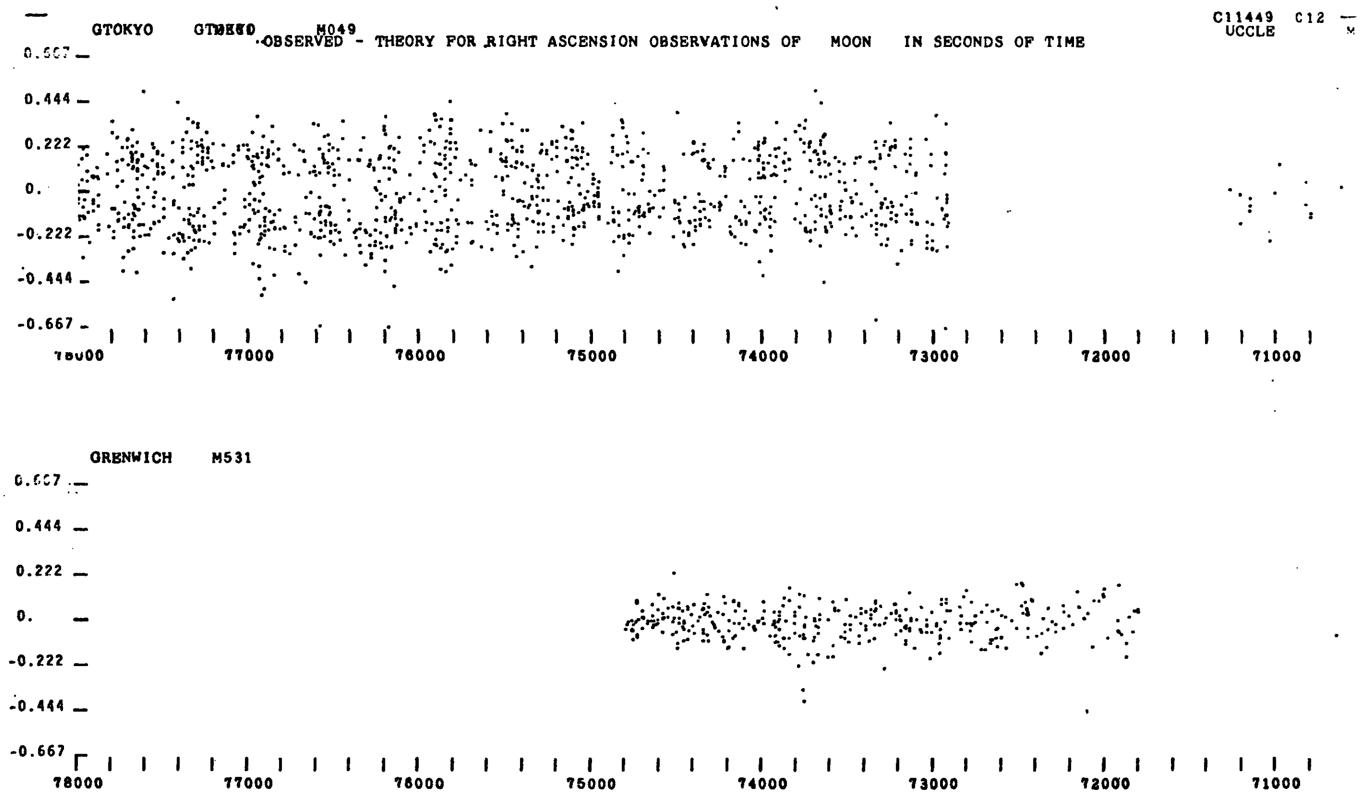

TIME OF OBSERVATION = JULIAN DAY NUMBER -2360000

7/10/71 90 2

Fig. 21

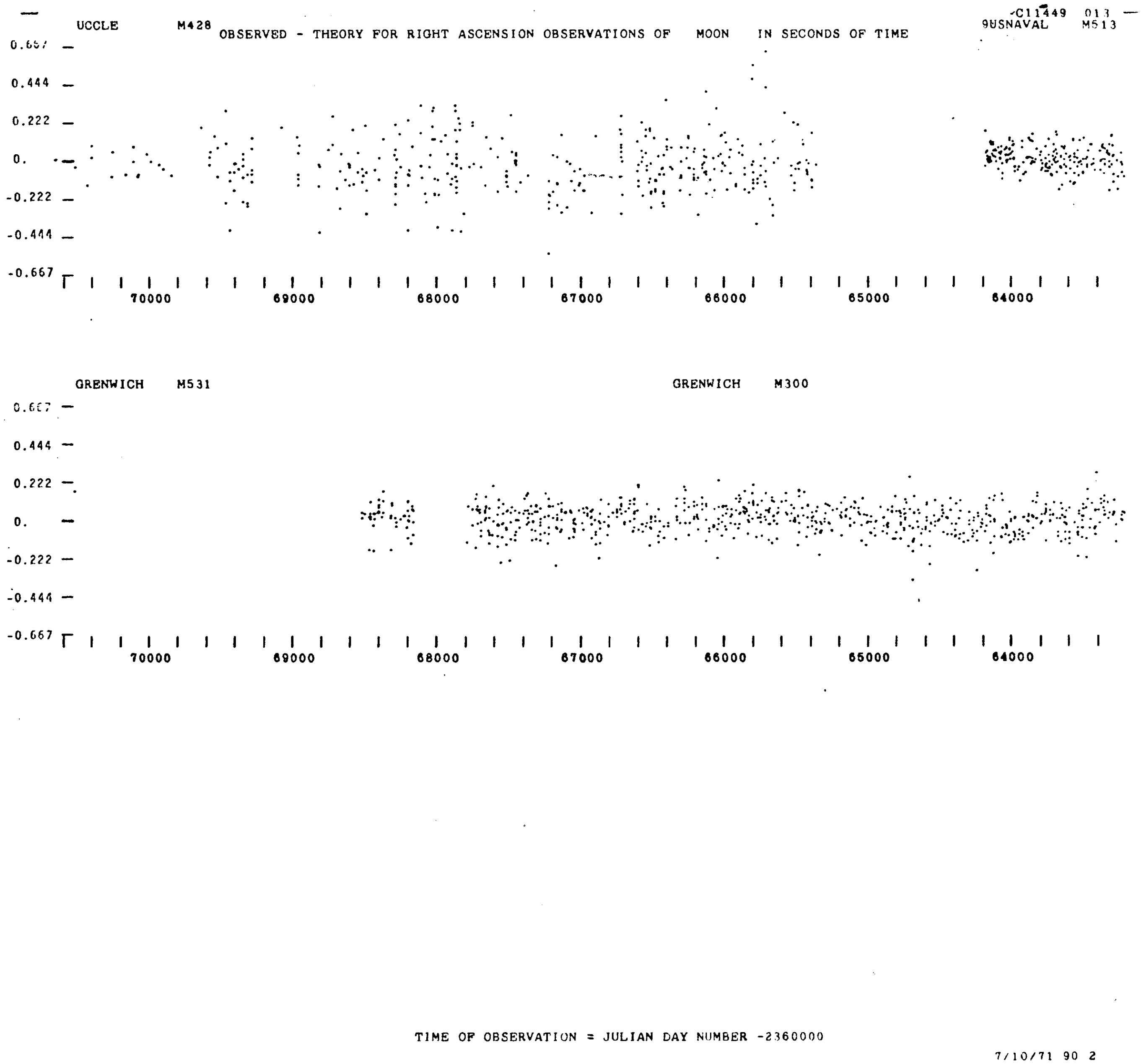
-C11449 013
UCCLE M428
OBSERVED - THEORY FOR RIGHT ASCENSION OBSERVATIONS OF MOON IN SECONDS OF TIME
9USNAVAL M513
0.444
0.222
0.
-0.222
-0.444
-0.667
70000
69000
68000
67000
66000
65000
64000
GRENWICH M531
GRENWICH M300
0.444
0.222
0.
-0.222
-0.444
-0.667
70000
69000
68000
67000
66000
65000
64000
TIME OF OBSERVATION = JULIAN DAY NUMBER -2360000
7/10/71 90 2

Fig. 21 (Cont.)

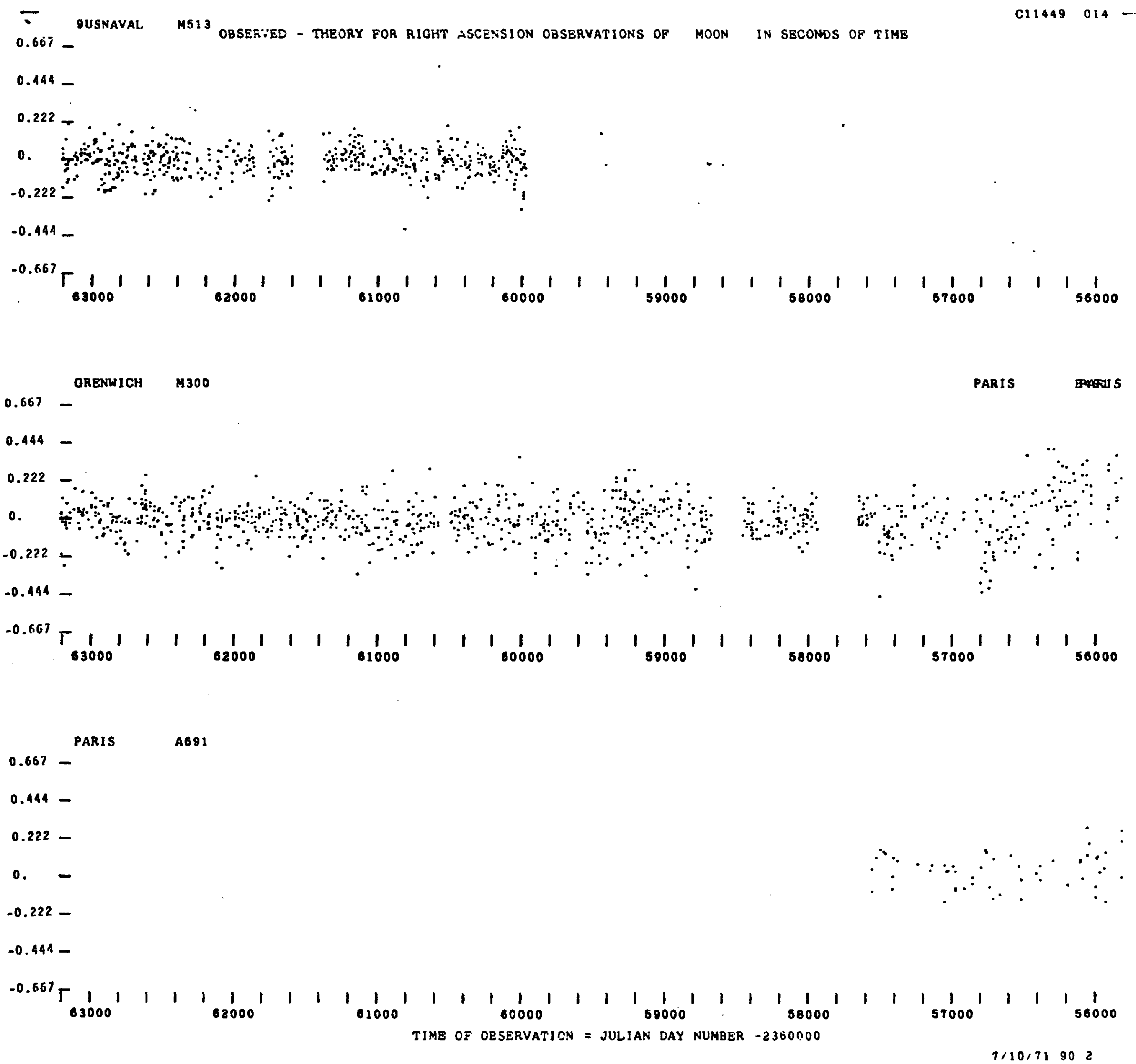
C11449 014
9USNAVAL M513
OBSERVED - THEORY FOR RIGHT ASCENSION OBSERVATIONS OF MOON IN SECONDS OF TIME
0.667
0.444
0.222
0.
-0.222
-0.444
-0.667
63000
62000
61000
60000
59000
58000
57000
56000
GRENWICH M300
PARIS
PARIS
PARIS A691
TIME OF OBSERVATION = JULIAN DAY NUMBER -2360000
7/10/71 90 2

Fig. 21 (Cont.)

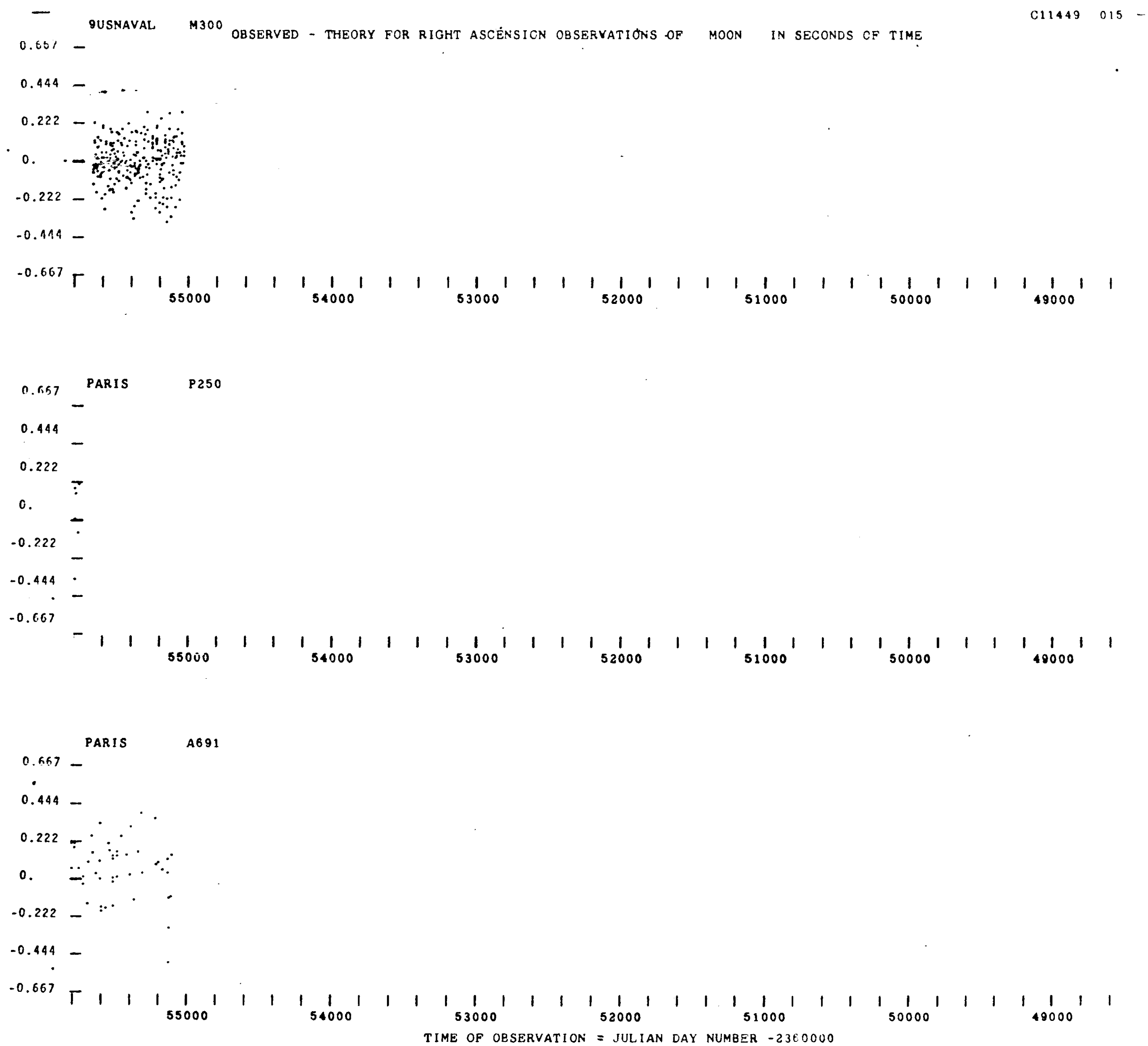
C11449 015
9USNAVAL M300 OBSERVED - THEORY FOR RIGHT ASCENSION OBSERVATIONS OF MOON IN SECONDS OF TIME
PARIS P250
PARIS A691
0.667
0.444
0.222
0.
-0.222
-0.444
-0.667
55000
54000
53000
52000
51000
50000
49000
TIME OF OBSERVATION = JULIAN DAY NUMBER -2360000
7/10/71

Fig. 21 (Cont.)

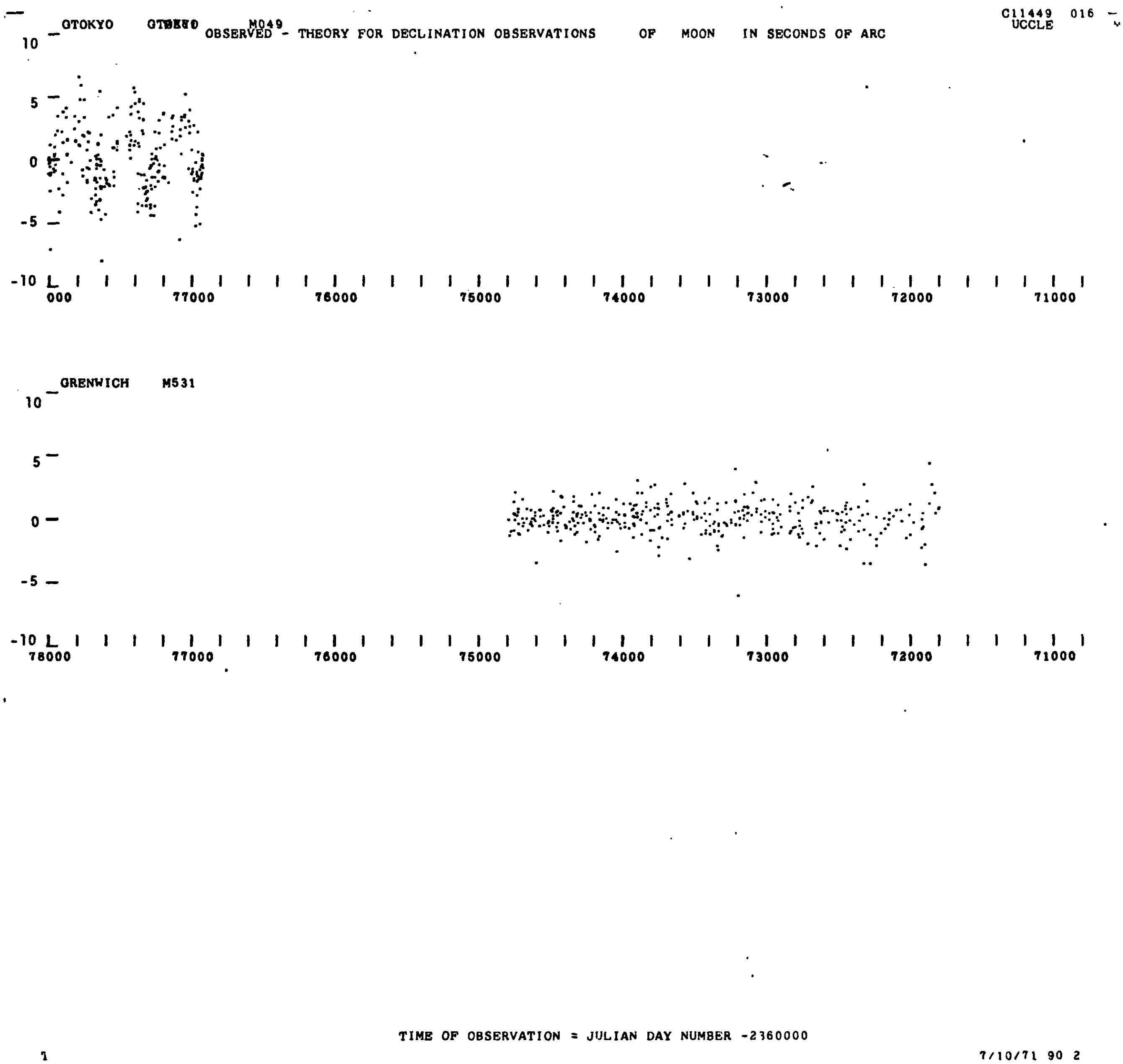

C11449 016
UCCLE
OTOKYO OTOKYO M049
OBSERVED - THEORY FOR DECLINATION OBSERVATIONS OF MOON IN SECONDS OF ARC
10
5
0
-5
-10
000
77000
76000
75000
74000
73000
72000
71000
GRENWICH M531
10
5
0
-5
-10
78000
77000
76000
75000
74000
73000
72000
71000
TIME OF OBSERVATION = JULIAN DAY NUMBER -2360000
1
7/10/71 90 2

Fig. 21 (Cont.)

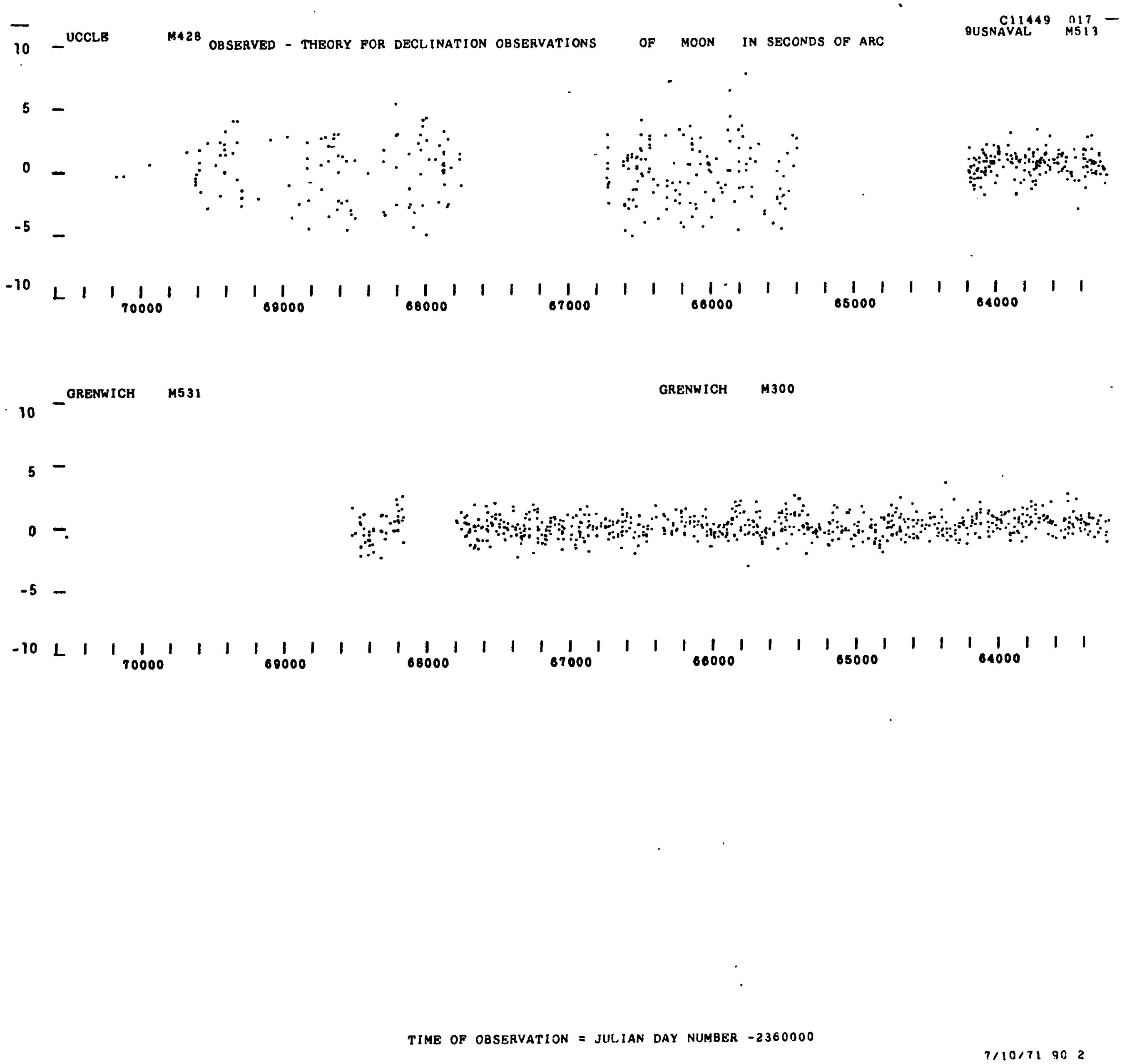
C11449 017
UCCLE M428
OBSERVED - THEORY FOR DECLINATION OBSERVATIONS OF MOON IN SECONDS OF ARC
9USNAVAL M513
10
5
0
-5
-10
70000
69000
68000
67000
66000
65000
64000
GRENWICH M531
GRENWICH M300
10
5
0
-5
-10
70000
69000
68000
67000
66000
65000
64000
TIME OF OBSERVATION = JULIAN DAY NUMBER -2360000
7/10/71 90 2

Fig. 21 (Cont.)

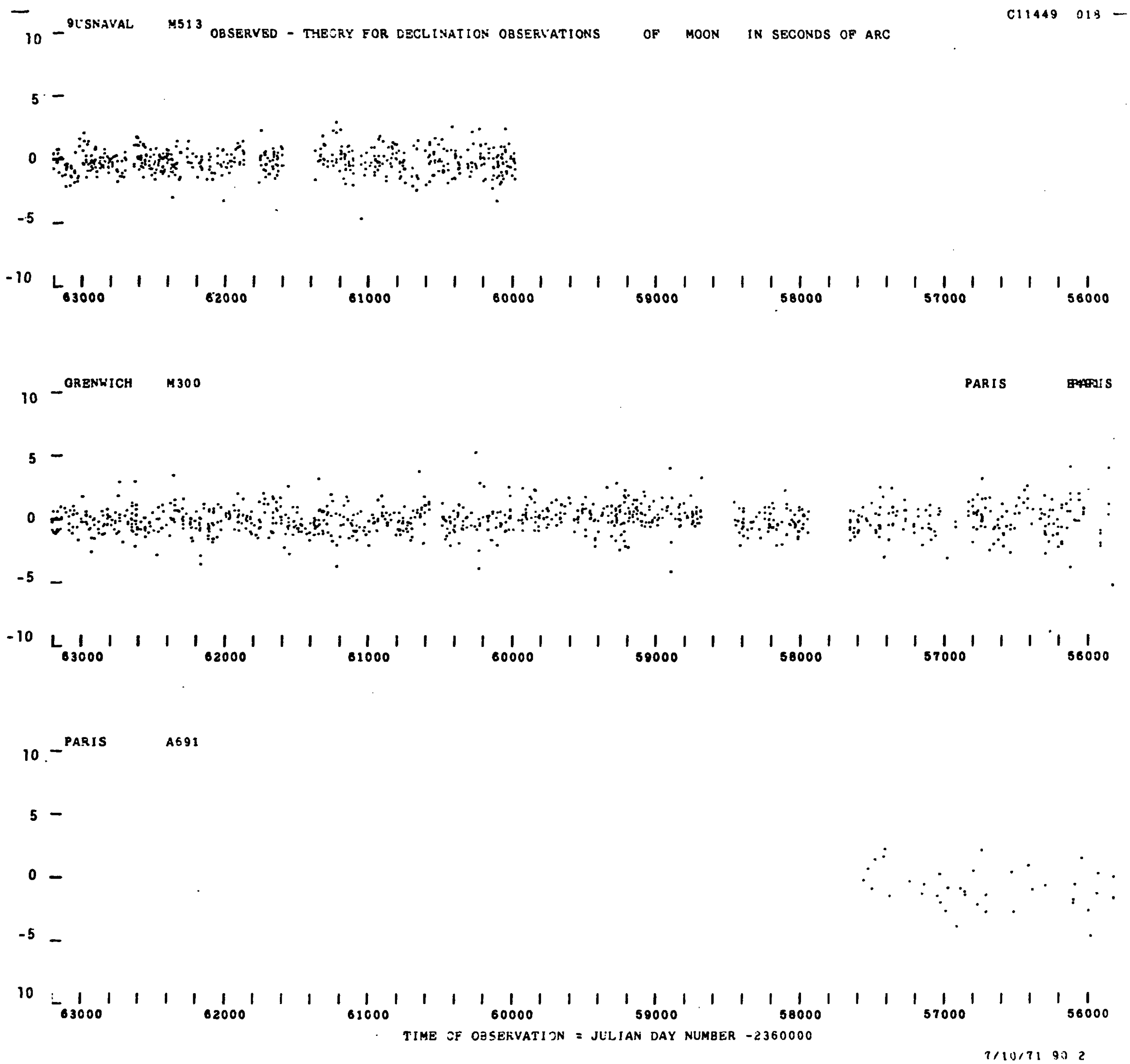

C11449 018
9USNAVAL M513 OBSERVED - THEORY FOR DECLINATION OBSERVATIONS OF MOON IN SECONDS OF ARC
10
5
0
-5
-10
63000
62000
61000
60000
59000
58000
57000
56000
GRENWICH M300
PARIS
PARIS A691
TIME OF OBSERVATION = JULIAN DAY NUMBER -2360000

Fig. 21 (Cont.)

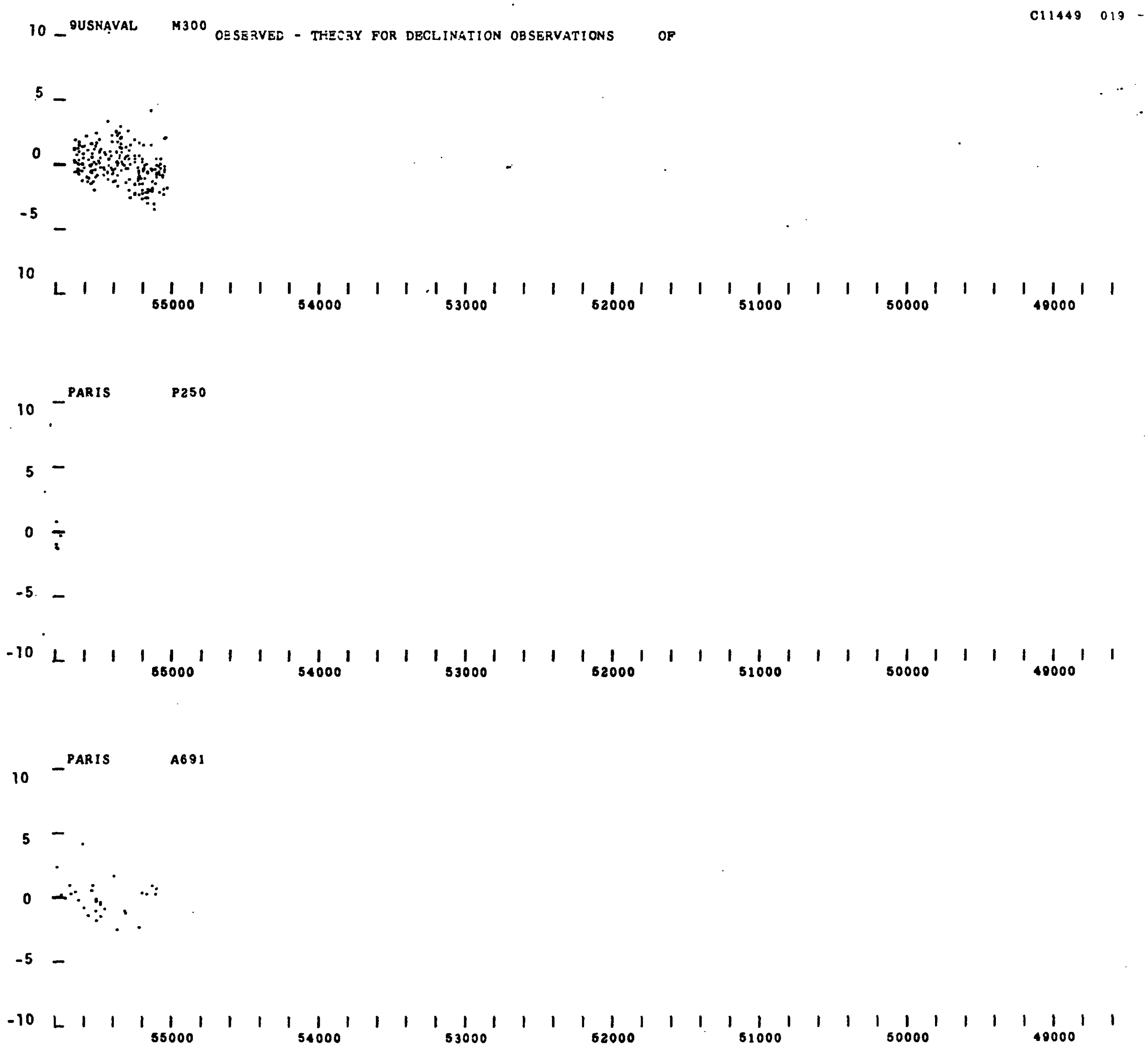
C11449 019
9USNAVAL M300 OBSERVED - THEORY FOR DECLINATION OBSERVATIONS OF
10
5
0
-5
10
55000
54000
53000
52000
51000
50000
49000
PARIS P250
10
5
0
-5
-10
55000
54000
53000
52000
51000
50000
49000
PARIS A691
10
5
0
-5
-10
55000
54000
53000
52000
51000
50000
49000

Fig. 21 (Cont.)

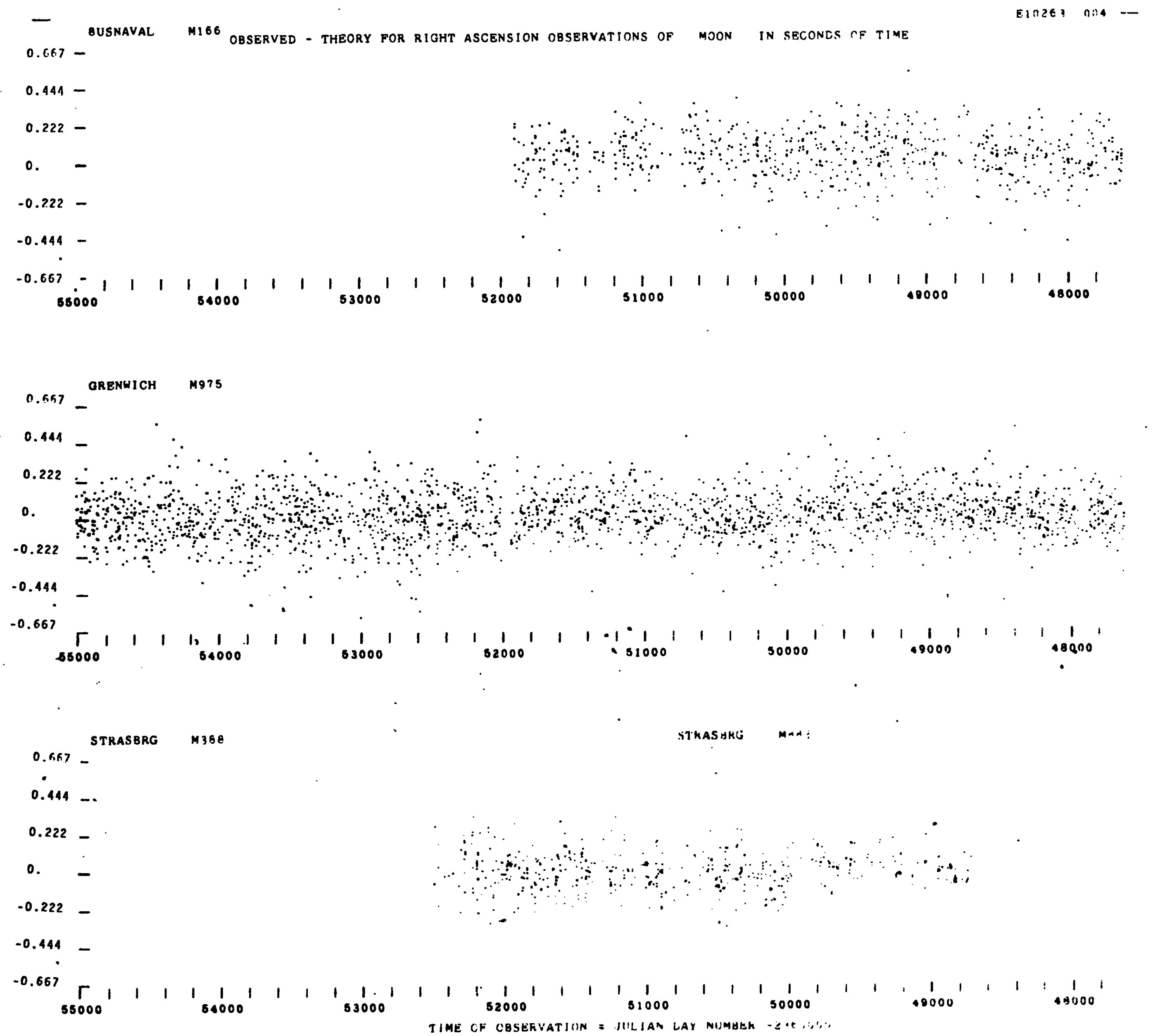

BUSNAVAL M166 OBSERVED - THEORY FOR RIGHT ASCENSION OBSERVATIONS OF MOON IN SECONDS OF TIME
0.667
0.444
0.222
0.
-0.222
-0.444
-0.667
55000
54000
53000
52000
51000
50000
49000
48000
GRENWICH M975
STRASBRG M368
STRASBRG
TIME OF OBSERVATION = JULIAN DAY NUMBER

Fig. 22

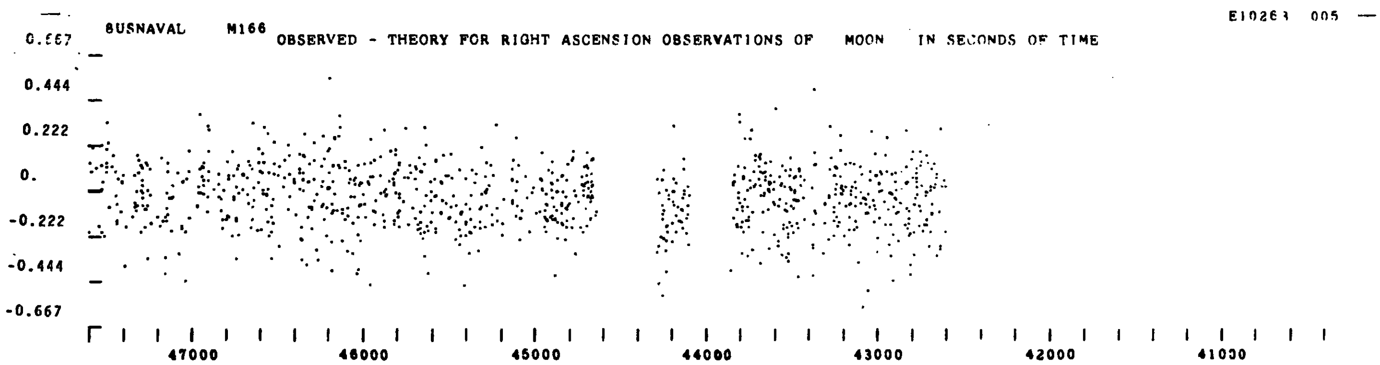

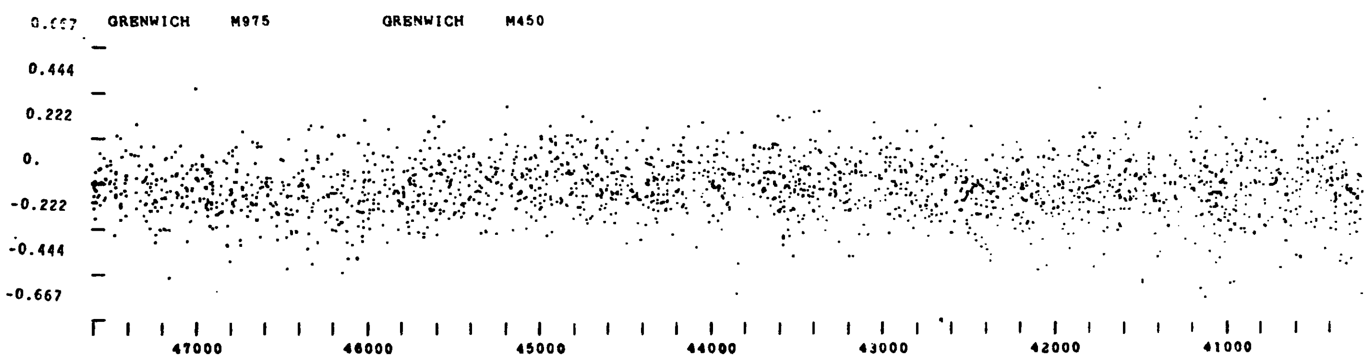

TIME OF OBSERVATION = JULIAN DAY NUMBER

Fig. 22 (Cont.)

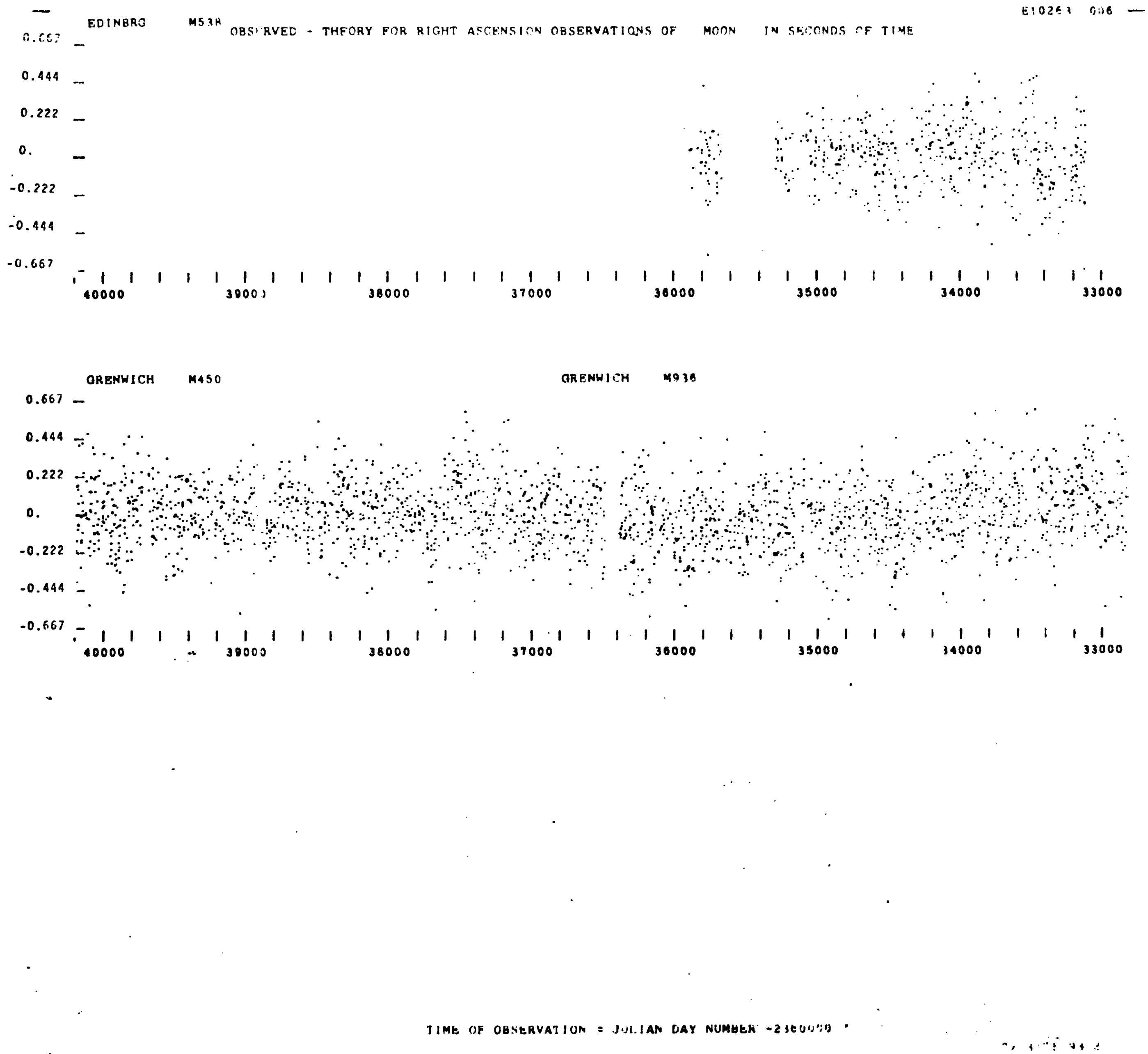
E10263 006
EDINBRG M538
OBSERVED - THEORY FOR RIGHT ASCENSION OBSERVATIONS OF MOON IN SECONDS OF TIME
0.667
0.444
0.222
0.
-0.222
-0.444
-0.667
40000
39000
38000
37000
36000
35000
34000
33000
GRENWICH M450
GRENWICH M936
TIME OF OBSERVATION = JULIAN DAY NUMBER -2360000

Fig. 22 (Cont.)

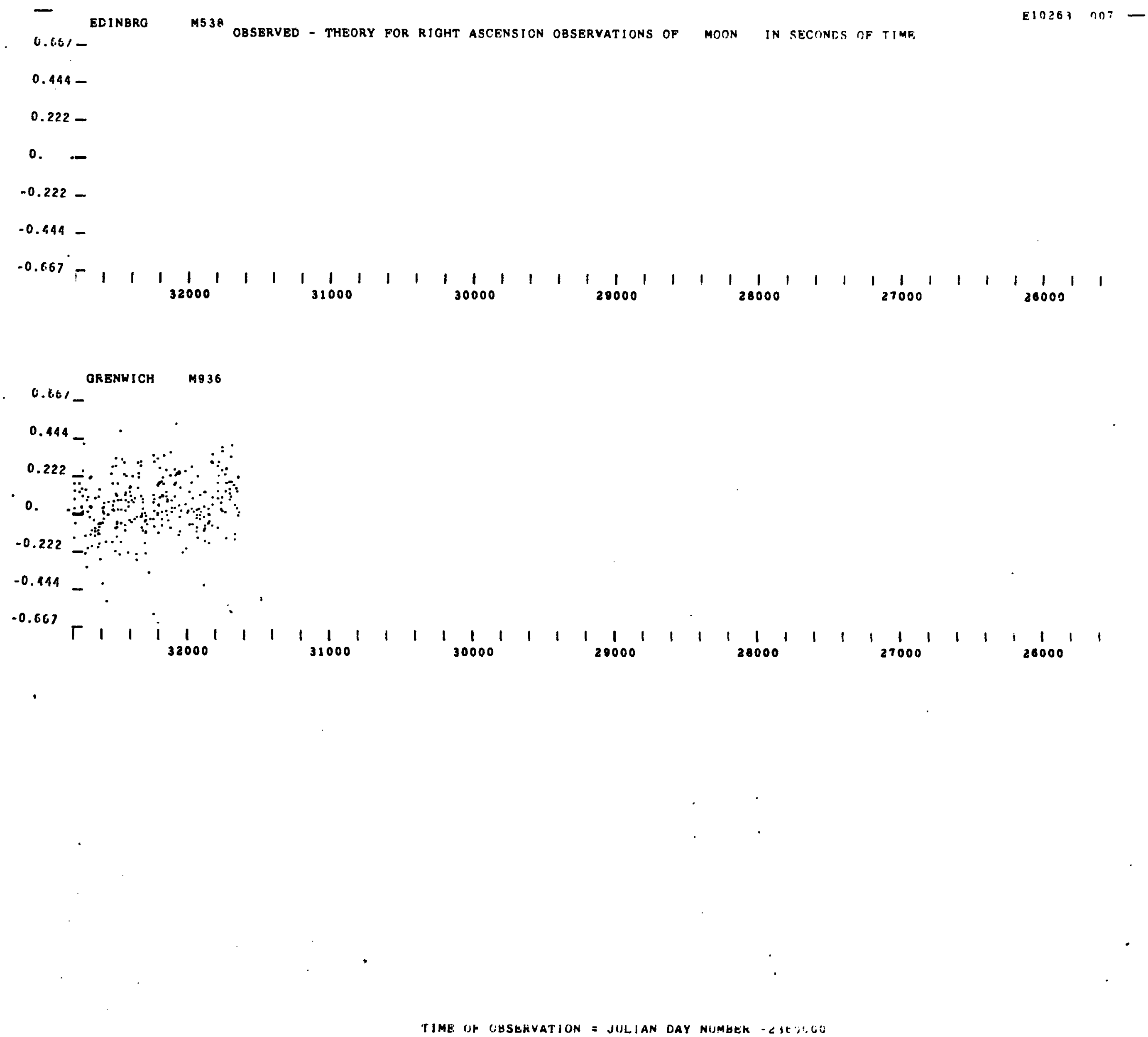
EDINBRG M538
OBSERVED - THEORY FOR RIGHT ASCENSION OBSERVATIONS OF MOON IN SECONDS OF TIME
0.444
0.222
0.
-0.222
-0.444
-0.667
32000
31000
30000
29000
28000
27000
26000
GRENWICH M936
0.444
0.222
0.
-0.222
-0.444
-0.667
32000
31000
30000
29000
28000
27000
26000
TIME OF OBSERVATION = JULIAN DAY NUMBER

Fig. 22 (Cont.)

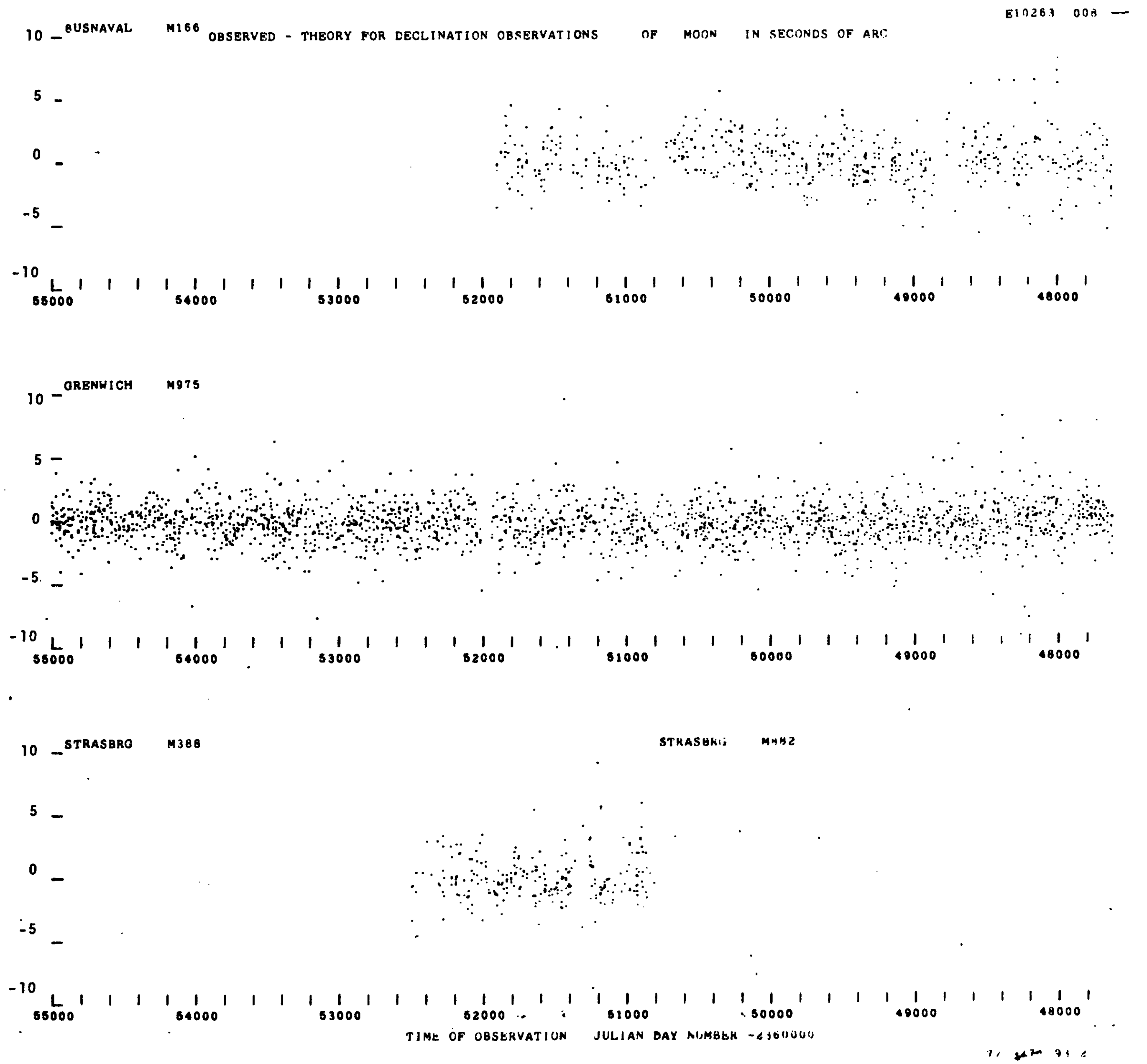
OBSERVED - THEORY FOR DECLINATION OBSERVATIONS OF MOON IN SECONDS OF ARC
USNAVAL M166
GRENWICH M975
STRASBRG M388
10
5
0
-5
-10
55000
54000
53000
52000
51000
50000
49000
48000
TIME OF OBSERVATION JULIAN DAY NUMBER

Fig. 22 (Cont.)

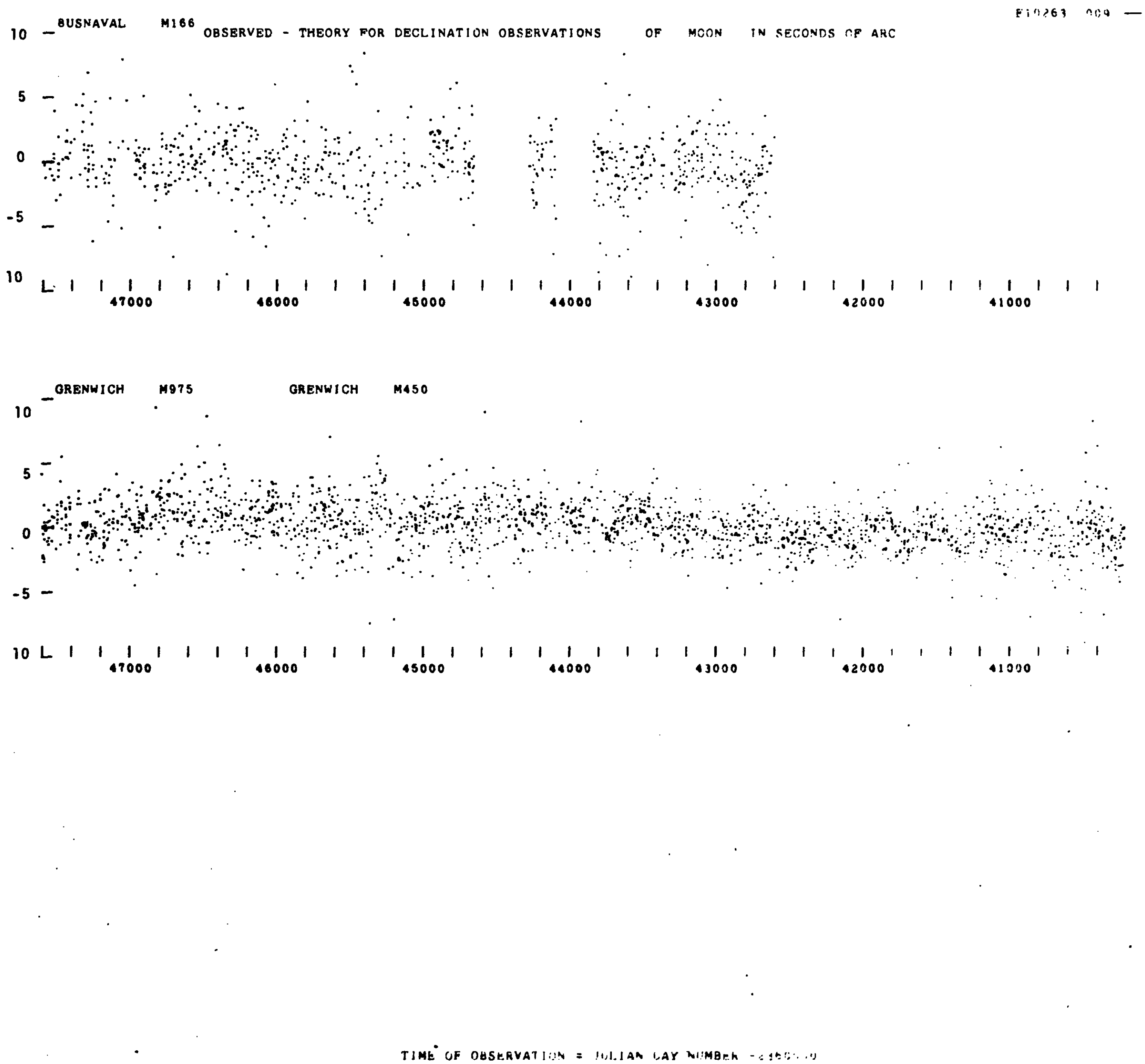
F10263 009
USNAVAL M166 OBSERVED - THEORY FOR DECLINATION OBSERVATIONS OF MOON IN SECONDS OF ARC
10
5
0
-5
10
47000
46000
45000
44000
43000
42000
41000
GRENWICH M975 GRENWICH M450
10
5
0
-5
10
47000
46000
45000
44000
43000
42000
41000
TIME OF OBSERVATION = JULIAN DAY NUMBER

Fig. 22 (Cont.)

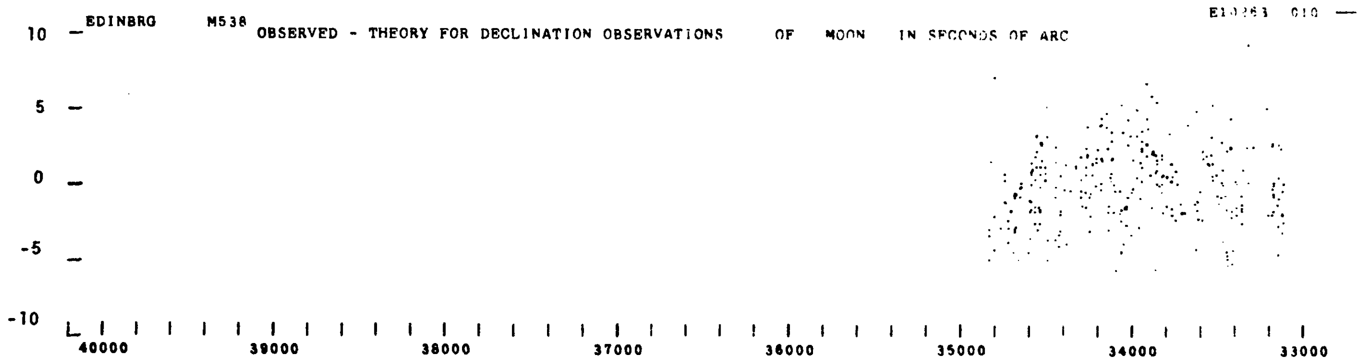

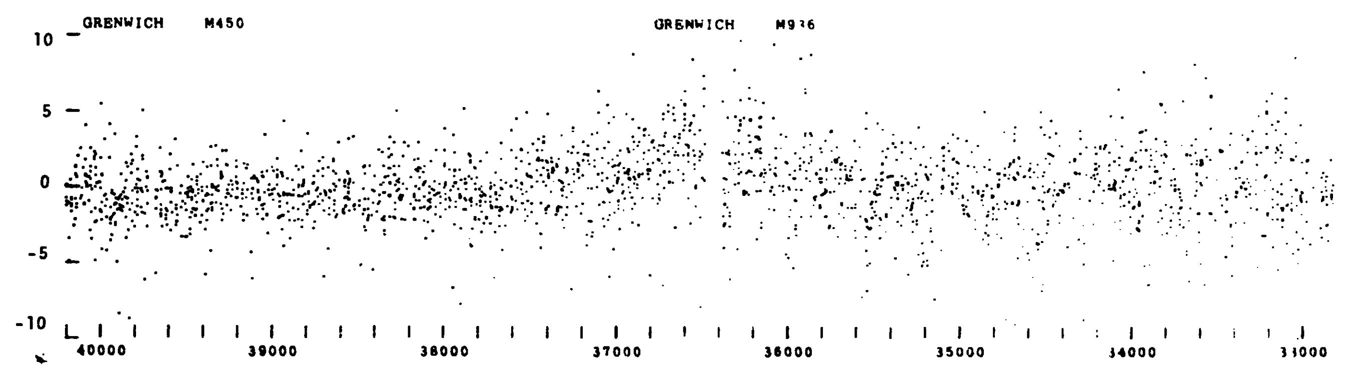

TIME OF OBSERVATION = JULIAN DAY NUMBER -2400000

Fig. 22 (Cont.)

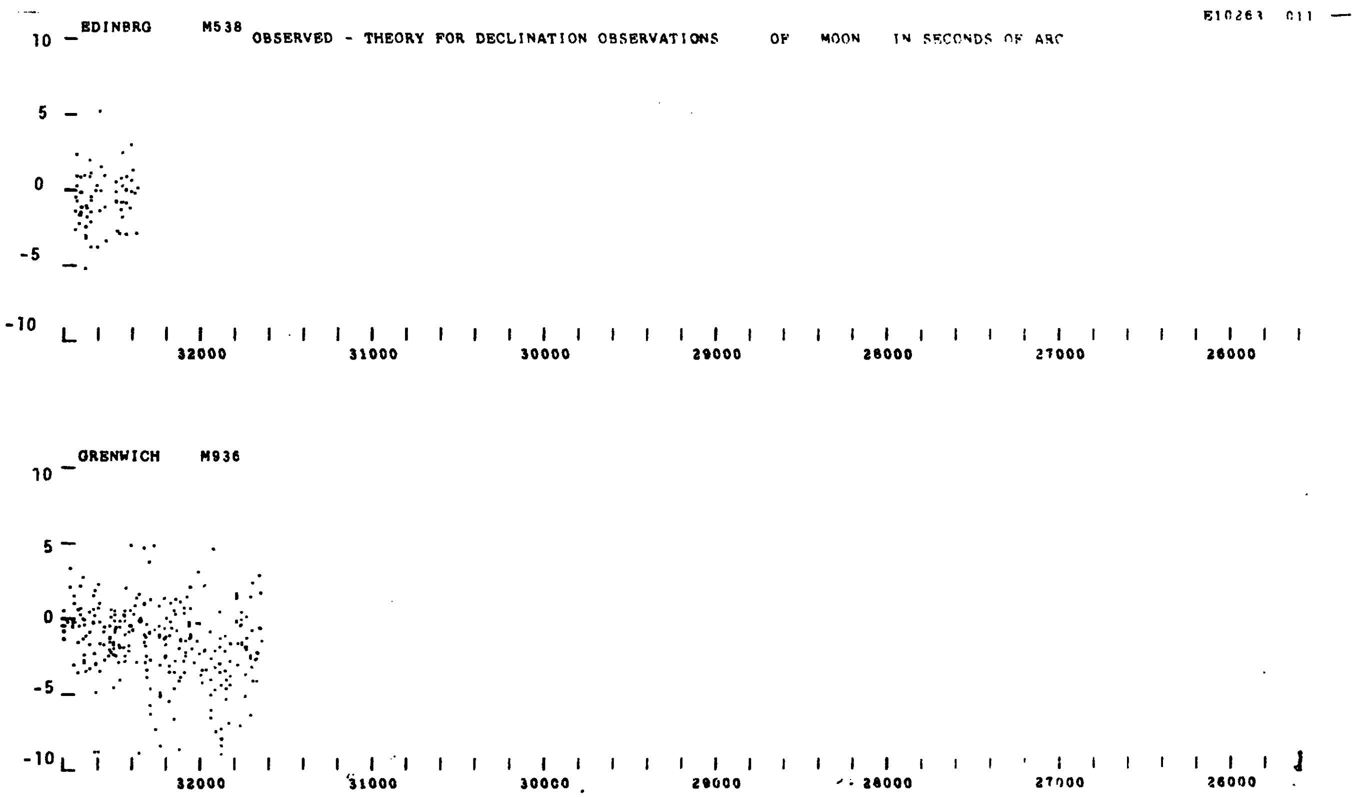

TIME OF OBSERVATION = JULIAN DAY NUMBER -2400000

Fig. 22 (Cont.)

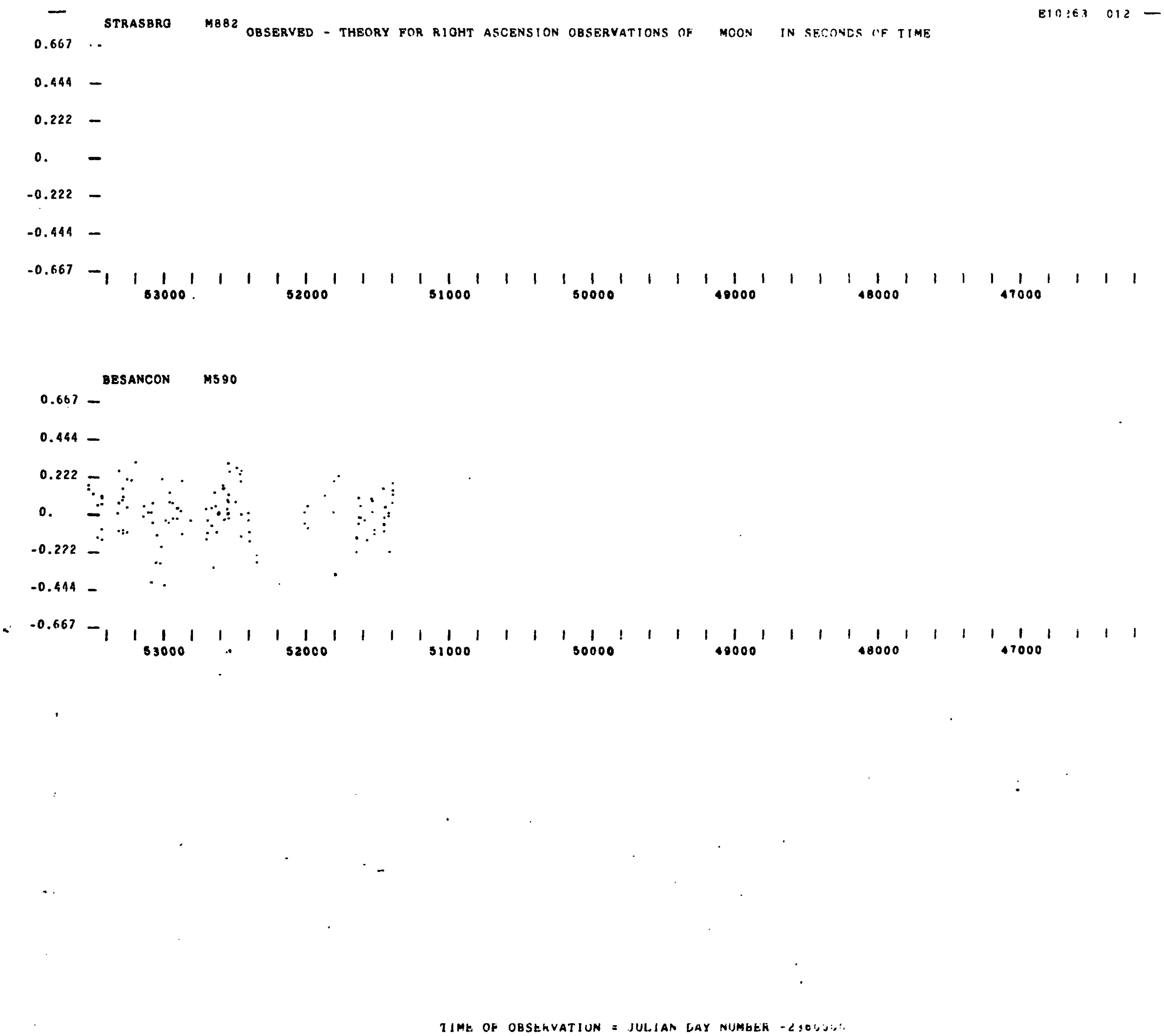
STRASBRG M882 OBSERVED - THEORY FOR RIGHT ASCENSION OBSERVATIONS OF MOON IN SECONDS OF TIME
0.667
0.444
0.222
0.
-0.222
-0.444
-0.667
53000
52000
51000
50000
49000
48000
47000
BESANCON M590
0.667
0.444
0.222
0.
-0.222
-0.444
-0.667
53000
52000
51000
50000
49000
48000
47000
TIME OF OBSERVATION = JULIAN DAY NUMBER

Fig. 23

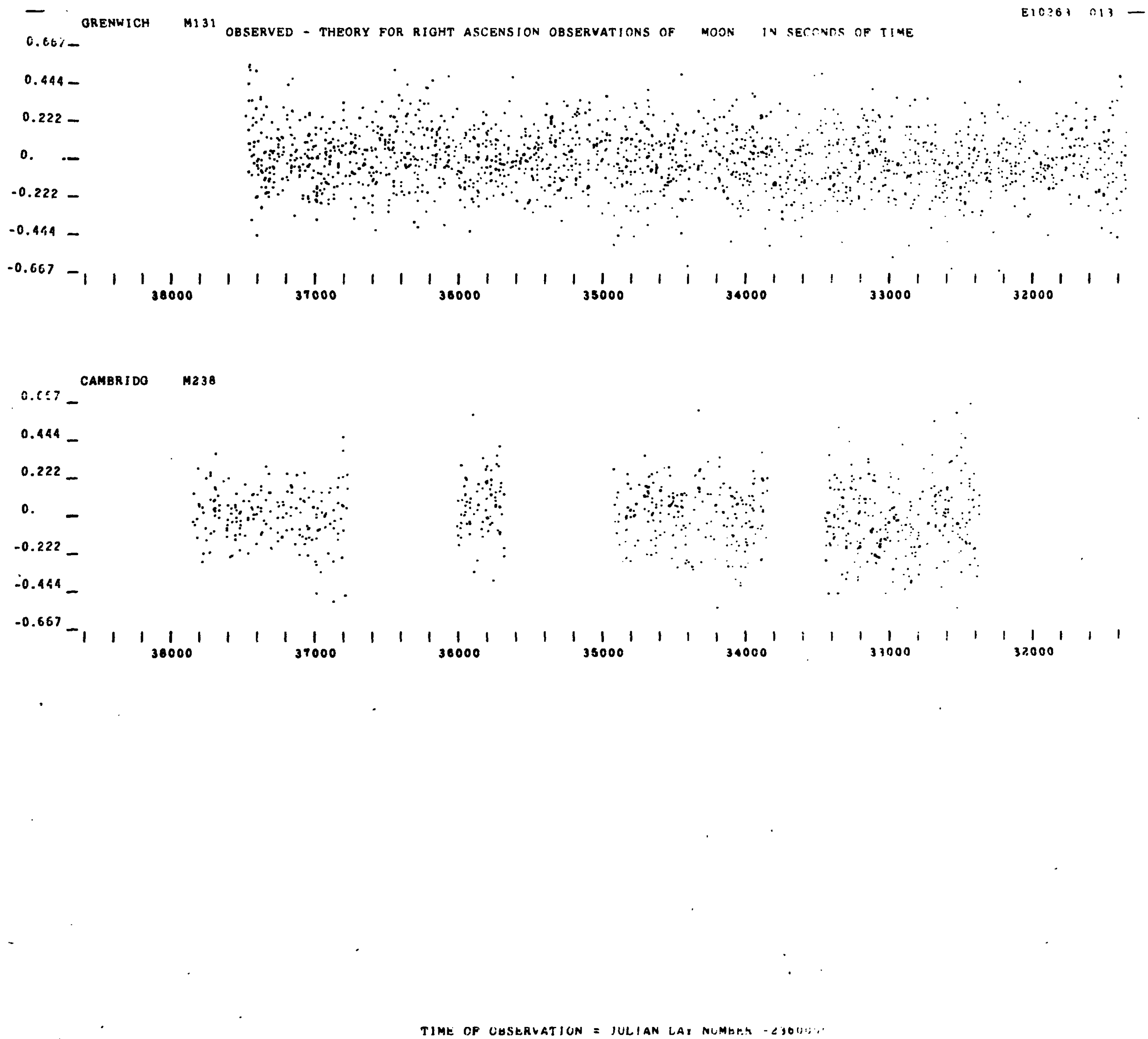
GRENWICH M131
OBSERVED - THEORY FOR RIGHT ASCENSION OBSERVATIONS OF MOON IN SECONDS OF TIME
0.667
0.444
0.222
0.
-0.222
-0.444
-0.667
38000
37000
36000
35000
34000
33000
32000
CAMBRIDG M238
0.ς57
0.444
0.222
0.
-0.222
-0.444
-0.667
38000
37000
36000
35000
34000
33000
32000
TIME OF OBSERVATION = JULIAN

Fig. 23 (Cont.)

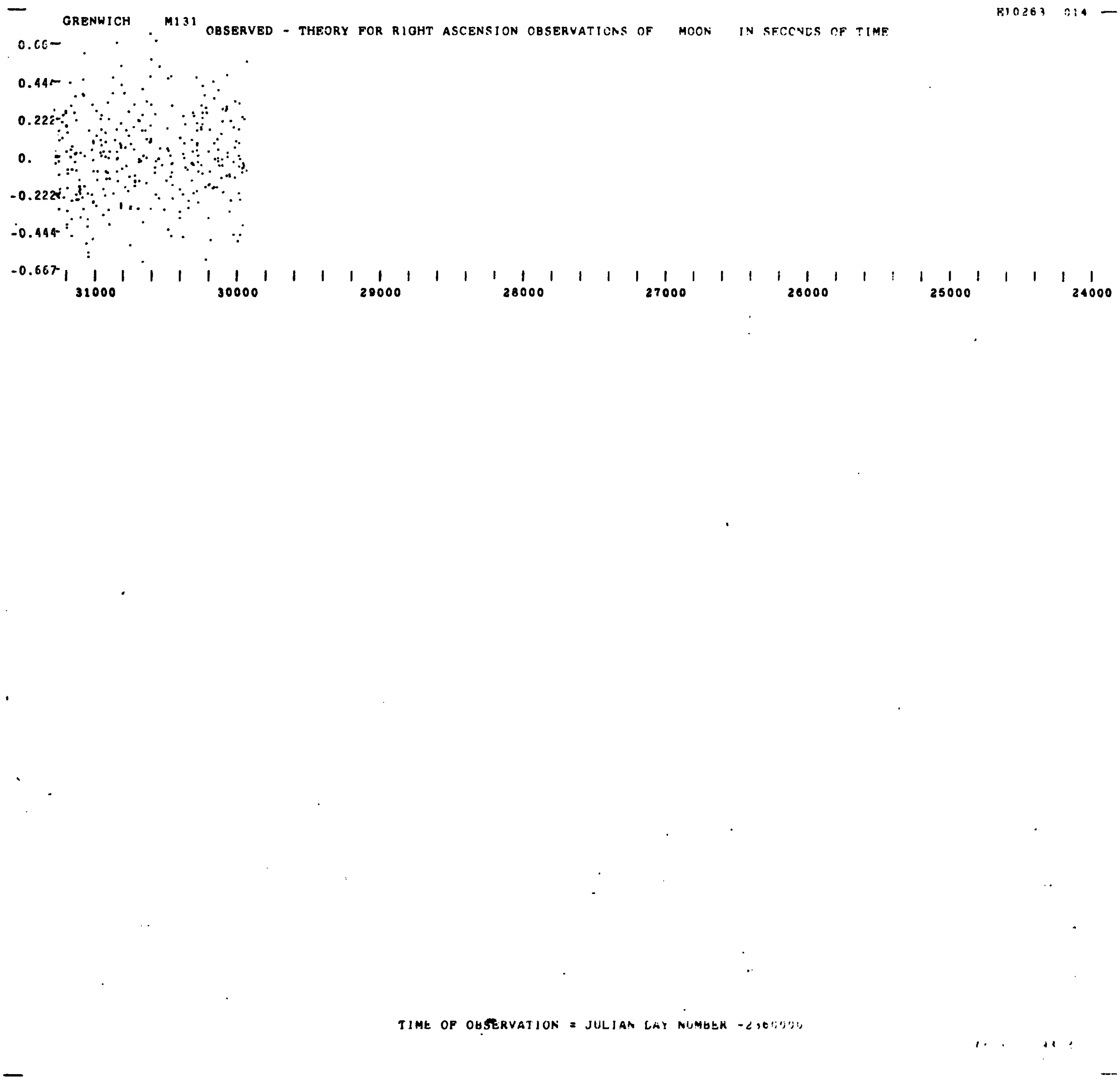
GRENWICH M131 OBSERVED - THEORY FOR RIGHT ASCENSION OBSERVATIONS OF MOON IN SECONDS OF TIME
0.444
0.222
0.
-0.222
-0.444
-0.667
31000
30000
29000
28000
27000
26000
25000
24000
TIME OF OBSERVATION = JULIAN DAY NUMBER

Fig. 23 (Cont.)

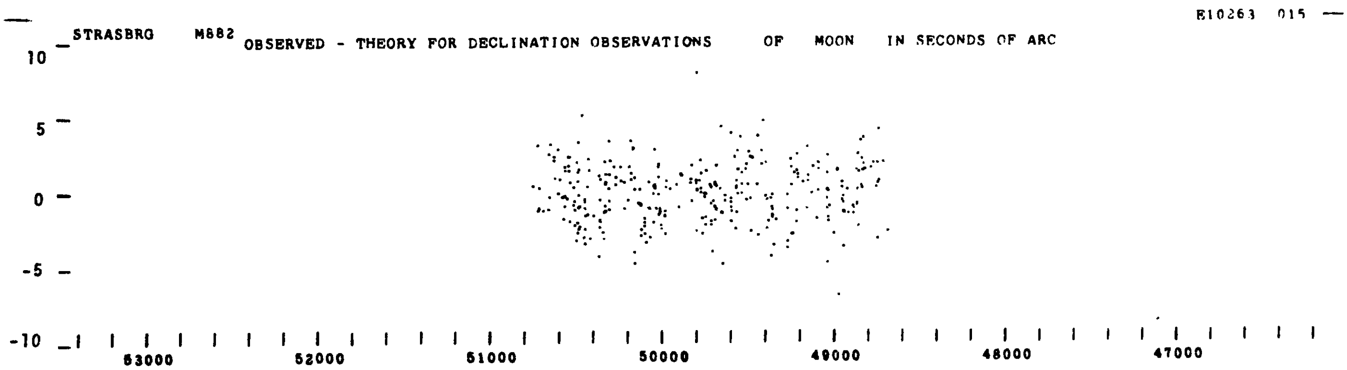

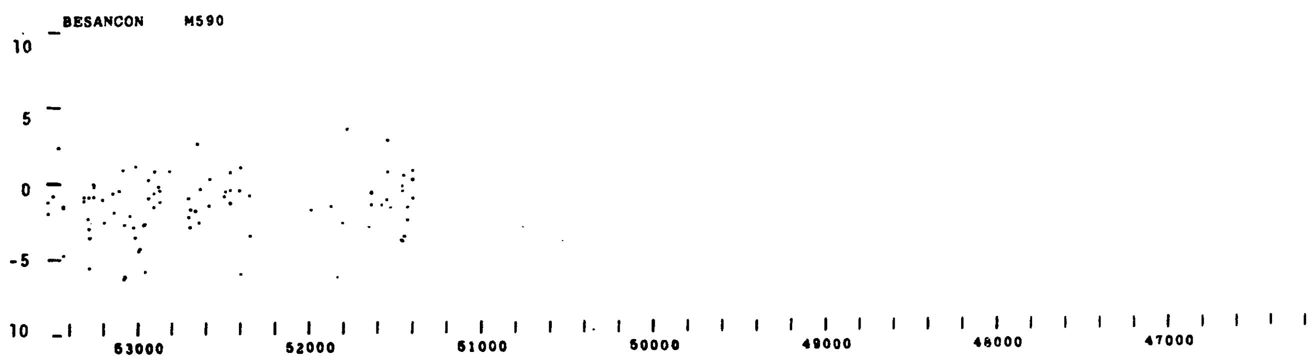

TIME OF OBSERVATION = JULIAN DAY NUMBER -236

Fig. 23 (Cont.)

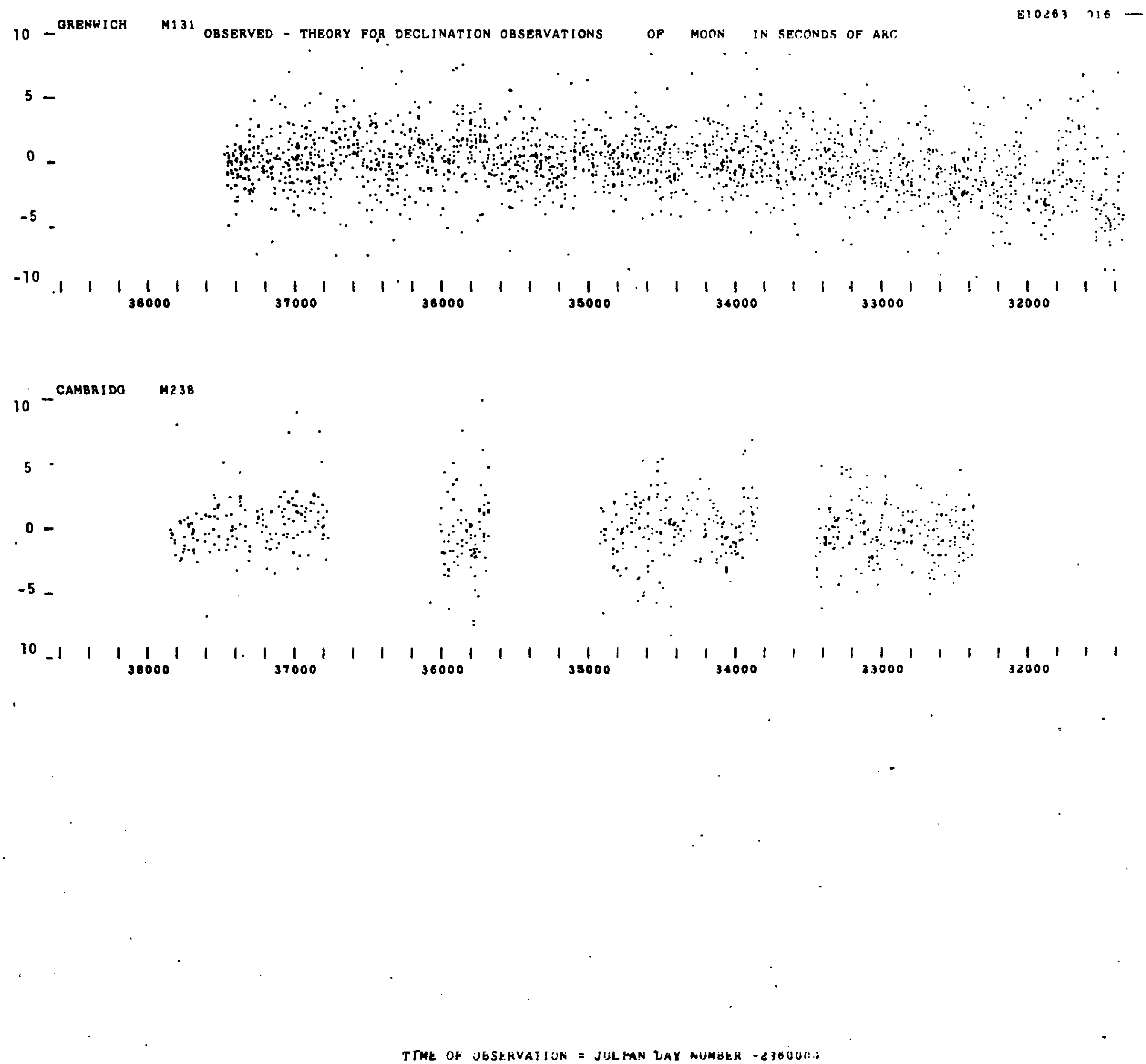
GRENWICH M131 OBSERVED - THEORY FOR DECLINATION OBSERVATIONS OF MOON IN SECONDS OF ARC
10
5
0
-5
-10
38000
37000
36000
35000
34000
33000
32000
CAMBRIDG M238
10
5
0
-5
10
38000
37000
36000
35000
34000
33000
32000

Fig. 23 (Cont.)

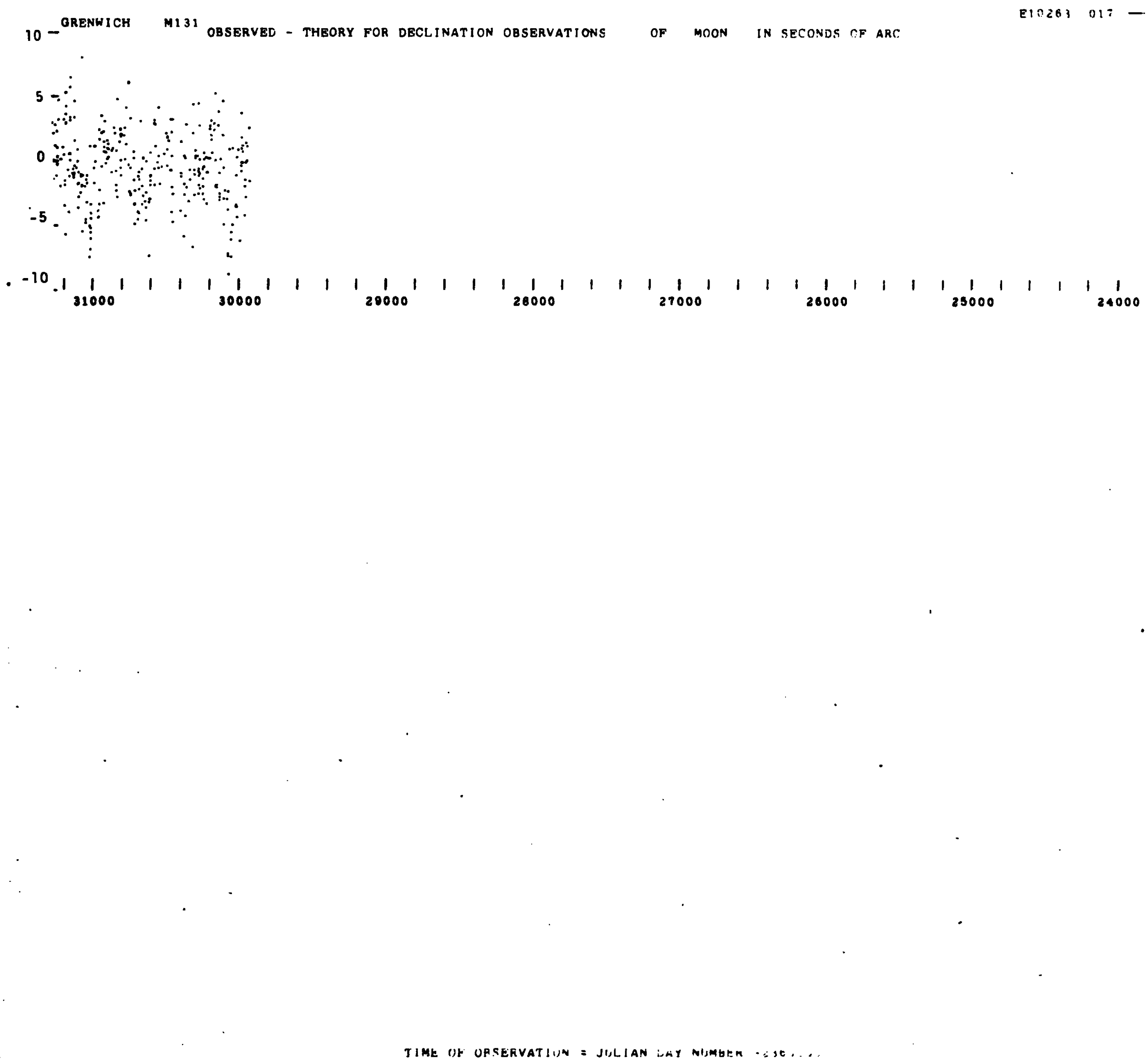
GRENWICH M131 OBSERVED - THEORY FOR DECLINATION OBSERVATIONS OF MOON IN SECONDS OF ARC
10
5
0
-5
-10
31000
30000
29000
28000
27000
26000
25000
24000

Fig. 23 (Cont.)

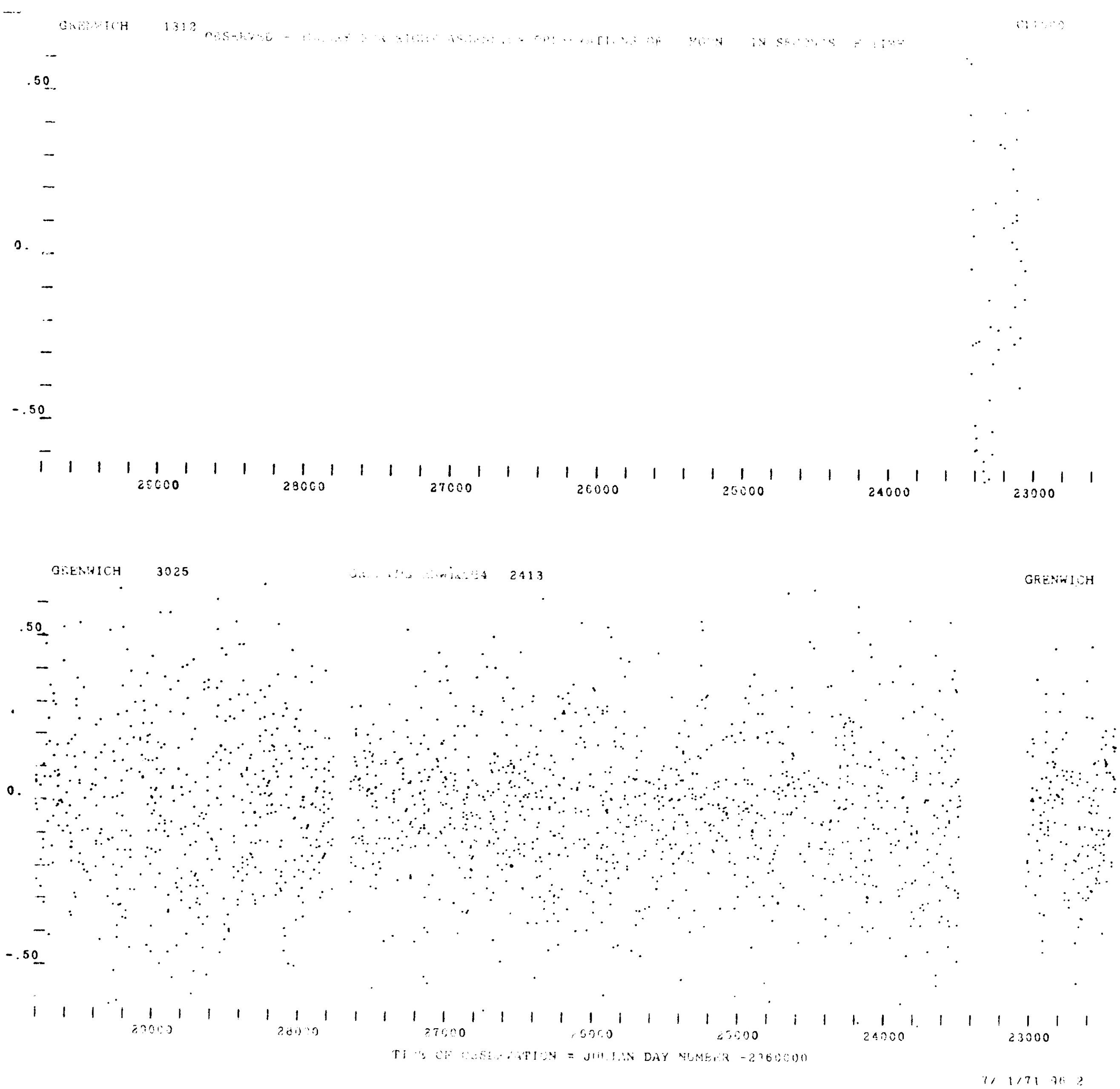
GREENWICH 1312
.50
0.
-.50
29000
28000
27000
26000
25000
24000
23000
GREENWICH 3025
2413
GREENWICH
TIME OF OBSERVATION = JULIAN DAY NUMBER -2360000

Fig. 24

OBSERVED - THEORY FOR RIGHT ASCENSION OBSERVATIONS OF MOON IN SECONDS OF TIME

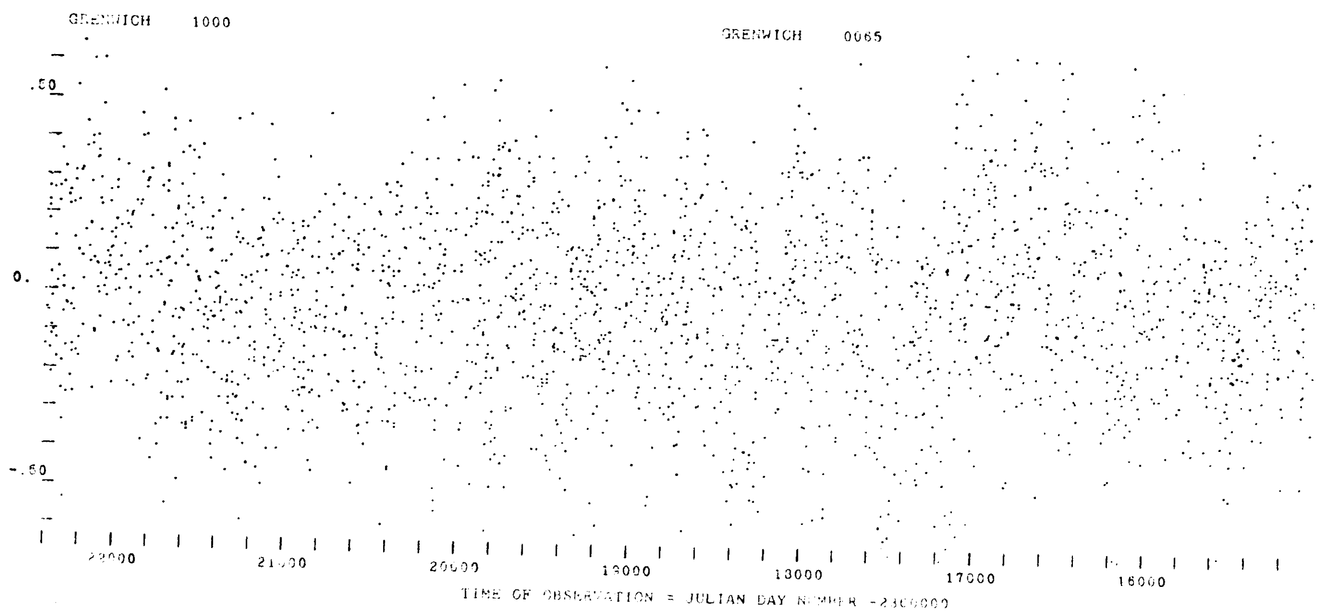

Fig. 24 (Cont.)

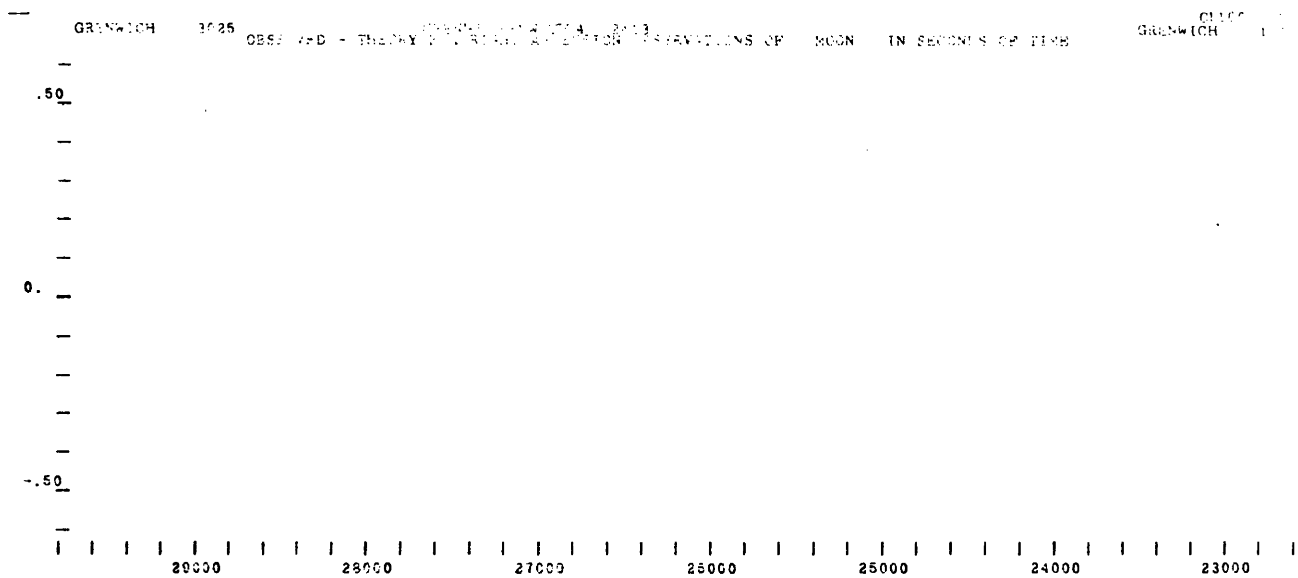
.50
0.
-.50
29000
28000
27000
26000
25000
24000
23000

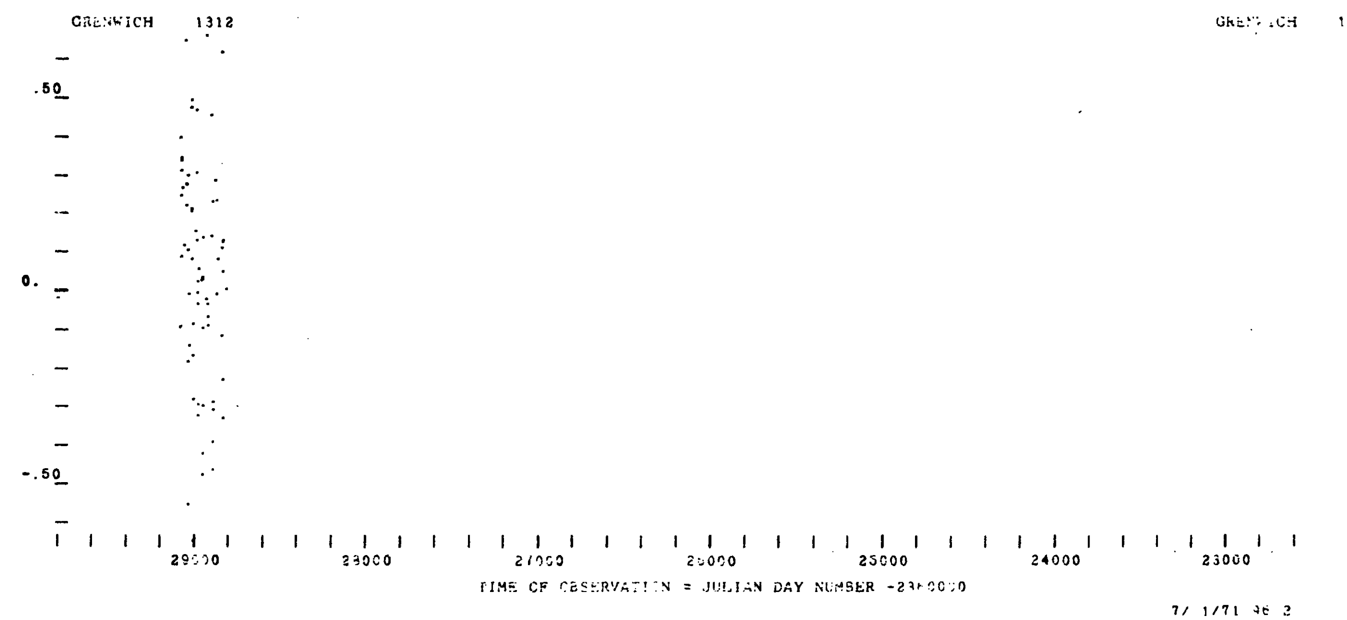
GRENWICH 1312
.50
0.
-.50
29000
28000
27000
26000
25000
24000
23000

Fig. 24 (Cont.)

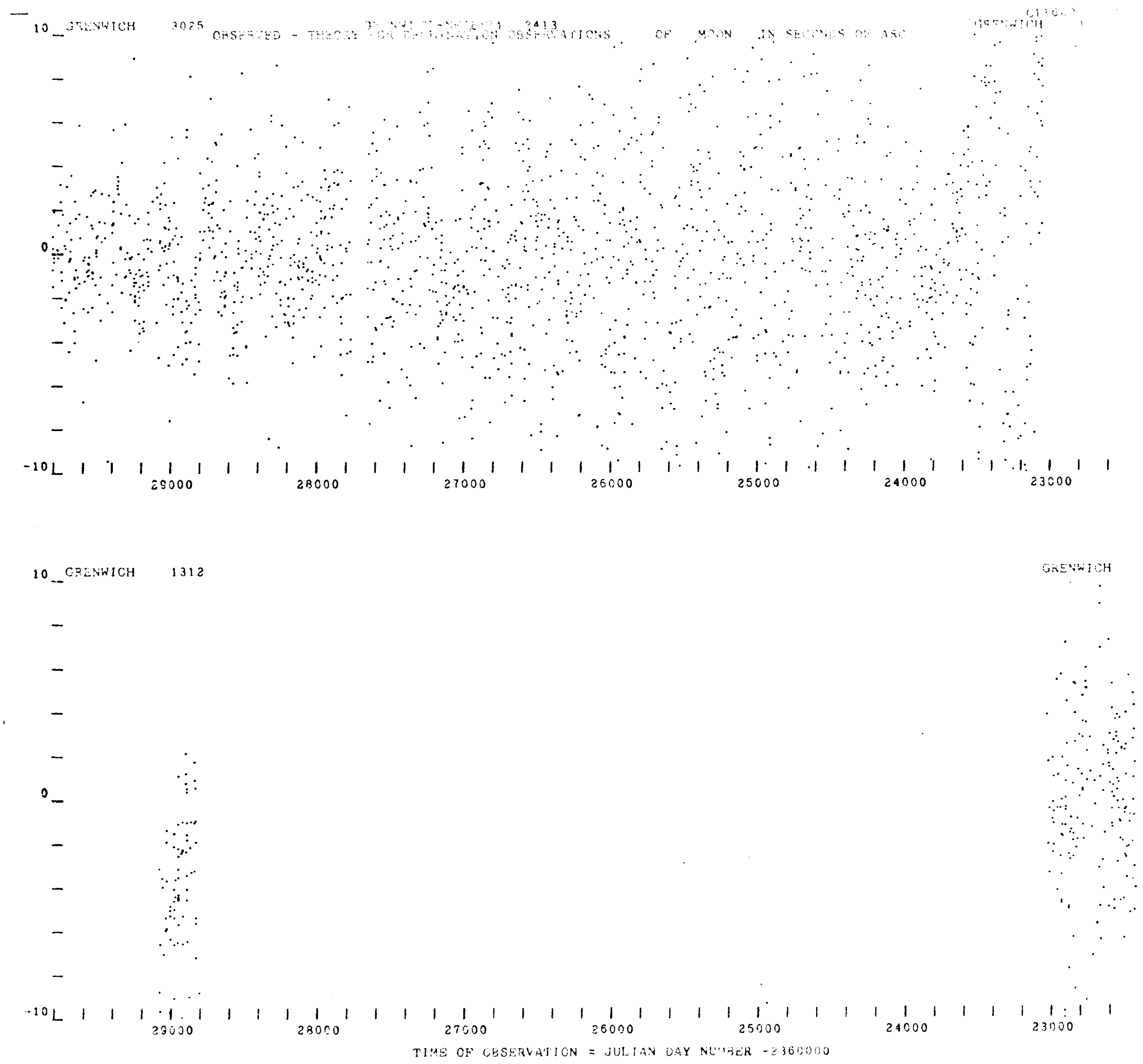

10
GRENWICH 3025
OF MOON IN SECONDS OF ARC
0
-10
29000
28000
27000
26000
25000
24000
23000
10
GRENWICH 1312
GRENWICH
0
-10
29000
28000
27000
26000
25000
24000
23000
TIME OF OBSERVATION = JULIAN DAY NUMBER -2360000

Fig. 24 (Cont.)

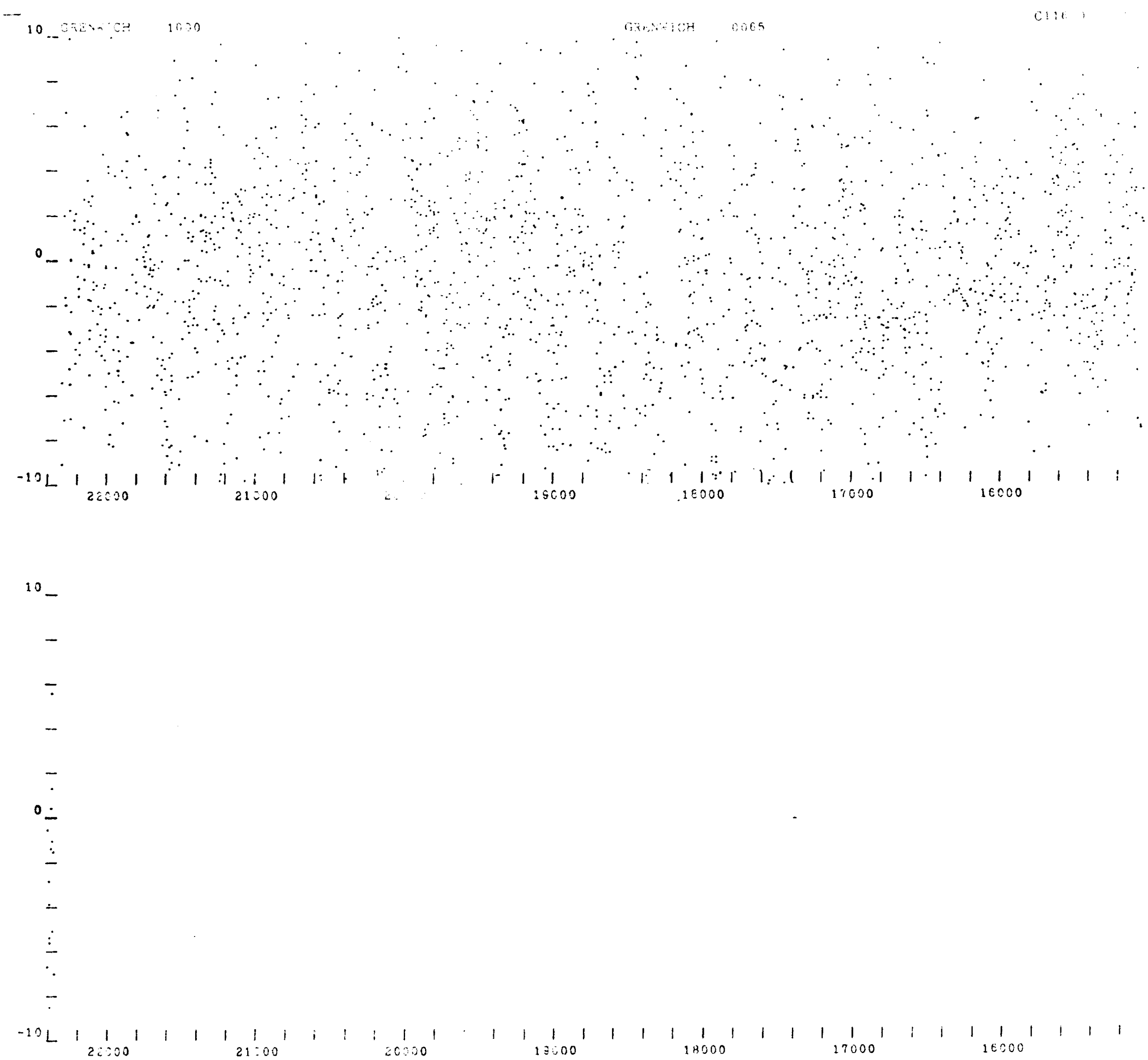
10
0
-10
22000
21000
19000
18000
17000
16000
10
0
-10
22000
21000
20000
19000
18000
17000
16000

Fig. 24 (Cont.)

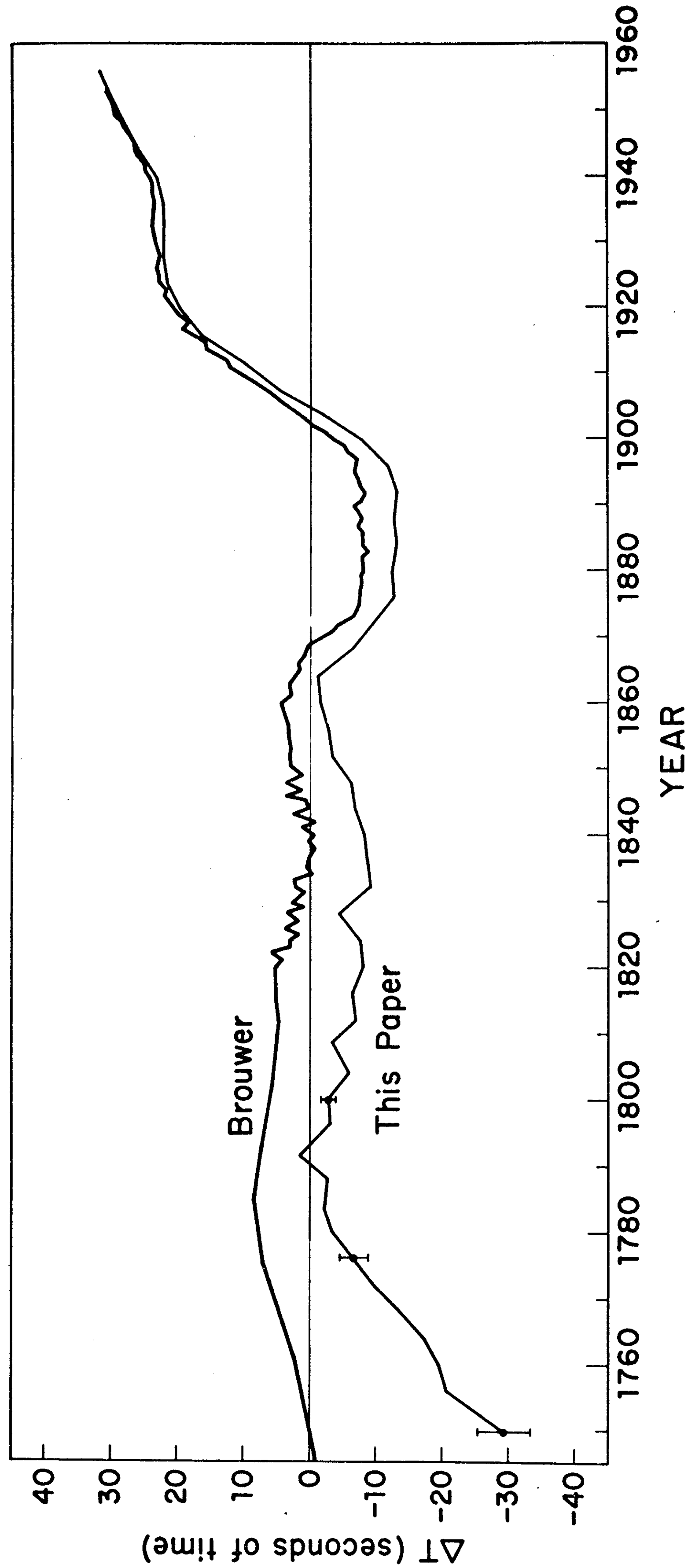
ΔT (seconds of time)
40
30
20
10
0
-10
-20
-30
-40
YEAR
1760
1780
1800
1820
1840
1860
1880
1900
1920
1940
1960
Brouwer
This Paper

Figure 25

REFERENCES

1. Adams, A.N., B.L.Klock, and D.K. Scott, 1969, Washington Meridian Observations of the Moon; Six Inch Transit Circle Results 1925-1968, Publication of the U.S. Naval Observatory, Second Series, Volume XIX, part III, U.S. Government Printing Office, Washington, D.C. (See also Vol. XIX, part II).
2. Anderson, D.L., and Kovach, R.L., 1964, "Attenuation in the Mantle and Rigidity of the Core from Multiply Reflected Core Phases", Proc. National Academy of Science, U.S., 51, 168-172.
3. Ash, Michael E., 1965a, "Generation of Planetary Ephemerides on an Electronic Computer", Lincoln Laboratory TR-391, Lexington, Mass.
4. Ash, Michael E., 1965b, "Generation of the Lunar Ephemeris on an Electronic Computer", Lincoln Laboratory TR-400, Lexington, Mass.
5. Ash, Michael E., I. Shapiro, and W.B. Smith, 1967, "Astronomical Constants and Planetary Ephemerides Deduced from Radar and Optical Observations", Astron. J., 72, 338-349.
6. Baierlein, Ralph, 1967, "Testing General Relativity with Laser Ranging to the Moon", Phys. Rev., 162, 1275-1288; Krogh, Christine, and Ralph Baierlein, "Lunar Laser Ranging and the Brans-Dicke Theory", Phys. Rev., 175, 1576-1579.

7. Ball, R.H., A.B. Kahle, and E.H. Vestine, 1968, "Variations in the Geomagnetic Field and in the Rate of the Earth's Rotation", Rand Corporation Memorandum, RM-5717-PR.

8. Brans, C., and R.H. Dicke, 1961, "Mach's Principle and a Relativistic Theory of Gravitation", Phys. Rev., 124, 925-935.

9. Brouwer, D., 1952, "A Study of the Changes in the Rate of Rotation of the Earth", Astronomical Journal, 57, 125-146.

10. Brown, E.W., 1910, Mem. Roy. Astron. Soc., 53, 39, 163; 54, 1; 57, 51; 59, 1.

11. Bullard, E.C., C. Friedman, H. Gillman, and J. Nixon, 1950, "The Westward Drift of the Earth's Magnetic Field", Phil. Trans. Roy. Soc., London, A293, 67

12. Chauvenet, W., 1891, Manual of Spherical and Practical Astronomy, reprinted Dover Publications, New York, 1960.

13. Clemence, G.M., 1966, "Inertial Frames of Reference", Q Quart. J. Royal. Astron. Soc., 7, 10-21.

14. Danby, J.M.A., 1969, Fundamentals of Celestial Mechanics, MacMillan and Co., New York.

15. de Sitter, W., 1916, "Planetary Motion and the Motion of the Moon According to Einstein's Theory", M.N. Roy. Astron. Soc., 76.

16. Dessler, A.J., 1967, "Solar Wind and Interplanetary Magnetic Fields", Rev. Geophysics, 5, 1.

17. Eckert, W.J., R. Jones, and H.K. Clark, 1954, Improved Lunar Ephemeris 1952-1959, U.S. Naval Observatory, Washington, D.C.

18. Eckert, W.J., 1965, "On the Motions of the Perigee and Node and the Distribution of Mass in the Moon", Astronomical Journal, 70, 787-792.

19. Eckert, W.J., 1966, "Transformation of the Lunar Coordinates and Orbital Parameters", Astronomical Journal, 71, 314.

20. Fock, V.A.,1939, J. Phys. USSR, 1, 81.

21. Fricke, Walter, 1967a, "Precession and Galactic Rotation Derived from McCormick and Cape Proper Motions in the Systems of FK3, N30, and FK4", Astromical Journal, 72, 642-649.

22. Fricke, Walter, 1967b, "Precession and Galactic Rotation Derived from Fundamental Proper Motions of Distant Stars , Astronomical Journal, 72, 1368-1369.

23. Fricke, W., and A. Kopff, 1963, Fourth Fundamental Catalogue (FK4), Veröffentlichungen des Astronomischen, Rechen-Instituts, Number 10, Heidelberg.

24. Goldreich, Peter, 1966, "History of the Lunar Orbit", Reviews of Geophysics, 4, 411-439.

25. Goldstein, Herbert, 1950, Classical Mechanics, Addison-Wesley, Cambridge.

26. Grove, G.V., 1960, "Motions of a Satellite in the Earth's Gravitational Field", Proc. Roy. Soc., London A254, 48-65.

27. Guinot, B., and Feissel, M., 1969, Annual Report for 1968, Bureau International de l'Heure, Paris.

28. Hildebrand, F.B., 1948, Advanced Calculus for Applications, Prentice-Hall, Englewood Cliffs, New Jersey.

29. Hildebrand, F.B., 1956, Introduction to Numerical Analysis, McGraw-Hill, New York.

30. Hill, G.W., 1884, Astron. Papers Am. Ephemeris, 3, U.S. Navy Department, Washington, D.C.

31. Holzman, R.E., 1965, User's Guide to the Tracking Data Processor, Jet Propulsion Laboratory, Pasadena, California, Reorder No. 65-205.

32. Isham, C.J., Abdus Salam, and J. Strathdee, 1971, Phys. Rev., D, 3, 867-873.

33. Jeffreys, H., 1968, "The Variation of Latitude", M.N.R.A.S., 141, 225.

34. Kaula, William M., 1964, "Tidal Dissipation by Solid Friction and the Resulting Orbital Evolution", Rev. Geophys, 2, 661-685.

35. Kaula, William M., 1969, "The Gravitational Field of the Moon", Science, 166, 1581-1588.

36. Knopoff, L., and G.J.F. MacDonald, 1958, "Attenuation of Small-Amplitude Stress Waves in Solids", Rev. Mod. Phys., 30, 1178-1192.

37. Kozai, Y., 1969, "Revised Value for Coefficients of Zonal Spherical Harmonics in the Geopotential", Smithsonian Astrophysical Observatory Spc. Report No. 295.

38. Koziel, K., 1962, "Libration of the Moon", in Physics and Astronomy of the Moon, Z. Kopal, ed., Academic Press, New York and London.

39. Lieske, Jay, 1967, "Expression for the Precession Quantities and their Partial Derivatives", Jet Propulsion Laboratory Tech. Report 32-1044.

40. Liu, A.S. and P.A. Loring, 1971, "Lunar Gravity Analysis from Long-Term Effects", Science, 173, 1017-1020.

41. Lorell, J., 1970, "Lunar Orbiter Gravity Analysis", The Moon, 1, 190-231.

42. MacDonald, G.J.F., 1964, "Tidal Friction", Rev. Geophys, 2, 467-541.

43. Markowitz, Wm., 1970, "Sudden Changes in Rotational Acceleration of the Earth and Secular Motion of the Pole", in Earthquake Displacement Fields and the Rotation of the Earth, ed. L. Manshinha, Springer Verlag, New York, 69-81.

44. Markowitz, W., R.G. Hall, L. Essen, and J.V.L. Parry, 1958, "Frequency of Cesium in Terms of Ephemeris Times", Phys. Rev. Letters, 1, 2040.

45. Melbourne, W.G., J.D. Mulholland, W.J. Sjogren, and F.M. Sturms, Jr., 1968, "Constants and Related Information for Astrodynamic Calculations, 1968, JPL Technical Report 32-1306, Jet Propulsion Laboratory, Pasadena, Cal.

46. Michael, W.H., Jr., W. T. Blackshear, and J.P. Gapcynski, 1969, paper presented to the 12th Plenary COSPAR Meeting, Prague, Czechoslovakia, "Results on the Mass and the Gravitational Field of the Moon as Determined from Dynamics of Lunar Satellites." COSPAR C.2:1.

47. Morrison, L.V. and F.M. Sadler, 1969, "An Analysis of Lunar Oscillation", M.N.R.A.S., 144, 129-141.

48. Mottinger, N.A., 1970, "Status of DSS Location Solutions from Deep Space Probe Missions", Jet Propulsion Laboratory Space Program Summary 37-60, Vol. II, 77-89.

49. Munk, W.H., and G.J.F. MacDonald, 1960, The Rotation of the Earth, Cambridge University Press, U.K.

50. Newcomb, Simon, 1895, Fundamental Constants of Astronomy, Supplement to the American Ephemeris and Nautical Almanac for 1897, Washington, D.C. Government Printing Office.

51. Newton, Robert R., 1969, Ancient Astronomical Observations and the Accelerations of the Earth and Moon, John Hopkins Press, Silver Spring, Md.

52. Nordsieck, A., 1962, "On Numerical Integration of Ordinary Differential Equations," Mathematics of Computation, 16, 22-49.

53. Papapetrou, A., 1955, Proc. Roy. Soc., A209, 248.

54. Press, F.P., 1966, "The Earth Beneath the Continents," Geophys. Monograph, 10, American Geophysical Union, Washington, D.C.

55. Rudnick, P., 1956, "The Spectrum of the Variation in Latitude", Trans. Am. Geophys. Union, 37, 137.

56. Shapiro, Irwin I.,"The Prediction of Ballistic Missile Trajectories from Radar Observations," Lincoln Laboratory Technical Report 129.

57. Shapiro, I.I., M.E. Ash, and M.J. Tausner, 1966, Verification of the Doppler formula", Phys. Rev. Lett., 17, 932-933.

58. Shapiro, Irwin I., William B. Smith, Michael E. Ash, Richard P. Tausner, and Gordon H. Pettengill, 1971, "Gravitational Constant: Experimental Bound on Its Time Variation", Phys. Rev. Letter, 26, 27-30.

59. Smith, William B., 1968, "Numerical Integration of Differential Equations by Three Methods -- Equations for Description of Computer Routines, Discussion of Results", Lincoln Laboratory Technical Note 1968-31.

60. Solloway, C.B., 1965,"Elements of the Theory of Orbit Determination", Engineering Planning Document, 225, Jet Propulsion Laboratory, Calif.

61. Spencer-Jones, H., 1939, "The Rotation of the Earth and the Secular Acceleration of the Sun, Moon and Planets, M.N.R.A.S., 99, 541-558.

62. Tausner, Manasha J., 1966, "General Relativity and Its Effects on Planetary Orbits and Interplanetary Observations", Lincoln Laboratory Technical Report 425.

63. van Flandern, T.C., 1969, A Discussion of 1950-1968 Occultations of Stars by the Moon, Ph.D. Thesis, Yale University, New Haven, Conn.

64. van Flandern, T.C., 1970, The Secular Acceleration of the Moon, Astron. J., 75, 657-658.

65. Vestine, E.H., and A.B. Kahle, 1968, "The Westward Drift and Geomagnetic Secular Change", Geophys. J. Royal Astron. Soc., 15, 39-37.

66. Watts, C.B., 1963, The Marginal Zone of the Moon, Astronomical Papers of the American Ephemeris, Vol XVII, U.S. Government Printing Office, Washington D.C.

67. Weinberg, Steven, 1972, Gravitation and Cosmology, Wiley, New York.

68. Winn, F.B., 1968, "Surveyor Post-Touchdown Analysis of Tracking Data" in Surveyor Project Final Report Part II, Jet Propulsion Laboratory Technical Report 32-1265, Pasadena.

APPENDIX I

The Inertial Reference Frame Determined from the FK4 Stellar Positions and Proper Motions

Fricke (1967a, 1967b) analyzed the measured proper motions of 512 stars in the FK3, N30, and FK4 catalogues for information about the motion with respect to a truly inertial system of the frame of reference that is nominally represented by Newcomb's relations for the precession matrix (Ch. II.C). This analysis depends upon three important assumptions:

1. The stellar motions used are distributed well enough over the sky so that, with proper weighting of different areas, the results obtained closely represent the results to be found from a dense distribution of measured proper motions covering the whole sky.
2. The stars have the property that the residual proper motion over the ensemble would vanish in a truly inertial frame once the solar motion and galactic rotation are removed.
3. The description of the motion of the reference frame compared to an inertial frame is adequately described by $\vec{\omega}$, a rigid rotation of one frame relative to the other (i.e. no distortion effects exist other than the simple model for shear from differential galactic rotation and the motion of the sun).

To explore the effects of these assumptions on the results, Fricke has carried out solutions for $\vec{\omega}$ in the various catalogues, in the same catalogue with different weightings, with different parallax groups, with right ascension proper motions μ_α, with declination motions μ_δ and with μ_α and μ_δ combined. To give the reader some feeling for the range of solutions (and hence their credibility) some sample solutions will be given. The FK4 "standard solution" designated (CO2.2) with declination motions weighted twice as much as right ascension motions, and with statistical parallax factors applied to different regions, is

$$\omega_1 = -0''.22 \pm 0''.04 \text{ per century}$$
$$\omega_2 = +0''.39 \pm 0''.04 \text{ per century}$$
$$\omega_3 = -0''.34 \pm 0''.04 \text{ per century}$$

The solution with μ_α alone and the same parallax factors gave

$$\omega_1 = -0''.60 \pm 0''.11 \text{ per century}$$
$$\omega_2 = +0''.34 \pm 0''.11 \text{ per century}$$
$$\omega_3 = -0''.26 \pm 0''.05 \text{ per century}$$

whereas the corresponding μ_δ solution gave

$$\omega_1 = -0\overset{''}{.}11 \pm 0\overset{''}{.}05 \text{ per century}$$
$$\omega_2 = +0\overset{''}{.}35 \pm 0\overset{''}{.}06 \text{ per century}$$

(ω_3 is not in the declination solution since μ_δ has no sensitivity to a motion in the plane of the equator.) The N30 solution corresponding to the FK4 standard solution gave:

$$\omega_1 = -0\overset{''}{.}18 \pm 0\overset{''}{.}04 \text{ per century}$$
$$\omega_2 = +0\overset{''}{.}40 \pm 0\overset{''}{.}04 \text{ per century}$$
$$\omega_3 = -0\overset{''}{.}28 \pm 0.04 \text{ per century}$$

Note that the FK4 and N30 catalogues are different treatments of greatly overlapping observational material.

Solutions were also made from two classes of stars:

(1) all stars closer than 250 parsecs (351 stars)

(2) stars further than 250 parsecs, restricted to galactic latitude $\pm$ 30° (137 stars)

The average results for N30 and FK4 combined were:

$$\text{Class 1} \begin{cases} \omega_1 = -0\overset{''}{.}18 \pm 0\overset{''}{.}05 \text{ per century} \\ \omega_2 = +0\overset{''}{.}42 \pm 0\overset{''}{.}06 \text{ per century} \\ \omega_3 = -0\overset{''}{.}38 \pm 0\overset{''}{.}07 \text{ per century} \end{cases}$$

$$\text{Class 2} \begin{cases} \omega_1 = -0''.24 \pm 0''.04 \text{ per century} \\ \omega_2 = +0''.33 \pm 0''.05 \text{ per century} \\ \omega_3 = -0''.28 \pm 0''.06 \text{ per century} \end{cases}$$

Fricke takes the solution which he feels is most reliable, and interprets the resulting $\vec{\omega}$ in terms of precession constant errors, equinox motion, and galactic rotation The result usually stated is that

$$\Delta(\mathbf{P}\cos\,\varepsilon) = +1''.10 \pm 0''.10 \text{ per century}$$

where $\mathbf{P}$ is Newcomb's constant for luni-solar precession, and ε is the obliquity of the ecliptic.

Let us instead compute what these results for $\vec{\omega}$ imply for the angles in the precession matrix $\underline{P}$. From the expressions in the report by Lieske (1967), we find the changes to the angles described in II.C that are implied by Fricke's result are:

$$\Delta\xi_0 \simeq \Delta z = -(0''.10 \pm 0''.05)T_{50}$$

$$\Delta W = +(0''.44 \pm 0''.04)T_{50}$$

where the errors reflect Fricke's assigned errors.

To see these results in another form, we can derive the changes in the precession in right ascension $\Delta\alpha$ and the precession in declination $\Delta\delta$ as

$$\Delta\alpha = \Delta\xi_0 + \Delta z = -(0''.20 \pm 0''.10)T_{50}$$

$$\Delta\delta = \Delta W = (0''.44 \pm 0''.04)T_{50}$$

These results are the basis for believing that $|\vec{\omega}| < 1''$ per century.

APPENDIX 2

Rotation Matrices and the Equations of Motion in a Rotating Frame

The assertion was made in Chapter II that the estimation of a certain rotation matrix was equivalent to estimation of the Coriolis term in a rotating coordinate system. This appendix contains the proof of that assertion.

Consider a small particle moving under Newtonian attraction about a massive body at the origin. The differential equation for the vector position $\vec{r}$ of the particle is given by

$$\frac{d^2\vec{r}}{dt^2} = -\frac{\mu}{|\vec{r}|^2}\hat{r} \tag{1}$$

in inertial coordinates. Now assume that we have another coordinate system with the same origin rotating with a constant angular velocity $\vec{\omega}$ with respect to the inertial system. We assume for simplicity that at t = 0, the coordinate systems coincide. The vector position $\vec{r}\,'$ for the particle in this new coordinate system obeys the differential equation:

$$\frac{d^2\vec{r}\,'}{dt^2} = -\frac{\mu}{|\vec{r}(\vec{r}\,')|^2}\hat{r}' - 2(\vec{\omega}\times\frac{d\vec{r}\,'}{dt}) - \vec{\omega}\times(\vec{\omega}\times\vec{r}(\vec{r}\,')) \tag{2}$$

We make the assumption that $|\vec{\omega}|$ is small enough so that the squares of distances of order $|\vec{\omega}||\vec{r}|T$ and velocities of order $|\vec{\omega}||\frac{d\vec{r}}{dt}|T$ (where T may be 2 or 3 centuries) are ignorable. For example, for T equal to 2 centuries, and $|\vec{r}|$ equal to one hundred astronomical units, the distance involved is $\sim 10^{-3}$ A.U. Therefore the last (centrifugal) term in the equation of motion can be ignored.

We wish to show that $\vec{r}\,'$ and $\vec{r}$ are related by the expression

$$\vec{r}\,' = (\underline{I} + \underline{\varepsilon})\vec{r} \tag{3}$$

where I is the identity matrix and

$$\underline{\varepsilon} = \begin{pmatrix} 0 & +\omega_z t & -\omega_y t \\ -\omega_z t & 0 & +\omega_x t \\ +\omega_y t & -\omega_x t & 0 \end{pmatrix} \tag{4}$$

That is, given that $\vec{r}$ is a solution of Equation (1), we wish to show that the $\vec{r}\,'$ defined by (3) is a solution of (2). Note that (3) at least satisfies the condition that, at $t = 0$, the systems coincide.

First, let us evaluate $|\vec{r}\,'|$

$$|\vec{r}'| = \sqrt{\vec{r}'\cdot\vec{r}'}$$

$$= \sqrt{\vec{r}\cdot\vec{r} + 2(\underline{\varepsilon}\vec{r})\cdot\vec{r} + |\underline{\varepsilon}\vec{r}|^2}$$

We find for the middle term that

$$2[\omega_z yxt - \omega_y zxt - \omega_z xyt + \omega_x zyt + \omega_y xzt - \omega_x yzt] = 0$$

So, not surprisingly, if we neglect terms of $0\ \varepsilon^2 r^2$, we have:

$$|\vec{r}'| = |\vec{r}|$$

Therefore

$$\hat{r}' = (\underline{I} + \underline{\varepsilon})\hat{r}$$

We can compute the following:

$$\frac{d\vec{r}'}{dt} = \frac{d\vec{r}}{dt} + \frac{d}{dt}(\underline{\varepsilon}\ \vec{r})$$

$$= \frac{d\vec{r}}{dt} + \frac{d}{dt}\begin{pmatrix} \omega_z ty - \omega_y tz \\ -\omega_z tx + \omega_x tz \\ \omega_y tx - \omega_x ty \end{pmatrix}$$

$$= \frac{d\hat{r}}{dt} + \begin{pmatrix} \omega_z y - \omega_y z + \omega_z t\dot{y} - \omega_y t\dot{z} \\ -\omega_z x + \omega_x z - \omega_z t\dot{x} + \omega_x t\dot{z} \\ \omega_y x - \omega_x y + \omega_y t\dot{x} - \omega_x t\dot{y} \end{pmatrix}$$

$$= \frac{d\vec{r}}{dt} + \underline{\varepsilon}\,\frac{d\vec{r}}{dt} - \vec{\omega}\times\vec{r}$$

$$\frac{d^2\vec{r}\,'}{dt^2} = \frac{d^2\vec{r}}{dt^2} + \frac{d}{dt}\left(\underline{\varepsilon}\,\frac{d\vec{r}}{dt}\right) - \vec{\omega}\times\frac{d\vec{r}}{dt}$$

$$= \frac{d^2\vec{r}}{dt^2} + \underline{\varepsilon}\,\frac{d^2\vec{r}}{dt^2} - 2\,\vec{\omega}\times\left(\frac{d\vec{r}}{dt}\right)$$

by analogy or direct calculation. Therefore the left-hand side of (2) is given by

$$(\underline{I} + \underline{\varepsilon})\,\frac{d^2\vec{r}}{dt^2} - 2\omega\times\frac{d\vec{r}}{dt}$$

and the right-hand side is given by

$$- \frac{\mu}{|r|^2} (\underline{I}+\underline{\varepsilon})\hat{r} - 2\vec{\omega}\times \frac{d\vec{r}}{dt}$$

$$= - \frac{\mu}{|r|^2} (\underline{I}+\underline{\varepsilon})\hat{r} - 2\vec{\omega}\times[\frac{d\vec{r}}{dt} + \underline{\varepsilon}\frac{d\vec{r}}{dt} - \vec{\omega}\times\vec{r}]$$

$$= - \frac{\mu}{|r|^2} (\underline{I}+\underline{\varepsilon})\hat{r} - 2\vec{\omega}\times \frac{d\vec{r}}{dt}$$

If we ignore terms of order $\omega_i\omega_j$. Multiplying both by $(\underline{I}+\underline{\varepsilon})^{-1}$, we see that (2) under substitution (3) gives

$$\frac{d^2\vec{r}}{dt^2} = - \frac{\mu}{|\vec{r}|^2}\hat{r}$$

APPENDIX 3

Angular Momentum and General Relativity

In this appendix, we wish to briefly indicate the theoretical development from general relativity for the geodesic precession.

Following the notation of Weinberg (1972), we consider the spin four vector

$$S_\alpha \equiv \varepsilon_{\alpha\beta\gamma\delta} J^{\beta\gamma} U^\delta \tag{1}$$

of a system for which an energy-momentum tensor $T^{\alpha\beta}$ exists. The factors in this expression are

$\varepsilon_{\alpha\beta\gamma\delta}$ - the antisymmetric Levi-Civita tensor

$U^\delta = \rho^\delta / (-\rho_\beta \rho^\beta)^{\frac{1}{2}}$ - the four vector velocity

$$\rho^\delta = \sum_n E_n \frac{d\vec{x}_n^\delta}{dt}$$

where E_n and $d\vec{x}_n/dt$ are the energy and coordinate velocity of the n^{th} particle in the system

$$T^{\alpha\beta}(\vec{x},t) = \sum_n \frac{\rho_n^\alpha \rho_n^\beta}{E_n} \delta^3(\vec{x}-\vec{x}_n(t))$$

$J^{\beta\gamma}$ is the "angular momentum" tensor defined below. To construct $J^{\beta\gamma}$ consider

$$M^{\alpha\beta\gamma} \equiv x^{\alpha}T^{\beta\gamma} - x^{\beta}T^{\alpha\gamma}$$

then

$$J^{\alpha\beta} \equiv \int d^3x \; M^{\alpha\beta 0}$$

Note that S_α will reduce to $(\vec{S},0)$ in the rest frame of the system (where $\vec{S}$ is the ordinary angular momentum about the center of mass of the system).

The covariant form of this vector in a general coordinate system x^μ is defined by

$$S_\mu \equiv \frac{\partial \xi^\alpha}{\partial x^\mu} S^f_\alpha$$

where S^f_α are components of S_α is the freely-falling coordinate system ξ^α. [Note that if S_α cannot be transformed into a locally freely-falling frame, then the covariant form of S_α cannot be defined in this way. The earth, for example, is large enough not to be considered strictly a test particle. Extended spinning bodies have been treated by Papepetrou (1955) and Fock (1939).]

The equation of motion for S_μ is the so-called "equation of parallel transport":

$$\frac{dS_\mu}{d\tau} = \Gamma^\lambda_{\mu\nu} U^\nu S_\lambda$$

where the affine connection is

$$\Gamma^{\lambda}_{\mu\varkappa} = \frac{\partial x^{\lambda}}{\partial \xi^{\alpha}} \frac{\partial^2 \xi^{\alpha}}{\partial x^{\mu} \partial x^{\nu}}$$

This equation, multiplied by $\frac{d\tau}{dt}$, becomes

$$\frac{dS_i}{dt} = \Gamma^{j}_{i0} S_j - \Gamma^{0}_{i0} v^j S_j$$

$$+ \Gamma^{j}_{ik} v^k S_j - \Gamma^{0}_{ik} v^k v^j S_j$$

To order $(\bar{v}^3/\bar{r})$ in the post-Newtonian approximation:

$$\overset{(3)}{\Gamma}{}^{j}_{0i} = \frac{1}{2} \left(\frac{\partial \xi_j}{\partial x^i} - \frac{\partial \xi_i}{\partial x^j} \right) - \delta_{ij} \frac{\partial \phi}{\partial t}$$

$$\overset{(2)}{\Gamma}{}^{0}_{0i} = \frac{\partial \phi}{\partial x^i}$$

$$\overset{(2)}{\Gamma}{}^{j}_{ik} = -\delta_{ij} \frac{\partial \phi}{\partial x^k} - \delta_{jk} \frac{\partial \phi}{\partial x^i} + \delta_{jk} \frac{\partial \phi}{\partial x^j}$$

$$\overset{(0)}{\Gamma}{}^{0}_{ik} = 0$$

where the number in parenthesis (n) indicates the equivalent order of $\bar{v}^n/\bar{r}$ of the component of the affine connection.

Parallel transport preserves the values of $S_\mu S^\mu$, or $\vec{S}^2 + 2\phi\vec{S}^2 - (\vec{v}\cdot\vec{S})^2$. To order $(|\vec{v}|^2|\vec{S}|^2)$, the quantity that is preserved is

$$\vec{\mathbf{S}} = (1+\phi)\vec{S} - \frac{1}{2}\vec{v}(\vec{v}\cdot\vec{S})$$

The equation of parallel transport is then

$$\frac{d\vec{\mathbf{S}}}{dt} = \vec{\Omega} \times \vec{\mathbf{S}}$$

where

$$\vec{\Omega} = -\frac{1}{2}\vec{\nabla}\times\vec{\xi} - \frac{3}{2}\vec{v}\times\vec{\nabla}\phi$$

where $\vec{\xi}$ and ϕ are the potentials defined in Chapter II.

APPENDIX 4

Programming of the Model for Tidal Friction

A. Definitions

For purposes of documentation, details of the implementation of the tidal model in the program are given here. The accelerations due to the tidal forces are expressed in a coordinate system referred to the equinox and equator of 1950.0 for insertion into PEP. The unit vector $\hat{u}$

$$\hat{u} = \frac{\vec{X}_{ME}}{|\vec{X}_{ME}|}$$

in the direction of the moon from earth is easily found from quantites in PEP. The velocity vector $\vec{V}_{☾-\oplus}$ of the moon relative to the earth is also available and can be used to form $\hat{n}$ as follows:

$$\hat{n} = \frac{\hat{u}\times\vec{v}_{☾-\oplus}}{|\hat{u}\times\vec{v}_{☾-\oplus}|}$$

(See Section II.D.3 for notation.) We have

$$\left(\frac{d^2\vec{r}_{☾-\oplus}}{dt^2}\right)_{tidal} = R\hat{u} + W\hat{n} + S\hat{t}$$

with the unit vector $\hat{t}$ found from $\hat{n}\times\hat{u}$ to complete the basis vectors.

The angle ϕ' must be expressed in terms of quantities in PEP. The earth's angular velocity vector $\vec{\Omega}$ can be used for this purpose. A unit vector $\hat{a}$ in the direction of the ascending node is given by

$$\hat{a} = \vec{\Omega}\times\hat{n}/\,|\vec{\Omega}\times\hat{n}|$$

and

$$\cos\phi' = \hat{a}\cdot\hat{u}$$

$$\sin\phi' = \sqrt{1-\cos^2\phi'}$$

The sign of sin ϕ' is the same as that of $\hat{u}\cdot\vec{\Omega}$.

B. Partial Derivatives

First we note that, in PEP, the symbol Z has been used for the function designated as S above

$$\ddot{\vec{r}} = R\hat{u} + W\hat{n} + Z\hat{t}$$

and thus

$$\therefore\ \frac{\partial\ddot{\vec{r}}}{\partial c_i} = \frac{\partial R}{\partial c_i}\hat{u} + \frac{\partial W}{\partial c_i}\hat{n} + \frac{\partial Z}{\partial c_i}\hat{t}$$

where

$$R = -A'C(r)\{3\cos^2\delta - 1 + D\}$$

$$Z = A'C(r)\{f(t)\}\sin 2\delta$$

$$W = -A'C(r)\{g(t)\}\sin 2\delta$$

where c_i is a parameter described below. In analogy with R. R. Newton's results, we have allowd for a time variation in tidal friction by setting

$$\sin 2\delta = c_1 - (c_2 + c_3 t)t$$

where t is the elapsed time from epoch. Using the relation

$$\frac{\partial}{\partial c_i}(\cos^2\delta) = \frac{\partial}{\partial c_i}\left[\frac{1}{2}\left(1+\sqrt{1-\sin^2(2\delta)}\right)\right]$$

$$= \frac{1}{2}\frac{\sin 2\delta}{\sqrt{1-\sin^2(2\delta)}}\frac{\partial}{\partial c_i}(\sin 2\delta)$$

we obtain

$$\frac{\partial R}{\partial c_1} = A'C(r)\ \frac{3}{2}\ \frac{\sin 2\delta}{\sqrt{1-\sin^2(2\delta)}}$$

$$\frac{\partial Z}{\partial c_1} = A'C(r)\{f(t)\}$$

$$\frac{\partial W}{\partial c_1} = -A'C(r)\{g(t)\}$$

$$\frac{\partial R}{\partial c_2} = -A'C(r)\ \frac{3}{2}\ \frac{(\sin 2\delta)t}{\sqrt{1-\sin^2(2\delta)}}$$

$$\frac{\partial Z}{\partial c_2} = -A'C(r)\{f(t)\}t$$

$$\frac{\partial W}{\partial c_2} = A'C(r)g(t)t$$

$$\frac{\partial R}{\partial c_3} = -A'C(r)\ \frac{3}{2}\ \frac{(\sin\ 2\delta)t^2}{\sqrt{1-\sin^2(2\delta)}}$$

$$\frac{\partial Z}{\partial c_3} = -A'C(r)\{f(t)\}t^2$$

$$\frac{\partial W}{\partial c_3} = A'C(r)g(t)t^2$$

APPENDIX 5

Everett Interpolation

In the Planetary Ephemeris Program (PEP), the tabular interval for each function to be interpolated is chosen so that the necessary accuracy can be obtained with Everett interpolation using eighth differences. Let f(t) be the function which we wish to evaluate at an arbitrary time t, given that we have a table of its values $f_i = f(t_i)$ at equally spaced tabular points t_i between t_0 and t_1. We define the even order differences for this tabulation by the inductive relations

$$\Delta_i^0 = f_i$$

$$\Delta_i^{2n} = \Delta_{i+1}^{2n-2} - 2\Delta_i^{2n-2} + \Delta_{i-1}^{2n-2} \qquad (1)$$

Let $h = t_{i-1}-t_i$ be the tabular interval and let $q = 1-p$. Then the Everett interpolation polynomial $g(t) = g(t_0+ph)$ [to be defined below] for $t_0 \leq t \leq t_1$, can be made to represent the actual value f(t) as accurately desired by appropriate choice of tabular interval h and highest order of differences used 2n if f possesses derivatives up to order 2n+2. See Hildebrand, "Introduction to Numerical Analysis", p. 103.

To find the value of f(t) for $t_0 \leq t \leq t_1$ by interpolation, tion, PEP determines the function g(t) from the formula

$$g(t) = g(t_0+ph) = p(y_1^1+p^2(y_1^2+p^2(y_1^3+p^2(y_1^4+p^2y_1^5))))$$

$$+q(y_0^1+q^2(y_0^2+q^2(y_0^3+q^2(y_0^4+q^2y_0^5))))$$

where the coefficients are defined by

$$y_i^1 = 1.7873015873015873f_i - 0.4960317460317460(f_{i+1}+f_{i-1})$$

$$+0.1206349206349206(f_{i+2}+f_{i-2})-0.1984126984126984\times10^{-1}$$

$$(f_{i+3}+f_{i-3})+0.1587301587301587\times10^{-2}(f_{i+4}+f_{i-4})$$

$$y_i^2 = -0.9359567901234568f_i+0.6057098765432098(f_{i+1}+f_{i-1})$$

$$-0.1632716049382716(f_{i+2}+f_{i-2})+0.2779982363315696\times10^{-1}$$

$$(f_{i+3}+f_{i-3}) -0.2259700176366843\times10^{-2}(f_{i+4}+f_{i-4})$$

$$y_i^3 = 0.1582175925925926f_i - 0.1171296296296296(f_{i+1}+f_{i-1})$$

$$+0.4606481481481481\times10^{-1}(f_{i+2}+f_{i-2}) - 0.8796296296296296\times10^{-3}$$

$$(f_{i+3}+f_{i-3}) + 0.7523148148148148\times10^{-3}(f_{i+4}+f_{i-4})$$

$$y_i^4 = -0.9755291005291005\times10^{-2}f_i + 0.7605820105820106\times10^{-2}$$

$$(f_{i+1}+f_{i=1}) - 0.3505291005291005\times10^{-2}(f_{i+2}+f_{i-2})$$

$$+0.8597883597883598\times10^{-3}(f_{i+3}+f_{i-3})$$

$$-0.8267195767195767\times10^{-4}(f_{i+4}+f_{i-4})$$

$$y_i^5 = 0.1929012345679012\times10^{-3}f_i - 0.1543209876543210\times10^{3}$$

$$(f_{i+1}+f_{i-1}) + 0.7716049382716048\times10^{-4}(f_{i+2}+f_{i-2})$$

$$-0.2204585537918871\times10^{-4}(f_{i+3}+f_{i-3})$$

$$+0.275573192398589\times10^{-5}(f_{i+4}+f_{i-4})$$

If the value of dr(t)/dt is needed in PEP and there is no tabulation for this function as there is for f(t), it is assumed that df(t)/dt = dg(t)/dt (numerical differentiation), where

$$h\,\frac{dg(t)}{dt} = y_1^1+p^2(3y_1^2+p^2(5y_1^3+p^7(7y_1^4+9p^2y_1^5)))$$

$$-y_0^1-q^2(3y_0^2+q^2(5y_0^3+q^2(7y_0^4+9q^2y_0^5)))$$

If the value of the second derivative is needed in PEP, it is assumed that $d^2f(t)/dt = d^2g(t)/dt$, where

$$h^2\,\frac{d^2g(t)}{dt} = p(6y_1^2+p^2(20y_1^3+p^2(42y_1^4+72p^2y_1^5)))$$

$$+q(6y_0^2+q^2(20y_0^3+q^2(42y_0^4+72q^2y_0^5)))$$

APPENDIX 6

Bibliography for Optical Observations

of the Sun, Moon, and Planets 1750-1970

1. Berlin (Germany).

Berlin, Germany. Astronomische Beobachtungen auf der Kaiserlichen Sternwarte zu Berlin.

	observations for
Band 2, 1844, p. xxv-xxxi.	1839-1842

2. Besançon (France). Université. Observatoire.

a. Bulletin Astronomique.

	observations for
Cinquiéme, 1890, p. C1-C10 and C12-C14.	1890
Sixiéme, 1891, p. C1-C5 and C7-C8.	1891
Septiéme, 1892, p. C1-C3 and C5.	1892
Huitiéme, 1893, p. C1-C3 and C5-C11.	1893
Neuviéme, 1894, p. C1-C2, C4-C6 and C8-C10.	1894
Dixiéme, 1895, p. C1-C6.	1895

b. Bulletin Astronomique, Paris.

	observations for
Tome XXVIII, 1911, p. 173-176.	1908

c. Journal des Observateurs, Marseilles.

		observations for
Vol. IV,	No. 8, 1921, p. 67-72.	1909-1914
Vol. VI,	No. 7, 1923, p. 49-51.	1921-1922
Vol. XVIII,	No. 1, 1935, p. 15-16.	1930-1934
Vol. XXI,	No. 7, 1938, p. 104.	1937

3. Cambridge (England). University.

a. Cambridge, England, University. Astronomical Observations made at the Observatory of Cambridge, George Bidell Airy.

		observations for
Vol. I	1829, p. 77-83.	1828
Vol. II,	1830, p. 105-107 and 109-116.	1829
Vol. IV,	1832, p. 122-131 and 133-136.	1831
Vol. V,	1833, p. 110-114 and 116-118.	1832
Vol. VI,	1834, p. 134-143 and 145-149.	1833
Vol. VII,	1835, p. 162-170 and 173-176.	1834
Vol. VIII,	1836, p. 124-132 and 134-136.	1835

b. Cambridge, England. University. Astronomical Observations made at the Observatory of Cambridge, James Challis.

	observations for
Vol. IX, 1837, p. 114-122 and 124-126.	1836

b. (continued)

			observations for
Vol. X,	1839,	p. 20-29 and 32-35.	1837
Vol. XI,	1840,	p. 26-34 and 36-39.	1838
Vol. XII,	1841,	p. 200-207 and 209-211.	1839
Vol. XIII,	1844,	p. 198-207.	1840-1841
Vol. XIV,	1845,	p. 242-248.	1842
Vol. XV,	1848,	p. 182-186.	1843
Vol. XVI,	1850,	p. 128-134.	1844-1845
Vol. XVII,	1854,	p. 76, 228-231, 233-235, 342 and 344.	1846-1848
Vol. XVIII,	1857,	p. 146, 280-283, 286, 406-408 and 412.	1849-1851
Vol. XIX,	1861,	p. 108-111, 115, 227-228, 231, 362-364 and 369.	1852-1854
Vol. XX,	1864,	p. 90-92, 94-95, 198-200, 203, 286-288, 292, 374-376 and 381.	1855-1860
Vol. XXI,	1879,	p. 87-88, 189-191, 303-305 and 421-423.	1861-1865
Vol. XXII,	1890,	p. 125-127, 207-209, 279-281, and 326-328.	1866-1869

4. Cape of Good Hope (South Africa). Royal Observatory.

a. Cape of Good Hope (South Africa). Royal Observatory. Annals of the Cape Observatory.

	observations for
Vol. II, Pt. 5, 1907, p. 34D-81D.	1884-1892
Vol. VIII, Pt. 4, 1915, p. 48D-78D.	1907-1911
Vol. VIII, Pt. 5, 1921, p. 51E-71E.	1912-1916
Vol. XIV, Pt. 4, 1950, p. 1-103.	1925-1936

b. Private communication, 6 July 1966.

	observations for
	1936-1959

5. Edinburgh (Scotland). Royal Observatory.

Astronomical Observations made at the Royal Observatory, Edinburgh.

	observations for
Vol. IV, 1841, p. 172-179 and 181-183.	1838
Vol. VI, 1847, p. 141-149 and 151-153.	1840
Vol. VII, 1848, p. 209-215 and 218-219.	1841
Vol. VIII, 1849, p. 257-267 and 269-271.	1842
Vol. IX, 1850, p. 209-216 and 219-221.	1843
Vol. X, 1852, p. 213-221 and 224-226.	1844
Vol. X, 1852, p. 287-292.	1845
Vol. X, 1852, p. 369.	1847

6. Greenwich (England). Royal Observatory. Observations appeared under various titles below:

a. Hurstmonceux (Herstmonceux), England. Royal Greenwich Observatory. Reduction of the Observations of the Planets made at the Royal Observatory, Greenwich from 1750 to 1830, under the superintendance of George Biddell Airy, London.

	observations for
1845, p. 164-227 and 244-311.	1750-1830

b. Hurstmonceux (Herstmonceux), England. Royal Greenwich Observatory. Reduction of the Observations of the Moon made at the Royal Observatory, Greenwich, from 1750 to 1830, under the superintendance of George Biddell Airy, London.

	observations for
Vol. 1, 1848, p. 1-495.	1750-1830
Vol. 2, 1848, p. 1-447.	1750-1830

c. Hurstmonceux (Herstmonceux), England. Royal Greenwich Observatory. Astronomical Observations made at the Royal Observatory Greenwich, in the months of (April, May, June) 1828, by John Pond, London.

	observations for
1828 (April-June).	1828
1828 (July-September).	1828
1828 (October-December).	1828

d. Hurstmonceux (Herstmonceux), England. Royal Greenwich Observatory. Reduction of the Observations of the Moon made at the Royal Observatory, Greenwich, from 1831 to 1851 under the superintendance of George Biddell Airy, London.

	observations for
1859, p. 2-39.	1831-1851

e. Hurstmonceux (Herstmonceux), England. Royal Greenwich Observatory. Astronomical Observations made at the Royal Observatory Greenwich in the year (date of observations), London.

	observations for
1834, p. 82-88.	1829
1833, p. 74-84.	1830
1832, p. 93-101.	1831
1833, p. 63-70.	1832
1834, p. 52-59.	1833
1834, p. 29-36.	1834
1835, p. 27-34.	1835
1837, p. 95-105.	1836
1838, p. 95-107.	1837
1840, p. 97-107.	1838
1843, p. 20-31.	1841 *

e. (continued)	<u>observations for</u>
1844, p. 17-28.	1842 *
1845, p. 17-28.	1843 *
1846, p. 19-29.	1844 *
1847, p. 27-39.	1845 *
1848, p. 25-34.	1846 *
1849, p. 21-32.	1847 *
1864, p. 19-25, and 31-34.	1862 **

f. Hurstmonceux, (Herstmonceux), England. Royal Greenwich Observatory. <u>Astronomical and Magnetical and Meteorological Observations made at the Royal Observatory Greenwich in the year (date of observations),</u> London.

	<u>observations for</u>
1840, p. 5-15.	1839
1842, p. 18-28.	1840
(see * above for observations for the years 1841-1847)	
1850, p. 18-30.	1848
1850, p. 26-34.	1849
1852, p. 29-35 and 39-42.	1850
1853, p. 20-27 and 30-33.	1851
1854, p. 27-33 and 38-40.	1852
1855, p. 21-25 and 29-32.	1853

f. (continued)	observations for
1856, p. 23-30 and 37-40.	1854
1857, p. 22-28 and 33-36.	1855
1858, p. 21-27 and 35-37.	1856
1859, p. 21-27 and 34-37.	1857
1860, p. 22-29 and 41-45.	1858
1861, p. 31-38 and 46-49.	1859
1862, p. 27-33 and 42-44.	1860
1863, p. 23-28 and 36-39.	1861
(see ** above for observations for the year 1862)	
1865, p. 25-31 and 39-42.	1863
1866, p. 33-39 and 48-50.	1864
1867, p. 41-47 and 57-59.	1865
1868, p. 43-48 and 58-61.	1866
1869, p. 35-40 and 50-53.	1867
1870, p. 28-35 and 44-47.	1868
1871, p. 23-29 and 41-43.	1869
1872, p. 23-29 and 37-39.	1870
1873, p. 27-34 and 39-41.	1871
1874, p. 33-39 and 47-50.	1872
1875, p. 34-40 and 51-54.	1873
1876, p. 33-39 and 47-50.	1874
1877, p. 28-34 and 42-45.	1875
1878, p. 32-37 and 48-51.	1876
1879, p. 27-33 and 39-41.	1877

f. (continued) observations for

1880, p. 41-46 and 51-54.	1878
1881, p. 33-38 and 44-46.	1879
1882, p. 38-43 and 46-49.	1880
1883, p. 34-40 and 45-48.	1881

(For observations in the years 1882-1909 the subtitle which follows is important because each section is individually numbered beginning with p. 1: <u>Right Ascension and North Polar Distances of the Sun, Moon and Planets</u>.)

1884, p. 38-43 and 47-50.	1882
1885, p. 56-62 and 65-68.	1883
1886, p. 50-56 and 60-63.	1884
1887, p. 47-53 and 56-59.	1885
1888, p. 43-50 and 55-58.	1886
1889, p. 45-52 and 57-60.	1887
1890, p. 45-51 and 55-58.	1888
1891, p. 43-49 and 54-56.	1889
1892, p. 51-59 and 63-66.	1890
1893, p. 45-52 and 55-57.	1891
1894, p. 44-53 and 55-58.	1892
1896, p. 66-76 and 79-82.	1893
1897, p. 72-81 and 85-87.	1894
1897, p. 64-74 and 77-79.	1895

f. (continued)

	observations for
1898, p. 78-88 and 90-93.	1896
1899, p. 110-119 and 121-123.	1897
1900, p. 110-118 and 120-122.	1898
1901, p. 118-129 and 131-134.	1899
1902, p. 106-115 and 117-120.	1900
1903, p. 100-110 and 112-115.	1901
1904, p. 212-223.	1902
1905, p. 307-321.	1903
1906, p. 314-321 and 323-325.	1904
1907, p. 264-277.	1905
1908, p. 97-104 and 106-107.	1906
1909, p. 130-143.	1907
1910, p. 150-164.	1908
1911, p. 140-154.	1909
1912, p. A99-A110.	1910
1913, p. A114-A130.	1911
1913, p. A98-A111.	1912
1915, p. A100-A111 and A113-A114.	1913
1918, p. A52-A66.	1914
1920, p. A38-A47.	1915
1921, p. A41-A52.	1916
1922, p. A39-A49.	1917
1922, p. A34-A44.	1918
1923, p. A37-A47.	1919

f. (continued)

	observations for
1923, p. A49-A59.	1920
1924, p. A48-A58.	1921
1924, p. A43-A57.	1922
1925, p. A40-A54.	1923
1926, p. A40-A55.	1924

g. Hurstmonceux (Herstmonceux), England. Royal Greenwich Observatory. Observations made at the Royal Observatory, Greenwich in the year (date of observations) in Astronomy, Magnetism and Meteorology under the direction of Sir Frank Dyson, London.

	observations for
1927, p. A44-A58.	1925
1928, p. A40-A55.	1926
1929, p. A54-A83.	1927
1930, p. A56-A72.	1928
p. A56-A73.	1929
1932, p. A52-A68.	1930
1933, p. A10-A25.	1931
1933, p. A10-A25.	1932
1934, p. A10-A27.	1933
1935, p. A10-A26.	1934
1937, p. A10-A25.	1935

g. (continued) <u>observations for</u>

1939, p. A10-A25.	1936
1957, p. A8-A10.	1947 ***

h. Hurstmonceux (Herstmonceux), England. Royal Greenwich Observatory. <u>Astronomical results from observations made at the Royal Observatory, Greenwich, in the year (date of observations) under the direction of H. Spencer Jones</u>, London, extracted from the Greenwich Observations.

	observations for
1951, p. A8-A22.	1937
1951, p. A8-A22.	1938
1953, p. A8-A22.	1939
1954, p. A8-A19.	1940
(no observations for the year	1941)
1955, p. A8-A22.	1942
1955, p. A6-A11.	1943
1955, p. A6-A10.	1944
1953, p. A6-A10.	1945
1955, p. A8-A19.	1946
(see *** above for observations for the year	1947)
1958, p. A9-A22.	1948
1957, p. A8-A25.	1949

h. (continued)

	observations for
1958, p. A8-A25.	1950
1958, p. A8-A27.	1951
1958, p. A8-A27.	1952
1959, p. A8-A26.	1953
1961, p. A8-A16.	1954

7. Nice (France). Observatoire. Observations for outer planets only.

a. Annales de l'Observatoire de Nice.

	observations for
Tome 12, 1910, p. B78.	1889
Tome 12, 1910, p. B115-B117.	1890
Tome 11, 1908, p. B166-B167.	1891
Tome 12, 1908, p. B288-B289.	1892
Tome 12, 1910, p. A115-A116	1893
Tome 12, 1910, p. A197-A198.	1894
Tome 12, 1910, p. B136.	1895
Tome 12, 1910, p. B154.	1896

b. Bulletin Astronomique, Paris.

		observations for
Tome XXIV,	1907, p. 5-6.	1905-1906
Tome XXV,	1908, p. 96-100.	1907
Tome XXVI,	1909, p. 75-77.	1908
Tome XXVII,	1910, p. 33-34 and 358-359.	1909-1910
Tome XXVIII,	1911, p. 276-277 and 350.	1910-1911

8. Ottawa (Canada). Dominion Observatory. Observations for sun and inner planets only.

Publications of the Dominion Observatory, Ottawa.

	observations for
Vol. XV, No. 2, 1952, p. 115-158.	1924-1935

9. Oxford (England). Radcliffe Observatory. Observations appeared under various titles listed below:

a. Radcliffe Observatory, Oxford. *Observations of the Reverend Thomas Hornsby, D.D., made with the transit instrument and quadrant at the Radcliffe Observatory, Oxford, in the years 1774 to 1798,* London, Oxford University Press.

	observations for
1932, p. 106-134.	1774-1798

b. *Radcliffe Observatory, Oxford. Astronomical Observations.*

	observations for
Vol. 1, 1842, p. 220-224 and 257-259.	1840
Vol. 2, 1843, p. 252-257.	1841
Vol. 3, 1844, p. 286-289.	1842
Vol. 4, 1845, p. 230-231.	1843
Vol. 5, 1846, p. 310-314.	1844
Vol. 6, 1847, p. 349-353.	1845

b. (continued)

	observations for
Vol. 7, 1848, p. 280-284.	1846
Vol. 8, 1849, p. 197-199.	1847
Vol. 9, 1850, p. 231-234.	1848
Vol. 10, 1851, p. 273-276.	1849
Vol. 11, 1852, p. 276-278.	1850
Vol. 12, 1853, p. 356-357.	1851
Vol. 13, 1854, p. 313-314.	1852

c. Radcliffe Observatory, Oxford. Astronomical and Meteorological Observations.

	observations for
Vol. 14, 1855, p. 257-258.	1853
Vol. 15, 1856, p. 243-244.	1854
Vol. 16, 1857, p. 143.	1855
Vol. 17, 1858, p. 248.	1856
Vol. 18, 1859, p. 243.	1857
Vol. 19, 1861, p. 255.	1858
Vol. 20, 1862, p. 81 and 165-166.	1859-1860
Vol. 21, 1863, p. 245-248.	1861
Vol. 22, 1864, p. 99-105.	1862
Vol. 23, 1865, p. 129-138.	1863
Vol. 24, 1866, p. 127-129 and 134-143.	1864

d. Radcliffe Observatory, Oxford. Results of Astronomical and Meteorological Observations.

	observations for
Vol. 25, 1867, p. 129-135.	1865
Vol. 26, 1868, p. 133-138.	1866
Vol. 27, 1869, p. 186-192.	1867
Vol. 28, 1870, p. 199-206.	1868
Vol. 29, 1871, p. 196-204.	1869
Vol. 30, 1872, p. 203-214.	1870
Vol. 31, 1873, p. 193-201.	1871
Vol. 32, 1874, p. 179-185.	1872
Vol. 33, 1875, p. 194-202.	1873
Vol. 34, 1876, p. 207-213.	1874
Vol. 35, 1877, p. 166-173.	1875
Vol. 36, 1878, p. 164-172.	1876
(no observations for the years 1877-1879)	
Vol. 38, 1883, p. 65-67.	1880
Vol. 39, 1884, p. 72-74.	1881
Vol. 40, 1885, p. 70-73.	1882
Vol. 41, 1886, p. 91-95.	1883
Vol. 42, 1887, p. 106-112.	1884
Vol. 43, 1889, p. 116-122.	1885
Vol. 44, 1890, p. 99-100 and 103-105.	1886
Vol. 45, 1891, p. 101-105.	1887
Vol. 46, 1896, p. 80-83 and 214-219.	1888-1889
Vol. 47, 1899, p. 104-110 and 223-224.	1890-1891

10. Paris (France). Observatoire.

a. Annales de l'Observatoire Imperial de Paris, Observations.

			observations for
Tome I,	1858,	p. 267-380.	1800-1829
Tome II,	1859,	p. 347-359.	1837-1838
Tome III,	1862,	p. 323-334.	1839-1840
Tome IV,	1862,	p. 278-289.	1841-1842
Tome V,	1862,	p. 246-262.	1843-1844
Tome VI,	1863,	p. 146-161.	1845-1846
Tome VII,	1863,	p. 111-123.	1847
Tome VIII,	1863,	p. 119-134.	1848-1849
Tome IX,	1865,	p. 102-115.	1850-1851
Tome X,	1866,	p. 225-239.	1852-1853
Tome XI,	1869,	p. 198-228.	1854-1855
Tome XII,	1860,	p. 303-316.	1856
Tome XIII,	1861,	p. 356-372.	1857
Tome XIV,	1861,	p. 479-497.	1858
Tome XV,	1861,	p. 312-330.	1859
Tome XVI,	1862,	p. 249-260.	1860
Tome XVII,	1863,	p. 125-137.	1861
Tome XVIII,	1863,	p. 130-139.	1862
Tome XIX,	1864,	p. I34-I52.	1863
Tome XX,	1865,	p. G9-G27.	1864
Tome XXI,	1866,	p. F9-F27.	1865
Tome XXII,	1867,	p. F9-F25.	1866

b. <u>Annales de l'Observatoire de Paris, Observations</u>.

	observations for
Tome XXIII, 1871, p. K8-K28.	1867
Tome XXIV, 1880, p. 13-24 and 43-45.	1868-1869
1881, p. 216-221 and 228-229.	1870
1882, p. D7-D12 and D17-D18.	1871
1882, p. D7-D14 and D21-D24.	1872
1882, p. D8-D15 and D26-D28.	1873
1876, p. D7-D15 and D23-D26.	1874
1878, p. D7-D16 and D25-D28.	1875
1879, p. D7-D15 and D25-D29.	1876
1880, p. D7-D13 and D19-D21.	1877
1881, p. E7-E12 and E18-E20.	1878
1882, p. E8-E17 and E23-E28.	1879
1883, p. E8-E19 and E26-E31.	1880
1885, p. E8-E18 and E27-E33.	1881
1887, p. E262-E274 and E283-E289.	1882
1889, p. E138-E160.	1883
1892, p. E93-E117.	1884
1893, p. E82-E101.	1885
1894, p. E83-E104.	1886
1894, p. E63-E79.	1887
1896, p. C51-C65.	1888
1898, p. C48-C61.	1889
1898, p. C51-C64.	1890

b. (continued)

	observations for
1907, p. A187-A193 and A199-A200.	1891
1910, p. A167-A175.	1892
1911, p. A208-A218.	1893
1899, p. A65-A69 and C153-C154.	1897
1902, p. A72-A77 and C151-C152.	1898
1904, p. A79-A84 and C92-C94.	1899
1904, p. A74-A79 and C103-C104.	1900
1905, p. A68-A73 and C142-C145.	1901
1906, p. A62-A67, C88-C90 and D111.	1902
1907, p. A53-A56, B137-B140 and C162-C166.	1903
1908, p. A55-A58, B127-B130 and C73-C74.	1904
1911, p. A53-A57, B109-B111 and C58-C59.	1905
1912, p. A59-A62, B102-B104 and C85-C86.	1906

c. Journal des Observateurs, Marseilles.

				observations for
Tome III,	No. 11,	1920,	p. 102-104.	1919
Tome IV,	No. 5,	1921,	p. 46-48.	1920
Tome V,	No. 9,	1922,	p. 72-75.	1921
Tome VI,	No. 7,	1923,	p. 54-56.	1922
Tome VII,	No. 8,	1924,	p. 90-92.	1923
Tome VIII,	No. 9,	1925,	p. 134-136.	1924-1925
Tome XIV,	No. 12,	1931,	p. 145-147.	1929-1930
Tome XVII,	No. 10,	1934,	p. 149-150.	1933

c. (continued)

	observations for
Tome XVIII, No. 11, 1935, p. 178.	1935
Tome XXI, No. 4, 1938, p. 45-46.	1936
Tome XXI, No. 5, 1938, p. 62.	1936-1937
Tome XXII, No. 8, 1939, p. 151.	1938

11. Strassburg (Germany).

Annalen der Kaiserlichen Universitätssternwarte in Strassburg, Karlsruhe.

	observations for
Band V, Teil III, 1926, seite C9-C52.	1883-1893

NOTE: This title was published, in German, from 1896 through 1926. When Strassburg was recovered by France after World War I, the title was changed to Annales de l'Observatoire de Strasbourg (Paris).

12. Tokyo (Japan). Tokyo Astronomical Observatory.

a. Tokyo Temmondai. Tokyo Astronomical Bulletin, 2nd Series.

	observations for
No. 28, (10 Jun 1950).	1949
No. 38, (25 Jun 1951).	1950
No. 50, (10 Oct 1952).	1951
No. 59, (20 Aug 1953).	1952
No. 68, (5 Aug 1954).	1953
No. 74, (20 Jul 1955).	1954

a. (continued)

	observations for
No. 85, (10 Jul 1956).	1955
No. 100, (5 Sep 1957).	1956
No. 108, (5 Aug 1958).	1957
No. 117, (25 Jul 1959).	1958
No. 131, (20 Jul 1960).	1959
No. 162, (10 Feb 1964).	1960
No. 153, (10 Jul 1962).	1961
No. 161, (5 Sep 1963).	1962

b. Private communication, 1966. Observations for Mars and outer planets only. <u>observations for</u> 1949-1962

13. Toulouse (France). Université. Observatoire. Observations of the moon and planets only.

a. <u>Bulletin Astronomique, Paris</u>.

	observations for
Tome XXVII, 1910, p. 171-172 and 442-443.	1908-1910
Tome XXX, 1913, p. 80-81.	1912

b. <u>Journal des Observateurs, Marseilles.</u>

	observations for
Tome I, No. 9, 1916, p. 87-89.	1912-1915
Tome II, No. 10, 1918, p. 127-129.	1914-1915

b. (continued)

	observations for
Tome II, No. 15, 1919, p. 159-160.	1911-1916
Tome III, No. 3, 1920, p. 26-29.	1912-1917
Tome II, No. 19, 1919, p. 195-196.	1916-1917
Tome IV, No. 2, 1921, p. 15-19.	1917-1918
Tome V, No. 5, 1922, p. 31-35.	1919-1920
Tome VI, No. 6, 1923, p. 41-45.	1919-1921
Tome VII, No. 10, 1924, p. 114-117.	1922
Tome IX, No. 12, 1926, p. 183-184.	1923-1924

14. Uccle (Belgium). Brussels. Observatoire Royal de Belgique. Bulletin Astronomique, Brussels, Observatoire Royal de Belgique.

			observations for
Vol. 1, No. 5,	1932,	p. 78-91.	1928-1930
Vol. 1, No. 2,3,	1931,	p. 23-28 and 46-48.	1931
Vol. 1, No. 5,7,8,	1932,	p. 76-77, 143 and 161.	1932
Vol. 1, No. 9,10,12,	1933,	p. 184-185,224-225 and 268.	1933
Vol. 1, No. 13,14,15,	1934,	p. 292-293,306 and 324.	1934
Vol. 2, No. 2,3,4,	1935,	p. 40,56 and 80-81.	1935
Vol. 2, No. 5,6,7,	1936,	p. 94, 124-125 and 154.	1936

14. (continued)

		<u>observations for</u>
Vol. 2, No. 8,10,	1937, p. 176 and 214.	1937
Vol. 2, No. 11,13,	1938, p. 232 and 282.	1938
Vol. 3, No. 1,2,3,	1939, p. 10,36 and 56-57.	1939
Vol. 3, No. 4,	1940, p. 88.	1940
Vol. 3, No. 5,	1941, p. 130.	1941
Vol. 3, No. 7,	1943, p. 198.	1942
Vol. 3, No. 8,	1944, p. 242.	1943
Vol. 3, No. 9,	1945, p. 280.	1944

15. Washington, D.C. (United States). U.S. Naval Observatory.

a. U.S. Naval Observatory. <u>Astronomical and Meteorological Observations made at the United States Naval Observatory.</u>

	<u>observations for</u>
1862, p. 336-340.	1861
1863, p. 569-579.	1862
1865, p. 353-362.	1863
1866, p. 365-374.	1864
1867, p. 414-425.	1865

b. U.S. Naval Observatory. <u>Publications of the United States Naval Observatory</u>, 2nd Series .

		<u>observations for</u>
Vol. IV, Pts. I-III,	1906, p. B3-B157.	1866-1891
Vol. I,	1900, p. 351-396.	1894-1899

b. (continued)

			observations for
Vol. IV,	Pts. I-III,	1906, p. A283-A318.	1900-1903
Vol. IX,	Pt. I,	1920, p. A3-A71.	1903-1911
Vol. XI,		1927, p. 153-179.	1911-1918
Vol. XIII,		1933, p. 102-155.	1913-1925
Vol. XVI,	Pt. I,	1949, p. 59-199.	1925-1941
Vol. XV,	Pt. V,	1948, p. 189-238.	1935-1945
Vol. XVI,	Pt. III,	1952, p. 397-445.	1941-1949
Vol. XIX,	Pt. I,	1964, p. 49-99.	1949-1956

c. United States Naval Observatory, Circular.

	observations for
No. 103, 9 Oct 1964.	1956-1962
No. 105, 27 Nov 1964.	1963-1964
No. 108, 1 Jul 1965.	1964
No. 115, 1 Feb 1967.	1965-1966
No. 118, 5 Jan 1968.	1966-1967
No. 124, 28 Feb 1969.	1967-1968
No. 127, 1 Apr 1970.	1968-1969

d. Private communication, P.K. Seidelmann.

observations for

1970

BIOGRAPHICAL NOTE

Martin A. Slade, III, was born on August 31, 1942 in Dunedin, Florida. He was raised in Lakeland, Florida, where he graduated from Lakeland Senior High School as valedictorian in 1960. He entered M.I.T. the following September as a National Merit Scholar. He received the degree of Bachelor of Science in the Department of Physics in June 1964.

Mr. Slade continued his studies at M.I.T. in the Department of Physics. In September of 1965, Mr. Slade was awarded a two year NASA Traineeship to pursue his graduate study. He received the degree of Master of Science in September of 1967. His S.M. thesis was entitled "Lifetime Measurement of Nuclear Excited States Using Doppler-Shift Attenuation Techniques".

In September of 1967, Mr. Slade entered the Department of Earth and Planetary Sciences. He held a Teaching Assistantship for that year, and a Research Assistantship in subsequent years. For the summers of 1969 and 1970, Mr. Slade held summer staff appointments at Haystack Research Facility of Lincoln Lab. (now Haystack Observatory of M.I.T).

Upon receipt of the degree of Doctor of Philosophy, Mr. Slade will join the staff of the Jet Propulsion Laboratory, California Institute of Technology, Pasadena, California.

ACKNOWLEDGEMENTS

I wish to express my greatest appreciation to Professor Irwin I. Shapiro and to Dr. Michael E. Ash. My thesis advisor, Professor Shapiro, provided unfailing inspiration and advice at every stage of this work. Working with him has been the greatest single contribution to my scientific education. Dr. Ash also advanced my knowledge of astronomy in many fruitful discussions. He supervised the interfacing of the additional programming for the moon with the existing structure of the Planetary Ephemeris Program and was a constant source of accurate information about this structure.

My sincerest thanks go to Mrs. Antonia Forni whose careful and diligent labor was indispensable to this work. Her clever solutions to programming difficulties and logistic problems have been invaluable. I would also like to thank William B. Smith who contributed the numerical integration procedures and aided in their implementation in the lunar data processing.

I also must thank Fernando Amuchastegui, Mark Hacker and Mrs. Katherine Becker for their programming assistance.

I am greatly indebted to Dr. Donald Eckhardt of the Air Force Cambridge Research Laboratory under whose contract this work was carried out. I woûld also like to thank Dr.

Thomas Clark and Mr. Gerald Marandino of Goddard Space Flight Center for much support and hospitality. For information on the Surveyor Doppler data, I thank Dr. Louis Friedman and F.B.Winn of the Jet Propulsion Laboratory. M. J. Davis of Stanford Electronics Research Center kindly supplied ionospheric electron densities. Dr.Stanley H. Zisk of Haystack Observatory provided much helpful information about the radar data. I am very grateful to Group 63, Lincoln Laboratory for a research assistantship during this work.

Prof. C.C. Counselman III is due special thanks for his careful reading and comments on a draft of this thesis. I would also like to thank Mrs. Ann Preston for her patient and careful preparation of the final copy of the manuscript.

I must thank my friends for their understanding and patience during this effort. Lastly the encouragement and support of my parents throughout my education is deeply appreciated.